4-5-2017 12:00 AM

Gatekeepers of nitrogen-fixing symbiosis: Cytokinin-ethylene crosstalk regulates symbiotic interaction in Lotus japonicus

Seyedehmandana Miri, *The University of Western Ontario*

Supervisor: Dr. Krzysztof Szczyglowski, *The University of Western Ontario*
Joint Supervisor: Dr. Denis Maxwell, *The University of Western Ontario*
A thesis submitted in partial fulfillment of the requirements for the Doctor of Philosophy degree in Biology

Abstract

Leguminous plants thrive under nitrogen-limited soil conditions because of their ability to symbiotically interact with nitrogen-fixing bacteria, known as rhizobia. In the presence of compatible strains of rhizobia, they develop specialized symbiotic organs, called root nodules, which host the bacteria and provide the appropriate conditions for symbiotic nitrogen fixation to occur. The plant hormone cytokinin is the key endogenous trigger for the inception of root nodule organogenesis. In the model legume *Lotus japonicus*, analysis of the cytokinin receptor gene *Lotus histidine kinase 1* (*Lhk1*) showed that it is required and also sufficient for the initiation of nodule organogenesis. However, mutant plants carrying loss-of-function *lhk1*alleles still form a limited number of nodules while being hyper-infected by their symbiotic partner, *Mesorhizobium loti*.

Here, I show that *L. japonicus* contains a small family of four cytokinin receptor genes, all of which respond to *M. loti* infection. Within the root cortex, LHK1 performs an essential role but also works partially redundantly with LHK1A and LHK3 to mediate cell divisions for nodule primordium formation. LHK1 is also shown to be critical in maintaining the homeostasis of *M. loti* entry into *L. japonicus* roots. The LHK1-dependent signaling is required to promote the development of infection threads within the root cortex but also to stimulate a negative feedback mechanism that restricts subsequent infections at the root epidermis. I have proposed and tested a hypothesis whereby the increased cytokinin activity in the root epidermis, as mediated by LHK1, enhances ethylene production, which in turn inhibits subsequent *M. loti* infections. My thesis work identifies a family of seven *ACS* genes that mediate ethylene biosynthesis in *L. japonicus* and shows that *ACS1* and *ACS2* are potential targets of LHK1-dependent regulation during symbiosis.

The results of this thesis work contribute to the understanding of the molecular mechanisms for hormonal, cytokinin-ethylene dependent, regulation of nitrogen-fixing symbiosis. In broader terms, this adds to knowledge of the principles that govern the beneficial plant-microbe interactions while bolstering the long-term goal of exploiting bio-fertilization through nutrient acquiring symbioses as a means of mitigating the negative environmental impacts associated with the use of industrial fertilizers in agriculture.

Keywords

Legumes, *Lotus japonicus*, root, rhizobia, nitrogen-fixing symbiosis, nodule organogenesis, cytokinin receptor, infection thread, ethylene biosynthesis

Co-Authorship Statements

The following thesis contains material from published and in-preparation manuscripts (Chapters 2-4). My supervisor, Krzysztof Szczyglowski provided insight and strategic direction of the projects and also critically edited the final manuscripts (Chapters 2-4).

CHAPTER 2

Mandana Miri, Mark Held, and Hongwei Hou designed the research, performed the experiments, analyzed the data and drafted the manuscript. Krzysztof Szczyglowski conceived the study and participated in its design. Christian Huynh participated in the cloning of *LhK* cDNA (Figure 2.18). Shusei Sato and Satoshi Tabata provided information for *Lhk* loci (Figure 2.1). Jillian Perry and Trevor Wang conducted the identification of all the mutations within *Lhk* loci via the TILLING approach (Table 2.2). Loretta Ross and Md Shakhawat Hossain helped in editing the manuscript. Mandana Miri, Mark Held, and Krzysztof Szczyglowski edited the manuscript. The experiments performed by Mandana Miri are listed in Section 2.1.

CHAPTER 3

Mandana Miri designed the research, performed the experiments and drafted the manuscript. Krzysztof Szczyglowski conceived the study and participated in its design. Mark Held performed the *NIN::GUS* epidermal expression experiment (Figure 3.3). Loretta Ross and Preetam Janakirama helped in editing the manuscript. Mandana Miri and Krzysztof Szczyglowski edited the manuscript.

CHAPTER 4

Mandana Miri designed the research, performed the experiments, analyzed the data, and drafted the manuscript. Krzysztof Szczyglowski conceived the study and participated in its design. Dugald Reid performed the ethylene measurement experiment (Figure 4.14) under the supervision of Jens Stougaard. Preetam Janakirama prepared materials and Stig Andersen performed the bioinformatic analysis for the RNAseq experiment (Figure 4.23). Mandana Miri and Krzysztof Szczyglowski edited the manuscript.

Dedication

To Reza Saberianfar,

without whom THIS thesis would not have been possible.

To my parents,

may they always know how loved they are.

Acknowledgments

Cooperation is crucial to the dynamics of all living organisms; therefore, the completion of my PhD project would have not been possible without the support of many people.

First, I would like to express my sincere gratitude to my supervisor and mentor, Dr. Krzysztof Szczyglowski, for giving me the opportunity to find my true passion through his guidance. I am foremost grateful for his endless support, trust and encouragement throughout my PhD program. I am immensely thankful for the time he spent reading and polishing my manuscripts and thesis.

I would like to thank my co-supervisor Dr. Denis Maxell for his support and the final reading of my thesis. I would also like to acknowledge the members of my advisory committee members Dr. Susanne Kohalmi and Dr. Kathleen Hill for providing helpful advice and feedback during my PhD studies. I especially wish to extend thanks to Dr. Kohalmi for her ongoing mentorship, advice and encouragement. I would also like to thank Dr. Danielle Way for careful reading of my thesis and her insightful comments.

A special thanks to Loretta Ross and Terry Huebert for their technical and intellectual assistance and for their never-ending friendship and patience. I am thankful to Alex Molnar for his assistance with the preparation of figures and posters. I would also like to extend my thanks to all the past and present Szczyglowski lab members, and colleagues and friends from Agriculture and Agri-Food Canada. Thanks for the companionship which made my time at work more enjoyable. A special thank goes to Farshid Manafi and Daryoush Karimi for helping me to stay sane along the way!

I would like to acknowledge the Department of Biology at University of Western Ontario and the private award donors who generously provided financial support throughout my graduate studies. Their support was encouraging and allowed me to focus on my project during my degree.

Lastly, I would like to thank my friends and family for supporting me throughout this research. In particular, I would like to thank Reza Saberianfar for his help, support, and encouragement during the most challenging parts of this degree.

Table of Contents

List of Tables

List of Figures

List of Appendices

List of Abbreviations

aa	amino acid
ACC	1-aminocyclopropane-1-carboxylic acid
ACO	ACC oxidase
ACS	ACC synthase
AM	arbuscular mycorrhiza
AMF	arbuscular mycorrhiza fungi
AMS	arbuscular mycorrhiza symbiosis
AVG	aminoethoxyvinylglycine
BA	6-benzylaminopurine
bp	base pairs
BTB	Broad complex/tramtrack/bric-a-brac
ca.	circa
CC	coiled-coil
CDPK	calcium-dependent protein kinase
CHASE	cyclases/histidine kinases associated sensory extracellular
CI	confidence interval
Cis-Z	cis-Zeatin
cITs	cortical infection threads
CSG	common symbiosis genes
Da	dalton
DAI	days after rhizobial inoculation
eITs	epidermal infection threads
EMS	ethyl methane sulfonate
EOL1	ETO1-like

ETO1	ethylene over producer1
Gal	Glucose
HK	histidine kinase
HPTs	histidine phosphor-transfer protein
ITs	infection thread
LORE1	*L. japonicus* retrotransposon 1
MAPK	mitogen-activated protein kinase
myc	mycorrhizal
NAA	1-naphthaleneacetic acid
NF	nodulation or nod factors
NFS	nitrogen-fixing symbiosis
NP	nodule primordia
ORF	open reading frame
RACE	Rapid amplification of cDNA ends
RNS	root nodule symbiosis
RRs	response regulator
SAM	S-adenosylemethionine
SAMS	SAM synthetase
SE	standard errors
SYM	symbiotic signaling
TCS	two component-output sensor
Tg	teragrams
TILLING	targeted induced localized lesions in genomes
TOE	target of ETO1
TPR	tetratrico petide repeat

Trans-Z	trans-Zeatin

Chapter 1

1 General introduction

1.1 Access to a usable form of nitrogen changed the world

The world we live in today has been dramatically shaped by a single discovery made in 1908, when a German chemist named Fritz Haber filed a patent on the "synthesis of ammonia from its elements", which included dinitrogen (Haber, 2002). Dinitrogen, though extremely abundant in the Earth's atmosphere, represents a chemically and biologically inert form, due to the triple bond connecting the two nitrogen atoms. Consequently, dinitrogen is unusable for most organisms. Haber's discovery was later industrialized by Carl Bosch. Haber and Bosch were awarded Nobel prizes in 1918 and 1931, respectively. Today, this technique is known as the Haber-Bosch process, whereby atmospheric dinitrogen is reduced in the presence of hydrogen and iron at high pressure and high temperature to ammonia, the most usable form of nitrogen (Townsend and Howarth, 2010).

The short- and long-term effects that have resulted from the Haber-Bosch discovery cannot be overestimated and may never be fully calculated. Throughout the 20th century, this chemical process was used to produce large quantities of nitrogen-based explosives that were used in weapons, resulting in the death of 100 - 150 million people in armed conflicts (Erisman et al., 2008). On the other hand, billons of people have been fed by an abundance of food made possible by nitrogen fertilizers manufactured through the Haber-Bosch process (Smil, 2002; Smil, 2004; Erisman et al., 2008) (Figure 1.1) The dichotomous influences that have resulted from this process recap, to some extent, the controversial origin of the Nobel Prize itself.

Synthetic fertilizers were pillars of the so-called "Green Revolution" of the mid-to late 20th century (Flavell, 2016). Pioneered by the work of a Nobel Laurate, Norman Borlaug, a set of advances and practices dramatically revolutionized the field of agriculture. During this period, the combined use of high-yielding cereal varieties and improved technologies and irrigation systems, in association with chemical fertilizers and agrochemicals significantly increased global agricultural productivity in many regions of the world (Evenson and Gollin, 2003). Nitrogen is one of the most growth-limiting factors in plants. Consequently, it has been estimated that between 1908 and 2008 the number of people supported per hectare of arable land has increased from 1.8 to 4.4

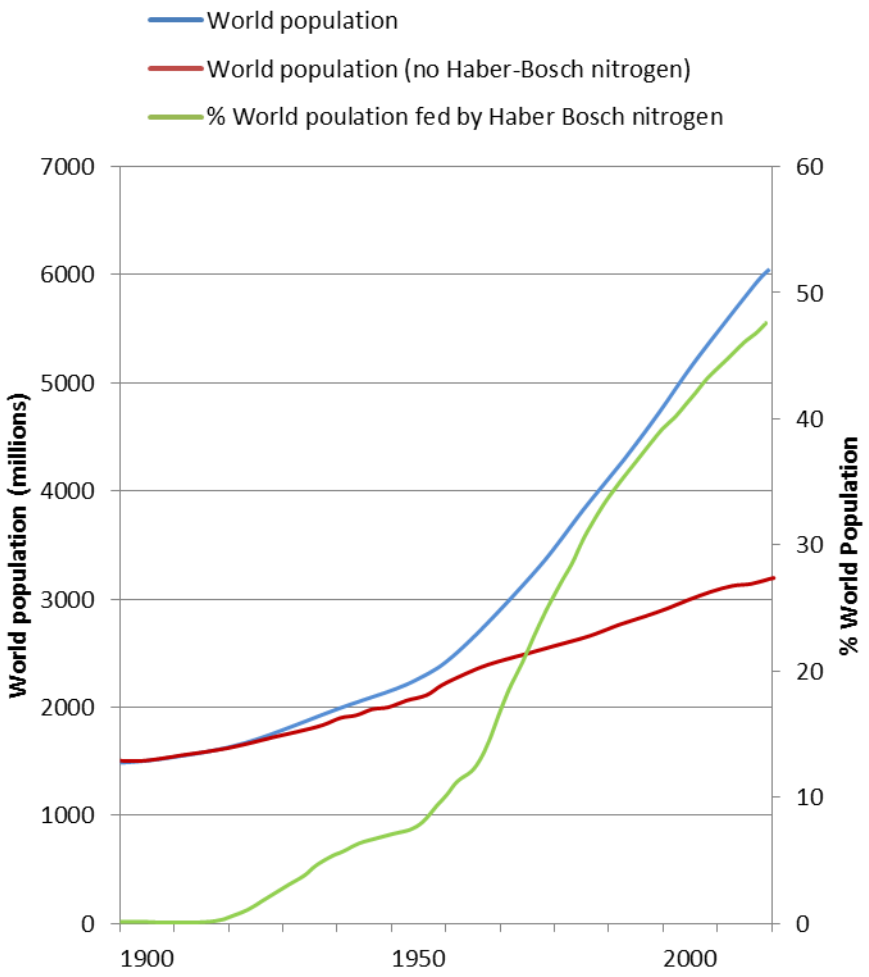

Figure 1.1 Trends in human population throughout the twentieth century.

Of the total world population (blue line), an estimate is made of the number of people that would have survived without reactive nitrogen from the Haber-Bosch process (red line), also shown as a percentage of the global population (green line). Figure modified from Erisman et al. (2008).

persons, mostly due to the nitrogen provided through the Haber-Bosch process (Erisman et al., 2008). Although it is hard to quantify the precise number of people whose lives depend on the fertilizer inputs, the updated estimate is that the existence of approximately 48% of the current human population was made possible by the availability of synthetic nitrogen fertilizers (Erisman et al., 2008) (Figure 1.1).

Approximately 80% of the reduced nitrogen manufactured through the Haber-Bosch process, is consumed in the production of fertilizers (Galloway et al., 2003; Galloway et al., 2004). To meet the rapid expansion in the global population, from 3.5 billion to over 7 billion people in the last 40 years, the amount of synthetic nitrogen fertilizer applied to crops worldwide has increased from 12 to almost 100 teragrams (Tg) per year (Mulvaney et al., 2009). Such intensive use of the nitrogen fertilizers, however, is not sustainable. It has been estimated that for wheat, rice, and maize typically around 66% of the applied nitrogen is lost to the environment (Raun and Johnson, 1999). In 2005, it was estimated that only approximately 17% of the nitrogen from the Haber-Bosch process was consumed by humans in crop, dairy, and meat products (Braun, 2007). A recent study suggested that 40% of the unused nitrogen was denitrified back to dinitrogen, which constitutes a massive waste of energy (Galloway et al., 2004). The rest of the excess nitrogen, however, by escaping into environmental reservoirs, has been of great concern (Townsend and Howarth, 2010). For instance, emissions of greenhouse gases such as nitric oxide (NO) and nitrous oxide (N_2O) to the atmosphere have increased about five-fold since pre-industrialized time (Galloway et al., 2004). Soluble nitrates, on the other hand, can find their way into aquatic systems, especially nitrogen-limited environments, resulting in unintentional nutrient-enrichment and hence, stimulating harmful algal blooms and creating coastal dead zones (Gruber and Galloway, 2008; Glendining et al., 2009). Nitrogen pollution has also been considered as one of the top three threats to biodiversity around the globe (Rockström et al., 2009; Townsend and Howarth, 2010). Furthermore, according to the National Institute of Health, the elevated nitrate concentrations in drinking water may contribute to a variety of health issues including several cancers and increased risk for Alzheimer's disease and diabetes (Townsend and Howarth, 2010). Although the value for Canada is not known, a report published in 2013 by the European Commission estimated the total annual cost to the European Union of

environmental impacts caused by nitrogen pollution to be between €70 billion and €320 billion. This raises the possibility that the costs of fertilization might outweigh the benefits (http://ec.europa.eu/environment/integration/research/newsalert/pdf/IR6_en.pdf).

In addition to the environmental and health concerns, the production of nitrogen fertilizers is expensive. The Haber-Bosch process consumes approximately 50% of the agricultural fossil fuel budget and is projected to reach 2% of global energy consumption by 2050 (Glendining et al., 2009). Figure 1.2 shows that nitrogen consumption is unbalanced across the planet. While farmers in developed countries of the West, and also in China and India, are heavy users of fertilizers, small holder farmers, for instance in sub-Saharan Africa, cannot afford fertilizers (Mueller et al., 2012). While the global average fertilizer application rate for maize is 134 kg ha^{-1}, in sub-Saharan Africa this rate is only around 3-5 kg ha^{-1} (Foley et al., 2011; Folberth et al., 2013).

Today, even with intensive agriculture, nearly a billion people suffer from chronic malnutrition across the globe. In sub-Saharan Africa in particular, more than 250 million people go hungry (Foley et al., 2011; Rogers and Oldroyd, 2014). By the middle of this century, it is predicted that the Earth will be home to more than nine billion people. Agriculture already faces tremendous pressure to meet the world's need with more food, fiber, and fuels. Nonetheless, population growth and increasing consumption of calorie- and meat-intensive diets are expected to roughly double human food demand by 2050 (Tilman et al., 2011). In the coming decades, a crucial challenge for humanity will be meeting food demands without substantial economic and environmental costs. Scientists have called for a second "Green Revolution" with emphasis on crops that can use nutrients such as nitrogen more efficiently (Zeigler and Mohanty, 2010; Flavell, 2016).

1.2 Legumes to the rescue for sustainable growth

Legumes have been grown for 5000 years in the eastern Mediterranean and Mesopotamian regions. Since ancient times, farmers have known that legumes such as peas, lentils, and clover are important for soil fertility. Practices such as green manuring, crop rotation, and intercropping have been known for millennia. Today, the legume family is the second most important plant family in terms of global economy (Graham and

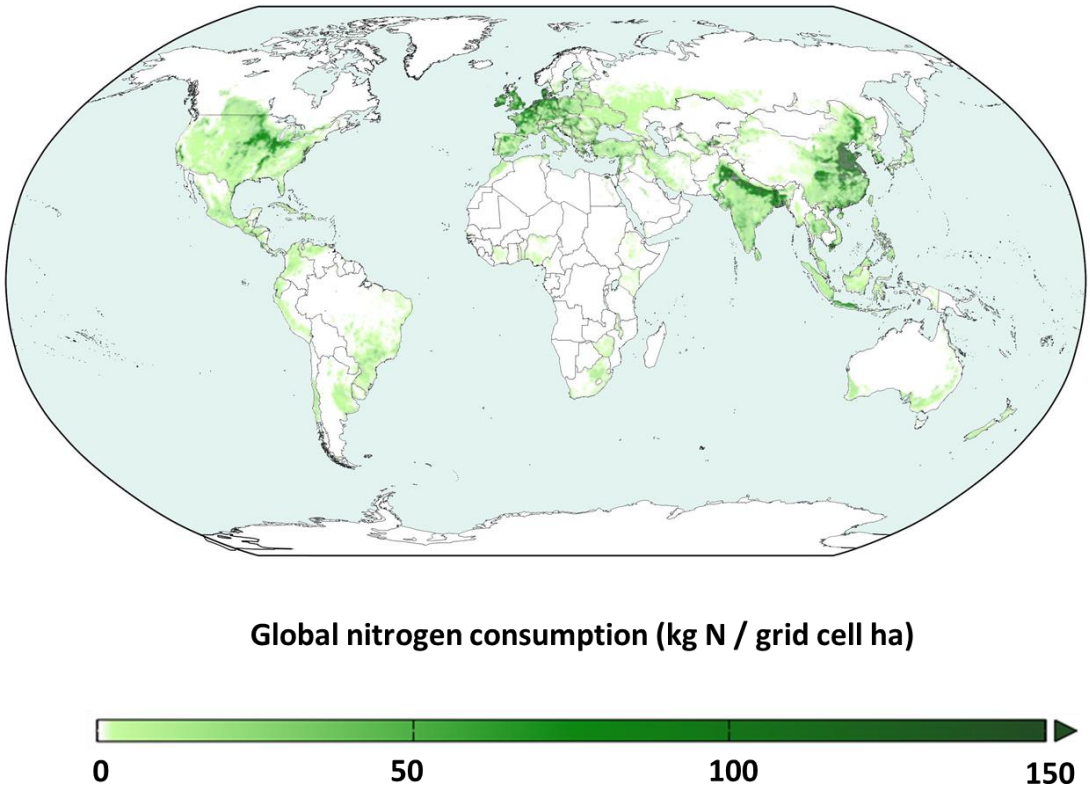

Figure 1.2 Usage of nitrogen fertilization varies widely across the world's crop land.

Figure modified from Mueller et al. (2012).

Vance, 2003). Legumes are important sources of protein, oils, vitamins, minerals, and fiber all around the world. Many species within this family are also valued for food and feed consumption as well as being used in dye and timber production, and as ornamentals (Graham and Vance, 2003; Szczyglowski and Stougaard, 2008). Importantly, legumes are also excellent natural, green fertilizers (Szczyglowski and Stougaard, 2008). In 1888, German scientists Hermann Hellriegel and Hermann Wilfarth discovered that legumes use atmospheric nitrogen for their growth. Although, they did not know the mechanism, they correctly concluded that legumes performed the trick in the "bumps" on their roots where bacteria convert atmospheric nitrogen to ammonia. Since that discovery, the nitrogen-fixing symbiosis (NFS) has been of great scientific interest.

Nitrogen-fixing symbioses, including plant-cyanobacteria symbiosis and root nodule symbiosis (RNS), have evolved independently at least ten times in land plants (Delaux et al., 2015a). RNS is restricted to several, but not all, species belonging to four orders of flowering plants in the Rosid I clade, namely, Fabales, Cucurbitales, Fagales, and Rosales (Sprent, 2007). The vast majority of these plants belong to a single Leguminosae family (Fabaceae) in the Fabales order (Doyle, 2011).

Legumes have evolved the ability to form endosymbiotic relationships with nitrogen-fixing soil bacteria, commonly known as rhizobia (Sprent, 2007; Werner et al., 2014). As a result of this association, the leguminous plants develop a novel root derived organ, called the root nodule (Oldroyd and Downie, 2008). Nodules host nitrogen-fixing rhizobial bacteria intracellularly, providing an environment conducive for the bacterially-encoded nitrogenase to carry out the reduction of dinitrogen to ammonia (Doyle, 2011). This association provides plants, on average, with fixed nitrogen that is estimated to be equivalent to approximately 120 Kg/ha^{-1} (Salvagiotti et al., 2008), thus allowing legumes to thrive in nitrogen-limited conditions.

1.3 Nutrient acquisition through root endosymbioses

Cooperation is essential to the biology of plants. The driving force behind the symbiotic associations between plants and their microorganism counterparts is the reciprocal need

for specific nutrients (Figure 1.3). The most elaborate form of beneficial interaction is the root nodule endosymbiotic relationship.

RNS is initiated by a molecular dialogue between legumes and rhizobia. In response to the flavonoids released by plants, their compatible microsymbionts synthesize lipochitooligosaccharides called Nodulation or Nod Factors (NF). In the model legumes *Lotus japonicus* and *Medicago truncatula* (Szczyglowski and Stougaard, 2008), as well as in other legumes such as soybeans, peas, and clover, perception of NFs by the host plant triggers a cellular signaling cascade which prepares the host plant for rhizobial accommodation (Madsen et al., 2010). In response to NF perception, two genetically-coordinated programs are initiated by the host plant; First the epidermal program initiates curling of the plant root hair to entrap rhizobia. Bacteria replicate inside the root hair and invagination of the plasma membrane results in the formation of infection threads (ITs) (Madsen et al., 2010). ITs are plant plasma membrane-derived conduits that extend inward from the tip of the root hair to direct rhizobia into the root cortex, the site of nodule initiation (Held et al., 2010). Second, concomitant to IT formation, the signaling cascade activates the cortical program, triggering cell divisions for initiation of nodule primordia (NP) formation. Nodules are specialized root organs that provide a suitable, oxygen-limited environment for the enzymatic function of the bacterial nitrogenase (Murray, 2011). Once ITs pass the epidermis, they ramify within the root cortex (Figure 1.4 A). Finally, the rhizobia are released from the ITs into the cortical cells, while remaining surrounded by a plant-derived membrane. In these organelle-like structures, called symbiosomes, rhizobia reduce atmospheric dinitrogen to ammonium (Suzaki et al., 2015). RNS constitutes a tremendous evolutionary innovation, which allows the host plant to access the atmospheric nitrogen at the expense of photosynthetic carbon which is supplied to the bacteria (Figure 1.3).

Evolved more than 450 million years ago, the symbiotic interaction between plants and members of the ancient phylum of fungi, Glomeromycota, is thought to be a vital contributor to the colonization of the terrestrial environment by plants (Kistner and Parniske, 2002; Parniske, 2008; Held et al., 2010; Delaux et al., 2015b). This arbuscular mycorrhizal symbiosis (AMS) provides water and nutrients, such as phosphate and

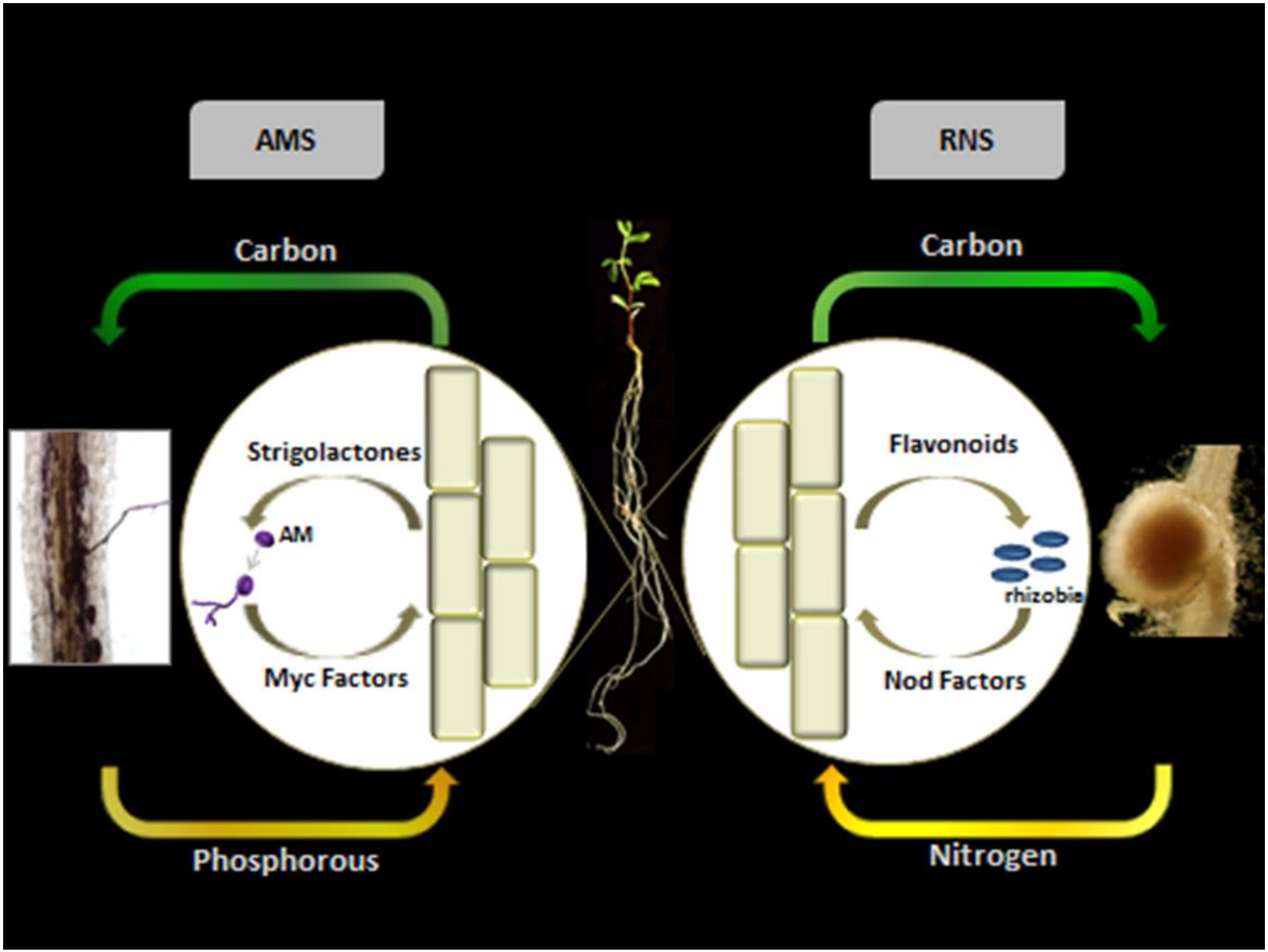
AMS
RNS
Carbon
Carbon
Strigolactones
AM
Myc Factors
Flavonoids
rhizobia
Nod Factors
Phosphorous
Nitrogen

Figure 1.3 Plants engage in intracellular symbioses with beneficial bacteria and fungi.

Rhizobia and arbuscular mycorrhizal fungi release Nod and Myc factors in response to plant flavonoid and strigolactone signals, respectively. This leads to establishment of root nodule (RNS) and arbuscular mycorrhiza (AMS) symbioses. Nodules and arbuscules are formed as a result of these associations, respectively. Photosynthetic carbon is provided to both bacterial and fungal partners in return for nitrogen and phosphorus, respectively. Figure by Mandana Miri.

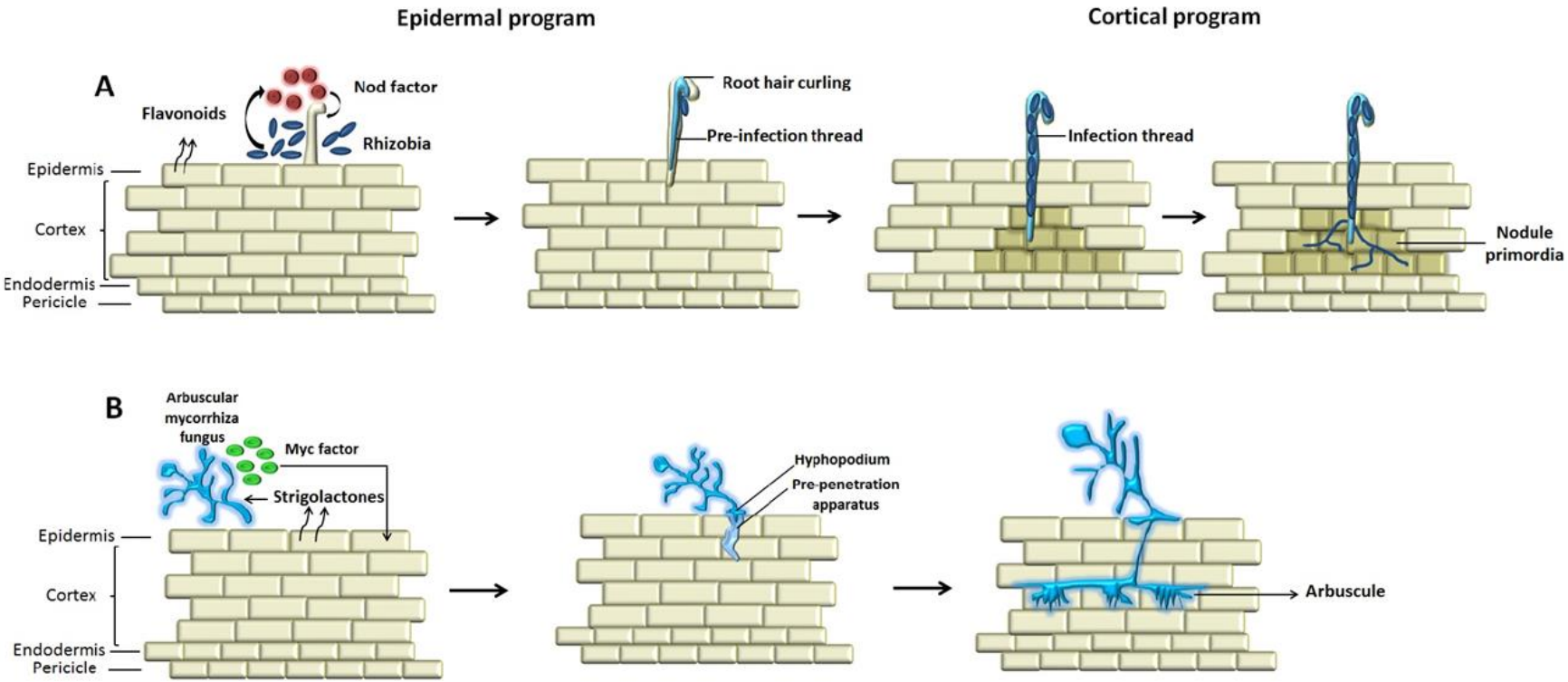
Epidermal program
Cortical program
A
Flavonoids
Nod factor
Rhizobia
Epidermis
Cortex
Endodermis
Pericicle
Root hair curling
Pre-infection thread
Infection thread
Nodule primordia
B
Arbuscular mycorrhiza fungus
Myc factor
Strigolactones
Epidermis
Cortex
Endodermis
Pericicle
Hyphopodium
Pre-penetration apparatus
Arbuscule

Figure 1.4 Rhizobial and mycorrhizal colonization.

(A) In response to flavonoids released by the plant root, rhizobia produce Nodulation factors (Nod factors) that are recognized by the plant. Rhizobia gain entry into the plant root through root hair cells. In response to Nod factors, the root hair curls around bacteria attached at the surface. Infection threads are invaginations of the plant cell that are initiated at the site of root hair curls and allow invasion of the rhizobia into the root tissue. Pre-infection threads (cytoplasmic bridges) are formed in the activated root cortex in advance, to guide the path of the infection thread growth. Nodule primordia are initiated in the subtending root cortex below the site of bacterial infection. The infection thread grows towards the nodule primordium, ramifies and releases rhizobia into the cells.

(B) Strigolactones released by the plant root promote spore germination and hyphal branching in arbuscular mycorrhizal fungi (AMF). AMF produce mycorrhizal factors (Myc factors) which activate the plant symbiosis signaling pathway. AMF form the hyphopodium, a penetration apparatus that allows fungal hyphae to grow into the root epidermal cell. The route of hyphal invasion in the root cortical region is predicted by a pre-penetration apparatus (similar to pre-infection threads describe dabove). The fungus colonizes the plant root cortex through intercellular hyphal growth. Arbuscules, highly branched hyphae, are formed in the inner root cortical cells from the intercellular hyphae.

Figure modified from Oldroyd (2013).

nitrogen, to the host plant. In return, it has been estimated that, approximately 20% of the plant photosynthesis-derived carbon is consumed by arbuscular mycorrhiza fungi (AMF) (Parniske, 2008) (Figure 1.3). AMS is probably the most widespread terrestrial symbiosis, formed by 70-90% of land plant species (Parniske, 2008). It has been hypothesized that species which are unable to interact with AMF, for instance, those in the Brassicaceae and Chenopodiaceae, have independently lost this ability (Delaux et al., 2013b).

Several molecular and genetic observations indicate that RNS, which is a relatively recent evolutionary innovation (around 60 million years ago), has evolved in part from a pre-existing pathway that regulates the more ancient AMS (Duc et al., 1989; Kistner et al., 2005; Markmann and Parniske, 2009; Delaux et al., 2015a). Similar to RNS, the host plant and the free-living organism communicate by chemical exchange during AMS (Parniske, 2008). Strigolactones released by the plant root are perceived by AMF in the rhizosphere, triggering spore germination and hyphal branching (Akiyama et al., 2005; Besserer et al., 2006). AMF produce mycorrhizal (Myc) factors (Maillet et al., 2011; Genre et al., 2013) which activate the symbiosis signaling pathway in the root. This association results in the formation of tree-shaped subcellular structures, called arbuscules, which similar to rhizobia, are accommodated by the host plant intracellularly. Nutrient exchange between the plant and fungal partners happens through these arbuscules (Figure 1.4 B) (Oldroyd, 2013).

1.4 The symbiosis signaling pathways in legumes

As mentioned above, molecular dialogue between the host plant and its compatible symbiotic partners leads to production of Myc and Nod factors by AMF and rhizobia, respectively. The perception of structurally-similar Myc or Nod factors (Maillet et al., 2011) activates an ancient signaling pathway called the common symbiotic signaling (SYM) pathway (Figure 1.5). Over the past two decades, thanks to various mutant analyses, tremendous advances have been made in our understanding of the genetic elements of the SYM pathway, especially in model legumes such as *L. japonicus* and *M. truncatula*.

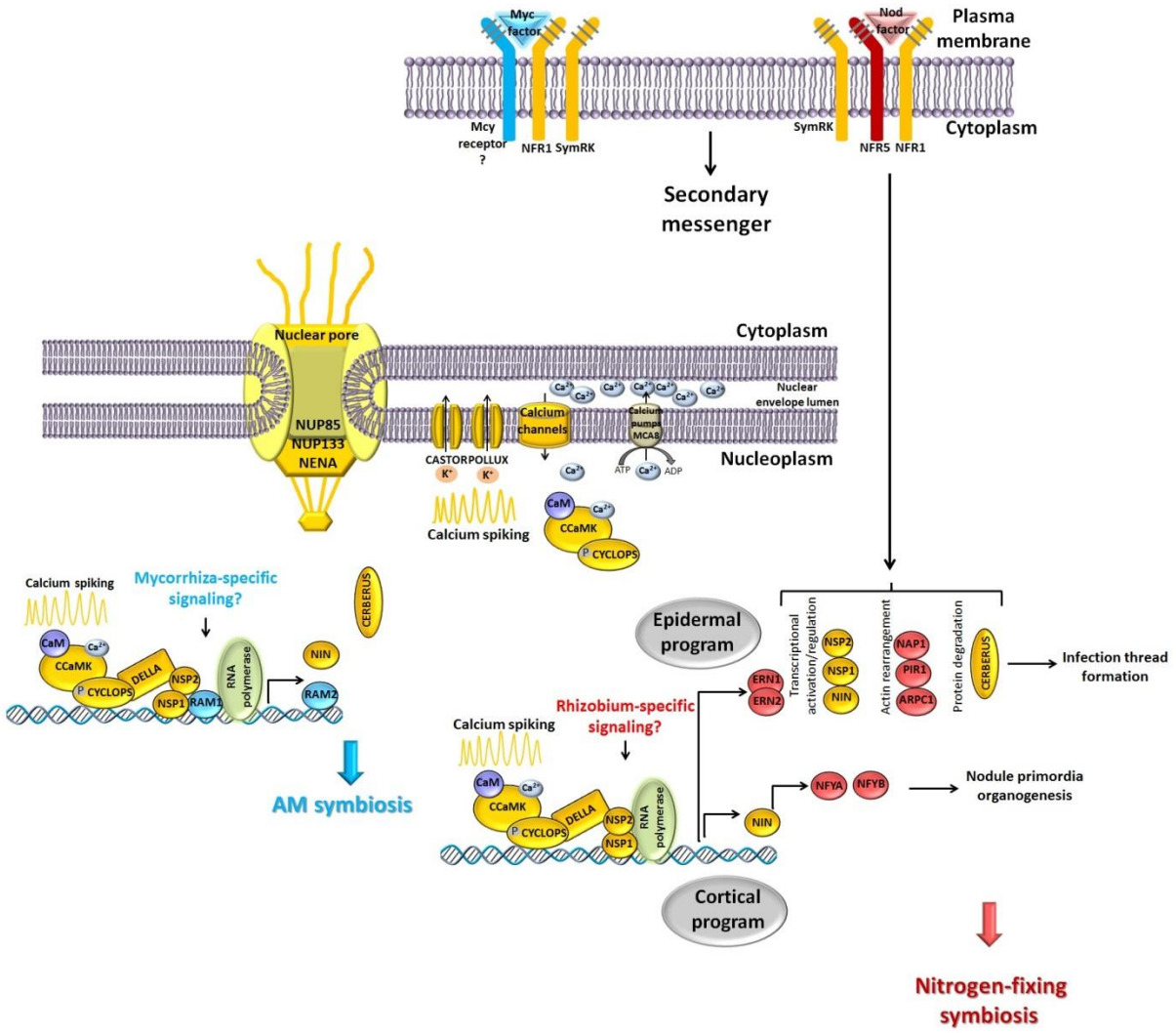
Myc factor
Nod factor
Plasma membrane
Mcy receptor ?
NFR1
SymRK
SymRK
NFR5
NFR1
Cytoplasm
Secondary messenger
Nuclear pore
NUP85
NUP133
NENA
Cytoplasm
Nuclear envelope lumen
Calcium channels
Calcium pump MCA8
CASTOR
POLLUX
ATP
ADP
Nucleoplasm
Calcium spiking
CaM
CCaMK
CYCLOPS
Calcium spiking
Mycorrhiza-specific signaling?
CERBERUS
CaM
CCaMK
DELLA
CYCLOPS
NSP2
NSP1
RAM1
RNA polymerase
NIN
RAM2
AM symbiosis
Epidermal program
Transcriptional activation/regulation
Actin rearrangement
Protein degradation
ERN1
ERN2
NSP2
NSP1
NIN
NAP1
PIR1
ARPC1
CERBERUS
Infection thread formation
Rhizobium-specific signaling?
Calcium spiking
CaM
CCaMK
DELLA
CYCLOPS
NSP2
NSP1
RNA polymerase
NIN
NFYA
NFYB
Nodule primordia organogenesis
Cortical program
Nitrogen-fixing symbiosis

Figure 1.5 Symbiotic signaling pathway.

In *L. japonicus*, Nod factor is recognized by the Nod factor receptors NFR1 and NFR5, embedded in the plasma membrane. This perception leads to the activation of SymRK, which is proposed to associate with as-yet-unknown mycorrhizal factor (Myc factor) receptors. Activation of these receptor complexes leads to the formation of a secondary messenger which initiates calcium spiking, driven by proteins in the nuclear envelope. Calcium spiking is dependent on three nuclear pore proteins, NENA, NUP85, and NUP133, the cation channels CASTOR and POLLUX, as well as the calcium pump MCA8 and calcium channels. Calcium spiking is perceived by the binding of calcium and calmodulin (CaM) to CCaMK. The activation of CCaMK results in the phosphorylation of CYCLOPS. Recently discovered DELLA proteins bridge the CCaMK/CYCLOPS complex to factors Nodulation Signaling Pathway 2 (NSP2). In the nitrogen-fixing symbiosis pathway, the transcription 1 (NSP1) and NSP2 are required and associate with the promoters of several plant genes that regulate RNS, such as *NIN*, *ERN1*, and *ERN2*. For mycorrhizal signaling, the same signaling complex is required, but NSP1 is replaced with Required for Arbuscular Mycorrhization 1 (RAM1) to drive expression of mycorrhiza-specific genes, such as *RAM2*. Independent of Common Signaling Genes (CSG), the NIN, NSP1, and NSP2 transcriptional regulators, are also required for infection thread (IT) formation. Additionally, the formation, maintenance, and progression of ITs require *NAP1*, *PIR1*, and *ARPC1* genes that encode proteins of the SCAR/WAVE/ARPC1/2 complex which activates actin rearrangement. CERBERUS, an E3 ubiquitin ligase has been recently shown to be essential for both symbiotic fungal and rhizobial infection. Components with dual function in nodulation and mycorrhizal signaling are shown in yellow. Nitrogen fixation-specific components are shown in red, while mycorrhizal signaling-specific components are shown in blue. Figure Mandana Miri.

NFs are perceived by a LysM-receptor kinase, located at the plasma membrane (Madsen et al., 2003). In *L. japonicus*, NFs produced by the compatible rhizobia, *Mesorhizobium loti*, are perceived by Nod Factor Receptor 1 (NFR1) and NFR5 which function in a non-redundant manner (Radutoiu et al., 2003; Broghammer et al., 2012). Lipochito-oligosaccharides produced by AMF (Maillet et al., 2011) are also perceived by LysM receptor-like kinases and recently it has been shown that NFR1 but not NFR5 is necessary for the recognition of AMF and the activation of the symbiosis signaling pathway (Zhang et al., 2015). There are at least 15 genes with dual function in both RNS and AMS, which are thus named the Common Symbiosis Genes (CSG) (Figure 1.5).

Nod/Myc factor perception induces a signal transduction pathway that activates the leucine rich-repeat, plasma membrane-bound Symbiosis Receptor Kinase (SymRK) (Endre et al., 2002; Stracke et al., 2002; Kosuta et al., 2011). Activation of this receptor complex leads to secondary signals that initiate perinuclear calcium oscillation, called calcium spiking, which constitutes the main outcome of the common SYM pathway (Wais et al., 2000; Walker and Downie, 2000). Three components of the nuclear pore, named NUP85, NUP133, and NENA (Kanamori et al., 2006; Saito et al., 2007; Groth et al., 2010), and two cation channels, CASTOR and POLLUX (Imaizumi-Anraku et al., 2005), are known to be essential for calcium spiking in the nucleus. Very recently, nuclear-localized calcium channels called cyclic nucleotide-gated channels (CNGCs) were shown to interact with POLLUX (MtDMI1) and to be required for nuclear calcium oscillations and subsequently the common SYM pathway in *M. truncatula* (Charpentier et al., 2016). Downstream from the calcium spiking, changes in calcium concentration are perceived by Calcium and Calmodulin-dependent receptor Kinase (CCaMK) (Lévy et al., 2004; Mitra et al., 2004; Tirichine et al., 2006). CCaMK associates with and subsequently phosphorylates CYCLOPS (Yano et al., 2008). It has been recently shown that in *M. truncatula*, DELLA proteins promote the formation of the CCaMK/CYCLOPS complex (Jin et al., 2016) and like CCaMK and CYCLOPS, are components of common symbiosis pathway (Yu et al., 2014; Jin et al., 2016). Whether DELLA proteins have similar function in *L. japonicus* has yet to be determined.

The CCaMK/CYCLOPS complex activates the symbiotic-specific effectors. Several nuclear-associated transcriptional regulators including two GRAS family proteins, Nodulation Signaling Pathway1 (NSP1) and NSP2, and Nodule INception (NIN) are required for IT formation as well as nodule organogenesis (Schauser et al., 1999; Kaló et al., 2005; Smit et al., 2005; Heckmann et al., 2006). NSP1 and NSP2 form a hetero-complex that associates with the promoter of Nod factor-inducible genes, such as ENOD11 and ERN1 (Hirsch et al., 2009). Interestingly, it has been recently shown that NSP1, NSP2, and NIN which were originally thought to be nodulation-specific, are also required for AMS (Liu et al., 2011; Maillet et al., 2011; Delaux et al., 2013a; Nagae et al., 2014; Guillotin et al., 2016).

Identification of several plant mutants has revealed that the epidermal and cortical programs for IT and nodule formation, respectively, can be uncoupled (Kosuta et al., 2011). In fact, there are several genes which are required specifically for bacterial entry inside the host root (Held et al., 2010). For instance, components associated with modification of plant cell cytoskeleton, including NAP1, PIR1, and ARPC1, have been shown to be required for the bacterial entry but not for AMS (Yokota et al., 2009; Miyahara et al., 2010; Hossain et al., 2012). This highlights a clear distinction between the two symbiotic mechanisms (Held et al., 2010).

1.5 Ubiquitous hormones function uniquely in nitrogen-fixing symbiosis

Several plant hormones have been reported to positively or negatively regulate RNS. These hormones might function at different stages during nodulation. Like any other plant developmental process, nodulation is modulated by interactions among multiple hormones.

Since their discovery in the 1950s, cytokinins have been shown to be involved in many plant growth and developmental processes throughout a plant's life, including seed development and germination, stem cell control in root and shoot, vascular differentiation, chloroplast development, root and shoot growth and branching, leaf

senescence, stress tolerance, interactions with pathogens, circadian rhythms and nodulation (Hwang et al., 2012).

Cytokinins act as important positive regulators of nodule organogenesis in roots. Early evidence dates back to 1994 when Cooper and Long demonstrated that cytokinins can partially mimic some of the morphological effects of NF (Cooper and Long, 1994). They showed that engineering the cytokinin trans-zeatin secreting system into a Nod^- (unable to produce NF) strain of *Sinorhizobium meliloti* led to formation of un-colonized nodule-like structures on *Medicago sativa* roots (Cooper and Long, 1994). Indeed, it has been shown that exogenous cytokinins trigger cortical cell divisions and formation of nodule-like structures on roots of several legumes in a manner similar to rhizobia and NF (Bauer et al., 1996; Fang and Hirsch, 1998; Mathesius et al., 2000; Heckmann et al., 2011).

Several genetic studies have highlighted the importance of cytokinin perception in nodule formation, including loss-of-function mutations or reduced histidine kinase cytokinin receptor gene expression in *LjLhk1* and *MtCre1* which result in defective nodulation in *L japonicus* and *M. truncatula*, respectively (Gonzalez-Rizzo et al., 2006; Murray et al., 2007; Plet et al., 2011). Furthermore, the *Spontaneous nodule formation 2* (*snf2)* gain-of-function mutation in the *L. japonicus* Histidine Kinase 1 (LHK1) cytokinin receptor confers hypersensitivity to cytokinin and is sufficient to induce cell division and nodule primordia formation in the absence of rhizobia (Tirichine et al., 2007).

Cytokinin perception and signaling is mediated by a multistep His-to-Asp phosphorelay pathway similar to the bacterial two-component system (Figure 1.6) (To and Kieber, 2008; Hwang et al., 2012; Spichal, 2012; Keshishian and Rashotte, 2015). Perception of cytokinins by hybrid histidine kinase cytokinin receptors triggers kinase activity. The cytokinin receptors auto-phosphorylate and transfer the signal via phosphorelay to histidine phosphor-transfer proteins (HPTs), which in turn, transfer the signal to a set of response regulators (RRs), proteins localized in the nucleus. Based on their sequence similarities, domain structure and transcriptional response to cytokinin, RRs are classified into two distinct subtypes: type-A and type-B. The type-A RRs are comprised of a receiver domain

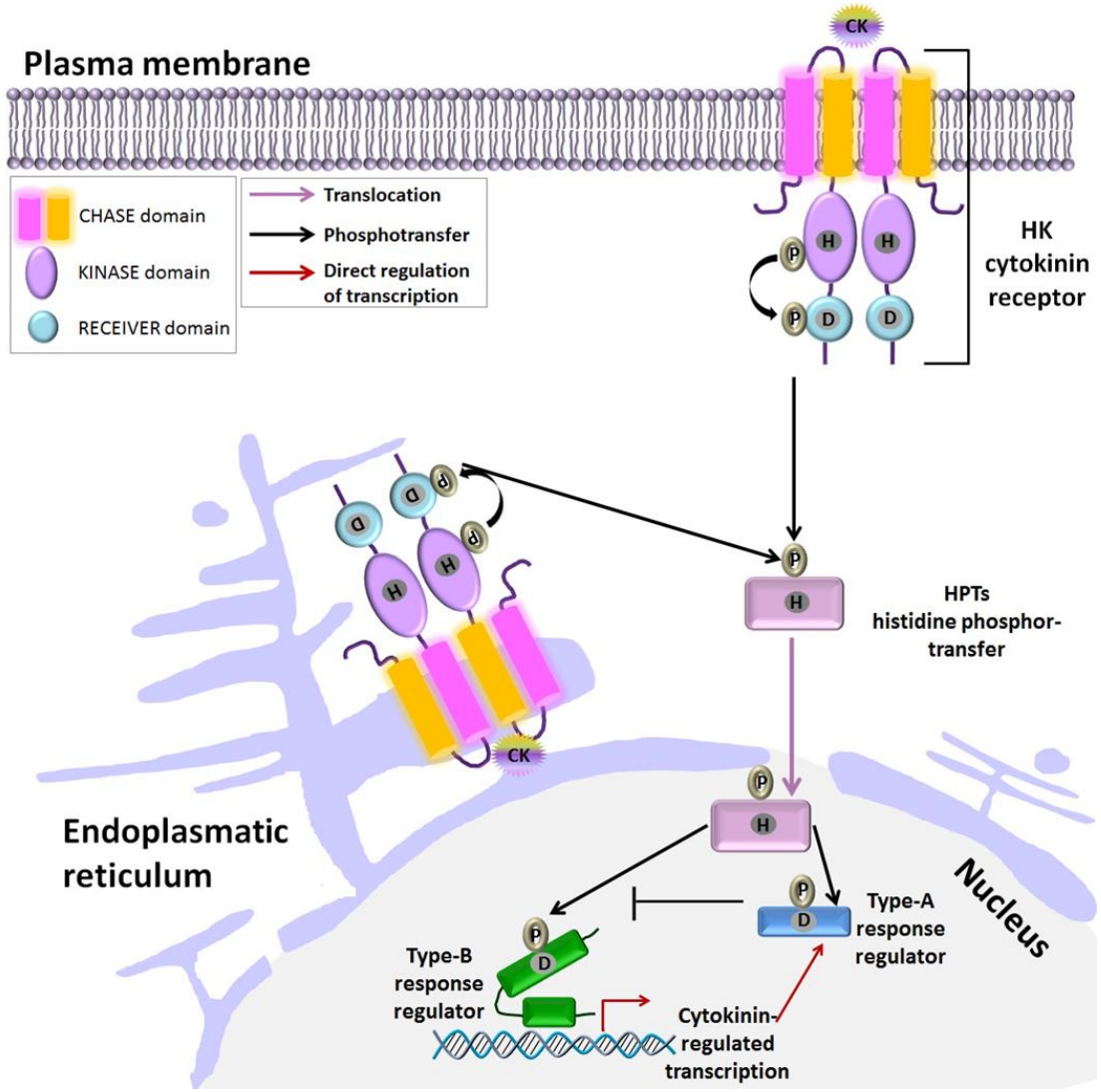
Plasma membrane
CK
CHASE domain
KINASE domain
RECEIVER domain
Translocation
Phosphotransfer
Direct regulation of transcription
HK cytokinin receptor
H
D
P
HPTs histidine phosphor-transfer
Endoplasmatic reticulum
Nucleus
Type-A response regulator
Type-B response regulator
Cytokinin-regulated transcription

Figure 1.6 Cytokinin signal transduction pathway.

In the cytokinin signal transduction pathway, hybrid histidine protein kinases (HKs), which are located at the plasma membrane and endoplasmatic reticulum, serve as cytokinin receptors. Histidine phosphotransfer proteins (HPTs) then transmit the signal from HKs to nuclear response regulators (RRs), which can either activate (type-B) or repress (type-A) transcription. Type-B RRs act directly to modulate gene expression of the effectors. There are four major steps in cytokinin signaling; HK sensing and signaling, HPT nuclear translocation, RR transcription activation, and a negative feedback loop through cytokinin-inducible RR gene products. Upon perception of cytokinin by the cyclases/histidine kinases associated sensory extracellular (CHASE) domain, HKs autophosphorylate on a conserved histidine (H) residue within the catalytic kinase domain. The phosphoryl group is then transferred to a conserved aspartic acid (D) residue in the C-terminal receiver domain. The phosphate group is through HPTs to RRs located within the nucleus. Figure by Mandana Miri.

and a short carboxyl terminus and their transcription is rapidly elevated in response to exogenous cytokinin; these are considered to be primary response genes and negative-feedback regulators. Type-B RRs, in addition to the receiver domain, have a carboxyl-terminal output domain that includes both a DNA-binding domain and a transcriptional activation domain. Type-B RRs are post-transcriptionally regulated by cytokinin. Activated type-B RRs mediate the majority of the transcriptional responses to cytokinin including the regulation of the type-A RRs. The activated type-A RRs act as repressors that mediate a negative feedback loop (To and Kieber, 2008; Hwang et al., 2012; Spichal, 2012; Keshishian and Rashotte, 2015).

The available data strongly suggest that recruitment of the cytokinin signaling pathway has been essential during the evolution of nitrogen-fixing RNS (Frugier et al., 2008). Downstream of cytokinin perception, RRs are activated during nodulation (Lohar et al., 2004; Breakspear et al., 2014). Localization of the GUS-fused *Arabidopsis* response regulator 5 (ARR5) in transgenic *L. japonicus* roots revealed a rapid cytokinin response after rhizobial inoculation in dividing cortical cells at different stages of nodule formation (Lohar et al., 2004). Similarly, using the endogenous *MtRR4* primary cytokinin response gene, Plet *et al.* showed activation of the cytokinin signaling pathway during nodulation in dividing cortical cells (Plet et al., 2011). In *M. truncatula* it has been shown that the expression of both *MtRR4* (type-A) and *MtRR1* (type-B) are induced in response to rhizobial infection and that upregulation depends on several components of the SYM pathway (Gonzalez-Rizzo et al., 2006; Ariel et al., 2012). Two additional type-A cytokinin RRs, namely *MtRR9* and *MtRR11* are induced by NF treatment in *M. truncatula* (Op den Camp et al., 2011). Furthermore, constitutive expression of *MtRR9* triggered the development of nodule primordia-like structures in *M. truncatula* and *L. japonicus* (Op den Camp et al., 2011). These findings collectively indicate that cytokinin signaling is essential, and also sufficient, for nodule organogenesis in roots.

The plant hormone ethylene, on the other contrary, is known as a negative regulator of both rhizobial infection and nodule formation. Exogenous ethylene or its precursor, 1-aminocyclopropane-1-carboxylic acid (ACC), reduces nodule formation (Grobbelaar et

al., 1971; Goodlass and Smith, 1979; Lee and LaRue, 1992; Penmetsa and Cook, 1997; Nukui et al., 2000; Lohar et al., 2009). Conversely, inhibitors of ethylene biosynthesis or perception, such as aminoethoxyvinylglycine (AVG) and silver ions, respectively, were shown to increase nodule number in several leguminous species, including *M. sativa*, *Pisum sativum*, and *L. japonicus* (Fearn and Larue, 1991; Guinel and LaRue, 1992; Penmetsa and Cook, 1997; Caba et al., 1998; Nukui et al., 2000; Oldroyd et al., 2001).

Ethylene is perceived by a family of membrane-bound receptors which act as negative regulators of the ethylene signaling pathway (Ju and Chang, 2012). These ethylene receptors control the activity of the Ethylene INsensitive2 (EIN2) protein, which is a positive regulator and one of the central components of the ethylene signaling transduction pathway (Lin et al., 2009; Ju and Chang, 2012). A pioneering study in *M. truncatula* showed that the *Mtein2* mutant, named *sickle*, is ethylene insensitive and is hyperinfected by *S. meliloti*, its nitrogen-fixing micro-symbiont (Penmetsa and Cook, 1997). In contrast to *M. truncatula*, plants that form determinate nodules, such as *L. japonicus*, soybeans and common beans, contain two copies of the *EIN2* gene (Miyata et al., 2013; Weller et al., 2015). In *L. japonicus*, simultaneous suppression of both *LjEIN2-1* and *LjEIN2-2* through an RNAi approach, leads to higher ethylene insensitivity and an increased number of nodules (Miyata et al., 2013). Similarly, overexpression of dominant negative forms of melon (Cm-ERS1/H70A) or *Arabidopsis* (*etr1-1*) ethylene receptors in *L. japonicus* leads to ethylene insensitivity, resulting in enhanced *M. loti* infection and increased nodule number (Nukui et al., 2004; Lohar et al., 2009). These results confirm the important role of ethylene and ethylene signaling in the regulation of nitrogen-fixing symbiosis regardless of the type of nodules (determinate or indeterminate) formed. This is also consistent with the observation made 20 years ago in *P. sativum*, that ethylene has a role in providing the positional information for nodule primordia to be formed across the root proto-xylem poles (Heidstra et al., 1997). Collectively, these observations demonstrate the importance of ethylene in the regulation of rhizobial infection and nodule formation in legumes.

1.6 Research goals and objectives

Inspired by the mutually beneficial relationships between legumes and rhizobia, multiple novel biotechnological approaches are being exploited toward the ultimate goal of developing nitrogen-fixing cereal crops (Beatty and Good, 2011; Oldroyd and Dixon, 2014; Rogers and Oldroyd, 2014). Should this prove successful, the nitrogen-fixing cereal will have tremendous potential towards food sovereignty without further undermining the integrity of the Earth's environmental systems. **Therefore, the overall objective of this thesis has been to obtain further knowledge and understanding of RNS, with the prospect of extending this useful process to non-legume crops.**

Although cytokinin is clearly one of the key endogenous signals during RNS, many questions remain unanswered. Comprehensive understanding of cytokinin signaling and its downstream effects during symbiosis is being considered here as an essential step in the rational consideration of extending RNS to non-legume crops. In the model legume *L. japonicus*, analysis of the *Lhk1* cytokinin receptor gene showed that LHK1 is required and also sufficient for the initiation of nodule organogenesis in a timely manner (Murray et al., 2007; Tirichine et al., 2007). Nonetheless, mutant plants carrying the loss-of-function *lhk1-1* allele still form a limited number of nodules while being hyper-infected by their symbiotic partner (Murray et al., 2007). To account for these observations, I followed a central hypothesis that other cytokinin receptors function in a partially redundant manner with LHK1 to mediate nodule formation. Furthermore, as *lhk-1* mutants show an aberrant rhizobial infection phenotype, this raises the possibility that cytokinin promotes not only nodule formation but also participates in the regulation of rhizobial infection. As such, the role of cytokinin during rhizobial entry into the root was also explored by my thesis research. Here, I have followed the hypothesis that the ethylene level was altered in the *lhk1-1* cytokinin receptor mutant, leading to excessive infection rates. Given the unique phenotype of the *lhk1-1* mutant, (hyperinfection in the initial absence of nodule formation (Murray et al., 2007)), understanding the underlying mechanisms could potentially bridge the gap between rhizobial infection in the epidermis and nodule organogenesis in the cortex. Given the above, the specific, detailed objectives of my thesis work were as follows:

1) To further assess the redundant role of cytokinin receptors during nodule primordia formation in the model legume *L. japonicus*.
2) To analyze the response of cytokinin receptors to cytokinin and rhizobial infection.
3) To assess the role of bacterial entry into roots in generating signaling for nodule primordia formation.
4) To evaluate whether a non-legume, *Arabidopsis* cytokinin receptor can functionally replace LHK1 during nodulation.
5) To investigate how cytokinin might regulate rhizobial infection.
6) To study whether cytokinin-ethylene crosstalk is involved in limiting rhizobial infection.

1.7 References

Akiyama, K., Matsuzaki, K.I., and Hayashi, H. (2005). Plant sesquiterpenes induce hyphal branching in arbuscular mycorrhizal fungi. Nature **435:** 824-827.

Ariel, F., Brault-Hernandez, M., Laffont, C., Huault, E., Brault, M., Plet, J., Moison, M., Blanchet, S., Ichanté, J.L., Chabaud, M., Carrere, S., Crespi, M., Chan, R.L., and Frugiera, F. (2012). Two direct targets of cytokinin signaling regulate symbiotic nodulation in *Medicago truncatula*. Plant Cell **24:** 3838-3852.

Bauer, P., Ratet, P., Crespi, M.D., Schultze, M., and Kondorosi, A. (1996). Nod factors and cytokinins induce similar cortical cell division, amyloplast deposition and *MsEnoD12A* expression patterns in alfalfa roots. Plant J. **10:** 91-105.

Beatty, P.H., and Good, A.G. (2011). Future prospects for cereals that fix nitrogen. Science **333:** 416-417.

Besserer, A., Puech-Pagès, V., Kiefer, P., Gomez-Roldan, V., Jauneau, A., Roy, S., Portais, J.C., Roux, C., Bécard, G., and Séjalon-Delmas, N. (2006). Strigolactones stimulate arbuscular mycorrhizal fungi by activating mitochondria. PLoS Biol. **4:** 1239-1247.

Braun, E. (2007). Reactive nitrogen in the environment: too much or too little of a good thing. (UNEP/Earthprint).

Breakspear, A., Liu, C., Roy, S., Stacey, N., Rogers, C., Trick, M., Morieri, G., Mysore, K.S., Wen, J., and Oldroyd, G.E. (2014). The root hair "infectome" of *Medicago truncatula* uncovers changes in cell cycle genes and reveals a requirement for auxin signaling in rhizobial infection. Plant Cell **26:** 4680-4701.

Broghammer, A., Krusell, L., Blaise, M., Sauer, J., Sullivan, J.T., Maolanon, N., Vinther, M., Lorentzen, A., Madsen, E.B., Jensen, K.J., Roepstorff, P., Thirup, S., Ronson, C.W., Thygesen, M.B., and Stougaard, J. (2012). Legume receptors perceive the rhizobial lipochitin oligosaccharide signal molecules by direct binding. Proc. Natl. Acad. Sci. U. S. A. **109:** 13859-13864.

Caba, J.M., Recalde, L., and Ligero, F. (1998). Nitrate-induced ethylene biosynthesis and the control of nodulation in alfalfa. Plant, Cell Environ. **21:** 87-93.

Charpentier, M., Sun, J., Martins, T.V., Radhakrishnan, G.V., Findlay, K., Soumpourou, E., Thouin, J., Véry, A.A., Sanders, D., Morris, R.J., and Oldroyd, G.E.D. (2016). Nuclear-localized cyclic nucleotide-gated channels mediate symbiotic calcium oscillations. Science **352:** 1102-1105.

Cooper, J.B., and Long, S.R. (1994). Morphogenetic rescue of *Rhizobium meliloti* nodulation mutants by *trans*-zeatin secretion. Plant Cell **6:** 215-225.

Delaux, P.M., Bécard, G., and Combier, J.P. (2013a). NSP1 is a component of the Myc signaling pathway. New Phytol. **199:** 59-65.

Delaux, P.M., Séjalon-Delmas, N., Bécard, G., and Ané, J.M. (2013b). Evolution of the plant-microbe symbiotic 'toolkit'. Trends Plant Sci. **18:** 298-304.

Delaux, P.M., Radhakrishnan, G., and Oldroyd, G. (2015a). Tracing the evolutionary path to nitrogen-fixing crops. Curr. Opin. Plant Biol. **26:** 95-99.

Delaux, P.M., Radhakrishnan, G., Jayaraman, D., Cheema, J., Malbreil, M., Volkening, J.D., Sekimoto, H., Nishiyama, T., Melkonian, M., Pokorny, L., Rothfels, C.J., Sederoff, H.W., Stevenson, D.W., Surek, B., Zhang, Y., Sussman, M.R., Dunand, C., Morris, R.J., Roux, C., Wong, G.K.S., Oldroyd, G.E.D., and Ane, J.M. (2015b). Algal ancestor of land plants was preadapted for symbiosis. Proc. Natl. Acad. Sci. U. S. A. **112:** 13390-13395.

Doyle, J.J. (2011). Phylogenetic perspectives on the origins of nodulation. Mol. Plant-Microbe Interact. **24:** 1289-1295.

Duc, G., Trouvelot, A., Gianinazzi-Pearson, V., and Gianinazzi, S. (1989). First report of non-mycorrhizal plant mutants (Myc-) obtained in pea (*Pisum sativum* L.) and fababean (*Vicia faba* L.). Plant Sci. **60:** 215-222.

Endre, G., Kereszt, A., Kevei, Z., Mihacea, S., Kaló, P., and Kiss, G.B. (2002). A receptor kinase gene regulating symbiotic nodule development. Nature **417:** 962-966.

Erisman, J.W., Sutton, M.A., Galloway, J., Klimont, Z., and Winiwarter, W. (2008). How a century of ammonia synthesis changed the world. Nat. Geosci. **1:** 636-639.

Evenson, R.E., and Gollin, D. (2003). Assessing the impact of the Green Revolution, 1960 to 2000. Science **300:** 758-762.

Fang, Y., and Hirsch, A.M. (1998). Studying early nodulin gene *ENOD40* expression and induction by nodulation factor and cytokinin in transgenic alfalfa. Plant Physiol. **116:** 53-68.

Fearn, J.C., and Larue, T.A. (1991). Ethylene inhibitors restore nodulation to *sym 5* mutants of *Pisum sativum* L. cv sparkle. Plant Physiol. **96:** 239-244.

Flavell, R.B. (2016). Greener revolutions for all. Nat. Biotechnol. **34:** 1106-1110.

Folberth, C., Yang, H., Gaiser, T., Abbaspour, K.C., and Schulin, R. (2013). Modeling maize yield responses to improvement in nutrient, water and cultivar inputs in sub-Saharan Africa. Agric. Syst. **119:** 22-34.

Foley, J.A., Ramankutty, N., Brauman, K.A., Cassidy, E.S., Gerber, J.S., Johnston, M., Mueller, N.D., O'Connell, C., Ray, D.K., West, P.C., Balzer, C., Bennett,

E.M., Carpenter, S.R., Hill, J., Monfreda, C., Polasky, S., Rockström, J., Sheehan, J., Siebert, S., Tilman, D., and Zaks, D.P.M. (2011). Solutions for a cultivated planet. Nature **478:** 337-342.

Frugier, F., Kosuta, S., Murray, J.D., Crespi, M., and Szczyglowski, K. (2008). Cytokinin: secret agent of symbiosis. Trends Plant Sci. **13:** 115-120.

Galloway, J.N., Aber, J.D., Erisman, J.W., Seitzinger, S.P., Howarth, R.W., Cowling, E.B., and Cosby, B.J. (2003). The nitrogen cascade. BioScience **53:** 341-356.

Galloway, J.N., Dentener, F.J., Capone, D.G., Boyer, E.W., Howarth, R.W., Seitzinger, S.P., Asner, G.P., Cleveland, C.C., Green, P.A., Holland, E.A., Karl, D.M., Michaels, A.F., Porter, J.H., Townsend, A.R., and Vörösmarty, C.J. (2004). Nitrogen cycles: Past, present, and future. Biogeochemistry **70:** 153-226.

Genre, A., Chabaud, M., Balzergue, C., Puech-Pagès, V., Novero, M., Rey, T., Fournier, J., Rochange, S., Bécard, G., Bonfante, P., and Barker, D.G. (2013). Short-chain chitin oligomers from arbuscular mycorrhizal fungi trigger nuclear Ca^{2+} spiking in *Medicago truncatula* roots and their production is enhanced by strigolactone. New Phytol. **198:** 190-202.

Glendining, M.J., Dailey, A.G., Williams, A.G., Evert, F.K.v., Goulding, K.W.T., and Whitmore, A.P. (2009). Is it possible to increase the sustainability of arable and ruminant agriculture by reducing inputs? Agric. Syst. **99:** 117-125.

Gonzalez-Rizzo, S., Crespi, M., and Frugier, F. (2006). The *Medicago truncatula* CRE1 cytokinin receptor regulates lateral root development and early symbiotic interaction with *Sinorhizobium meliloti*. Plant Cell **18:** 2680-2693.

Goodlass, G., and Smith, K.A. (1979). Effects of ethylene on root extension and nodulation of pea (*Pisum sativum* L.) and white clover (*Trifolium repens* L.). Plant Soil **51:** 387-395.

Graham, P.H., and Vance, C.P. (2003). Legumes: Importance and constraints to greater use. Plant Physiol. **131:** 872-877.

Grobbelaar, N., Clarke, B., and Hough, M.C. (1971). The nodulation and nitrogen fixation of isolated roots of *Phaseolus vulgaris* L. - III. The effect of carbon dioxide and ethylene. Plant Soil **35:** 215-223.

Groth, M., Takeda, N., Perry, J., Uchid, H., Dräxl, S., Brachmann, A., Sato, S., Tabata, S., Kawaguchi, M., Wang, T.L., and Parniskea, M. (2010). *NENA*, a *Lotus japonicus* homolog of *Sec13*, is required for rhizodermal infection by arbuscular mycorrhiza fungi and rhizobia but dispensable for cortical endosymbiotic development. Plant Cell **22:** 2509-2526.

Gruber, N., and Galloway, J.N. (2008). An Earth-system perspective of the global nitrogen cycle. Nature **451:** 293-296.

Guillotin, B., Couzigou, J.M., and Combier, J.P. (2016). NIN is involved in the regulation of arbuscular mycorrhizal symbiosis. Front. Plant Sci. **7**.

Guinel, F.C., and LaRue, T.A. (1992). Ethylene inhibitors partly restore nodulation to pea mutant E107 (*brz)*. Plant Physiol. **99:** 515-518.

Haber, F. (2002). The synthesis of ammonia from its elements Nobel Lecture, June 2, 1920. Resonance **7:** 86-94.

Heckmann, A.B., Lombardo, F., Miwa, H., Perry, J.A., Bunnewell, S., Parniske, M., Wang, T.L., and Downie, J.A. (2006). *Lotus japonicus* nodulation requires two GRAS domain regulators, one of which is functionally conserved in a non-legume. Plant Physiol. **142:** 1739-1750.

Heckmann, A.B., Sandal, N., Bek, A.S., Madsen, L.H., Jurkiewicz, A., Nielsen, M.W., Tirichine, L., and Stougaard, J. (2011). Cytokinin induction of root nodule primordia in *Lotus japonicus* is regulated by a mechanism operating in the root cortex. Mol. Plant-Microbe Interact. **24:** 1385-1395.

Heidstra, R., Yang, W.C., Yalcin, Y., Peck, S., Emons, A., Van Kammen, A., and Bisseling, T. (1997). Ethylene provides positional information on cortical cell division but is not involved in Nod factor-induced root hair tip growth in *Rhizobium*-legume interaction. Development **124:** 1781-1787.

Held, M., Hossain, M.S., Yokota, K., Bonfante, P., Stougaard, J., and Szczyglowski, K. (2010). Common and not so common symbiotic entry. Trends Plant Sci. **15:** 540-545.

Hirsch, S., Kim, J., Muñoz, A., Heckmann, A.B., Downie, J.A., and Oldroyd, G.E.D. (2009). GRAS proteins form a DNA binding complex to induce gene expression during nodulation signaling in *Medicago truncatula*. Plant Cell **21:** 545-557.

Hossain, M.S., Liao, J., James, E.K., Sato, S., Tabata, S., Jurkiewicz, A., Madsen, L.H., Stougaard, J., Ross, L., and Szczyglowski, K. (2012). *Lotus japonicus* ARPC1 is required for rhizobial infection. Plant Physiol. **160:** 917-928.

Hwang, I., Sheen, J., and Müller, B. (2012). Cytokinin signaling networks. In Annual Review of Plant Biology, pp. 353-380.

Imaizumi-Anraku, H., Takeda, N., Charpentier, M., Perry, J., Miwa, H., Umehara, Y., Kouchi, H., Murakami, Y., Mulder, L., Vickers, K., Pike, J., Downie, J.A., Wang, T., Sato, S., Asamizu, E., Tabata, S., Yoshikawa, M., Murooka, Y., Wu, G.J., Kawaguchi, M., Kawasaki, S., Parniske, M., and Hayashi, M. (2005). Plastid proteins crucial for symbiotic fungal and bacterial entry into plant roots. Nature **433:** 527-531.

Jin, Y., Liu, H., Luo, D., Yu, N., Dong, W., Wang, C., Zhang, X., Dai, H., Yang, J., and Wang, E. (2016). DELLA proteins are common components of symbiotic rhizobial and mycorrhizal signalling pathways. Nat. Commun. **7**.

Ju, C., and Chang, C. (2012). Advances in ethylene signalling: protein complexes at the endoplasmic reticulum membrane. AoB Plants **2012:** pls031.

Kaló, P., Gleason, C., Edwards, A., Marsh, J., Mitra, R.M., Hirsch, S., Jakab, J., Sims, S., Long, S.R., Rogers, J., Kiss, G.B., Downie, J.A., and Oldroyd, G.E.D. (2005). Nodulation signaling in legumes requires NSP2, a member of the GRAS family of transcriptional regulators. Science **308:** 1786-1789.

Kanamori, N., Madsen, L.H., Radutoiu, S., Frantescu, M., Quistgaard, E.M.H., Miwa, H., Downie, J.A., James, E.K., Felle, H.H., Haaning, L.L., Jensen, T.H., Sato, S., Nakamura, Y., Tabata, S., Sandal, N., and Stougaard, J. (2006). A nucleoporin is required for induction of Ca^{2+} spiking in legume nodule development and essential for rhizobial and fungal symbiosis. Proc. Natl. Acad. Sci. U. S. A. **103:** 359-364.

Keshishian, E.A., and Rashotte, A.M. (2015). Plant cytokinin signalling. Essays Biochem. **58:** 13-27.

Kistner, C., and Parniske, M. (2002). Evolution of signal transduction in intracellular symbiosis. Trends Plant Sci. **7:** 511-518.

Kistner, C., Winzer, T., Pitzschke, A., Mulder, L., Sato, S., Kaneko, T., Tabata, S., Sandal, N., Stougaard, J., Webb, K.J., Szczyglowski, K., and Parniske, M. (2005). Seven *Lotus japonicus* genes required for transcriptional reprogramming of the root during fungal and bacterial symbiosis. Plant Cell **17:** 2217-2229.

Kosuta, S., Held, M., Hossain, M.S., Morieri, G., MacGillivary, A., Johansen, C., Antolín-Llovera, M., Parniske, M., Oldroyd, G.E.D., Downie, A.J., Karas, B., and Szczyglowski, K. (2011). *Lotus japonicus* symRK-14 uncouples the cortical and epidermal symbiotic program. Plant J. **67:** 929-940.

Lee, K.H., and LaRue, T.A. (1992). Exogenous ethylene inhibits nodulation of *Pisum sativum* L. cv sparkle. Plant Physiol. **100:** 1759-1763.

Lévy, J., Bres, C., Geurts, R., Chalhoub, B., Kulikova, O., Duc, G., Journet, E.P., Ané, J.M., Lauber, E., Bisseling, T., Dénarié, J., Rosenberg, C., and Debellé, F. (2004). A putative Ca^{2+} and calmodulin-dependent protein kinase required for bacterial and fungal symbioses. Science **303:** 1361-1364.

Lin, Z., Zhong, S., and Grierson, D. (2009). Recent advances in ethylene research. J. Exp. Bot. **60:** 3311-3336.

Liu, W., Kohlen, W., Lillo, A., den Camp, R.O., Ivanov, S., Hartog, M., Limpens, E., Jamil, M., Smaczniak, C., Kaufmann, K., Yang, W.C., Hooiveld, G.J.E.J.,

Charnikhova, T., Bouwmeester, H.J., Bisseling, T., and Geurts, R. (2011). Strigolactone biosynthesis in *Medicago truncatula* and rice requires the symbiotic GRAS-type transcription factors NSP1 and NSP2. Plant Cell **23:** 3853-3865.

Lohar, D., Stiller, J., Kam, J., Stacey, G., and Gresshoff, P.M. (2009). Ethylene insensitivity conferred by a mutated *Arabidopsis* ethylene receptor gene alters nodulation in transgenic *Lotus japonicus*. Ann. Bot. **104:** 277-285.

Lohar, D.P., Schaff, J.E., Laskey, J.G., Kieber, J.J., Bilyeu, K.D., and Bird, D.M. (2004). Cytokinins play opposite roles in lateral root formation, and nematode and Rhizobial symbioses. Plant J. **38:** 203-214.

Madsen, E.B., Madsen, L.H., Radutoiu, S., Olbryt, M., Rakwalska, M., Szczyglowski, K., Sato, S., Kaneko, T., Tabata, S., Sandal, N., and Stougaard, J. (2003). A receptor kinase gene of the LysM type is involved in legume perception of rhizobial signals. Nature **425:** 637-640.

Madsen, L.H., Tirichine, L., Jurkiewicz, A., Sullivan, J.T., Heckmann, A.B., Bek, A.S., Ronson, C.W., James, E.K., and Stougaard, J. (2010). The molecular network governing nodule organogenesis and infection in the model legume *Lotus japonicus*. Nat. Commun. **1:** 10.

Maillet, F., Poinsot, V., André, O., Puech-Pagés, V., Haouy, A., Gueunier, M., Cromer, L., Giraudet, D., Formey, D., Niebel, A., Martinez, E.A., Driguez, H., Bécard, G., and Dénarié, J. (2011). Fungal lipochitooligosaccharide symbiotic signals in arbuscular mycorrhiza. Nature **469:** 58-64.

Markmann, K., and Parniske, M. (2009). Evolution of root endosymbiosis with bacteria: how novel are nodules? Trends Plant Sci. **14:** 77-86.

Mathesius, U., Charon, C., Rolfe, B.G., Kondorosi, A., and Crespi, M. (2000). Temporal and spatial order of events during the induction of cortical cell divisions in white clover by *Rhizobium leguminosarum* bv. *trifolii* inoculation or localized cytokinin addition. Mol. Plant-Microbe Interact. **13:** 617-628.

Mitra, R.M., Gleason, C.A., Edwards, A., Hadfield, J., Downie, J.A., Oldroyd, G.E.D., and Long, S.R. (2004). A Ca^{2+}/calmodulin-dependent protein kinase required for symbiotic nodule development: Gene identification by transcript-based cloning. Proc. Natl. Acad. Sci. U. S. A. **101:** 4701-4705.

Miyahara, A., Richens, J., Starker, C., Morieri, G., Smith, L., Long, S., Downie, J.A., and Oldroyd, G.E.D. (2010). Conservation in function of a SCAR/WAVE component during infection thread and root hair growth in *Medicago truncatula*. Mol. Plant-Microbe Interact. **23:** 1553-1562.

Miyata, K., Kawaguchi, M., and Nakagawa, T. (2013). Two distinct *EIN2* genes cooperatively regulate ethylene signaling in *Lotus japonicus*. Plant Cell Physiol. **54:** 1469-1477.

Mueller, N.D., Gerber, J.S., Johnston, M., Ray, D.K., Ramankutty, N., and Foley, J.A. (2012). Closing yield gaps through nutrient and water management. Nature **490:** 254-257.

Mulvaney, R.L., Khan, S.A., and Ellsworth, T.R. (2009). Synthetic nitrogen fertilizers deplete soil nitrogen: A global dilemma for sustainable cereal production. J. Environ. Qualit. **38:** 2295-2314.

Murray, J.D. (2011). Invasion by invitation: Rhizobial infection in legumes. Mol. Plant-Microbe Interact. **24:** 631-639.

Murray, J.D., Karas, B.J., Sato, S., Tabata, S., Amyot, L., and Szczyglowski, K. (2007). A cytokinin perception mutant colonized by *Rhizobium* in the absence of nodule organogenesis. Science **315:** 101-104.

Nagae, M., Takeda, N., and Kawaguchi, M. (2014). Common symbiosis genes *CERBERUS* and *NSP1* provide additional insight into the establishment of arbuscular mycorrhizal and root nodule symbioses in *Lotus japonicus*. Plant Signaling Behav. **9**.

Nukui, N., Ezura, H., and Minamisawa, K. (2004). Transgenic *Lotus japonicus* with an ethylene receptor gene *Cm-ERS1/H70A* enhances formation of infection threads and nodule primordia. Plant Cell Physiol. **45:** 427-435.

Nukui, N., Ezura, H., Yuhashi, K.I., Yasuta, T., and Minamisawa, K. (2000). Effects of ethylene precursor and inhibitors for ethylene biosynthesis and perception on nodulation in *Lotus japonicus* and *Macroptilium atropurpureum*. Plant Cell Physiol. **41:** 893-897.

Oldroyd, G.E.D. (2013). Speak, friend, and enter: Signalling systems that promote beneficial symbiotic associations in plants. Nat. Rev. Microbiol. **11:** 252-263.

Oldroyd, G.E.D., and Downie, J.A. (2008). Coordinating nodule morphogenesis with rhizobial infection in legumes. In Annual Review of Plant Biology, pp. 519-546.

Oldroyd, G.E.D., and Dixon, R. (2014). Biotechnological solutions to the nitrogen problem. Curr. Opin. Biotechnol. **26:** 19-24.

Oldroyd, G.E.D., Engstrom, E.M., and Long, S.R. (2001). Ethylene inhibits the Nod factor signal transduction pathway of *Medicago truncatula*. Plant Cell **13:** 1835-1849.

Op den Camp, R.H.M., de Mita, S., Lillo, A., Cao, Q., Limpens, E., Bisseling, T., and Geurts, R. (2011). A phylogenetic strategy based on a legume-specific whole genome duplication yields symbiotic cytokinin type-A response regulators. Plant Physiol. **157:** 2013-2022.

Parniske, M. (2008). Arbuscular mycorrhiza: The mother of plant root endosymbioses. Nat. Rev. Microbiol. **6:** 763-775.

Penmetsa, R.V., and Cook, D.R. (1997). A legume ethylene-insensitive mutant hyperinfected by its rhizobial symbiont. Science **275:** 527-530.

Plet, J., Wasson, A., Ariel, F., Le Signor, C., Baker, D., Mathesius, U., Crespi, M., and Frugier, F. (2011). MtCRE1-dependent cytokinin signaling integrates bacterial and plant cues to coordinate symbiotic nodule organogenesis in *Medicago truncatula*. Plant J. **65:** 622-633.

Radutoiu, S., Madsen, L.H., Madsen, E.B., Felle, H.H., Umehara, Y., Grønlund, M., Sato, S., Nakamura, Y., Tabata, S., Sandal, N., and Stougaard, J. (2003). Plant recognition of symbiotic bacteria requires two LysM receptor-like kinases. Nature **425:** 585-592.

Raun, W.R., and Johnson, G.V. (1999). Improving nitrogen use efficiency for cereal production. Agron. J. **91:** 357-363.

Rockström, J., Steffen, W., Noone, K., Persson, Å., Chapin, F.S., Lambin, E.F., Lenton, T.M., Scheffer, M., Folke, C., Schellnhuber, H.J., Nykvist, B., De Wit, C.A., Hughes, T., Van Der Leeuw, S., Rodhe, H., Sörlin, S., Snyder, P.K., Costanza, R., Svedin, U., Falkenmark, M., Karlberg, L., Corell, R.W., Fabry, V.J., Hansen, J., Walker, B., Liverman, D., Richardson, K., Crutzen, P., and Foley, J.A. (2009). A safe operating space for humanity. Nature **461:** 472-475.

Rogers, C., and Oldroyd, G.E.D. (2014). Synthetic biology approaches to engineering the nitrogen symbiosis in cereals. J. Exp. Bot. **65:** 1939-1946.

Saito, K., Yoshikawa, M., Yano, K., Miwa, H., Uchida, H., Asamizu, E., Sato, S., Tabata, S., Imaizumi-Anraku, H., Umehara, Y., Kouchi, H., Murooka, Y., Szczyglowski, K., Downie, J.A., Parniske, M., Hayashi, M., and Kawaguchi, M. (2007). Nucleoporin85 is required for calcium spiking, fungal and bacterial symbioses, and seed production in *Lotus japonicus*. Plant Cell **19:** 610-624.

Salvagiotti, F., Cassman, K.G., Specht, J.E., Walters, D.T., Weiss, A., and Dobermann, A. (2008). Nitrogen uptake, fixation and response to fertilizer N in soybeans: A review. Field Crops Res. **108:** 1-13.

Schauser, L., Roussis, A., Stiller, J., and Stougaard, J. (1999). A plant regulator controlling development of symbiotic root nodules. Nature **402:** 191-195.

Smil, V. (2002). Nitrogen and food production: Proteins for human diets. AMBIO **31:** 126-131.

Smil, V. (2004). Enriching the earth: Fritz Haber, Carl Bosch, and the transformation of world food production. (MIT press).

Smit, P., Raedts, J., Portyanko, V., Debellé, F., Gough, C., Bisseling, T., and Geurts, R. (2005). NSP1 of the GRAS protein family is essential for rhizobial nod factor-induced transcription. Science **308:** 1789-1791.

Spichal, L. (2012). Cytokinins - Recent news and views of evolutionally old molecules. Funct. Plant Biol. **39:** 267-284.

Sprent, J.I. (2007). Evolving ideas of legume evolution and diversity: A taxonomic perspective on the occurrence of nodulation. New Phytol. **174:** 11-25.

Stracke, S., Kistner, C., Yoshida, S., Mulder, L., Sato, S., Kaneko, T., Tabata, S., Sandal, N., Stougaard, J., Szczyglowski, K., and Parniske, M. (2002). A plant receptor-like kinase required for both bacterial and fungal symbiosis. Nature **417:** 959-962.

Suzaki, T., Yoro, E., and Kawaguchi, M. (2015). Leguminous plants: Inventors of root nodules to accommodate symbiotic bacteria. In International review of cell and molecular biology (Elsevier Inc.), pp. 111-158.

Szczyglowski, K., and Stougaard, J. (2008). *Lotus* genome: pod of gold for legume research. Trends Plant Sci. **13:** 515-517.

Tilman, D., Balzer, C., Hill, J., and Befort, B.L. (2011). Global food demand and the sustainable intensification of agriculture. Proc. Natl. Acad. Sci. U. S. A. **108:** 20260-20264.

Tirichine, L., Sandal, N., Madsen, L.H., Radutoiu, S., Albrektsen, A.S., Sato, S., Asamizu, E., Tabata, S., and Stougaard, J. (2007). A gain-of-function mutation in a cytokinin receptor triggers spontaneous root nodule organogenesis. Science **315:** 104-107.

Tirichine, L., Imaizumi-Anraku, H., Yoshida, S., Murakami, Y., Madsen, L.H., Miwa, H., Nakagawa, T., Sandal, N., Albrektsen, A.S., Kawaguchi, M., Downie, A., Sato, S., Tabata, S., Kouchi, H., Parniske, M., Kawasaki, S., and Stougaard, J. (2006). Deregulation of a Ca^{2+}/calmodulin-dependent kinase leads to spontaneous nodule development. Nature **441:** 1153-1156.

To, J.P.C., and Kieber, J.J. (2008). Cytokinin signaling: two-components and more. Trends Plant Sci. **13:** 85-92.

Townsend, A.R., and Howarth, R.W. (2010). Fixing the global nitrogen problem. Sci. Am. **302:** 64-71.

Wais, R.J., Galera, C., Oldroyd, G., Catoira, R., Penmetsa, R.V., Cook, D., Gough, C., Dénarié, J., and Long, S.R. (2000). Genetic analysis of calcium spiking responses in nodulation mutants of *Medicago truncatula*. Proc. Natl. Acad. Sci. U. S. A. **97:** 13407-13412.

Walker, S.A., and Downie, J.A. (2000). Entry of *Rhizobium leguminosarum* bv. *viciae* into root hairs requires minimal nod factor specificity, but subsequent infection thread growth requires *nodO* or *nodE*. Mol. Plant-Microbe Interact. **13:** 754-762.

Weller, J.L., Foo, E.M., Hecht, V., Ridge, S., Vander Schoor, J.K., and Reid, J.B. (2015). Ethylene signaling influences light-regulated development in pea. Plant Physiol. **169:** 115-124.

Werner, G.D.A., Cornwell, W.K., Sprent, J.I., Kattge, J., and Kiers, E.T. (2014). A single evolutionary innovation drives the deep evolution of symbiotic N_2-fixation in angiosperms. Nat. Commun. **5**.

Yano, K., Yoshida, S., Müller, J., Singh, S., Banba, M., Vickers, K., Markmann, K., White, C., Schuller, B., Sato, S., Asamizu, E., Tabata, S., Murooka, Y., Perry, J., Wang, T.L., Kawaguchi, M., Imaizumi-Anraku, H., Hayashi, M., and Parniske, M. (2008). CYCLOPS, a mediator of symbiotic intracellular accommodation. Proc. Natl. Acad. Sci. U. S. A. **105:** 20540-20545.

Yokota, K., Fukai, E., Madsen, L.H., Jurkiewicz, A., Rueda, P., Radutoiu, S., Held, M., Hossain, M.S., Szczyglowski, K., Morieri, G., Oldroyd, G.E.D., Downie, J.A., Nielsen, M.W., Rusek, A.M., Sato, S., Tabata, S., James, E.K., Oyaizu, H., Sandal, N., and Stougaard, J. (2009). Rearrangement of actin cytoskeleton mediates invasion of *Lotus japonicus* roots by *Mesorhizobium loti*. Plant Cell **21:** 267-284.

Yu, N., Luo, D., Zhang, X., Liu, J., Wang, W., Jin, Y., Dong, W., Liu, J., Liu, H., Yang, W., Zeng, L., Li, Q., He, Z., Oldroyd, G.E.D., and Wang, E. (2014). A DELLA protein complex controls the arbuscular mycorrhizal symbiosis in plants. Cell Res. **24:** 130-133.

Zeigler, R.S., and Mohanty, S. (2010). Support for international agricultural research: Current status and future challenges. New Biotechnol. **27:** 565-572.

Zhang, X., Dong, W., Sun, J., Feng, F., Deng, Y., He, Z., Oldroyd, G.E.D., and Wang, E. (2015). The receptor kinase CERK1 has dual functions in symbiosis and immunity signalling. Plant J. **81:** 258-267.

Chapter 2

2 *Lotus japonicus* cytokinin receptors work partially redundantly to mediate nodule formation

Mark Held[1,2,*], Hongwei Hou[1,*], **Mandana Miri**[1,2,*], Christian Huynh[1], Loretta Ross[1], Md Shakhawat Hossain[1], Shusei Sato[3], Satoshi Tabata[3], Jillian Perry[4], Trevor L. Wang[4], and Krzysztof Szczyglowski[1,2]

[1]Agriculture and Agri-Food Canada, Southern Crop Protection and Food Research Centre, London, Ontario, N5V 4T3 Canada

[2]Department of Biology, University of Western Ontario, London, Ontario, N6A 5BF Canada

[3]Kazusa DNA Research Institute, 2-6-7 Kazusa-Kamatari, Kisarazu, Chiba, 292-0818 Japan

[4]John Innes Centre, Norwich Research Park Colney, Norwich NR4 7UH, United Kingdom

[*]**These authors contributed equally to this work.**

A version of this chapter has been published in *The Plant Cell* Journal. Permission has been granted for inclusion of the article "*Lotus japonicus* cytokinin receptors work partially redundantly to mediate nodule formation" published in *The Plant Cell*, Volume 26, pages 678-694, February 2014, in this thesis.

2.1 Contributions made by Mandana Miri

- Analyzed the symbiotic phenotype for single and double *lhk* mutant (Figure 2.7)
- Identified insertional LORE1 mutant alleles and performed the symbiotic phenotype analysis (Figure 2.8)
- Studied the transcriptional response of cytokinin receptors in response to ectopic cytokinin in *L. japonicus* wild-type and *lhk1-1* roots (Figure 2.10)
- Studied the transcriptional response of cytokinin receptors to rhizobial inoculation at several time points in *L. japonicus* wild-type and *lhk1-1* roots (Figure 2.15)
- Studied the necessity of bacterial entry inside the root cortex for nodule formation in *lhk1-1* by performing the phenotypic analyses of *lhk1-1 arpc1-1* and *lhk1-1 symRK-14* mutants (Figure 2.16)
- Performed the symbiotic and non-symbiotic phenotypic analyses of the *lhk1-1 lhk1a-1 lhk3-1* cytokinin receptor triple mutant (Figure 2.17)
- Performed the hairy root transformation experiments (Figure 2.18 and Figure 2.19)

This chapter shows that in Lotus japonicus, the LHK1 cytokinin receptor performs an essential function but also works partially redundantly with LHK1A and LHK3 to mediate nodule primordium formation within the root cortex. LHK1 is also expressed in the root epidermis, where it likely participates in signaling to restrict rhizobial infection.

2.2 Introduction

Cytokinins are a group of adenine-based phytohormones which are involved in many developmental and growth processes, including nodulation (Amasino, 2005; Frugier et al., 2008). In the majority of legume-*Rhizobium* systems that have been analyzed, the main stimulus which initiates nodule formation comes from compatible bacteria in the form of chemically decorated lipochitinoligosaccharide molecules, known as nodulation or Nod factors (NFs) (Lerouge et al., 1990; Bek et al., 2010). Perception of NFs by the host plant LysM motif kinase receptors (Madsen et al., 2003; Radutoiu et al., 2003) activates cascades of intracellular responses including calcium spiking (Wais et al., 2000; Walker and Downie, 2000; Sieberer et al., 2012). The changes in calcium concentration are perceived by calcium and calmodulin-dependent receptor kinase (CCaMK) (Hayashi et al., 2010; Singh and Parniske, 2012). This leads to activation of downstream effectors for rhizobial infection and nodule formation.

A growing body of evidence indicates that cytokinin signaling, activated downstream of NF perception and CCaMK, is one of the key endogenous effectors of nodulation (Frugier et al., 2008). An elegant study by Cooper and Long demonstrated that the cytokinin trans-zeatin synthesis and secretion system engineered into *Sinorhizobium meliloti* functionally replaced NF in its ability to incite nodule primordia formation in *Medicago sativa* (Cooper and Long, 1994). A similar effect can be obtained without bacteria by external application of a small amount of cytokinin to legume roots, including *Lotus japonicus* (Bauer et al., 1996; Heckmann et al., 2011).

To date, no direct evidence exists to support the involvement of bacterially-produced cytokinin in nodule formation. To the contrary, the identification of spontaneous nodule formation phenotypes in tetraploid alfalfa (*M. sativa*) (Truchet et al., 1989) and in

mutants of diploid *L. japonicus* (Tirichine et al., 2006) indicates the presence of an inherent plant signaling process for nodule formation.

Current data are most consistent with a model where the NF-dependent activation of CCaMK leads to local accumulation of cytokinin which, in turn, stimulates root cortical cell divisions for nodule primordium formation (Frugier et al., 2008). Such an interpretation is in agreement with the observation that *L. japonicus* plants carrying the *spontaneous nodule formation 1* (*snf1*) (Gleason et al., 2006), gain-of-function allele of CCaMK do not produce spontaneous nodules in the absence of the functional *L. japonicus* histidine kinase 1 (LHK1) cytokinin receptor (Madsen et al., 2010). Conversely, the *L. japonicus snf2*, gain-of-function allele of *Lhk1*, induces spontaneous nodule formation independent of CCaMK, supporting an epistatic relationship, where *Lhk1* acts downstream from CCaMK (Tirichine et al., 2007).

Functional analyses of loss-of-function and gain-of-function alleles of LHK1 defined this cytokinin receptor as being required and also sufficient for nodule organogenesis in *L. japonicus* (Murray et al., 2007; Tirichine et al., 2007; Heckmann et al., 2011). Unlike the *M. truncatula cre1* mutant, the *L. japonicus* mutant carrying a loss-of function *lhk1-1* allele, formerly known as *hit1*, (Murray et al., 2007) is hyperinfected by *Mesorhizobium loti*, with infection threads (ITs) heavily present in segments of the root epidermis and cortex in the initial absence of nodule organogenesis (Murray et al., 2007). *lhk1-1* develops a limited number of nodules at a later time-point upon inoculation by *M. loti* (Murray et al., 2007), suggesting the presence of an LHK1-independent signaling mechanism for nodule formation. We have, therefore, tested a hypothesis that other cytokinin receptors function in at least a partially redundant manner with LHK1 to mediate nodule organogenesis in *L. japonicus*. Our data demonstrate that LHK1 exerts a unique function in the root epidermis but works partially redundantly with LHK1A and LHK3 within the root cortex to mediate nodule formation.

2.3 Results

2.3.1 The *L. japonicus* cytokinin receptor gene family comprises at least four members

A search of the *L. japonicus* genome and cDNA sequences resulted in the prediction of a small family of four *Lotus histidine kinase* (*Lhk*) cytokinin receptor genes, including the previously described *Lhk1* and *Lhk2* (Murray et al., 2007). Based on the clustering pattern of the corresponding LHK proteins with *Arabidopsis thaliana* cytokinin receptors, the *Lhk2* gene was renamed as *Lhk1A*, while the two putative cytokinin receptors genes described in this study were named *Lhk2* and *Lhk3*. The corresponding *L. japonicus* proteins are referred to as LHK1, LHK1A, LHK2, and LHK3 (Figure 2.1).

Full-length transcripts were obtained for three *Lhk* mRNAs (i.e. *Lhk1A*, *Lhk2*, and *Lhk3*) and these were used to decipher the corresponding gene structures. Like *Lhk1*, the *Lhk3* gene has 11 exons while 12 and 14 exons are predicted for the *Lhk1A* and *Lhk2* genes, respectively. The length of the predicted open reading frames was found to be 2991 bp, 3654 bp, and 2958 bp for *Lhk1A*, *Lhk2*, and *Lhk3*, respectively which reflect the corresponding proteins of 997, 1218, and 986 amino acids.

2.3.2 LHK proteins contain domains characteristic of known cytokinin receptors

To test the prediction that, like LHK1, the LHK1A, LHK2 and LHK3 proteins constitute *bona fide* cytokinin receptors, their amino acid sequences were analyzed. Subsequently, functional assays in heterologous yeast and *Escherichia coli* systems were performed (see Section 2.3.5).

The identity and similarity of LHK protein sequences within the predicted *L. japonicus* cytokinin receptor family and to representatives from *A. thaliana* are summarized in Table 2.1. Briefly, LHK1 and LHK1A are the most similar, sharing 80% identity at the amino acid level. Conservation between these two proteins and the *Arabidopsis* AHK4 cytokinin receptor is also high at 68 and 69%, respectively. In contrast, LHK1 and LHK1A share only ~50% identity with LHK2 and LHK3. Amino acid sequence conservation is greater between LHK2 and LHK3 and also to their presumed orthologues

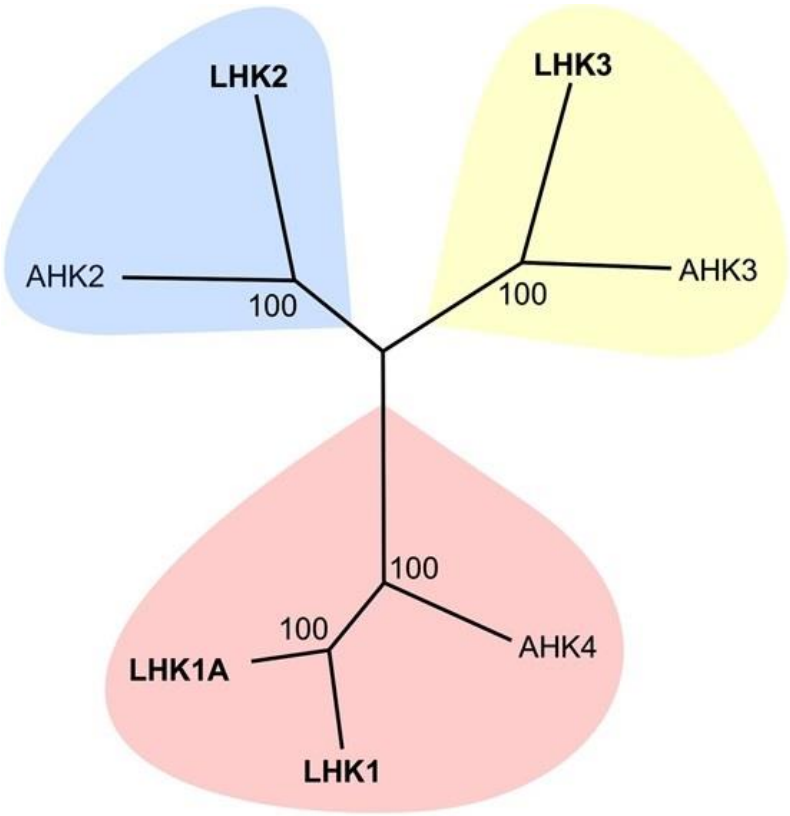

Figure 2.1 The *L. japonicus* LHK protein family.

This unrooted relationship tree is based on an amino acid alignment of full-length sequences from *L. japonicus* (LHK1, LHK1A [formerly LHK2; (Murray et al., 2007)], LHK2, and LHK3) and *Arabidopsis* (AHK4, AHK2, and AHK3). Protein sequences were aligned with Clustal Omega using the default settings, and the MEGA 6.0.5 phylogeny tool was used to portray the relationships between proteins. The numbers represent a measure of support where 100 represents maximal support. The LHK3 variant 1 protein (Figure 2.5) was used for the alignment.

from *A. thaliana* (AHK2 and AHK3, respectively) than between these two proteins and LHK1 or LHK1A (Table 2.1).

The N-terminal portions of all four LHKs contain a predicted cyclase/histidine kinase associated sensory extracellular (CHASE) domain (Heyl et al., 2012), which is highly-conserved within the LHK family and also between LHKs and CHASE domains of other known cytokinin receptors, such as *Arabidopsis* AHK4 (Figure 2.2).

As expected, the predicted cytosolic portion of the LHK proteins contains the highly conserved kinase domain (Hwang et al., 2012) with the canonical H, N, G1, F, and G2 consensus motifs and a highly conserved histidine (H) residue (Figure 2.3).

Downstream, a C-terminal receiver or output domain is also present in all predicted LHK receptors. This domain is known to participate in the phosphotransfer from the kinase domain to downstream signaling elements, such as histidine phosphotransfer (HPT) proteins (Ferreira and Kieber, 2005). The functional receiver domain carries three characteristic motifs named the DD, D, and K motifs for their conserved amino-acid residues (Ueguchi et al., 2001). All of these conserved motifs are present in the predicted LHK receptors, including an absolutely invariant aspartic acid residue in the D motif (Figure 2.4).

2.3.3 The *Lhk3* transcript undergoes altenative splicing

A survey of *L. japonicus* gene atlas data (http://ljgea.noble.org/v2/) (Verdier et al., 2013), shows that the *Lhk* transcripts are present in all organs analyzed, including roots, stems, leaves and nodules. Two variants of the *Lhk3* mRNA (variant 1 and 2) were identified through 5'-RACE experiments (Figure 2.5). These variants differ in length, with *Lhk3* mRNA variant no. 2 being longer by 228 bp in comparison with variant no. 1. Transcript-specific primers were designed against each predicted *Lhk3* mRNA variant and the presence of both mRNA species was confirmed via RT-PCR of *L. japonicus* nodule total RNA (Figure 2.5B).

Table 2.1 Amino acid conservation among *L. japonicus* LHK proteins and with their presumed *Arabidopsis* counterparts.

Name	Length	Name	Length	Identity (%)	Similarity (%)
LHK1	993	LHK1A	997	80	86
LHK1	993	LHK2	128	52	67
LHK1	993	LHK3	986	49	66
LHK1	993	AHK4	1057	68	78
LHK1A	997	LHK2	1218	53	68
LHK1A	997	LHK3	986	51	68
LHK1A	997	AHK4	1057	69	79
LHK2	1218	LHK3	986	54	69
LHK2	1218	AHK2	1176	59	71
LHK3	986	AHK3	1036	68	80

Figure 2.2 Amino acid sequence alignment to protein regions containing the CHASE domain, as predicated for *L. japonicus* LHKs and *Arabidopsis* AHK4.

The alignment was created using CLUSTALW2 and analyzed by the BoxShade software. A threshold of ≥80% conservation was used. Green shading indicates identical residues, whereas yellow indicates conservative substitutions. Asterisks denote conserved amino-acid positions corresponding to the *Arabidopsis* AHK4 receptor residues W244, T301, F304, R305 and T3017, all shown to be important for cytokinin binding (Heyl et al., 2007).

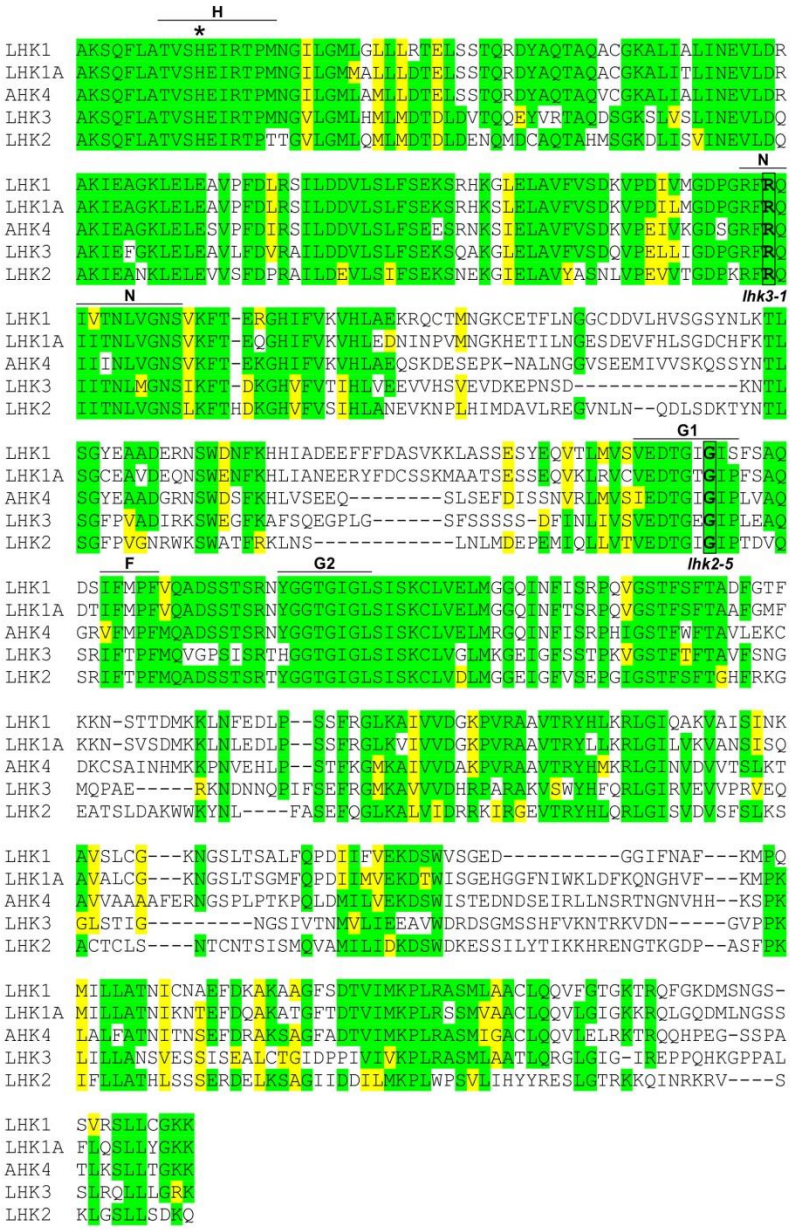

Figure 2.3 Amino acid sequence alignment of the protein kinase domain, as predicted for *L. japonicus* LHK proteins and compared to *Arabidopsis* AHK4.

The conserved H, N, G1, F, and G2 box motifs are indicated. An asterisk denotes the presence of a conserved histidine (H) residue required for the phosphorelay. Boxed and highlighted R and G residues correspond to position of *lhk3-1* and *lhk2-5* mutations, respectively (see Section 2.3.4). The alignment was created as before (see Figure 2.2).

Figure 2.4 Amino acid sequence alignment of the receiver domains, as predicted for *L. japonicus* LHK proteins and *Arabidopsis* AHK4.

The conserved DD, D, and K motifs are indicated. An asterisk denotes the presence of conserved aspartic acid (D) residue required for the phosphorelay. The alignment was created as before (see Figure 2.2).

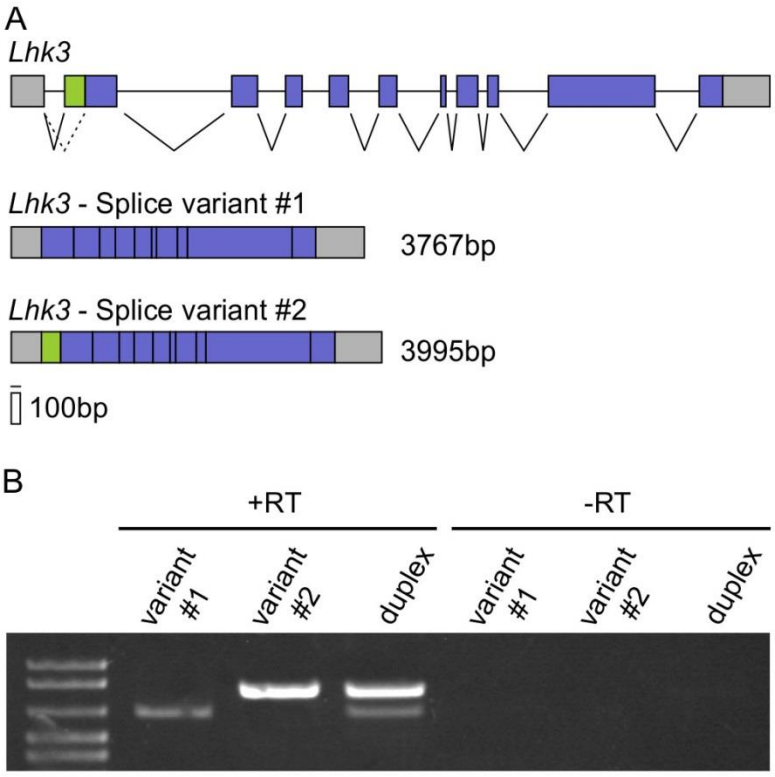

Figure 2.5 Alternative splicing of *Lhk3*.

(A) Alternative splicing at the intron 1/exon 2 junction of the *Lhk3* locus results in the production of two *Lhk3* splice variants (named *Lhk3* - Splice variant #1 and *Lhk3* - Splice variant #2, differing by 228 bp (green box).

(B) RT-PCR and transcript-specific primers were used to detect and sequence the two splice variants from *L. japonicus* nodule RNA.

2.3.4 Identification of cytokinin receptor mutant alleles

The Targeted Induced Localized Lesions IN Genomes (TILLING) approach was employed to identify mutations in the *Lhk1A*, *Lhk2*, and *Lhk3* loci. A 1 kb region within the highly-conserved kinase domain was targeted. Several *L. japonicus* lines carrying single nucleotide substitutions were identified in the *Lhk1A*, *Lhk2*, and *Lhk3* genes (Table 2.2). For *Lhk1A*, a mutant line carrying the G4439 to A transition (named *lhk1a-1*) was chosen for detailed analyses as this was predicted to change a tryptophan residue in the kinase domain to a premature stop codon (W565 to STOP; Table 2.2). For the *Lhk2* and *Lhk3* loci, mutant lines carrying the *lhk2-5* and *lhk3-1* alleles were selected as the corresponding mutations were predicted to change invariant residues within the conserved G1 (Gly605 to Arg) and N (Arg561 to Gln) box motifs of the kinase domain, respectively (see Figure 2.3). The original TILLING lines were back-crossed to wild-type *L. japonicus* Gifu and homozygote *lhk1a-1*, *lhk2-5*, and *lhk3-1* single mutant individuals were selected from among segregating F2 populations. Their progeny were used in subsequent analyses.

2.3.5 *Lhk1A* and *Lhk3* encode functional cytokinin receptors

2.3.5.1 *Lhk1A* confers cytokinin-responsive growth to the *sln1Δ* mutant of *Saccharomyces cerevisiae*

Wild-type and mutant alleles were used in parallel to functionally evaluate different LHKs in the *sln1Δ* mutant of *S. cerevisiae* (Maeda et al., 1994). This yeast strain was previously used to demonstrate the cytokinin-responsive function of the LHK1 receptor and the deleterious nature of the *lhk1-1* mutation (Murray et al., 2007).

Like *Lhk1*, the wild-type *Lhk1A* cDNA restored the viability of the *sln1Δ* strain in a cytokinin-dependent fashion. In contrast, the *lhk1a-1* cDNA failed to do so, demonstrating the deleterious nature of the *lhk1a-1* mutation (Figure 2.6A).

Repeated attempts to perform a similar functional study with *Lhk2* and the two variants of the *Lhk3* cDNA have failed due to an apparent toxicity of these cDNAs in the yeast cells. Therefore, an alternative approach based on an *E. coli* two-component phosphorelay assay (Yamada et al., 2001; Tirichine et al., 2007) was used.

Table 2.2 A list of *lhk1a, lhk2,* and *lhk3* mutant alleles as identified by a TILLING approach.

DNA: nucleotide changes are listed; Amino acid: predicted amino-acid changes are listed. Adenine in the predicted ATG initiation codon was set as 1 for defining the position of a given mutation in DNA. Similarly, a predicted initiating methionine residue was set as 1 to calculate the position of any given amino acid change.

Plant line Number	Mutant allele	Mutation change (DNA)	Mutation change (Amino acid)
SL761-1	*lhk1a-1*	G_{4439} - *A*	W_{565} - *STOP*
SL1481-1	*lhk1a-2*	C_{4808} - *T*	L_{689} - *F*
SL3496-1	*lhk1a-3*	C_{4808} - *T*	L_{689} - *F*
SL4275-1	*lhk1a-4*	G_{4725} - *A*	G_{661} - *E*
SL5603-1	*lhk1a-5*	G_{4929} - *A*	S_{729} - *N*
SL4559-1	*lhk1a-6*	C_{4388} - *T*	H_{549} - *T*
SL871-1	*lhk1a-7*	G_{3934} - *A*	*None - Intronic*
SL1169-1	*lhk1a-8*	C_{4504} - *T*	*None - synonomous*
SL3064-1	*lhk1a-9*	C_{4031} - *T*	*None - Intronic*
SL4389-1	*lhk1a-10*	G_{4933} - *A*	*None - synonomous*
SL4340-1	*lhk2-1*	G_{5499} - *A*	A_{517} - *T*
SL4236-1	*lhk2-2*	G_{5532} - *A*	D_{528} - *N*
SL404-1	*lhk2-3*	G_{5547} - *A*	E_{533} - *K*
SL577-1	*lhk2-4*	G_{5551} - *A*	G_{534} - *D*
SL965-1	*lhk2-5*	G_{5769} - *A*	G_{605} - *R*
SL1482-1	*lhk2-6*	G_{5817} - *A*	A_{621} - *T*
SL2025-1	*lhk2-7*	G_{5836} - *A*	R_{627} - *Q*
SL5335-1	*lhk2-8*	G_{5899} - *A*	G_{648} - *E*
SL80-1	*lhk2-9*	G_{5908} - *A*	G_{651} - *E*
SL390-1	*lhk2-10*	G_{6051} - *A*	D_{699} - *N*
SL1428-1	*lhk2-11*	C_{5645} - *T*	*None - synonomous*
SL1535-1	*lhk2-12*	C_{5248} - *T*	*None - Intronic*
SL314-1	*lhk2-13*	C_{5335} - *T*	*None - synonomous*
SL6570-1	*lhk2-14*	C_{5691} - *T*	*None - synonomous*
SL5401-1	*lhk2-15*	G_{5260} - *A*	*None - Intronic*
SL201-1	*lhk3-1*	G_{4558} - *A*	R_{561} - *Q*
SL577-1	*lhk3-2*	G_{5219} - *A*	V_{596} - *I*
SL1972-1	*lhk3-3*	G_{6057} - *A*	S_{875} - *N*
SL780-1	*lhk3-4*	C_{4782} - *T*	*None - Intronic*
SL1767-1	*lhk3-5*	G_{4973} - *A*	*None - Intronic*

2.3.5.2 *Lhk3* confers cytokinin-responsiveness to the sensor-negative SRC122 *E. coli* mutant strain

The introduction of a functional histidine kinase receptor and an appropriate ligand to the SRC122 *E. coli* strain results in activation of the *cps::LacZ* reporter fusion (Yamada et al., 2001). Application of cytokinin to the SRC122 *E. coli* strain carrying wild-type copies of either of the two splice variants of *Lhk3* cDNA significantly induced the β-galactosidase activity above the control level of the untreated samples, thus confirming their cytokinin-responsive function (Figure 2.6B and 2.6C). The *lhk3-1* mutation completely abolished the cytokinin responsiveness, irrespective of the cDNA variant used, which indicates that the *lhk3-1* mutant form is non-functional (Figure 2.6D and 2.6E).

When transformed into SRC122, the *Lhk2* cDNA-containing replicon was highly unstable such that no intact receptor sequence could be recovered. This outcome was not entirely unexpected given the reports on similar problems with the *A. thaliana* AHK2 gene (Yamada et al., 2001). Thus, the LHK2 receptor remains functionally undefined by this work and is considered here after as a presumed cytokinin receptor.

2.3.6 Single and double mutants of *lhk1a-1*, *lhk2-5*, and *lhk3-1* do not affect nodule formation

Early events that characterize the epidermal program for symbiosis, such as the formation of bacterial microcolonies trapped within curled root hairs and subsequent development of ITs, were evaluated 7 days after inoculation (DAI) with a *M. loti* strain carrying the *hemA::LacZ* reporter gene fusion. Unlike the hyperinfected root phenotype of *lhk1-1* (Murray et al., 2007), *lhk1a-1*, *lhk2-5*, and *lhk3-1* single mutants displayed a wild-type number of infection events (Figure 2.7A). Furthermore, the numbers of nodule primordia and nodules were at wild-type levels in *lhk1a-1* and *lhk3-1* single mutants (Figure 2.7B). The *lhk2-5* mutant formed slightly but significantly fewer nodules than wild-type (Figure 2.7B). However, this is likely an indirect effect, as the overall growth of the *lhk2* mutant, including root elongation (Figure 2.9B), was also significantly affected. Under the same growth conditions, *lhk1-1* formed a strongly reduced number of nodules, confirming the

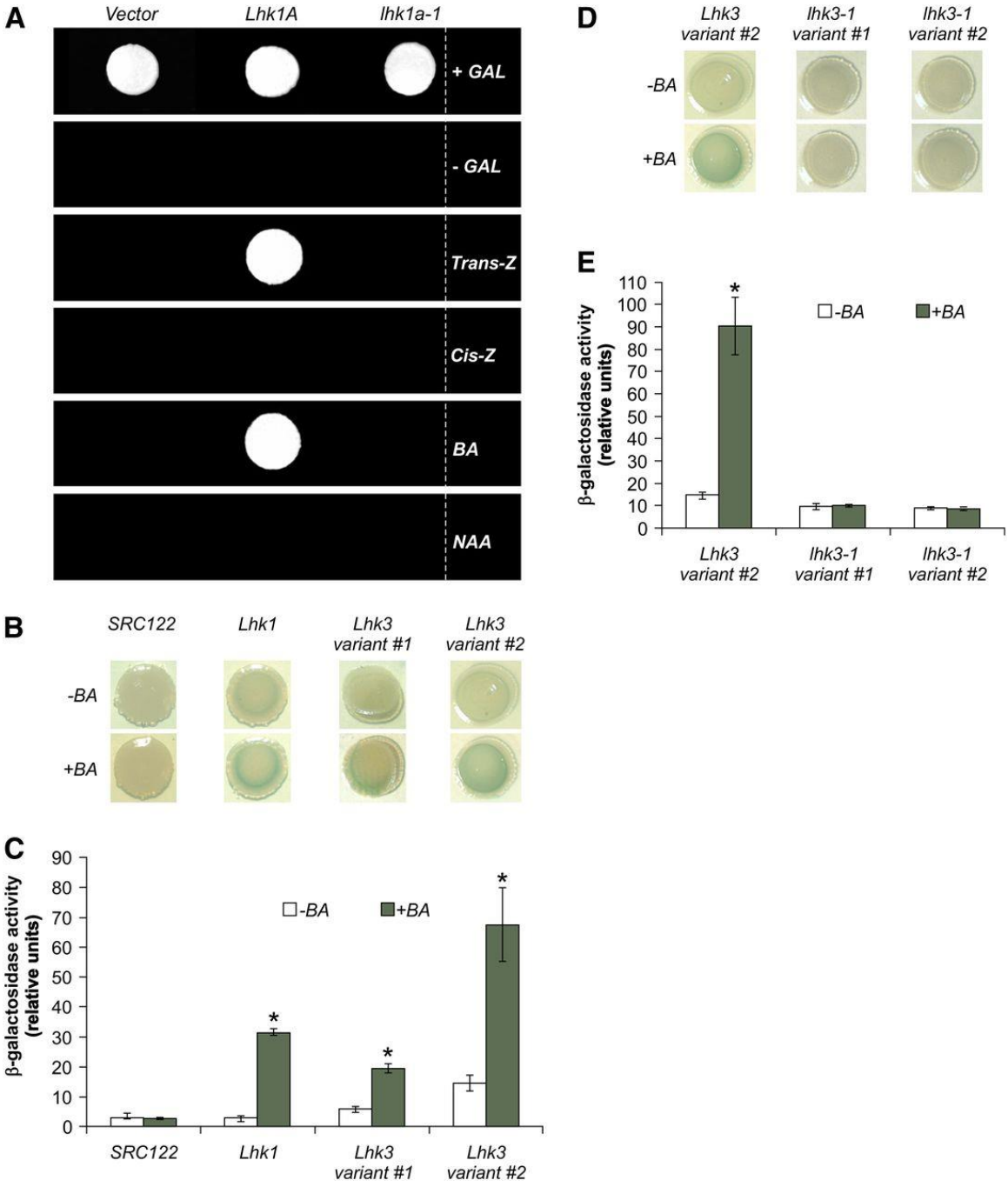
A
Vector
Lhk1A
lhk1a-1
+ GAL
- GAL
Trans-Z
Cis-Z
BA
NAA
B
SRC122
Lhk1
Lhk3 variant #1
Lhk3 variant #2
-BA
+BA
C
β-galactosidase activity (relative units)
-BA
+BA
SRC122
Lhk1
Lhk3 variant #1
Lhk3 variant #2
D
Lhk3 variant #2
lhk3-1 variant #1
lhk3-1 variant #2
-BA
+BA
E
β-galactosidase activity (relative units)
-BA
+BA
Lhk3 variant #2
lhk3-1 variant #1
lhk3-1 variant #2

Figure 2.6 *Lhk1A* and *Lhk3* encode functional cytokinin receptors.

(A) In the absence of galactose (-GAL), the wild-type *Lhk1A* cDNA confers cytokinin (Trans-Z and BA)-dependent growth of the *sln1Δ* mutant of *S. cerevisiae*. The *lhk1a-1* mutant cDNA is unable to do so. +GAL, 2% Gal supplement; Trans-Z, trans-zeatin; Cis-Z, cis-zeatin; BA, 6-benzylaminopurine; NAA, 1-naphthaleneacetic acid.

(B) to **(E)** Wild-type ([B] and [C]) and *lhk3-1* mutant ([D] and [E]) cDNAs corresponding to the two *Lhk3* mRNA variants (variants 1 and 2) were cloned into the pSTV28 expression vector and transformed into the sensor-negative *E. coli* SRC122 strain. The *Lhk1* cDNA was used as a positive control for the experiments shown in (B) and (C). Upon application of BA, a noticeable increase in the β-galactosidase reporter activity (blue color) can be observed in the presence of *Lhk1* and both wild-type variants of Lhk3 cDNA ([B] and [D]). Quantification of the β-galactosidase activity as driven by different *Lhk* cDNAs in the presence or absence of BA is shown in (C) and (E). SRC122 is the sensor-negative *E. coli* strain used as a negative control. The *lhk3-1* mutation abolishes the cytokinin-responsive function of the LHK3 receptor ([D] and [E]). The wild-type *Lhk3* variant 2 was used as a positive control in (D) and (E). In all cases, values represent means ± 95% confidence interval (n = 3). Asterisks denote significant differences (Student's t test, $P < 0.05$).

previous data (Murray et al., 2007). All double receptor mutants also had wild-type or close to wild-type (in the case of plants carrying the *lhk2-5* allele; see above) nodulation phenotypes, except for those carrying the *lhk1-1* allele, where a greatly reduced number of nodules was apparent (Figure 2.7B).

2.3.7 Insertional and single-nucleotide substitution mutant alleles of the cytokinin receptor genes share the symbiotic phenotype

As described above, *lhk1-1*, *lhk1a-1* and *lhk3-1* mutations generate non-functional cytokinin receptors (Section 2.3.5). Nevertheless, whether these alleles and also *lhk2-5*, which could not be tested in heterologous systems due to toxicity/instability of the cDNA, behave as nulls *in planta* remained uncertain. Fortunately, the *L. japonicus* retrotransposon (LORE1) has been introduced as a mutational tool (Madsen et al., 2005; Fukai et al., 2010; Fukai et al., 2012; Urbański et al., 2012). LORE1 is a stable, long terminal repeat (LTR) germline-specific retro-transposon that amplifies in the *L. japonicus* genome by a copy-and-paste mechanism (Malolepszy et al., 2016). The insertion of the 5.041 kb long LORE1 sequence in the coding region introduces multiple premature, translational stop codons (Urbański et al., 2012). It had been previously shown that the activity of LORE1 leads to gene inactivation and generation of null mutant alleles (Madsen et al., 2005). A large LORE1 insertion population is publicly available (http://users-mb.au.dk/pmgrp/). By screening this population candidate lines carrying LORE1 insertions in exons of *Lhk1*, *Lhk1a, Lhk2* and *Lhk3* were identified. These alleles were designated as *lhk1-4*, *lhk1a-12*, *lhk1a-13, lhk2-17*, *lhk2-18, lhk3-6* and *lhk3-7* (Figure 2.8A). The progeny of the plants homozygous for these LORE1 containing alleles were tested for their symbiotic phenotype 21 DAI with *M. loti* alongside the selected TILLING mutant lines (Figure 2.8B).

As shown in Figure 2.8B, nodulation was significantly reduced in *lhk1-1* and *lhk1-4* while it remained unaffected in all other mutant lines tested, which confirms the data obtained with the selected *lhk* TILLING mutants (Figure 2.7B and Figure 2.8B). Therefore, the substitution mutation alleles were used for further analysis of the role of LHK cytokinin receptors in nodulation.

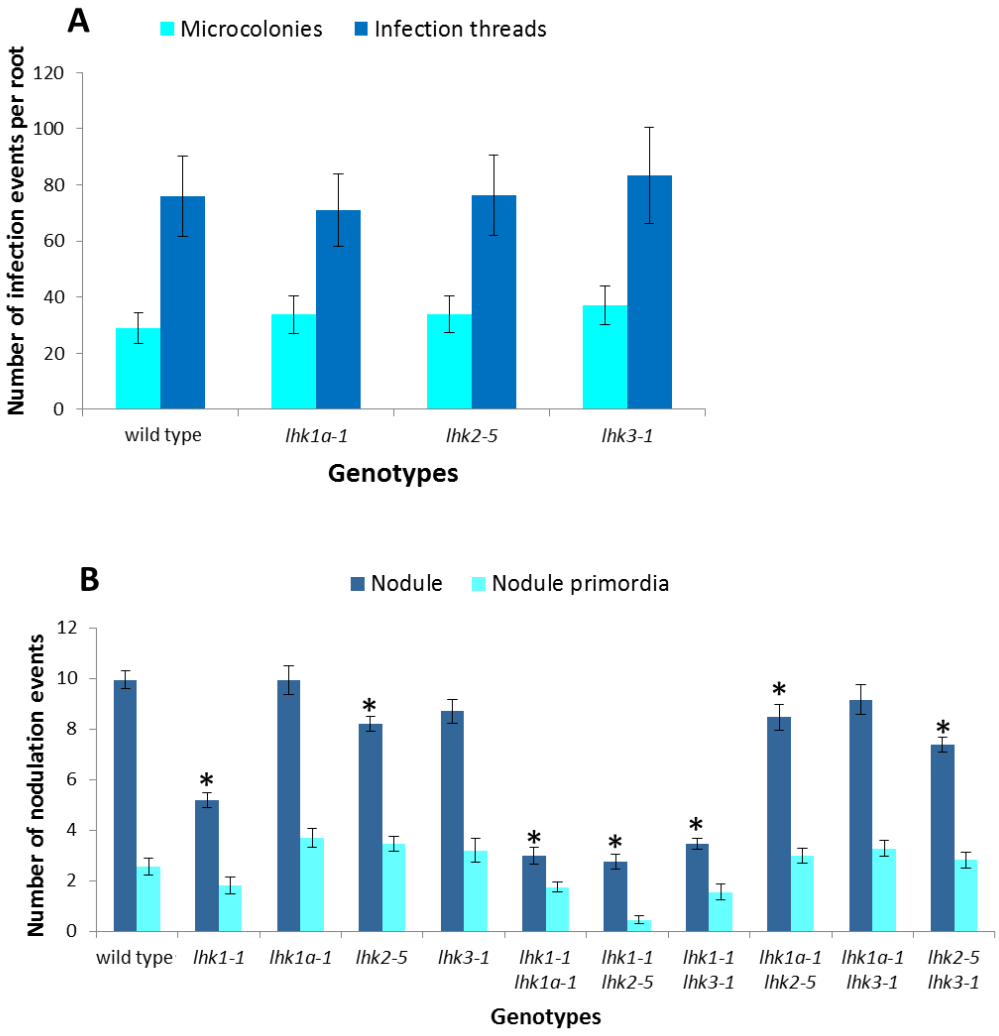

Figure 2.7 Bacterial infection and nodule formation are mostly unaffected by *lhk1a-1*, *lhk2-5*, and *lhk3-1* mutations.

(A) The number of microcolonies and infection threads was scored in *lhk* single mutants at 7 DAI with the *M. loti* strain tagged with the *hemA::LacZ* reporter and this was compared to the *L. japonicus* wild-type control. In all cases, values reported are the mean ± 95% CI (confidence interval) (n = 10).

(B) Nodule and nodule primordia formation in *lhk1-1*, *lhk1a-1*, *lhk2-5*, and *lhk3-1* single and the corresponding double mutants were scored 21 DAI. In all cases, values reported represent the mean ± 95% CI (n = 29-50). An asterisk denotes significant differences between the mutant and wild-type control (Student's t-Test, $P<0.05$).

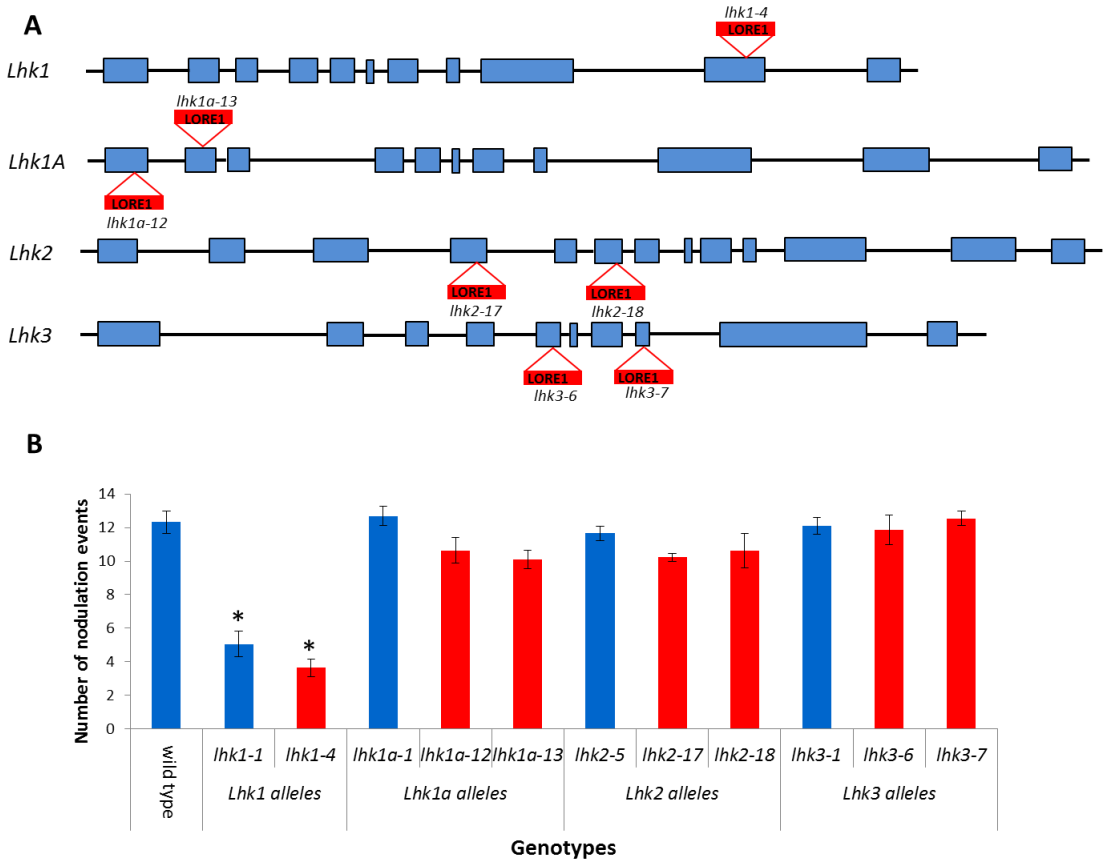

Figure 2.8 Nodulation phenotypes are similar in the mutant plants carrying either retrotransposon or single nucleotide substitution alleles of *Lhk* cytokinin receptor genes.

(A) The intron-exon structures of the *Lhk1*, *Lhk1a*, *Lhk2*, and *Lhk3* genes are shown. Boxes represent predicted exons while lines denote 5' and 3' UTRs and introns. *lhk1-4*, *lhk1a-12*, *lhk1a-13*, *lhk2-17*, *lhk2-18*, *lhk3-6*, and *lhk3-7* denote mutant alleles carrying the *L. japonicus* LORE1 retrotransposon insertion at the indicated positions.

(B) Number of nodulation events in different *lhk1*, *lhk1a*, *lhk2*, and *lhk3* mutant lines was scored 21 DAI. In all cases, values reported represent the mean ± 95% SE (n = 20). An asterisk denotes significant differences between the mutant and wild-type control (Student's t-Test, $P<0.05$).

2.3.8 LHK1 is the main sensor of exogenous cytokinin

In wild-type *L. japonicus* plants, root elongation is significantly inhibited by external application of cytokinin (Murray et al., 2007). Deleterious mutations in the *Lhk1* receptor gene, such as *lhk1-1*, render mutant roots insensitive to exogenous 6-benzylaminopurine (BA) up to 1 x 10^{-7} M (Murray et al., 2007). This indicates that in addition to its significant role during nodule organogenesis, the LHK1 receptor mediates root responses to external signals, such as cytokinin. To analyze whether other *L. japonicus* cytokinin receptors partake in this physiological response, all *L. japonicus lhk* mutant lines, including *lhk1-1*, were subjected to the root elongation assay in the presence or absence of BA. In contrast to *lhk1-1*, which was insensitive to external cytokinin, *lhk1a-1*, *lhk2-5*, and *lhk3-1* mutants responded to the exogenous BA by reducing root growth in a manner similar to the wild-type *L. japonicus* (Figure 2.9A). It is worth noting here that the growth of untreated *lhk1-1*, *lhk1a-1*, and *lhk3-1* mutant roots was not significantly different from wild type. The root length of *lhk2-5*, however, was slightly yet significantly affected (Figure 2.9B).

To further understand the unique role of LHK1 during the response of *L. japonicus* roots to ectopic cytokinin, we quantified steady state levels of the *Lhk1* mRNA upon application of 50 nM BA. The four remaining cytokinin receptor mRNAs, including two variants of *Lhk3*, were also included in this analysis. The level of the *Lhk1* mRNA was strongly and significantly up-regulated within 6 hours of BA treatment and this increase was further enhanced at 12 hours (Figure 2.10 A and B). In contrast, the steady-state levels of the *Lhk1A*, *Lhk2*, and both variants of *Lhk3* mRNA were significantly up-regulated only after a prolonged, 12 hour treatment with BA (Figure 2.10B). Importantly, this increase in levels of *Lhk1A*, *Lhk2*, and *Lhk3* mRNAs in response to BA was not observed in *lhk1-1* roots (Figure 2.10C and 2.10D), while the *lhk1-1* mRNA still responded by a slight but significant increase after 12 hours of the BA treatment (Figure 2.10D).

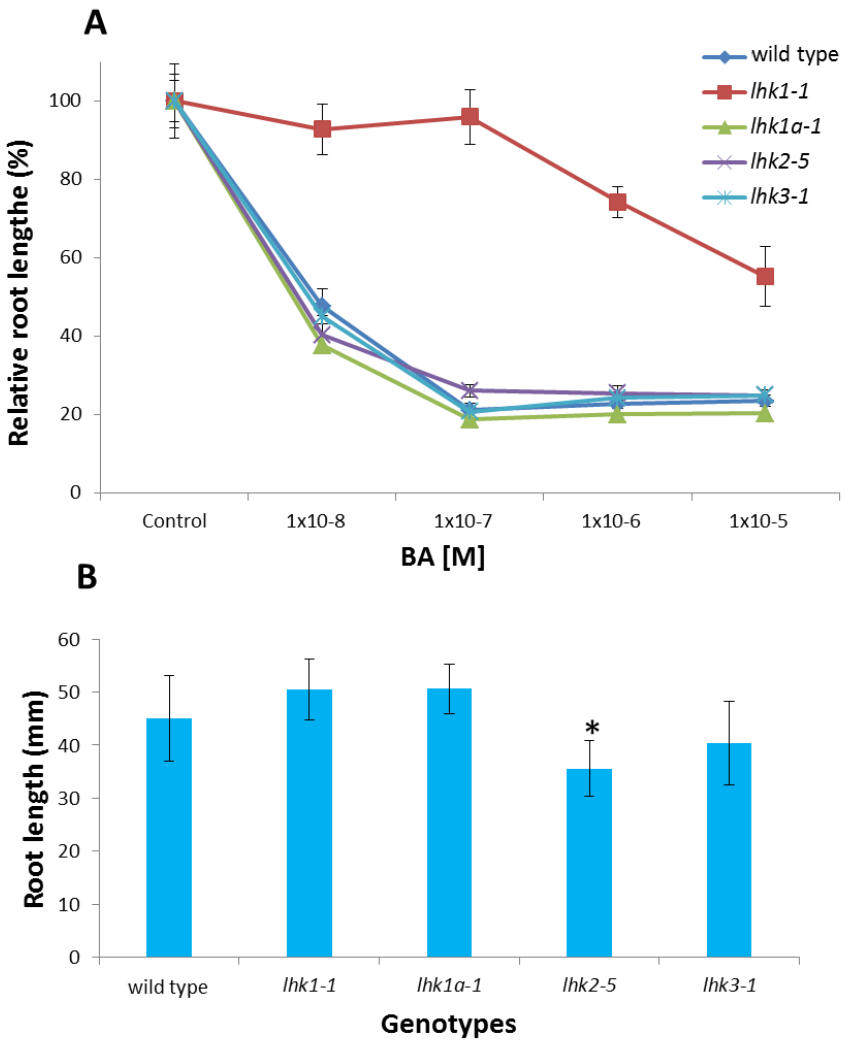

Figure 2.9 Responses of the *L. japonicus* wild-type and *lhk* mutant roots to exogenous cytokinin and root growth.

(A) Plants were grown on the surface of agar plates in the dark, in the presence of increasing concentrations of cytokinin (BA). The root length was measured 7 days after sowing. The relative root length is given, where the length of control roots that were grown in the absence of BA was set as 100%. BA: 6-benzylaminopurine.

(B) The average length of control, untreated roots for given genotypes are shown. Values in panels (A) and (B) represent the mean ±95% CI ($n \geq 10$). An asterisk denotes significant difference with the wild-type value (Student's t-Test, $P<0.05$).

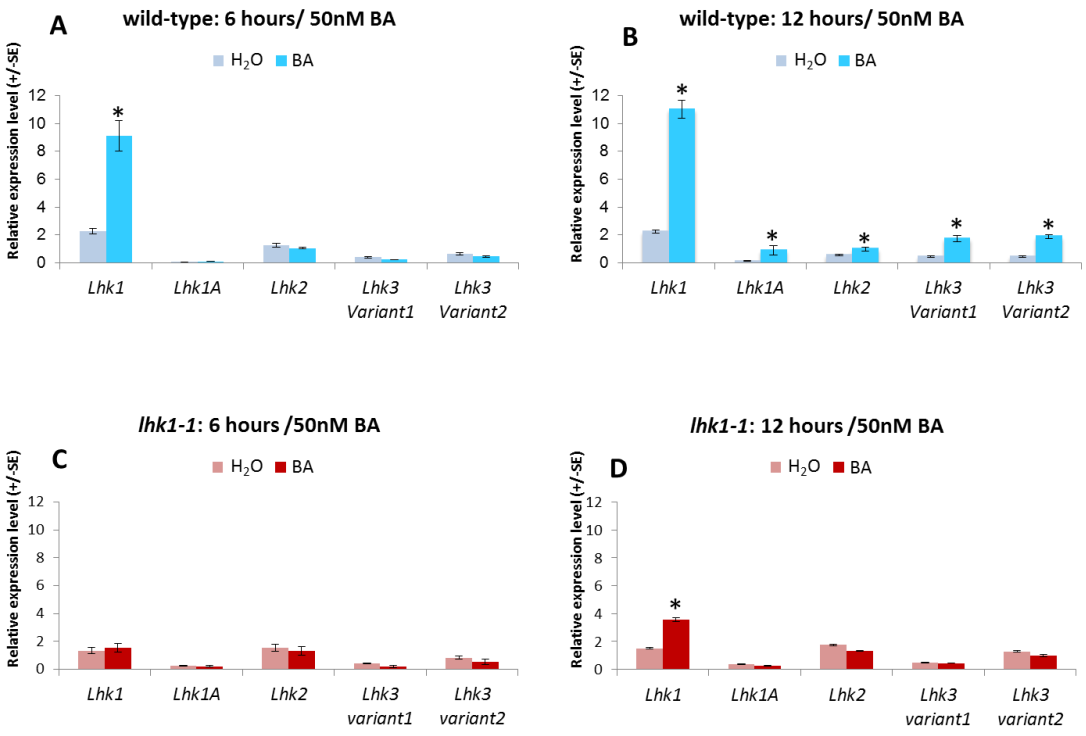

Figure 2.10 Ectopic cytokinin increases the steady state level of cytokinin receptor mRNAs.

The relative steady state levels of *Lhk1*, *Lhk1A*, *Lhk2*, and *Lhk3* transcripts in untreated (H_2O) and cytokinin-treated (BA) *L. japonicus* roots are given. Values (means ± SE of three biological replicates) for *L. japonicus* wild-type (**[A]** and **[B]**) and *lhk1-1* mutant (**[C]** and **[D]**) roots that were incubated in the absence or presence of 50 nM BA for 6 h ([A] and [C]) and 12 h ([B] and [D]) are shown. Asterisks denote significant differences between the corresponding untreated control and BA-treated samples (Student's t-Test, $P<0.05$).

2.3.9 The transcriptional output of cytokinin signaling during nodule formation

The results described above have suggested a unique role for the LHK1 receptor in mediating nodule organogenesis and also in root responses to exogenous cytokinin. To explore this further, stable *L. japonicus* transgenic lines carrying the cytokinin two-component-output sensor *(TCS)::GUS* reporter (Müller and Sheen, 2008) or one of the four *Lhk* promoters transcriptionally fused to the GUS reporter gene (Lhk_{pro}*::GUS*) were analyzed to map their expression domains.

Following *M. loti* inoculation, the *TCS*-mediated GUS activity was initially detectable in the sub-epidermal and the second and third cortical cell layers, with the latter two showing most of the activity (Figure 2.11A and 2.11B). At this early stage in nodule development, GUS staining was observed only intermittently in the root epidermis and if present, it was weak. At a slightly later developmental stage, GUS staining was present in cell layers encompassing the entire region from the root epidermis to pericycle (Figure 2.11C and 2.11D), and continued to intensify across all cell layers that were actively engaged in nodule formation and also in the associated epidermis, including root hairs (Figure 2.11E and 2.11F). GUS activity was present in most cells of young nodules that had just emerged from the root epidermis (Figure 2.11G), but it was undetectable in fully mature nodules, except for a weak activity in the nodule parenchyma and vascular bundles (Figure 2.11H).

In comparison, during lateral root development, the *TCS*-driven GUS activity maxima were associated with a subset of proliferating cells at the base of developing primordia (Figure 2.11I) and, later on, also with the root apex (Figure 2.11J), consistent with the previous report (Lohar et al., 2004). In mature roots, GUS staining was mostly confined to the root apex and the root transition zone but was much weaker within the root proximal meristem (Figure 2.11K).

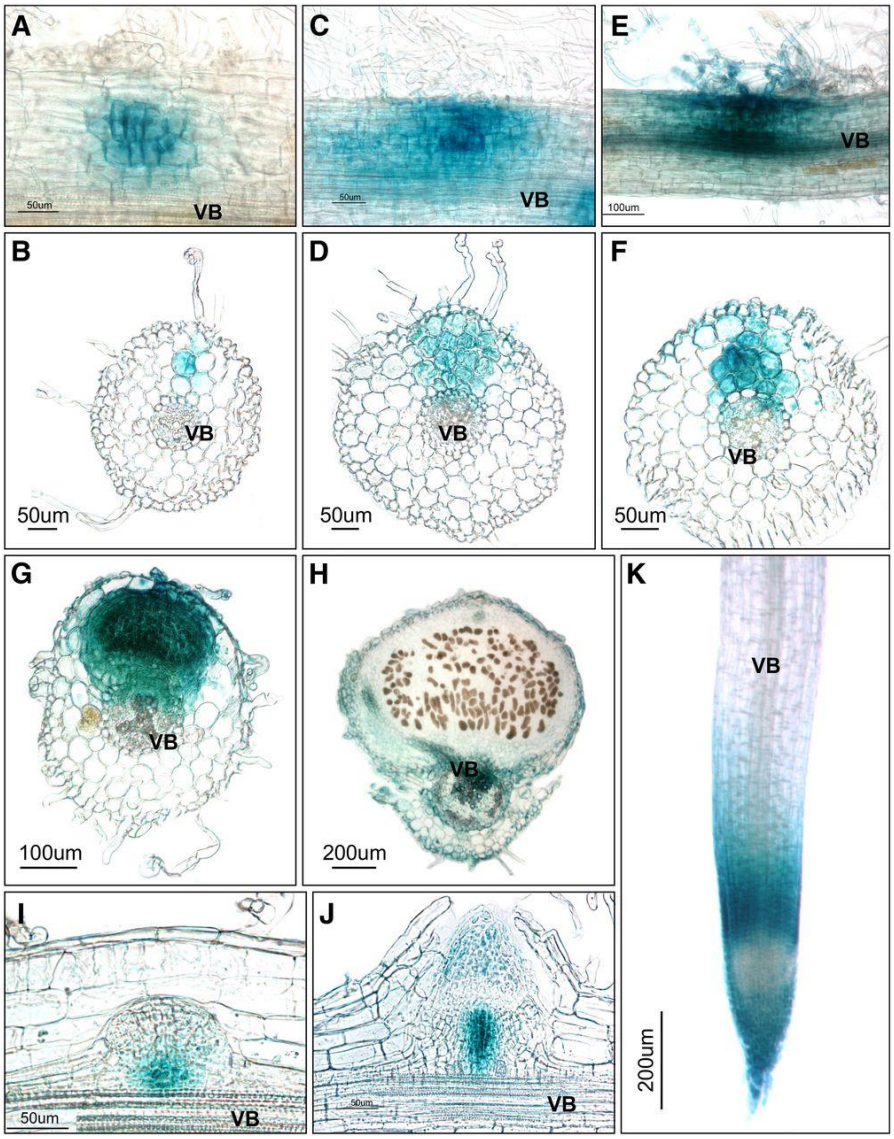

Figure 2.11 Cytokinin responses during nodule and root development.

The *TCS::GUS* cytokinin output reporter activities are depicted (blue color) as associated with various stages of developing nodules (**[A]** to **[H]**), lateral roots (**[I]** and **[J]**), and the apical region of the main root **(K)**. All images represent specimens collected at 7 or 14 DAI with *M. loti*. (A), (C), (E), and (K) represent whole mounts, and the other panels show 35 μm sections. VB, vascular bundles.

2.3.10 Expression of *Lhk1*, *Lhk1A*, *Lhk2*, and *Lhk3* in uninoculated *L. japonicus* roots

Lhk1$_{pro}$::GUS plants showed strong histochemical staining along the entire roots (Figure 2.12), including the root apex and a portion that is defined as a susceptible zone for *M. loti* infection which spans the region positioned between 2-5 mm above the root tip (Figure 2.12C). Longitudinal sectioning of several independent samples of *Lhk1*$_{pro}$*::GUS* roots that were stained at room temperature showed GUS activity in all root cell layers, including the root epidermis; however GUS staining was much weaker or entirely absent from cells of the proximal meristem (Figure 2.12B) and in root cells located in a more proximal part of the root, above the root transition zone.

None of the other three *Lhk* promoters paralleled the activity of the *Lhk1* promoter. As driven by the *Lhk1A* promoter, GUS activity was only barely detectable in root cap cells (Figure 2.12D) and in pericycle cells associated with lateral root emergence (see Figure 2.14D), but not within the susceptible zone (Figure 2.12E). *Lhk2* was active in the root vasculature (Figure 2.12G) but GUS staining was undetectable in the root tip region (Figure 2.12F), including the susceptible zone. Finally, *Lhk3* was active in the proximal root meristem (Figure 2.12H) but its activity was undetectable in the meristem proper or the main root vasculature (Figure 2.12H and 2.12I).

2.3.11 Activity of the *Lhk1* promoter during nodule formation

In order to monitor the activity of the *Lhk1* promoter during nodule development, the temperature under which GUS staining was performed was reduced from 37°C to room temperature. This decreased the overall intensity of root staining, making it possible to detect the GUS activity maxima.

At early stages of nodule primordium formation, where only very limited cortical cell divisions are present, GUS activity was detectable in a few sub-epidermal cells and the second and third cortical layers (Figure 2.13A and 2.13B). GUS staining was also detectable, albeit rather weakly and intermittently, in the associated root epidermis. With the advancement of cell divisions, the intensity of GUS staining increased across all cell layers and was now clearly detectable in the root epidermis, including root hairs (Figure

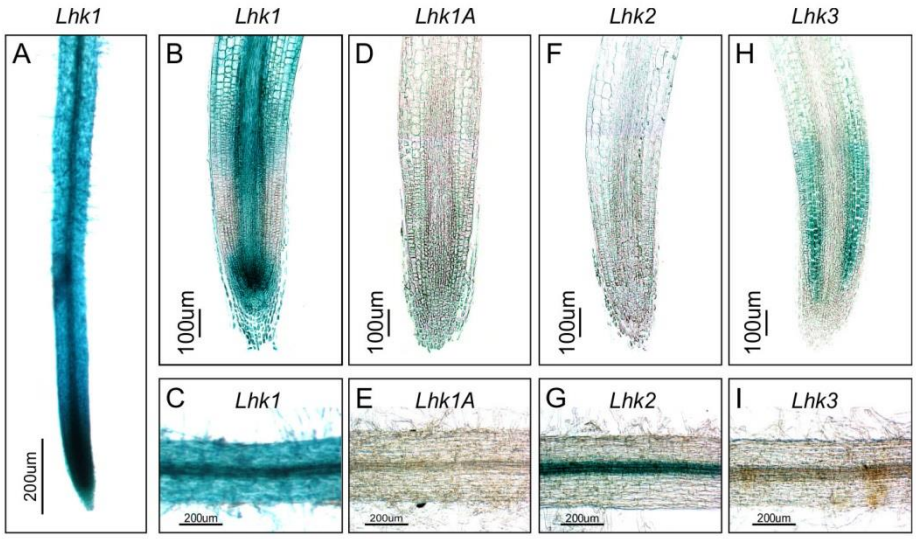

Figure 2.12 Activities of *Lhk1*, *Lhk1A*, *Lhk2* and *Lhk3* promoters in uninoculated *L. japonicus* roots.

Whole mounts (A, C, E, G and I) and 35 µm thick longitudinal sections (B, D, F and H) are shown. *Lhk1*$_{pro}$*::GUS* activity in *L. japonicus* root (A), root apical region (B) and a root segment within a zone susceptible to *M. loti* infection approx. 2-5 mm above the root tip (C). Activities of *Lhk1A*$_{pro}$*::GUS* (D and E), *Lhk2*$_{pro}$*::GUS* (F and G) and *Lhk3*$_{pro}$*::GUS* (H and I) reporter constructs in the corresponding apical and root susceptible zones. All images represent specimens collected at 7 or 14 days after sowing.

2.13C and 2.13D). This pattern of GUS staining persisted to the point of nodule emergence from the root epidermis (Figure 2.13E). In mature nodules, however, GUS activity was restricted to the nodule parenchyma and nodule vasculature, but was undetectable in centrally-located infected cells (Figure 2.13F).

In comparison to nodules, GUS activity associated with lateral root development was observed in a discrete region of the root pericycle and was associated with all cells of the developing primordium (Figure 2.13G) before localizing to the apex in the emerging lateral root (Figure 2.13H). In fully-emerged, growing lateral roots, the pattern of the *Lhk1*-dependent GUS activity was identical to the main root, showing strong staining within the meristematic region but also in other parts of the root (Figure 2.13I).

2.3.12 The *Lhk1A* and *Lhk3* promoters show partially overlapping activities with *Lhk1* during nodule primordia formation

As observed for *Lhk1*, the activities of *Lhk1A* and *Lhk3* promoters were clearly induced upon rhizobial infection (Figure 2.14). GUS staining was specifically associated with dividing cortical cells of young nodule primordia but was absent from surrounding root cortical cells (Figure 2.14A, 2.14B and 2.14I). GUS activity could not be detected in the epidermal cells associated with the developing nodule primordium, even at later stages. Mature nodules showed GUS staining in the parenchyma and vasculature (Figure 2.14C) or only in the vasculature (Figure 2.14J and 2.14K) for *Lhk1A* and *Lhk3*, respectively.

Both promoters rendered rather different GUS activity profiles during lateral root development, with *Lhk1A* conferring a barely detectable histochemical signal in subtending pericycle cells (Figure 2.14D) and $Lhk3_{pro}$*::GUS* plants showing rather strong GUS staining along the root vasculature and within the proximal meristem (Figure 2.14L).

Similar to uninoculated plants, the $Lhk2_{pro}$*::GUS* reporter construct showed activity in the vasculature of roots and also nodules, but not in dividing cortical cells of nodule primordia or emerging nodules (Figure 2.14E, 2.14F and 2.14G). Transverse sections of roots showed specific localization of the $Lhk2_{pro}$-driven GUS activity in the pericycle cells that were positioned opposite root protoxylem poles (Figure 2.14H).

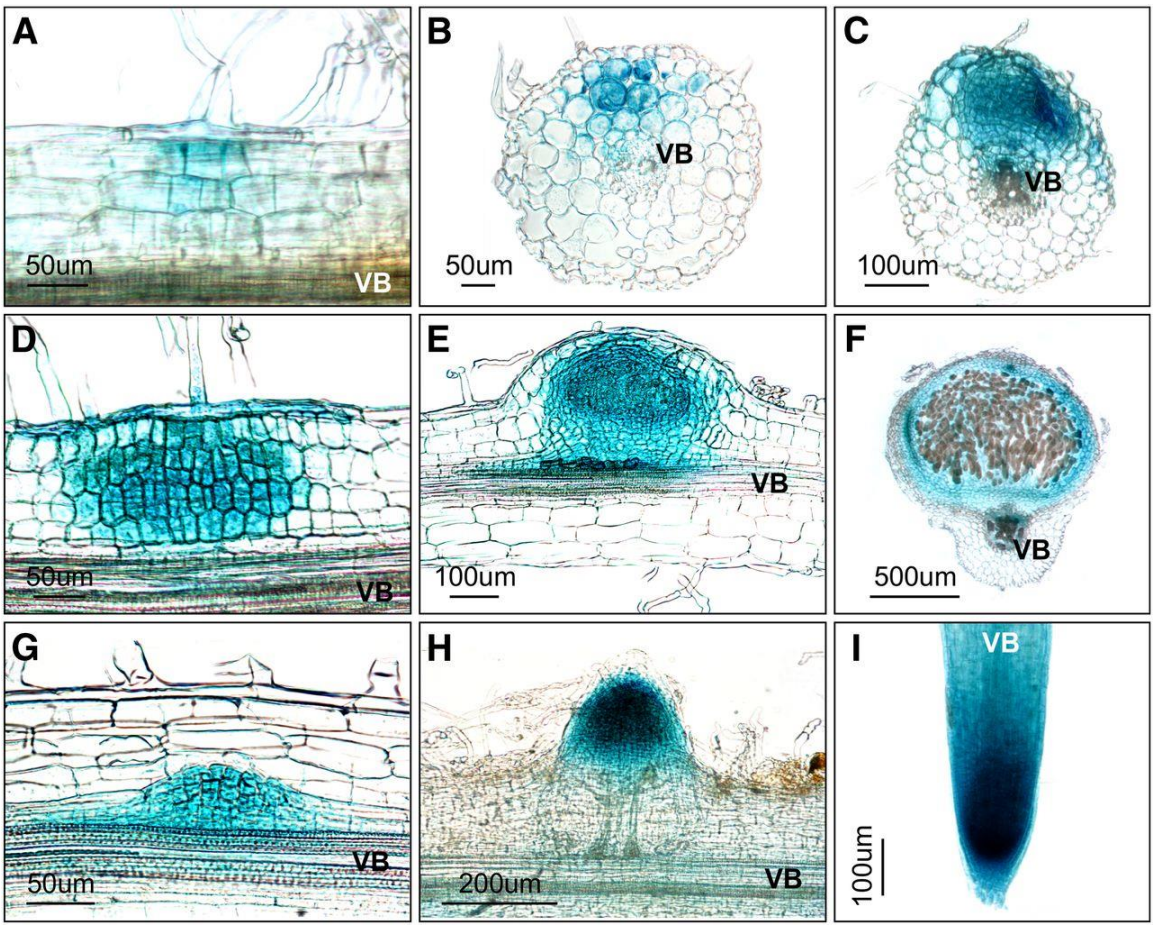

Figure 2.13 Activity of the *Lhk1* promoter during nodule and lateral root development.

Whole mounts (**[A]** and **[I]**) and 35-µm-thick root/nodule sections ([B] to [H]) are shown. (A) to (F) *Lhk1*$_{pro}$*::GUS* reporter activity (blue color) associated with the progressive stages in nodule development. Note that (B) shows a transverse section through a root region where nodule primordium formation has been initiated. (D) depicts the presence of GUS activity in the associated root hair. (G) to (I) *Lhk1*$_{pro}$*::GUS* activity during lateral root formation. (I) depicts the apical portion of a fully emerged lateral root. All images represent specimens collected at 7 or 14 DAI with *M. loti*. VB, vascular bundles.

2.3.13 All four *Lhk* promoters respond to *M. loti* inoculation

To support the histochemical data, the steady-state level of *Lhk1*, *Lhk1A*, *Lhk2*, and *Lhk3* transcripts was quantified in uninoculated control roots and roots collected 2, 3 and 7 days after inoculation with *M. loti*. In uninoculated wild-type *L. japonicus* roots, the level of the *Lhk1* mRNA was the highest and that of *Lhk1A* was the lowest (approx. 13-33 times lower than the *Lhk1* mRNA depending on the specific time point), while steady-state levels of *Lhk2* and *Lhk3* mRNA were intermediate (Figure 2.15). Consistent with the histochemical observations, the steady-state levels of *Lhk1*, *Lhk1A* and *Lhk3* transcripts were elevated upon inoculation. Quantitative PCR results also revealed that the steady-state level of the *Lhk2* transcript was also up-regulated upon *M. loti* infection (Figure 2.15).

Significant changes were observed in the *lhk1-1* mutant. The steady-state level of *Lhk1* mRNA was markedly lower than in wild-type roots, regardless of whether inoculated or uninoculated root samples were analyzed. *Lhk1* remained responsive to *M. loti* inoculation; however, at 2 and 3 DAI, its mRNA reached only approximately 50% of the levels in corresponding wild-type roots (Figure 2.15). Both *Lhk2* and *Lhk3* were rendered unresponsive to the infection but the level of the *Lhk2* mRNA in uninoculated *lhk1-1* roots was elevated in comparison to wild-type roots. As in wild-type, the *Lhk1A* mRNA remained a relatively minor component and was still able to respond to *M. loti* infection (Figure 2.15).

2.3.14 Bacterial entry inside the root cortex is required for nodule formation in *lhk1-1*

Previously, it was shown that initial colonization of the root cortex by *M. loti* occurs in *lhk1-1* without concomitant nodule primordia formation, but that a few nodules are eventually formed (Murray et al., 2007). We have, therefore, tested the hypothesis that a prior colonization of the root cortex by *M. loti* is required for the nodule primordium inception in the *lhk1-1* mutant. In the absence of functional LHK1, this was presumed to be mediated by bacterial signaling from within the root cortex through a partially redundant

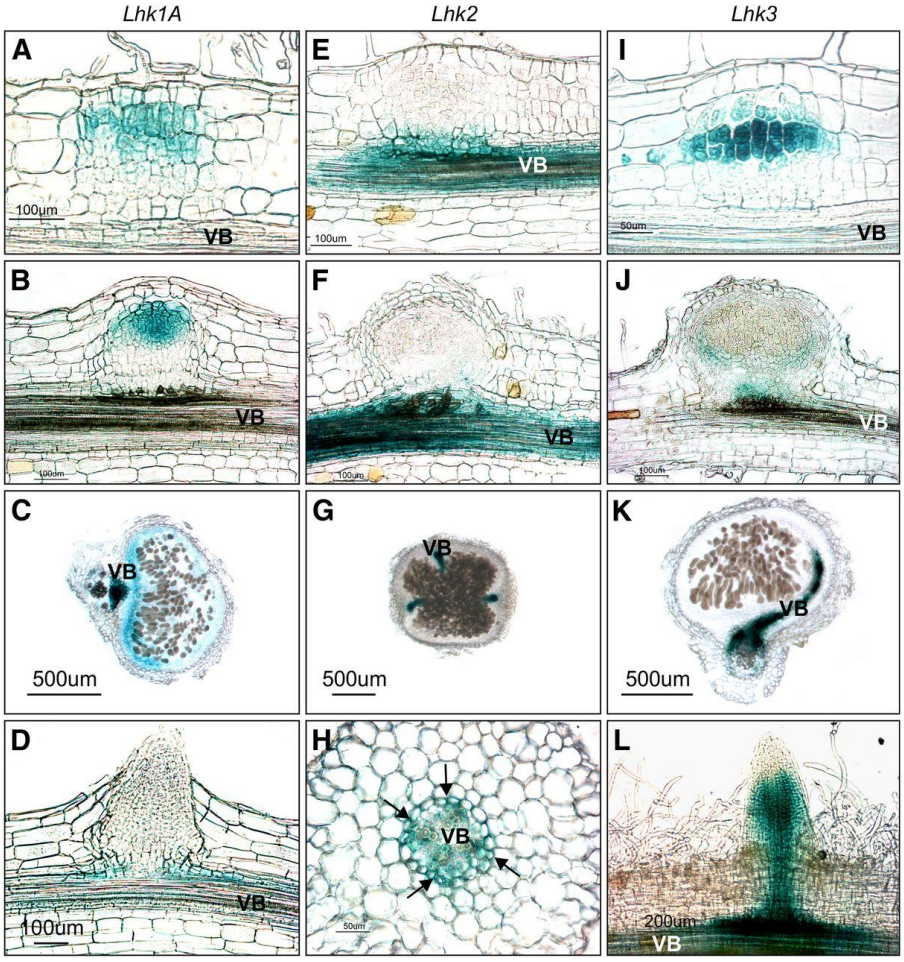

Figure 2.14 Activities of the *Lhk1A*, *Lhk2* and *Lhk3* promoters during nodule and lateral root development.

A-D *Lhk1A*$_{pro}$*::GUS* reporter activity (blue) associated with nodule (A-C) and lateral root (D) development.

E-H *Lhk2*$_{pro}$*::GUS* reporter activity associated with nodule (E-G) and lateral root (H) development; note the specific GUS staining in root pericycle cells positioned opposite protoxylem poles (arrows in H).

I-L *Lhk3*$_{pro}$*::GUS* reporter activity associated with nodule (I-K) and lateral root (L) development. Panel (L) represents a whole mount image while the remaining panels depict 35 µm sections.

All images represent specimens collected at 7 or 14 DAI with *M. loti*.

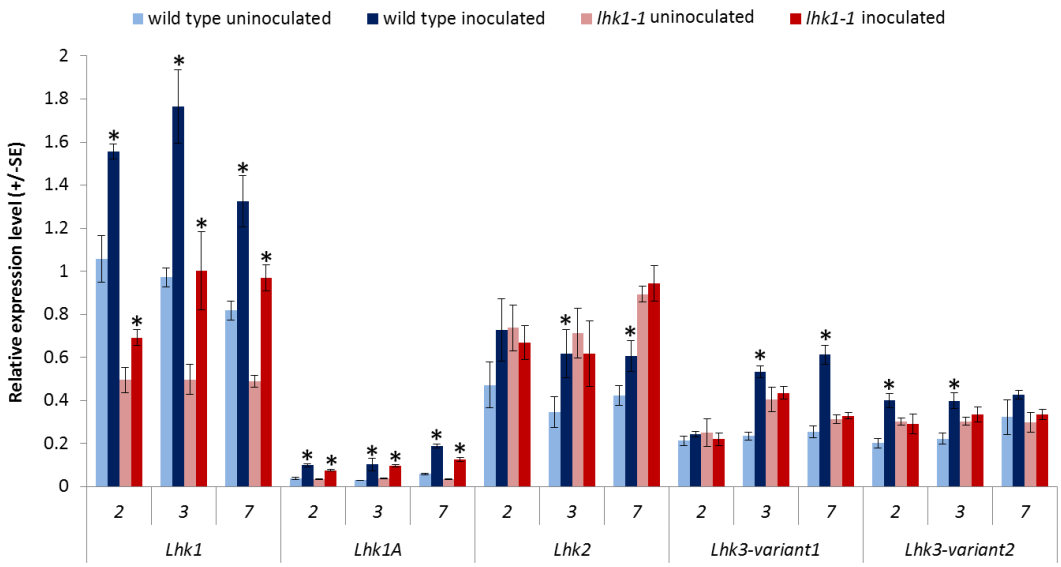

Figure 2.15 All four *Lhks* respond to *M. loti* inoculation.

The relative steady-state levels of all four *Lhk* transcripts in uninoculated roots and roots for the same age harvested, 9, 10 and 14 days after sowing are given. Note that plants were inoculated with *M. loti* 7 days after sowing such that each of the time points (i.e. 9, 10 and 14) reflect the measurement at 2, 3 and 7 DAI, respectively, for the inoculated samples. Average values for three biological replicates ± SE are given. Asterisks denote significant differences between the corresponding inoculated and uninoculated samples (Student's t test, $P < 0.05$).

function of LHK1A and LHK3. Two previously characterized *L. japonicus* mutations, namely *symRK-14* (Kosuta et al., 2011) and *arpc1-1* (Hossain et al., 2012), which abort root hair-dependent bacterial entry inside the root while leaving the nodule organogenesis intact or even enhanced, were used to test this hypothesis. We reasoned that if bacterial entry is indeed needed to form nodules in the *lhk1-1* background, combining these mutations with *lhk1-1* should prevent infection of the root cortex, resulting in a non-nodulating (Nod-) phenotype. In agreement with this prediction, both *symRK-14* and *arpc1-1* mutations almost entirely aborted bacterial entry inside *lhk1-1* roots when examined 21 and 35 DAI. While all three single mutants, *lhk1-1*, *symRK-14* and *arpc1-1* formed nodules and nodule primordia, the *lhk1-1 symRK-14* and *lhk1-1 arpc1-1* double mutants did not develop any nodules when analyzed 21 DAI with *M. loti*. This was also the case for the 35 DAI time point, except for *lhk1-1 symRK-14*, where one nodule-like structure was found among 15 roots analyzed (Figure 2.16).

2.3.15 The *lhk1-1 lhk1a-1 lhk3-1* cytokinin receptor triple mutant does not form nodules

We additionally tested the hypothesis that the LHK1, LHK1A and LHK3 receptors work partially redundantly to mediate nodule formation by constructing and then analyzing the phenotype of the triple mutant line that combined mutations in these cytokinin receptors genes.

Although viable and relatively healthy, the growth of the *lhk1-1 lhk1a-1 lhk3-1* triple mutant was significantly affected compared to wild-type *L. japonicus*. The average shoot and root mass of uninoculated triple mutant plants grown in the presence of potassium nitrate was only approximately half of the corresponding wild-type values when analyzed 28 days after sowing (Figure 2.17A and 2.17B). The length of the main root remained wild-type (Figure 2.17C), but the number of lateral and higher order roots was at least 5 times lower in the triple mutant (Figure 2.17D). When analyzed 7 DAI with *M. loti*, the triple mutant formed significantly more infection threads than wild-type *L. japonicus* Gifu of the same age (Figure 2.17E), but no nodule primordia or nodules were present in the mutant roots (Figure 2.17F and G). As overall growth of the triple mutant is slower,

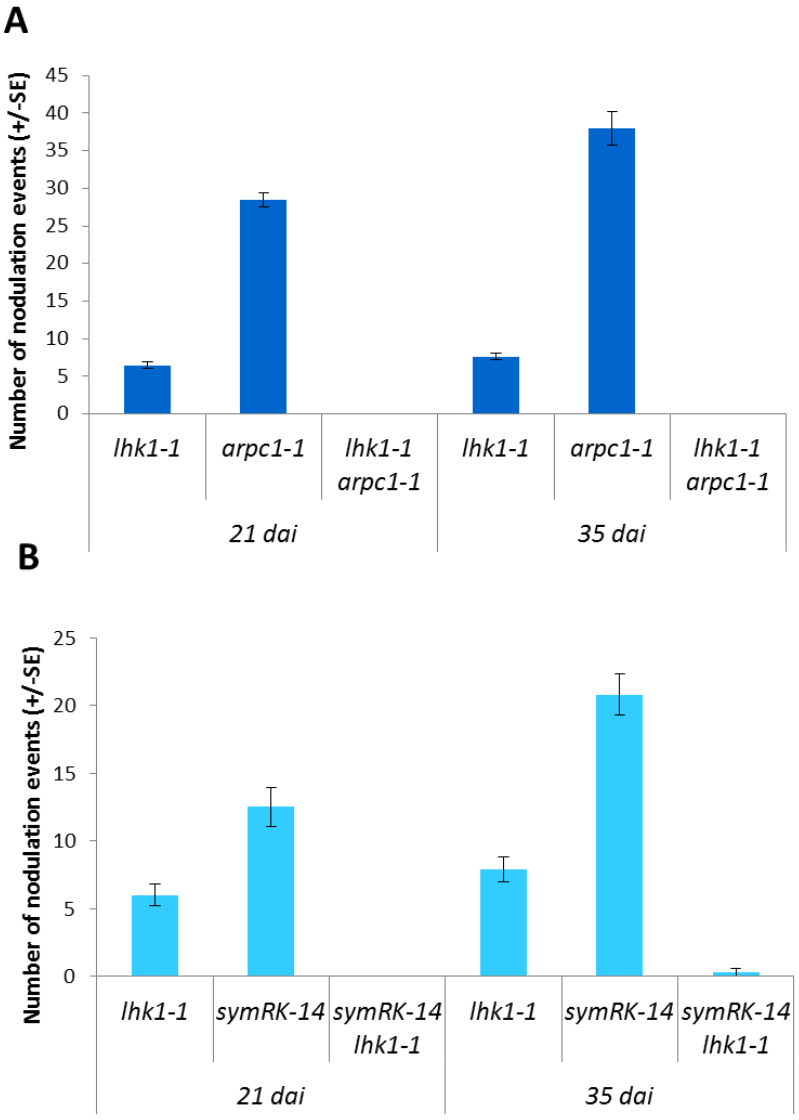

Figure 2.16 Signaling from within the root cortex.

The combined scores of nodule primordia and nodules (nodulation events) are given for *lhk1-1 arpc1-1* **(A)** and *lhk1-1 symRK-14* **(B)** double mutants and the corresponding single mutant lines. In all cases, values reported represent the mean ± SE (n = 10-15). The nodulation phenotypes were evaluated 21 and 35 days after infection with *M. loti*.

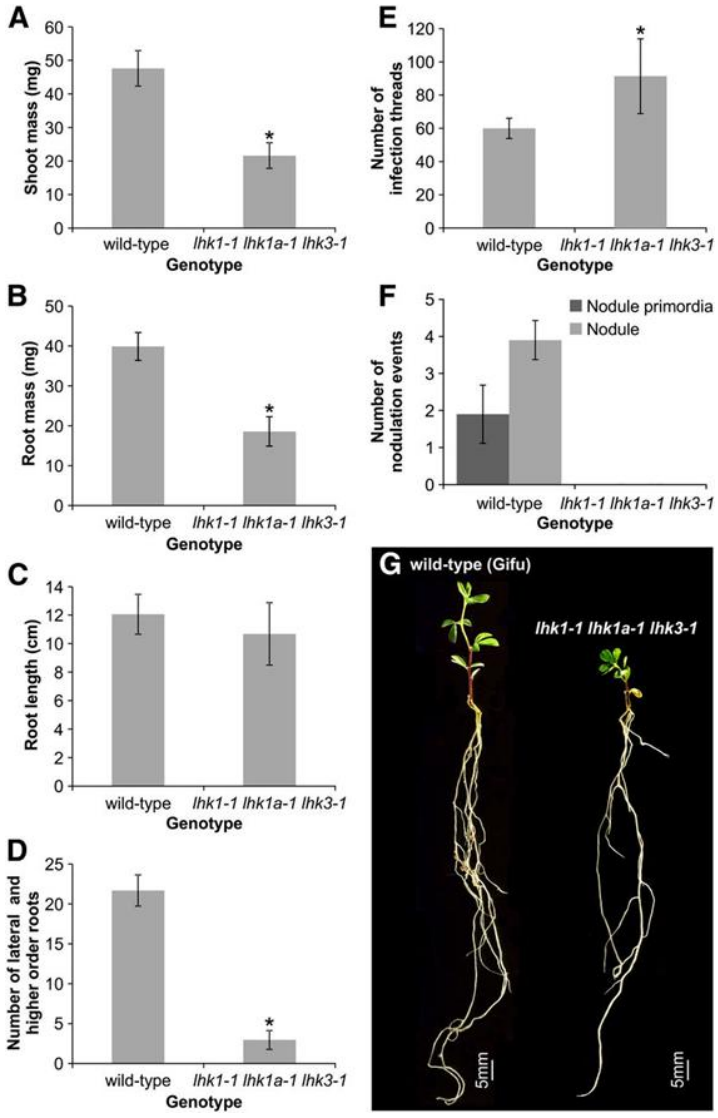

Figure 2.17 The *lhk1-1 lhk1a-1 lhk3-1* triple mutant does not form nodules.

(A) to **(D)** Shoot (A) and root (B) masses, as well as the root length (C) and the number of lateral and higher order roots (D), were scored in 28-day-old uninoculated *L. japonicus* (Gifu) wild-type and *lhk1-1 lhk1a-1 lhk3-1* triple receptor mutant plants grown in the presence of KNO_3. **(E)** and **(F)** Scores of infection threads (E) and nodulation events (i.e., nodule primordia and nodules) (F) are given for the *L. japonicus* wild type (Gifu) and the triple receptor mutant. All values reported represent means ± 95% confidence interval (*n* = 10 to 35) as measured 28 d after sowing ([A] to [D]) or 7 DAI with *M. loti* ([E] and [F]) for nodulation counts. Asterisks denote significant differences (Student's *t* test, $P < 0.05$). **(G)** Phenotypes of the wild type and the triple mutant are shown 21 DAI.

we additionally tested its nodulation phenotype at 21 and 35 DAI. While wild-type *L. japonicus* formed on average 9 ± 0.74 (n = 32) and 24 ± 3.55 (n = 20) fully developed nodules, respectively, the triple mutant (n = 19-35) did not develop any nodules or nodule primordia (Figure 2.17F).

2.3.16 Other receptors can substitute for LHK1 during nodule formation

Given the prominent role of LHK1, we asked whether other cytokinin receptors can substitute for its essential function in mediating nodule organogenesis. One important aspect of this was to test whether a non-legume cytokinin receptor could function in the nodulation pathway. If confirmed, this would indicate that the ability to respond to rhizobial signalling and or ectopic cytokinin by inciting nodule formation is not due to neo-functionalization of cytokinin receptors in legumes.

Hairy roots induced on *lhk1-1* mutant shoots via *Agrobacterium rhizogenes*-mediated transformation exaggerate the mutant nodulation phenotype, which results in a non-nodulating (Nod^-) or almost Nod^- phenotype (Murray et al., 2007). It has been previously demonstrated that nodulation can be restored to hairy roots formed on *lhk1-1* shoots by expressing the wild-type *Lhk1* gene (Murray et al., 2007). A similar complementation result was obtained in this study with the *Lhk1* cDNA expressed under the control of a constitutive CaMV 35S promoter (Figure 2.18). Nodulation was also restored to *lhk1-1* hairy roots by expressing either of the two *Lhk3* cDNA variants; however, *Lhk1A* and *Lhk2* cDNAs failed to complement the *lhk1-1* mutant phenotype (Figure 2.18). We then tested whether the *Arabidopsis AHK4* gene, including its own promoter and terminator, could restore nodule formation to *lhk1-1* transgenic hairy roots and indeed, this was the case (Figure 2.19).

A

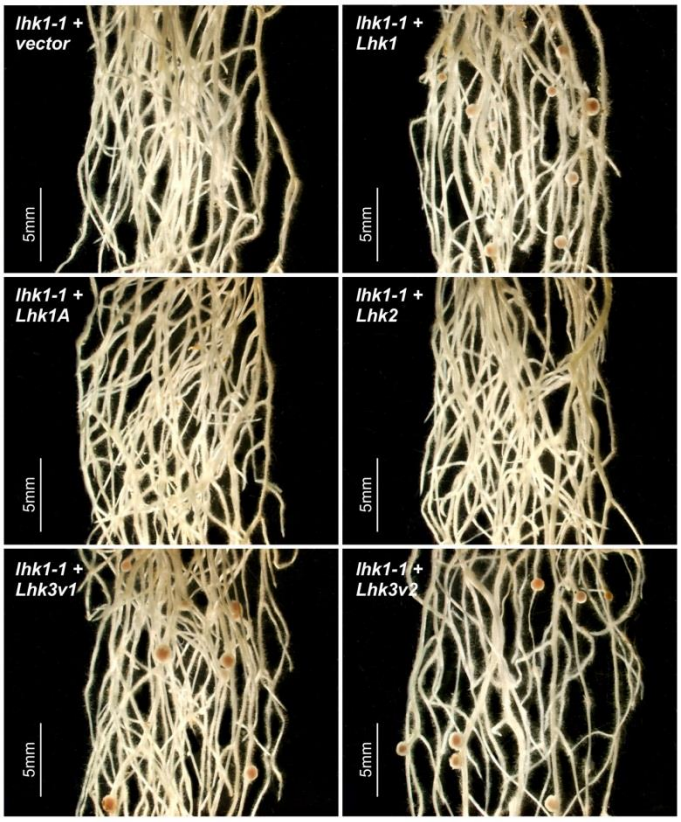

B

	Total # of plants	# Nodulated plants	Nodules/ nodulated plant
lhk1-1 + vector	32	0	0
lhk1-1 + Lhk1	20	16	17.8 ± 2.0
lhk1-1 + Lhk1A	29	0	0
lhk1-1 + Lhk2	3	0	0
lhk1-1 + Lhk3 variant #1	30	25	15.8 ± 2.7
lhk1-1 + Lhk3 variant #2	21	10	5.8 ± 1.4

Figure 2.18 *Lhk3* functionally replaces *Lhk1*.

The five *Lhk* cDNAs (*Lhk1*, *Lhk1A*, *Lhk2*, *Lhk3v1* and *Lhk3v2*) were expressed under the control of CaMV 35S promoter in the *lhk1-1* mutant background via *A. rhizogenes*-mediated hairy root transformation.

(A) Representative images of transgenic hairy roots are shown at 21 DAI with *M. loti.*

(B) Quantitative data for plants used and nodule frequency obtained are given. For *Lhk2*, only 3 plants were scored due to an apparent suppression of hairy root formation. In all cases, values represent the mean ± 95% CI.

B

	Total # of plants	# Nodulated plants	Nodules/ nodulated plant
Gifu	17	16	19.9 ± 7.7
lhk1-1 + vector	11	0	0
lhk1-1 + Lhk1	12	8	6.1 ± 2.7
lhk1-1 + AHK4	15	11	6.1 ± 3.8

Figure 2.19 *Arabidopsis* cytokinin receptor can mediate nodule organogenesis.

(**A**) Nodulation phenotypes of hairy roots formed on wild-type and *lhk1-1* mutant shoots after transformation with the *A. rhizogenes* strain AR12 containing empty vector (+vector), the entire *Lhk1*gene, including 5' and 3' UTRs (+*Lhk1*), or a vector containing the *Arabidopsis AHK4* gene, including its cognate promoter and terminator (+*AHK4*) (see Methods).

(**B**) The nodulation phenotypes were scored 21 DAI with *M. loti*. Numbers of plants and nodules in each transformation category are given. Wild-type *L. japonicus* ecotype Gifu transformed with *A. rhizogenes* AR12 was used as a positive control. In all cases, values represent the mean ± 95% CI.

2.4 Discussion

We show that *L. japonicus* contains a small family of four cytokinin receptor genes, including *Lhk2* that encodes a presumed cytokinin receptor, which all respond to *M. loti* infection. While further highlighting the prominent role of LHK1 (Murray et al., 2007; Tirichine et al., 2007; Heckmann et al., 2011), our data also demonstrate the involvement of other cytokinin receptors during *L. japonicus* nodule formation. We showed that only *Lhk1* is expressed in the root epidermis but it is also essential within the root cortex, where it mediates cell divisions for nodule primordia formation in a partially redundant manner with *Lhk1A* and *Lhk3*. *Lhk2* is not expressed in the root cortex and is unlikely, therefore, to be involved in the stimulation of cortical cell divisions, as mediated by LHK1, LHK1A, and LHK3. Consistent with this, the presence of *Lhk2* is not sufficient to induce nodule primordia formation in the *lhk1-1 lhk1a-1 lhk3-1* triple mutant.

2.4.1 *Arabidopsis* AHK4 mediates nodule organogenesis

The loss-of-function allele, *lhk1-1*, had roots that were insensitive to growth inhibition by applied cytokinin; none of the mutations in other cytokinin receptor genes had this effect. In this respect, LHK1 resembles its closest homolog in *Arabidopsis*, AHK4, which is the main sensor of external cytokinin in that species (Inoue et al., 2001; Nishimura et al., 2004). The similarity in the function of the two genes extends to their promoters, both of which are active almost ubiquitously in roots (Nishimura et al., 2004). We show, however, that *Lhk1* is less active in the *L. japonicus* root proximal meristem. Unlike *Lhk1*, expression of *Lhk2* and *Lhk3* in *L. japonicus* uninoculated roots was detectable only in the vasculature and the proximal meristem, respectively. This is different from the expression patterns described for their presumed *Arabidopsis* counterparts, *AHK2* and *AHK3* (Nishimura et al., 2004).

Our data show that *AHK4*, a cytokinin receptor gene from a non-legume species which does not form nodular symbiosis with rhizobia, can functionally substitute for *Lhk1* in mediating nodule organogenesis in *L. japonicus* upon *M. loti* infection. *Lhk3* also rescued the *lhk1-1* nodulation defect in hairy root experiments but this effect could not be achieved with *Lhk1A* or *Lhk2* cDNAs. The lack of complementation by *Lhk1A*, which is

the closest *L. japonicus* homolog of *Lhk1*, is puzzling and may reflect a need for additional regulatory sequences, beyond the cDNA used herein. Regardless, the ability of *AHK4* to complement nodulation suggests that the evolution of signaling for nodule primordia formation involved recruitment of a cytokinin receptor that has not been subjected to major, legume-specific modifications (Szczyglowski and Amyot, 2003). Consequently, the specificity of cytokinin signaling during nodule formation must be exerted downstream from the cytokinin perception. We cannot, however, rule out the possibility that the capacity for nodule formation is orchestrated by other cues that provide a unique legume-specific context to cytokinin signaling.

2.4.2 Unique properties of *Lhk1*

A distinct role for LHK1 is supported by several additional observations. *Lhk1*, but not other *Lhk* promoters, directs GUS activity to the root epidermis. External application of cytokinin to *L. japonicus* roots induced an increase in the steady-state level of the *Lhk1* mRNA within the first three hours, a response not mimicked by other *Lhk* mRNAs. This increase appears to be largely the consequence of an auto-regulatory mechanism, because it necessitates a functional copy of the *Lhk1* gene (Figure 2.10). The steady-state level of *Lhk1* mRNA was lower in untreated *lhk1-1* mutant roots as compared to wild-type roots, which further supports the existence of an inherent auto-regulatory feed-back mechanism.

Upregulation of *Lhk1A*, *Lhk2* and *Lhk3* mRNA levels after a prolonged, 12-hour treatment with BA was also *Lhk1*-dependent. The level of *Lhk1* mRNA in the *lhk1-1* mutant roots was still somewhat increased under these conditions (i.e. 12 hours/50 nM BA) (Figure 2.10D), perhaps due to effects of other cytokinin receptors.

When grown in soil in the presence or absence of *M. loti*, the existence of a regulatory relationship between different cytokinin receptors was also discernible. The steady-state level of *Lhk1* was significantly diminished in the *lhk1-1* mutant. *Lhk2* and *Lhk3* genes became unresponsive to, while the *Lhk1* mRNA was elevated by, *M. loti* infection, although its level remained at or below that of the uninoculated wild-type roots (Figure 2.15).

Taken together, these data demonstrate the prominent role of LHK1 during the perception and response of *L. japonicus* roots to both applied cytokinin and *M. loti* infection. They also suggest some degree of regulatory capacity, where LHK1 appears to exert a dominant role over its own expression but also over those of other cytokinin receptors. The underlying mechanism is unknown; nevertheless, given the rather distinct expression domains for *Lhk* genes, a functional link might be required to maintain homeostasis during root development.

2.4.3 LHK1 mediates signaling without bacterial entry into roots

Unlike wild-type *L. japonicus*, the *lhk1-1* mutant is unable to form nodules upon application of BA (Heckmann et al., 2011), but it does so in response to *M. loti* inoculation, albeit with noticeable delay and significant reduction in nodule number (see also (Murray et al., 2007). Thus, bacterial infection must be exerting an effect beyond what is being mimicked by ectopic cytokinin.

Consistent with this prediction, we show that formation of *lhk1-1* nodules is prevented by blocking bacterial entry inside roots with either *symRK-14* or *arpc1-1* mutations (Figure 2.16). This is unlike in *L. japonicus* plants carrying the wild-type *Lhk1* gene, where empty or initially empty nodules readily develop in the presence of various mutations that affect infections (Karas et al., 2005; Yokota et al., 2009; Groth et al., 2010), including *symRK-14* and *arpc1-1* (Kosuta et al., 2011; Hossain et al., 2012).

The simplest explanation for these observations is to assume that LHK1 participates, either directly or indirectly, in transducing a signal from the root epidermis to the subtending root cortex, regardless of whether the initial stimulus is ectopic cytokinin or *M. loti* NF. In the *lhk1-1* mutant, applied cytokinin would, therefore, be expected to fail in inducing nodule formation, which indeed is the case (Heckmann et al., 2011). Bacterial infection, however, could bypass the epidermis and initiate signaling for cell divisions from within the root cortex via redundantly acting LHK1A and/or LHK3 receptors. Although we cannot entirely rule out this explanation, our histochemical data point to a more complex signaling circuit during the response to bacterial infection.

2.4.4 LHK1, the master of symbiotic events

It has been shown that the induction of nodule primordia organogenesis in *L. japonicus* is regulated by a cytokinin-dependent mechanism that operates in the root cortex (Heckmann et al., 2011). Consistent with this, *M. loti* infection-dependent cytokinin signaling (as monitored by the *TCS*::*GUS* histochemical activity) was initially localized to the second and/or third cortical layers. This is where cell divisions for nodule primordia formation are first initiated in *L. japonicus* (van Spronsen et al., 2001). This expression pattern was paralleled, at least to some extent, by GUS activity driven by the *Lhk1* promoter, which also peaked initially within the middle cortex, although by default the *Lhk1* promoter is also active in the root epidermis.

A similar, inner cortex-localized primary cytokinin response was documented in *M. truncatula* roots responding to *S. melilloti* infection (Plet et al., 2011). It is therefore likely that another NF-dependent mechanism generates a cell non-autonomous signaling event that originates in the root epidermis and is rapidly translocated to incite the initial peak accumulation of bioactive cytokinin in the inner cortex. This could explain why a much longer time is needed to induce nodule formation in *L. japonicus* upon external application of cytokinin than upon bacterial infection (Heckmann et al., 2011).

We postulate that the initial cytokinin burst, as perceived by LHK1 within the root cortex, leads to an LHK1-dependent auto-stimulation (Figure 2.20A). This is manifested by a local increase in the level of the *Lhk1* mRNA. Our results show that in addition to *Lhk1*, the activities of *Lhk1A*, *Lhk2* and *Lhk3* promoters are also enhanced by *M. loti* infection. We have interpreted these events as leading to a local increase in cell sensitivity to cytokinin, a mechanism that is primarily reliant on LHK1 and by which a sufficient threshold is reached to initiate first cortical cell divisions for nodule primordia formation.

In the absence of functional LHK1, cell divisions for nodule primordia formation are initiated only upon bacterial entry (see also (Murray et al., 2007)) and we show that the presence of *Lhk1A* or *Lhk3* is critical in this context (Figure 2.20B). Lack of functional LHK1 leads to significantly reduced levels of *Lhk1*, which could explain why the

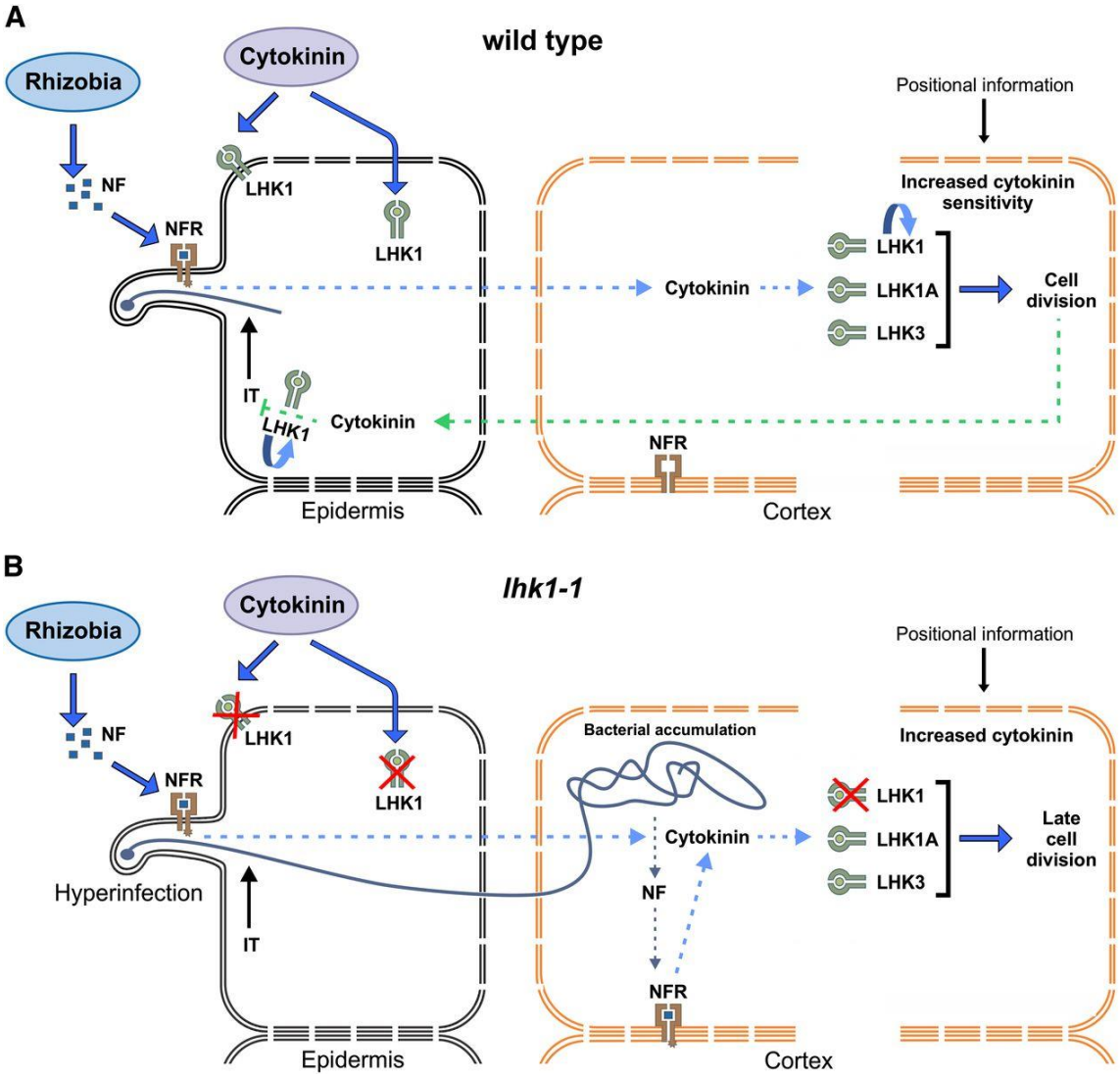
A
wild type
Rhizobia
Cytokinin
NF
NFR
LHK1
LHK1
Positional information
Increased cytokinin sensitivity
LHK1
LHK1A
LHK3
Cell division
Cytokinin
IT
LHK1
Cytokinin
NFR
Epidermis
Cortex
B
lhk1-1
Rhizobia
Cytokinin
NF
NFR
LHK1
LHK1
Positional information
Bacterial accumulation
Increased cytokinin
LHK1
LHK1A
LHK3
Late cell division
Cytokinin
NF
Hyperinfection
IT
NFR
Epidermis
Cortex

Figure 2.20 Working models for LHK1-dependent and LHK1-independent signaling for *L. japonicus* nodule formation.

(A) In wild-type *L. japonicus*, *M. loti* infection generates a presumed cell non-autonomous signaling event (dotted blue arrow), which triggers the accumulation of bioactive cytokinin and the subsequent stimulation of cortical cell divisions for nodule primordium formation prior to bacterial entry into the root. A feedback loop is induced downstream from advancing cell divisions, which results in the accumulation of cytokinin in the root epidermis; this is presumed to locally block subsequent infections (IT) in an LHK1-dependent manner.

(B) In the *lhk1-1* mutant, bacterial entry and accumulation inside the root are required for the initiation of cortical cell divisions (leading to late cell divisions). Lack of the LHK1-dependent feedback loop results in the hyperinfection of root epidermis and cortex. The "U-turn" arrows in (A) denote autostimulation of LHK1 expression. Ectopic cytokinin can be perceived either at the plasma membrane or upon movement inside the cell by the endoplasmic reticulum-localized cytokinin receptors (Wulfetange et al., 2011). "Positional information" refers to as yet undefined spatial information that dictates the position of the first cortical cell division for nodule primordium formation. NFR, nodulation factor receptor complex. For further details, see text.

threshold required for the stimulation of cortical cell divisions is not reached during the initial bacterial signaling, prior to their entry within the root cortex. Following heavy colonization of *lhk1-1* roots by *M. loti*, direct perception of NF within the root cortex might contribute to overcoming this limitation, which eventually leads to cell divisions (Figure 2.20B).

The evidence for NF perception in the root cortex was provided in the context of transcellular cortical infection threads, as formed by the *L. japonicus nfr1 nfr5 snf1 symrk-3* quadruple mutant (Madsen et al., 2010). The same mechanism likely accounts for delayed nodulation in the *lhk1-1* mutant. In many legumes, rhizobia can bypass the root epidermis, entering the root by a crack-entry mechanism (Sprent and James, 2007). It has been shown that a crack-entry like mechanism also operates in *L. japonicus* (Karas et al., 2005; Madsen et al., 2010; Kosuta et al., 2011) and signaling for nodule formation from within the root cortex in *lhk1-1* likely reflects this latent ability.

Rapid expansion and/or intensification of the cytokinin signaling in the root epidermis, including root hairs, was clearly observable early on, following some initial advancement in nodule primordia formation. This was true for the cytokinin response as well as the activity of the *Lhk1* promoter. Unlike *M. truncatula cre1* (Gonzalez-Rizzo et al., 2006), the *lhk1-1* mutant is hyperinfected by *M. loti* (Murray et al., 2007). Hence, LHK1, in addition to being the master of cortical events, may also prove to be the master of epidermal infections. In subsequent chapters, we consider the hypothesis that the increased cytokinin activity as mediated by LHK1 in the root epidermis prevents hyperinfection of *L. japonicus* roots by restricting subsequent infection events.

2.5 Experimental Procedures

2.5.1 Plant growth conditions

Seeds of wild-type Gifu and mutant *Lotus japonicus* plants were scarified lightly with sand paper and surface-sterilized following the previously established methods (Szczyglowski et al., 1998). Briefly, seeds were washed using the solution of 70% (v/v) ethanol and 0.1% (W/V) sodium dodecyl sulfate (SDS) for 1 minute, followed by a solution containing 20% bleach and 0.1% SDS for 1 minute. Sterilized seeds were rinsed at least 10 times with sterile Milli-Q water and allowed to imbibe overnight. Imbibed seeds were left to germinate on Petri plates containing sterilized Whatman filter paper moistened with sterilized Milli-Q water. Plates were sealed with parafilm and placed under continuous light at 23 ºC for a period of 7 days.

To assess the extent of root growth of the various genotypes, the previously established protocol was followed (Wopereis et al., 2000). Briefly, two day-old seedlings were transferred to vertical plates containing ½ B5 with minimal organics, 2.5 mM 2-(*N*-morpholino) ethanesulfonic acid (MES), 4.5% sucrose, and 0.8% phytagel. Roots were allowed to elongate for 7 days at room temperature in total darkness. Root elongation was scored and averaged for 10-20 roots per genotype. Where appropriate, cytokinin (6-benzylaminopurine, BA) was added (10^{-8}, 10^{-7}, 10^{-6}, and 10^{-5} M).

For studying the response of *L. japonicus* wild-type and *lhk1-1* plants to exogenous cytokinin, 10 day-old sand-vermiculate grown plants were transferred to beakers containing either sterile water or 50 nM BA, and incubated at room temperature with constant aeration. Roots were collected 6 and 12 hours post treatment and used for total RNA extraction as described (Murray et al., 2007).

2.5.2 Assessment of symbiotic phenotypes

Under sterile conditions, seven-day-old seedlings were transplanted into pots containing a 6:1 mixture of vermiculite and sand soaked with 1X B and D nutrient solution (Broughton and Dilworth, 1971), supplemented with 0.5 mM KNO3, under the standard growth condition of 18 hours light at 23 ºC and 6 hours dark at 18 ºC with 80% humidity.

After seven days, the seedlings were inoculated with either the wild-type *M. loti* strain NZP 2355 or *M. loti* containing the *hemA::LacZ* reporter cassette for visualization of bacterial infection (Wopereis et al., 2000). For histochemical analysis of β-galactosidase reporter gene activity, roots were fixed, stained, and cleared (Wopereis et al., 2000) at different time points as stated for each experiment.

2.5.3 Alternative splicing at the *Lhk3* locus

Primers were designed for PCR-based detection and expression-based studies of the two, alternative splice variants produced by the *Lhk3* locus (named *Lhk3* variant #1 and variant #2). For the comparative analysis of these two alternatively-spliced transcripts, 5'-end products were amplified from cDNA templates using a common reverse primer and a transcript-specific, forward primer (Table 2.3). The PCR cycling program was as follows: 5 min at 94 ºC, followed by 30 cycles of 94 ºC 30sec, 58 ºC 30sec, 68 ºC 1min, followed by a 7min at 68 ºC.

2.5.4 The *Lhk* mutants

The *lhk1-1* mutant has been described (Murray et al., 2007). Targeted Induced Localized Lesions IN Genomes (TILLING) was utilized for the identification of mutant alleles at the *Lhk1A*, *Lhk2*, and *Lhk3* loci. Briefly, TILLING is a mutagenesis technique which uses a chemical mutagen such as ethyl methanesulfonate (EMS) with a sensitive DNA screening-technique that identifies single base mutations (Perry et al., 2009). The primers used to generate amplicons for TILLING are listed in the Table 2.3. All selected TILLING mutant lines were back-crossed once to wild-type *L. japonicus* Gifu before extensive phenotypic analyses were conducted. To genotype plants carrying point mutations in *lhk* alleles, combinations of sequence analysis, cleavage amplification polymorphisms (CAPS), and derived CAPS (dCAPS) markers were used. The primers used for genotyping were listed in the Table 2.3.

Double mutants were developed by genetic crosses between primary homozygous single mutants for each of the two loci being analyzed. The F1 plants were allowed to self-fertilize and produce F2 segregating populations, from which the homozygous *lhk* double

mutants were selected. The F3 progenies from confirmed, homozygous double mutants were utilized for phenotypic evaluation.

The *lhk1-1 lhk1a-1 lhk3-1* cytokinin receptor triple mutant was selected from the F2 population of cross between homozygous *lhk1-1 lhk3-1* and *lhk1-1 lhk1a-1*. For the analysis of non-symbiotic phenotypes in uninoculated plants, including shoot and root mass, root length, and lateral root number, seven-day-old wild-type and triple mutant seedlings were transferred to pots containing a mixture of vermiculite and coarse sand and were supplemented with Hoagland's nutrient solution containing 6mM KNO3 (Hoagland and Arnon, 1950). Plants were harvested and analyzed 28 days after sowing. The symbiotic phenotype of the triple mutant was assessed as described above.

The additional alleles called *lhk1-4* (line no. 30016353), *lhk1a-12* (line no. 30006025), *lhk1a-13* (line no. 30007419), *lhk2-17* (line no. 30008546), *lhk2-18* (line no. 30006521), *lhk3-6* and *lhk3-7* were identified from the *L. japonicus* LORE1 retrotransposon mutant resource (https://lotus.au.dk/).The R3 generation seeds (3rd generation of tissue culture regenerated plants) carrying LORE1 insertions were received from *Lotus Base.* R3 is a segregation population. Therefore, seeds of the LORE1 insertion lines for each allele were sown and the seedlings were subjected to PCR-based genotyping using the gene and LORE1 specific primers, following the procedure (Urbański et al., 2012). The primers used for genotyping are listed in the Table 2.3.

2.5.5 Cytokinin-responsive assay in *S. cerevisiae*

All *Lhk* cDNAs were directionally cloned into the multi-cloning site of a yeast expression vector (P415CYC; Mumberg et al. 1995). The previously analyzed *Lhk1* cDNA was used as a positive control (Murray et al., 2007). Resultant constructs were transformed into the *sln1Δ* mutant of *S. cerevisiae* (kind gift from Tatsuo Kakimoto, Osaka University, Japan) and analyzed for response to treatments with different plant hormones, including 6-benzylaminopurine (BA), trans-zeatin (tZ), cis-zeatin (cZ) and the non-specific ligand, 1-naphthaleneacetic acid (NAA) as described (Murray et al., 2007). Putative loss-of-function mutant cDNAs were also analyzed using this assay.

2.5.6 Cytokinin-responsive assay in *E. coli*

The mutant and wild-type *Lhk* cDNAs were cloned into the *E. coli* expression vector pSTV28 (Tirichine et al., 2007). The resultant constructs were transformed into the sensor-negative *E. coli* SRC122 strain (kind gift from Dr. Takafumi Yamashino; Japan). Following transformation, colonies were grown on LB plates or in liquid LB medium containing 40 mM sodium phosphate buffer and 20 mM glucose, with or without the addition of 200 μM BA. For analysis of β-galactosidase activity, a standard assay was used as described (Tirichine et al., 2007).

2.5.7 Stable transgenic lines and GUS staining

To develop promoter-GUS fusions for *Lhk1*, *Lhk1A*, *Lhk2*, and *Lhk3*, approximately 4 kb promoter fragments were first amplified and cloned into the pKGWFS7,0 destination vector (GUS and GFP reporters) using the Gateway™ technology (Invitrogen).

A synthetic, cytokinin two-component-output sensor (TCS) was used to follow the presence of bioactive cytokinin. TCS harbours the concatemerized B-type *Arabidopsis* response regulator (ARR)-binding motifs and a minimal 35S promoter, followed by the TMV-omega sequence, as described (Müller and Sheen 2008). The TCS promoter was amplified from the TCS min35S-ΩeGFP ER vector (pCB302; kind gift from Dr. Jen Sheen) and was cloned into the pKGWFS7,0 destination vector using the Gateway™ technology (Invitrogen). The list of the primers used is under localization analysis in Table 2.3.

After validation of the insert by sequencing, the corresponding vectors were transferred to *Agrobacterium tumefaciens* LBA4404. Standard transformation protocols (Lombari et al., 2005) were used to regenerate fully transgenic plants from hypocotyl segments of wild-type (ecotype ‘Gifu’) *L. japonicus* plants. At least seven independent transgenic plants were used for analyses of promoter expression.

Detection of the GUS reporter activity was routinely conducted using a staining solution which contained 0.1M potassium phosphate buffer, 5 mM EDTA, 0.5 mM potassium ferric- and ferrous-cyanides, and 0.5 mg/ml 5-bromo-4-chloro-3-indolyl glucuronide

cyclohexylammonium salt (X-GLUC; Fermentas). All tissues were vacuum-infiltrated for 15 min, stained overnight at room temperature or 37^{0}C and cleared, as described previously (Wopereis et al., 2000).

2.5.8 Quantitative real-time RT-PCR assay

Total RNA was extracted using an RNeasy Plant Mini Kit (Qiagen) and was treated with DNase I. The concentration and purity of RNA was determined by measuring absorbance at 260/280 nm. cDNA was prepared from 1 µg of total RNA using the High Capacity cDNA Synthesis Kit (Applied Biosystems) with random primers. Negative control reactions to which no reverse transcriptase was added (-RT) were included for each RNA sample. Quantitative RT-PCR reactions were performed in triplicate (i.e. three biological and three technical replicates) on a CFX-96 Real-Time PCR Detection System (BioRad) using PerfeCTa SYBR Green FastMix (Quanta Biosciences). Five reference genes, including UBC (ubiquitin-conjugating enzyme), PP2A (protein phosphatase 2A), TB2C (tubulin beta chain), ATP-S (ATP synthase), and PubQ (ubiquitin) were used to normalize results as previously described (Tirichine et al. 2007). Primer sequences used for the real time qPCR expression analyses can be found in Table 2.3.

2.5.9 Complementation of the *lhk1-1* nodulation defect

For hairy root complementation, the binary vector BIN19 containing the entire Arabidopsis Histidine Kinase 4 (AHK4) gene, including its cognate promoter and terminator regions was used (kind gift from Dr. Chiharu Ueguchi, Nagoya University, Japan).

To overexpress different *Lhk* mRNA in the *lhk1-1* mutant background, *Lhk* cDNAs were cloned into the pEarleyGate100 destination vector using the Gateway^{TM} technology and subsequently transformed into *A. rhizogenes* strain AR1193. Standard *A. rhizogenes*-mediated transformation procedures were followed to induce the formation of hairy roots on *lhk1-1* mutant shoots (Petit et al., 1987). The chimeric plants witch developed hairy roots were transferred to soil and at least 10 independent plants per genotype were assessed for presence of nodules 21 DAI with *M. loti*.

2.5.10 Microscopy and image analysis

All microscopic observations were performed on a Nikon SMZ1500 (Nikon, Japan) dissecting or Zeiss Axioskop 2 (Zeiss, Germany) compound light microscope. Both microscopes were integrated with a Nikon DXM1200 digital camera using the ACT1 media software (Nikon). All images captured were taken in a TIFF format at a resolution of 3840 X 3072. Longitudinal and cross-sections of root and/or nodule segments were generated by embedding specimens in 3% (w/v) agar blocks and sectioning to 35 μm thickness using a Leica VT 1000S vibratome (Leica Microsystems Inc., USA).

2.5.11 Statistical analyses

In all cases, means were calculated from data ranges containing no fewer than 10 plants per genotype or per treatment. Pair-wise comparisons were made using a Student's t-Test assuming unequal variance.

2.5.12 Phylogenetic analysis

All sequence alignments were generated in Clustal Omega (http://www.ebi.ac.uk/Tools/msa/clustalo/) using default settings. The Maximum Likelihood method of the MEGA 6.0.5 package (http://www.megasoftware.net/mega.php) and branch support test from 1000 bootstrap repetitions were used.

2.5.13 Computer analyses

Databases were searched with standard protein BLAST (http://www.ncbi.nlm.nih.gov/), which also predicts putative conserved domains.

2.5.14 Accession numbers

Sequence data from this article can be found in the GenBank/EMBL libraries under the following accession numbers: *Lhk1* (ABI48271); *Lhk1A* (DQ848998; former *Lhk2*, see Murray et al., 2007); *Lhk2* (KJ361851) and *Lhk3* (KJ361852); *AHK4* (NP_565277.1); *AHK2* (NP_568532.1); and *AHK3* (NP_564276.1).

Table 2.3 Full primer sequences used in this study.

Name of primers	**Primer sequence (5'-3')**
Alternative splicing at the *Lhk3* locus	
Lhk3 variant #1-FWD	CTTATATGAAGGGTGGTTTTGG
Lhk3 variant #2-FWD	GGTTGGTTACTGTTGTGGATGA
Lhk3 common-REV	CTTTCCAGAAAGCACGTCAAC
Generate amplicon for TILLING experiment	
LHK1A-FWD	TGTCCATGCTTCGAGCCCAATGAGTCC
LHK1A-REV	AAACCCACCCAGAATGGAAAATATGTC
LHK2-FWD	ACAGTTGGCTGTTTATGCATCT
LHK2-REV	TTTTTAGGCAGCGCTCTAATGCCAATG
LHK3-FWD	TGATGTACGGGCAATTCTGGATGATGT
LHK3-REV	GCTTACCCATCCATTTCTGGCATTTGA
Genotyping for the point mutations in *lhk* alleles	
lhk1-1-CAPS-BccI-FWD	CCTTTGATGTTGAGTCCCTTGT
lhk1-1-CAPS-BccI-REV	CTGCTGATAATTGATAAACCACTGA
lhk1a-1-Seq-FWD	CTCACAAGGGACTTGCTGATT
lhk1a-1-Seq-REV	AAACCCACCCAGAATGGAAAATATGTC
lhk2-5-Seq-FWD	GCGATCCTAAACGATTCCGGCAAATAA
lhk2-5-Seq-REV	TTTTAGGCAGCGCTCTAATGCCAATG
lhk3-1-dCAPS-SalI-FWD	TAATAGGTGATCCAGGAAGGTGTC
lhk3-1-dCAPS-SalI-REV	GGTGCATGCCTATAAGGAAAGA
Genotyping for LORE1 insertional *lhk* alleles	
lhk1-4-30016353-FWD	GCAAGTGGATTGCACAACATTGCCC
lhk1-4-30016353-REV	GCAGCTTTGCCACTTGCTGCACAT
lhk1a-12-30006025-FWD	TTTGTCCACAATTCCGCAACGCAG
lhk1a-12-30006025-REV	GCAGCCCAGTGAATTTGCTGCTGA
lhk1a-13-30007419-FWD	CGGAATTGTGGACAAATGCGGGTC
lhk1a-13-30007419-REV	GCTTTCCCAGTGGCCCTAGCCCTT
lhk2-17-30008546-FWD	TTGAGAACCAGCATGGGTGGACAA
lhk2-17-30008546-REV	TTGATGTTGGTAAGTGAGGCACCCA
lhk2-18-30006521-FWD	CCAGATGCAACAGTGGAGCAGCGT
lhk2-18-30006521-REV	CCAAGGGTGTGGAGGCCTTTGCTT
lhk3-6-30000134-FWD	TGTCAGAACAGCGCAGGACAGTGG
lhk3-6-30000134-REV	GAATCCCTCCCAGCTCTTGCGGAT
lhk3-7-30011166 -FWD	CCACGGATGCGTTCTATCATGTCAGC
lhk3-7-30011166 -REV	AAACCTGCCACACTTTGGGCCTGA
LORE1-specifc-P2	CCATGGCGGTTCCGTGAATCTTAGG
Localization analysis	
LHK1-Promoter-GW-FWD	AAAAAGCAGGCTCAGGCTTTCTCAGGAGAG GTT
LHK1-Promoter-GW-REV	AGAAAGCTGGGTTTTTCTCTGGTGGGTTGAT

	TG
LHK1A-Promoter-FWD	AAAAAGCAGGCTTAGCGATGAAGGAGACAAACCT
LHK1A-Promoter-REV	AGAAAGCTGGGTCGTGAAACTGCTACTGGTCTTG
LHK2-Promoter-FWD	AAAAAGCAGGCTATGAAGTAACATGCACGACGAT
LHK2-Promoter-REV	AGAAAGCTGGGTATGAAGTAACATGCACGACGAT
LHK3-Promoter-FWD	AAAAAGCAGGCTACATATTCACACCAGGTCACCA
LHK3-Promoter-REV	AGAAAGCTGGGTGCTGTCTTATCCACCCAATAGC
TCS-FWD	GGGGACAAGTTTGTACAAAAAAGCAGGCTGAAGCTTATGCTAGCAAAATCT
TCS-REV	GGGGACCACTTTGTACAAGAAAGCTGGGTTGTTATATCTCCTTGGATCGAT
qRT-PCR expression analysis	
Lhk1-qPCR-FWD	GTGCTTAAATTGTGGGATGGA
Lhk1-qPCR-REV	ATTGATGCTGGGAGAAGTTGA
Lhk1A-qPCR-FWD	TCAAAGCCATTTGAGGAACAG
Lhk1A-qPCR-REV	GCATAGTTTACCTGCAACATCTG
Lhk2-qPCR-FWD	ATGGATGGCTACGTGTCAAAG
Lhk2-qPCR-REV	GCATACGTTGTTGATTGAATGC
Lhk3-variant 1-qPCR-FWD	CTTATATGAAGGGTGGTTTTGG
Lhk3-variant 1-qPCR-REV	TTGTCTCTTCACTCCCTTGGA
Lhk3-variant 2-qPCR-FWD	TCAGCTGCAATTCACAAACTC
Lhk3-variant 2-qPCR-REV	ACAACCCAGCAACATAGCACT
UBC-FWD	ATGTGCATTTTAAGACAGGG
UBC-REV	GAACGTAGAAGATTGCCTGAA
PP2A-FWD	GTAAATGCGTCTAAAGATAGGGTCC
PP2A-REV	ACTAGACTGTAGTGCTTGAGAGGC
TB2C-FWD	GCTCACCACCCCAAGCTTTGG
TB2C-REV	TGTCAATGGAGCAAACCCAACC
ATP-S-FWD	AACACCACTCTCGATCATTTCTCTG
ATP-S-REV	CAATGTCGCCAAGGCCCATGGTG
PUB-FWD	ATGCAGATCTTTTGTGAAGAC
PUBQ-REV	ACCACCACGGAAGACGGAG

2.6 References

Amasino, R. (2005). 1955: Kinetin arrives. The 50th anniversary of a new plant hormone. Plant Physiol. **138:** 1177-1184.

Bauer, P., Ratet, P., Crespi, M.D., Schultze, M., and Kondorosi, A. (1996). Nod factors and cytokinins induce similar cortical cell division, amyloplast deposition and *MsEnoD12A* expression patterns in alfalfa roots. Plant J. **10:** 91-105.

Bek, A.S., Sauer, J., Thygesen, M.B., Duus, J.Ø., Petersen, B.O., SørenThirup, James, E., Jensen, K.J., Stougaard, J., and Radutoiu, S. (2010). Improved characterization of nod factors and genetically based variation in LysM receptor domains identify amino acids expendable for nod factor recognition in *Lotus* spp. Mol. Plant-Microbe Interact. **23:** 58-66.

Broughton, W.J., and Dilworth, M.J. (1971). Control of leghaemoglobin synthesis in snake beans. Biochem. J. **125:** 1075-1080.

Cooper, J.B., and Long, S.R. (1994). Morphogenetic rescue of *Rhizobium meliloti* nodulation mutants by *trans*-zeatin secretion. Plant Cell **6:** 215-225.

Ferreira, F.J., and Kieber, J.J. (2005). Cytokinin signaling. Curr. Opin. Plant Biol. **8:** 518-525.

Frugier, F., Kosuta, S., Murray, J.D., Crespi, M., and Szczyglowski, K. (2008). Cytokinin: secret agent of symbiosis. Trends Plant Sci. **13:** 115-120.

Fukai, E., Umehara, Y., Sato, S., Endo, M., Kouchi, H., Hayashi, M., Stougaard, J., and Hirochika, H. (2010). Derepression of the plant chromovirus *LORE1* induces germline transposition in regenerated plants. PLoS Genet. **6**.

Fukai, E., Soyano, T., Umehara, Y., Nakayama, S., Hirakawa, H., Tabata, S., Sato, S., and Hayashi, M. (2012). Establishment of a *Lotus japonicus* gene tagging population using the exon-targeting endogenous retrotransposon *LORE1*. Plant J. **69:** 720-730.

Gleason, C., Chaudhuri, S., Yang, T., Muñoz, A., Poovaiah, B.W., and Oldroyd, G.E.D. (2006). Nodulation independent of rhizobia induced by a calcium-activated kinase lacking autoinhibition. Nature **441:** 1149-1152.

Gonzalez-Rizzo, S., Crespi, M., and Frugier, F. (2006). The *Medicago truncatula* CRE1 cytokinin receptor regulates lateral root development and early symbiotic interaction with *Sinorhizobium meliloti*. Plant Cell **18:** 2680-2693.

Groth, M., Takeda, N., Perry, J., Uchid, H., Dräxl, S., Brachmann, A., Sato, S., Tabata, S., Kawaguchi, M., Wang, T.L., and Parniskea, M. (2010). *NENA*, a

Lotus japonicus homolog of *Sec13*, is required for rhizodermal infection by arbuscular mycorrhiza fungi and rhizobia but dispensable for cortical endosymbiotic development. Plant Cell **22:** 2509-2526.

Hayashi, T., Banba, M., Shimoda, Y., Kouchi, H., Hayashi, M., and Imaizumi-Anraku, H. (2010). A dominant function of CCaMK in intracellular accommodation of bacterial and fungal endosymbionts. Plant J. **63:** 141-154.

Heckmann, A.B., Sandal, N., Bek, A.S., Madsen, L.H., Jurkiewicz, A., Nielsen, M.W., Tirichine, L., and Stougaard, J. (2011). Cytokinin induction of root nodule primordia in *Lotus japonicus* is regulated by a mechanism operating in the root cortex. Mol. Plant-Microbe Interact. **24:** 1385-1395.

Heyl, A., Riefler, M., Romanov, G.A., and Schmülling, T. (2012). Properties, functions and evolution of cytokinin receptors. Eur. J. Cell Biol. **91:** 246-256.

Heyl, A., Wulfetange, K., Pils, B., Nielsen, N., Romanov, G.A., and Schmülling, T. (2007). Evolutionary proteomics identifies amino acids essential for ligand-binding of the cytokinin receptor CHASE domain. BMC Evol. Biol. **7**.

Hoagland, D.R., and Arnon, D.I. (1950). The water culture method for growing plants without soil. Calif. Agric. Exp. Stn. Circ. **347:** 347.

Hossain, M.S., Liao, J., James, E.K., Sato, S., Tabata, S., Jurkiewicz, A., Madsen, L.H., Stougaard, J., Ross, L., and Szczyglowski, K. (2012). *Lotus japonicus* ARPC1 is required for rhizobial infection. Plant Physiol. **160:** 917-928.

Hwang, I., Sheen, J., and Müller, B. (2012). Cytokinin signaling networks. In Annual Review of Plant Biology, pp. 353-380.

Inoue, T., Higuchi, M., Hashimoto, Y., Seki, M., Kobayashi, M., Kato, T., Tabata, S., Shinozaki, K., and Kakimoto, T. (2001). Identification of CRE1 as a cytokinin receptor from Arabidopsis. Nature **409:** 1060-1063.

Karas, B., Murray, J., Gorzelak, M., Smith, A., Sato, S., Tabata, S., and Szczyglowski, K. (2005). Invasion of *Lotus japonicus root hairless 1* by *Mesorhizobium loti* involves the nodulation factor-dependent induction of root hairs. Plant Physiol. **137:** 1331-1344.

Kosuta, S., Held, M., Hossain, M.S., Morieri, G., MacGillivary, A., Johansen, C., Antolín-Llovera, M., Parniske, M., Oldroyd, G.E.D., Downie, A.J., Karas, B., and Szczyglowski, K. (2011). *Lotus japonicus* symRK-14 uncouples the cortical and epidermal symbiotic program. Plant J. **67:** 929-940.

Lerouge, P., Roche, P., Faucher, C., Maillet, F., Truchet, G., Promé, J.C., and Dénarié, J. (1990). Symbiotic host-specificity of *Rhizobium meliloti* is determined by a sulphated and acylated glucosamine oligosaccharide signal. Nature **344:** 781-784.

Lohar, D.P., Schaff, J.E., Laskey, J.G., Kieber, J.J., Bilyeu, K.D., and Bird, D.M. (2004). Cytokinins play opposite roles in lateral root formation, and nematode and Rhizobial symbioses. Plant J. **38:** 203-214.

Lombari, P., Ercolano, E., El Alaouri, E., and Chiurazzi, M. (2005). *Agrobacterium*-mediated in vitro transformation. *Lotus japonicus* Handbook**:** 87-95.

Madsen, E.B., Madsen, L.H., Radutoiu, S., Olbryt, M., Rakwalska, M., Szczyglowski, K., Sato, S., Kaneko, T., Tabata, S., Sandal, N., and Stougaard, J. (2003). A receptor kinase gene of the LysM type is involved in legume perception of rhizobial signals. Nature **425:** 637-640.

Madsen, L.H., Fukai, E., Radutoiu, S., Yost, C.K., Sandal, N., Schauser, L., and Stougaard, J. (2005). LORE1, an active low-copy-number TY3-*gypsy* retrotransposon family in the model legume *Lotus japonicus*. Plant J. **44:** 372-381.

Madsen, L.H., Tirichine, L., Jurkiewicz, A., Sullivan, J.T., Heckmann, A.B., Bek, A.S., Ronson, C.W., James, E.K., and Stougaard, J. (2010). The molecular network governing nodule organogenesis and infection in the model legume *Lotus japonicus*. Nat. Commun. **1:** 10.

Maeda, T., Wurgler-Murphy, S.M., and Saito, H. (1994). A two-component system that regulates an osmosensing MAP kinase cascade in yeast. Nature **369:** 242-245.

Malolepszy, A., Mun, T., Sandal, N., Gupta, V., Dubin, M., Urbański, D., Shah, N., Bachmann, A., Fukai, E., Hirakawa, H., Tabata, S., Nadzieja, M., Markmann, K., Su, J., Umehara, Y., Soyano, T., Miyahara, A., Sato, S., Hayashi, M., Stougaard, J., and Andersen, S.U. (2016). The *LORE1* insertion mutant resource. Plant J. **88:** 306-317.

Müller, B., and Sheen, J. (2008). Cytokinin and auxin interaction in root stem-cell specification during early embryogenesis. Nature **453:** 1094-1097.

Murray, J.D., Karas, B.J., Sato, S., Tabata, S., Amyot, L., and Szczyglowski, K. (2007). A cytokinin perception mutant colonized by *Rhizobium* in the absence of nodule organogenesis. Science **315:** 101-104.

Nishimura, C., Ohashi, Y., Sato, S., Kato, T., Tabata, S., and Ueguchi, C. (2004). Histidine kinase homologs that act as cytokinin receptors possess overlapping functions in the regulation of shoot and root growth in arabidopsis. Plant Cell **16:** 1365-1377.

Perry, J., Brachmann, A., Welham, T., Binder, A., Charpentier, M., Groth, M., Haage, K., Markmann, K., Wang, T.L., and Parniske, M. (2009). TILLING in *Lotus japonicus* identified large allelic series for symbiosis genes and revealed a bias in functionally defective ethyl methanesulfonate alleles toward glycine replacements. Plant Physiol. **151:** 1281-1291.

Petit, A., Stougaard, J., Kühle, A., Marcker, K.A., and Tempé, J. (1987). Transformation and regeneration of the legume *Lotus corniculatus*: A system for molecular studies of symbiotic nitrogen fixation. MGG **207:** 245-250.

Plet, J., Wasson, A., Ariel, F., Le Signor, C., Baker, D., Mathesius, U., Crespi, M., and Frugier, F. (2011). MtCRE1-dependent cytokinin signaling integrates bacterial and plant cues to coordinate symbiotic nodule organogenesis in *Medicago truncatula*. Plant J. **65:** 622-633.

Radutoiu, S., Madsen, L.H., Madsen, E.B., Felle, H.H., Umehara, Y., Grønlund, M., Sato, S., Nakamura, Y., Tabata, S., Sandal, N., and Stougaard, J. (2003). Plant recognition of symbiotic bacteria requires two LysM receptor-like kinases. Nature **425:** 585-592.

Sieberer, B.J., Chabaud, M., Fournier, J., Timmers, A.C.J., and Barker, D.G. (2012). A switch in Ca^{2+} spiking signature is concomitant with endosymbiotic microbe entry into cortical root cells of *Medicago truncatula*. Plant J. **69:** 822-830.

Singh, S., and Parniske, M. (2012). Activation of calcium- and calmodulin-dependent protein kinase (CCaMK), the central regulator of plant root endosymbiosis. Curr. Opin. Plant Biol. **15:** 444-453.

Sprent, J.I., and James, E.K. (2007). Legume evolution: Where do nodules and mycorrhizas fit in? Plant Physiol. **144:** 575-581.

Szczyglowski, K., and Amyot, L. (2003). Symbiosis, inventiveness by recruitment? Plant Physiol. **131:** 935-940.

Szczyglowski, K., Shaw, R.S., Wopereis, J., Copeland, S., Hamburger, D., Kasiborski, B., Dazzo, F.B., and De Bruijn, F.J. (1998). Nodule organogenesis and symbiotic mutants of the model legume *Lotus japonicus*. Mol. Plant-Microbe Interact. **11:** 684-697.

Tirichine, L., James, E.K., Sandal, N., and Stougaard, J. (2006). Spontaneous root-nodule formation in the model legume *Lotus japonicus*: A novel class of mutants nodulates in the absence of rhizobia. Mol. Plant-Microbe Interact. **19:** 373-382.

Tirichine, L., Sandal, N., Madsen, L.H., Radutoiu, S., Albrektsen, A.S., Sato, S., Asamizu, E., Tabata, S., and Stougaard, J. (2007). A gain-of-function mutation in a cytokinin receptor triggers spontaneous root nodule organogenesis. Science **315:** 104-107.

Truchet, G., Barker, D.G., Camut, S., de Billy, F., Vasse, J., and Huguet, T. (1989). Alfalfa nodulation in the absence of *Rhizobium*. MGG **219:** 65-68.

Ueguchi, C., Koizumi, H., Suzuki, T., and Mizuno, T. (2001). Novel family of sensor histidine kinase genes in *Arabidopsis thaliana*. Plant Cell Physiol. **42:** 231-235.

Urbański, D.F., Małolepszy, A., Stougaard, J., and Andersen, S.U. (2012). Genome-wide *LORE1* retrotransposon mutagenesis and high-throughput insertion detection in *Lotus japonicus*. Plant J. **69:** 731-741.

van Spronsen, P.C., Grønlund, M., Bras, C.P., Spaink, H.P., and Kijne, J.W. (2001). Cell biological changes of outer cortical root cells in early determinate nodulation. Mol. Plant-Microbe Interact. **14:** 839-847.

Verdier, J., Torres-Jerez, I., Wang, M., Andriankaja, A., Allen, S.N., He, J., Tang, Y., Murray, J.D., and Udvardi, M.K. (2013). Establishment of the *Lotus japonicus* Gene Expression Atlas (LjGEA) and its use to explore legume seed maturation. Plant J. **74:** 351-362.

Wais, R.J., Galera, C., Oldroyd, G., Catoira, R., Penmetsa, R.V., Cook, D., Gough, C., Dénarié, J., and Long, S.R. (2000). Genetic analysis of calcium spiking responses in nodulation mutants of *Medicago truncatula*. Proc. Natl. Acad. Sci. U. S. A. **97:** 13407-13412.

Walker, S.A., and Downie, J.A. (2000). Entry of *Rhizobium leguminosarum* bv. *viciae* into root hairs requires minimal nod factor specificity, but subsequent infection thread growth requires *nodO* or *nodE*. Mol. Plant-Microbe Interact. **13:** 754-762.

Wopereis, J., Pajuelo, E., Dazzo, F.B., Jiang, Q., Gresshoff, P.M., De Bruijn, F.J., Stougaard, J., and Szczyglowski, K. (2000). Short root mutant of *Lotus japonicus* with a dramatically altered symbiotic phenotype. Plant J. **23:** 97-114.

Wulfetange, K., Lomin, S.N., Romanov, G.A., Stolz, A., Heyl, A., and Schmülling, T. (2011). The cytokinin receptors of arabidopsis are located mainly to the endoplasmic reticulum. Plant Physiol. **156:** 1808-1818.

Yamada, H., Suzuki, T., Terada, K., Takei, K., Ishikawa, K., Miwa, K., Yamashino, T., and Mizuno, T. (2001). The Arabidopsis AHK4 histidine kinase is a cytokinin-binding receptor that transduces cytokinin signals across the membrane. Plant Cell Physiol. **42:** 1017-1023.

Yokota, K., Fukai, E., Madsen, L.H., Jurkiewicz, A., Rueda, P., Radutoiu, S., Held, M., Hossain, M.S., Szczyglowski, K., Morieri, G., Oldroyd, G.E.D., Downie, J.A., Nielsen, M.W., Rusek, A.M., Sato, S., Tabata, S., James, E.K., Oyaizu, H., Sandal, N., and Stougaard, J. (2009). Rearrangement of actin cytoskeleton mediates invasion of *Lotus japonicus* roots by *Mesorhizobium loti*. Plant Cell **21:** 267-284.

Chapter 3

3 Into the root: how cytokinin controls rhizobial infection

Mandana Miri[1,2], Preetam Janakirama[1], Mark Held[1], Loretta Ross[1] and Krzysztof Szczyglowski[1,2*]

[1]Agriculture and Agri-Food Canada, Southern Crop Protection and Food Research Centre, London, Ontario, Canada, NV5 4T3.

[2]Department of Biology, University of Western Ontario, London, Ontario, Canada, N6A 5BF.

A version of this chapter has been published in the *Trends in Plant Science* Journal. Permission has been granted for inclusion of the article “Into the root: how cytokinin controls rhizobial infection” published in the *Trends in Plant Science*, Volume 21, pages 178-186, March 2016, in this thesis (Appendix A).

In this chapter, it is postulated that cytokinin participates in orchestrating the signaling events that promote rhizobial colonization of the root cortex and limit the extent of subsequent infection at the root epidermis, thus maintaining homeostasis of the symbiotic interaction. Accordingly, it is shown that plant mutants with defects in cytokinin receptors display aberrant rhizobial infection phenotypes.

3.1 Introduction

The perception of nodulation factors (NF) by the host plant LysM motif receptor kinase complex (Broghammer et al., 2012) initiates a range of primary cellular responses, including the root hair tip-localized calcium influx and calcium spiking (Morieri et al., 2013). Acting as a secondary messenger, the NF-induced calcium evolutions facilitate links with intrinsic plant developmental pathways. This is achieved, at least in part, through the regulation of calcium and calmodulin-dependent receptor kinase (CCaMK) (Lévy et al., 2004; Liao et al., 2012; Miller et al., 2013). The resultant signaling outputs lead to activation of several transcription regulators, including the NODULE INCEPTION activator *Nin* (Schauser et al., 1999). These and other regulators partake in the transcriptional reprograming (Suzaki and Kawaguchi, 2014) that mediates the infection thread (IT)-dependent entrance of rhizobia inside the root (Fournier et al., 2015) and also stimulates a subset of susceptible cells to form a nodule primordium within the subtending root cortex (Oldroyd et al., 2011; Suzaki et al., 2015).

Artificial activation of several components that participate in the symbiotic signaling, including NF receptors, CCaMK or CYCLOPS, induces the formation of empty nodules independent of *Rhizobium* and/or NF (Gleason et al., 2006; Tirichine et al., 2007; Ried et al., 2014; Saha et al., 2014; Singh et al., 2014). Ectopic cytokinin is also sufficient to stimulate nodule structure formation on at least some leguminous roots (Cooper and Long, 1994; Heckmann et al., 2011). It has become clear that cytokinin signaling, induced downstream from the NF perception and CCaMK, represents one of the key endogenous effectors of nodule differentiation (Cooper and Long, 1994; Gonzalez-Rizzo et al., 2006; Murray et al., 2007; Tirichine et al., 2007; Frugier et al., 2008; Madsen et al., 2010; Heckmann et al., 2011; Plet et al., 2011; Held et al., 2014). In *Lotus japonicus*, this process is mediated by the Lotus Histidine Kinase 1 (LHK1) cytokinin receptor with a

partially redundant involvement of LHK1A and LHK3 (see Chapter 2), requiring several cytokinin-regulated effectors, including NIN and Nodulation Signaling Pathway 2 (NSP2) (Schauser et al., 1999; Murray et al., 2007; Tirichine et al., 2007; Held et al., 2010; Heckmann et al., 2011; Soyano et al., 2014).

Current data also implicate cytokinin in the regulation of root colonization by rhizobia, but the underlying mechanism remains unclear. In this work, I further consider the aberrant infection phenotype of *L. japonicus* cytokinin receptor mutants and propose a conceptual model for the cytokinin-dependent regulation of *Mesorhizobium loti* infection in *L. japonicus*.

3.2 Results and discussion

3.2.1 Cytokinin is not essential during epidermal infection thread formation

In both *lhk1-1* and the *lhk1-1 lhk1a-1 lhk3-1* triple receptor mutant, defects in nodule formation are accompanied by hyperinfection of the root epidermis by *M. loti* (Figure 3.1 and Figure 3.2) (Murray et al., 2007; Held et al., 2014). This implies that cytokinin signaling, as mediated by LHK1 and possibly other cytokinin receptors, is not only essential for nodule structure formation but also partakes, directly or indirectly, in establishing homeostasis of the symbiotic infection. Neither of the *lhk1a-1* and *lhk3-1* single mutants nor the corresponding *lhk1a-1 lhk3-1* double mutant are hyperinfected by *M. loti* (Held et al., 2014), which indicates that in *L. japonicus*, LHK1 is not only required but is also sufficient to restrict the epidermal infection thread formation events.

In most legumes, including *L. japonicus* and *Medicago truncatula*, the primary mode of rhizobial entry inside the root is by root hair epidermal infection threads (eIT) (Fournier et al., 2015). Only a small proportion of eITs will enter the subtending nodule primordium (Penmetsa and Cook, 1997), becoming persistent, cortical ITs (cITs). These deliver rhizobia into the cytosol of the nodule cells, where they are subjected to differentiation into bacteroides, which are the symbiotic form of rhizobia that reside with the plant cells and fix atmospheric nitrogen to ammonia (Kereszt et al., 2011).

Mounting evidence points to different requirements for plant functions that support eIT and cIT formation (Karas et al., 2005; Groth et al., 2010; Madsen et al., 2010; Kosuta et al., 2011; Hayashi et al., 2014). Mutant plants, such as *L. japonicus symrk-14* and *nena*, are specifically impaired in epidermal responses to *M. loti* infection, including calcium spiking and *Nin* gene expression. While defective in eIT formation, they develop normal cortical infection threads (Groth et al., 2010; Kosuta et al., 2011). Furthermore, activation of CCaMK by calcium/calmodulin is reported to be critical only for eIT formation (Hayashi et al., 2014).

It has been known that the transcription factor *Nin* is essential during remodeling of the root hair infection chamber, which leads to eIT initiation (Fournier et al., 2015). The

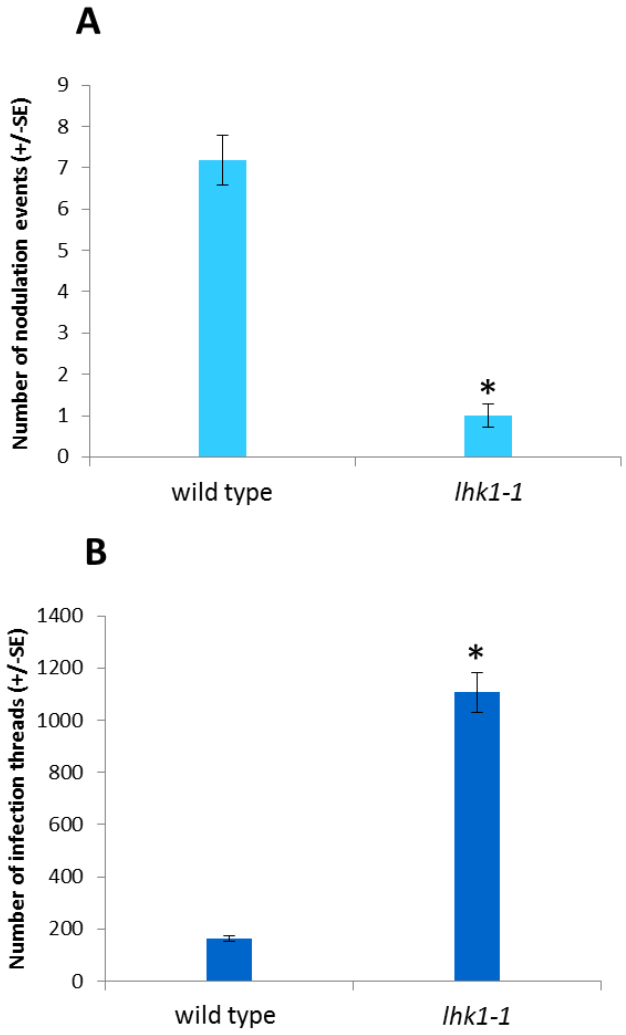

Figure 3.1 The *L. japonicus* LHK1 cytokinin receptor regulates both nodulation and infection thread formation.

The *lhk1-1* mutant forms a low number of nodules but is hyperinfected by *M. loti*. The scores of nodulation events (combination of nodules and nodule primordia) **(A)** and infection threads **(B)** are given for wild type and the *lhk1-1* mutant. In all cases, values reported represent the mean ± SE (n = 10). The phenotypes were evaluated 10 days after inoculation (DAI) with *M. loti*.

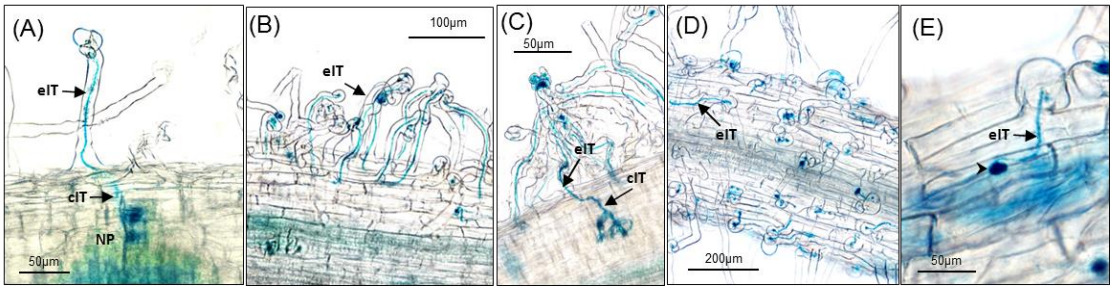

Figure 3.2 The *L. japonicus lhk1-1* single and *lhk1-1 lhk1a-1 lhk3-1* triple cytokinin receptor mutants are hyperinfected by *M. loti* at the root epidermis.

(A) An image of a wild-type *L. japonicus* epidermal infection thread (eIT) that traverses a root hair and enters the root cortex to become a cortical infection thread (cIT). The cIT ramifies within the subtending nodule primordium (NP). Images showing abundant eITs on the root surface of the *lhk1-1* single **(B)** and *lhk1-1 lhk1a-1 lhk3-1* triple **(D)** cytokinin receptor mutants. **(C)** The *lhk1-1* mutant is able to form sporadic cITs. **(E)** Close-up of a single eIT that successfully traverses the root hair of the triple cytokinin mutant but bulges (arrowhead) at the bottom of the cell, unable to enter the root cortex.

rhizobial infection rapidly induces *Nin* expression within the root epidermis (*Nin*-epidermis) and also in the subtending root cortex (*Nin*-cortex), but these cellular responses can be genetically uncoupled (Kosuta et al., 2011). While ectopic cytokinin fails to mimic this epidermal response, it does, like bacterial infection, induce the *Nin*-cortex expression (Heckmann et al., 2011). Consistent with the presence of eITs in the *lhk1-1* mutant (Figure 3.1A and Figure 3.2B), activation of the *Nin*-epidermis upon *M. loti* inoculation is LHK1-independent (Figure 3.3). Together with the apparent lack of detectable cytokinin activity in the *L. japonicus* root epidermis in the earliest stages following *M. loti* infection (Held et al., 2014) (see Figure 2.11), this further supports the notion that cytokinin is not essential during epidermal infection thread formation.

Recent data on the *M. truncatula* root hair "infectome" highlight the requirement for auxin signaling to initiate eIT formation (Breakspear et al., 2014). The *Mtcre1-1* mutant, carrying a deleterious lesion in the presumed *M. truncatula* orthologue of the *L. japonicus Lhk1* locus, is similarly capable of initiating eITs (Plet et al., 2011), indicating that the MtCRE1-dependent cytokinin signaling is also nonessential in this process.

I propose that in epidermal cells responding to NF, active repression of cytokinin signaling by auxin-dependent mechanisms (Chandler and Werr, 2015) is required for eIT formation. Indeed, expression of type-A response regulators, which negatively regulate cytokinin signaling, is rapidly upregulated by NF application and/or rhizobial infection (Op den Camp et al., 2011; Breakspear et al., 2014; Liu et al., 2015) and presumably that this response is auxin-dependent in the root epidermis.

3.2.2 Infection of the root cortex requires cytokinin signaling

In *L. japonicus*, three cytokinin receptors, LHK1, LHK1A, and LHK3, have no apparent role during the initial eIT formation (Figure 3.2), but in their absence, in the *lhk1-1 lhk1a-1 lhk3-1* triple receptor mutant, cITs do not develop (Figure 3.2D and 3.2E). Among the four cytokinin receptor genes that are present in the *L. japonicus* genome only the *Lhk1* promoter has detectable activity in the root epidermis (See Figure 2.13) (Held et al., 2014). Given that *lhk1-1* forms an abundance of eITs (Figure 3.1A), the competency to carry out eIT formation must be LHK1-independent.

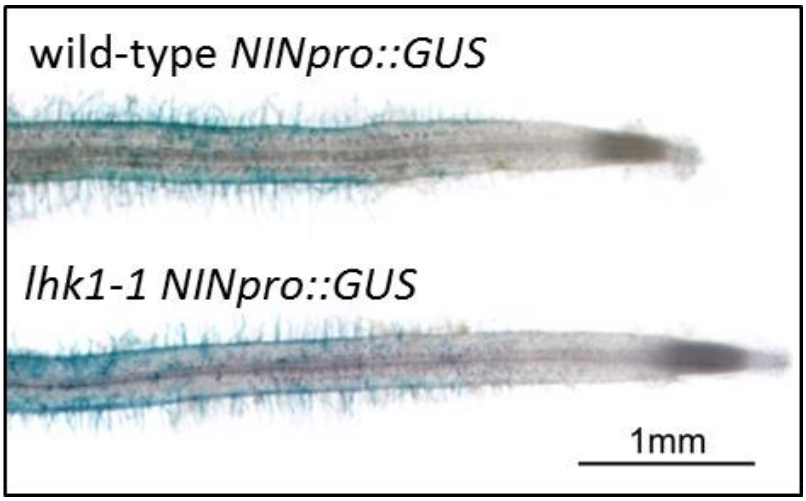

Figure 3.3 Expression of the *Nodule Inception::β-Glucuronidase* (*Nin*::*GUS*) reporter in the root epidermis upon *M. loti* inoculation.

Segments of *L. japonicus* wild-type and *lhk1-1* mutant roots from transgenic plants expressing the GUS reporter gene (blue color) under the control of the *L. japonicus Nin* promoter are shown. The roots were stained for GUS activity 48 hours after inoculation with *M. loti*.

Although delayed, cITs are formed in inoculated *lhk1-1* roots (Figure 3.2C) (Murray et al., 2007; Held et al., 2014). This indicates that LHK1 is not absolutely required for cIT formation. The presence of cITs in *lhk1-1* is associated with cortical cell divisions which give rise to a low nodule number phenotype (Figure 3.1B) (Murray et al., 2007). I have shown that this nodulation phenotype reflects partially redundant function of LHK1 with LHK1A and LHK3 within the *L. japonicus* root cortex (see Chapter 2) (Held et al., 2014). The ability of *lhk1-1* to sustain the cIT development is likely also due to partially overlapping function of these receptors in the root cortex. Consistent with this notion, the *lhk1-1 lhk1a-1 lhk3-1* triple receptor mutant, although hyperinfected at the root epidermis, does not develop cITs (Figure 3.2D and 3.2E). This phenotype highlights the essential role of the cytokinin receptor-dependent signaling in controlling the colonization of the root cortex by *M. loti*. This is supported by the phenotype of the *L. japonicus daphne* mutant, which carries a cytokinin-insensitive allele of *Nin*. Like the *lhk1-1 lhk1a-1 lhk3-1* triple receptor mutant, *daphne* is hyperinfected by *M. loti* at the root epidermis (which confirms that the cytokinin regulation of *Nin* is not required for eIT formation), lacks cITs and does not form nodules (Suzaki et al., 2015). The *Mtcre1-1* mutant does not initially form cITs either (Gonzalez-Rizzo et al., 2006; Plet et al., 2011). Thus, cytokinin might be the primary, plant endogenous signal that conditions cortical cells for upcoming rhizobial infections.

Cytokinin induces *Nin* gene expression in the *L. japonicus* root cortex (Heckmann et al., 2011), which must depend on at least one of the three cytokinin receptors. A similar symbiotic defect in the triple receptor and *daphne* mutants is congruent with this notion. This further suggests that signaling events which promote the development of cITs and stimulate the negative feedback mechanism to restrict subsequent eIT formation, both originate within the activated *L. japonicus* root cortex and require the cytokinin-induced *Nin*-cortex gene expression (Held et al., 2014; Yoro et al., 2014). Interestingly, ethylene-responsive factors have been suggested as potential candidates for the NIN-dependent regulation (Yoro et al., 2014).

The role of cytokinin in promoting cIT formation is indirect and likely relates to its propensity for reprograming a subset of root cortical cells toward symbiotic functions in

legumes (Oldroyd et al., 2009). At which point downstream from the cytokinin and *Nin*-cortex activation the competency of root cortical cells for rhizobial infection is reached and what exactly this entails remains uncertain. However, the ability to control the cell cycle machinery and the formation of associated pre-infection threads, hypothesized to be the result of the modified cell division process, appear to be critical to reaching the infection-permissive stage in the root cortex (Yang et al., 1994). Basic cellular functions such as the cell-cycle switch protein CCS52A (Kondorosi and Kondorosi, 2004) and components of the *L. japonicus* topoisomerase VI, complex (Sasaki et al., 2014; Yoon et al., 2014) have been highlighted as important and are among those likely targeted by cytokinin (Jain et al., 2006; Takahashi et al., 2013). Incidentally, in *M. truncatula*, changes in expression of cell-cycle genes accompany the eIT formation (Breakspear et al., 2014). This could mean that although the primary hormonal response to the NF perception is root cell-layer specific, with presumed high auxin/low cytokinin activity in the epidermis and high cytokinin/low auxin in the cortex, reaching the stage that is permissive for rhizobial infection involves common, downstream alterations to the cellular apparatus.

3.2.2.1 Mutation in the predicted *M. truncatula* orthologue of *Lhk1* does not lead to hyperinfection

Unlike *lhk1-1*, the *Mtcre1-1* mutant is not hyperinfected by *Sinorhizobium meliloti*, a natural microsymbiont of *M. truncatula* (Figure 3.4) (Gonzalez-Rizzo et al., 2006; Plet et al., 2011). This indicates that either MtCRE1 does not participate in a mechanism that restricts subsequent eIT formation or it functions in a redundant manner with other cytokinin receptors to carry out this process. When grown in soil, *Mtcre1-1* recovers a nearly wild type nodulation phenotype three weeks after inoculation (Figure 3.4B), suggesting the existence of a partially redundant function(s) or presence of an independent mechanism. Additional studies are needed to fully comprehend the importance of these apparent, species-specific differences. *Lotus* and *Medicago* have dissimilar nodule development programs (determinate versus indeterminate, respectively), which must reflect differences in relevant hormonal signals. This is also likely to be consequential for the regulation of rhizobial infection in these two species.

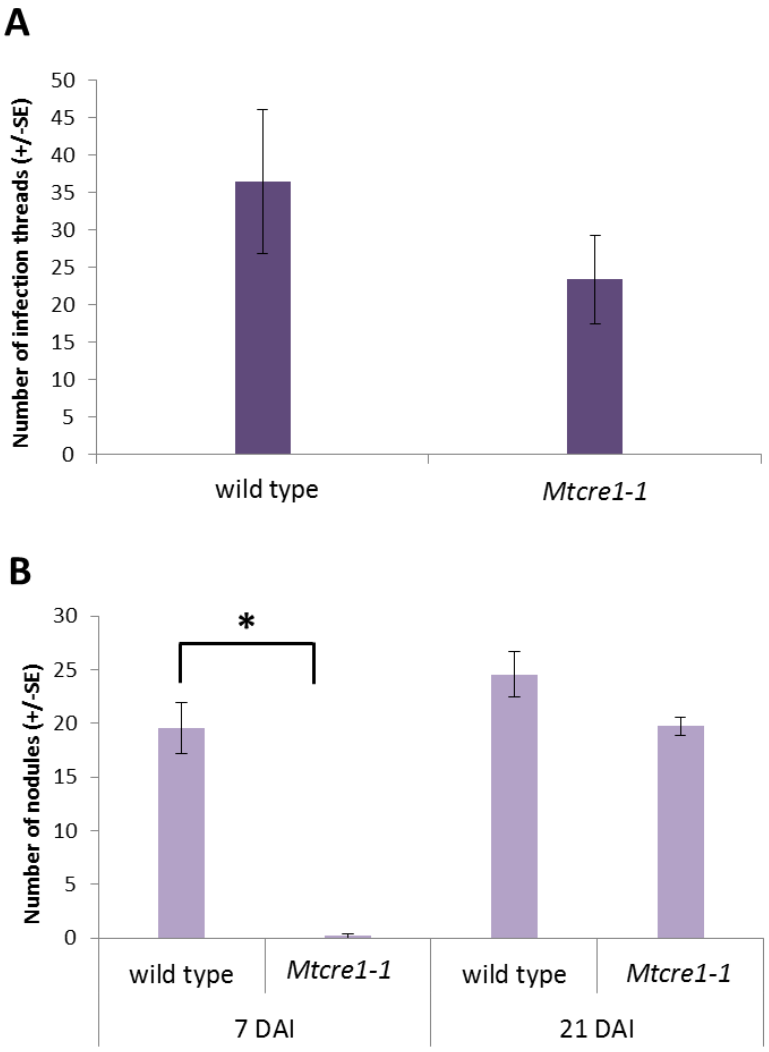

Figure 3.4 Infection thread number and nodulation in the *M. truncatula cre1-1* mutant.

The number of infection threads at 7 DAI **(A)** and nodulation events (combination of nodules and nodule primordia) at 7 and 21 DAI **(B)** were scored in *M. truncatula* wild-type and *Mtcre1-1* mutant plants. In all cases, values reported represent the mean ± SE (n = 10). An asterisk denotes significant differences between the mutant and the wild-type control (Student's t-Test, $P<0.05$).

3.2.3 Cytokinin-ethylene crosstalk limits subsequent epidermal infections

When applied to roots, cytokinin stimulates ethylene production, which in turn limits root elongation (Dugardeyn and Van Der Straeten, 2008). Ethylene is a potent inhibitor of early responses to NF and was shown to dynamically regulate infection and nodule formation events by inhibiting or modulating the epidermal calcium influx and calcium spiking in a concentration-dependent manner (Heidstra et al., 1997; Oldroyd and Downie, 2006; Morieri et al., 2013).

We have postulated that upon *M. loti* infection, symbiotic cytokinin induces ethylene production. In *L. japonicus*, this effect would primarily be LHK1-dependent and is presumed here to represent a locally operating mechanism that restricts subsequent infection events at the root epidermis (Figure 3.5). This could explain why the *lhk1-1* mutant is hyperinfected by *M. loti* (Murray et al., 2007; Held et al., 2014).

Using the two component-output sensor (*TCS*)::GUS reporter (Müller and Sheen, 2008), we showed that two successive peaks of cytokinin activity follow root inoculation by *M. loti* (Held et al., 2014) (See Figure 2.11). The first peak is detectable in a discreet region within the root cortex, where cell divisions for nodule primordia formation are initiated. The second peak occurs only after the initial cell divisions create a microscopically visible nodule primordium (i.e. a distinct region of cell divisions) within the root cortex. In *L. japonicus*, this stage is marked by enhanced *TCS*::GUS reporter gene activity, which extends to include root hairs and is accompanied by increased activity of the *Lhk1* promoter (See Figure 2.11) (Held et al., 2014). Whether the onset of the second cytokinin peak relates in any way to the systemic autoregulation of nodulation (AON) which operates to limit subsequent nodule formation via a shoot-to-root cytokinin transport (Soyano et al., 2014; Wang et al., 2014) remains unknown. The extent of *M. loti* infection in *lhk1-1* roots appears to be further enhanced in the presence of the *har1-1* mutation which blocks functioning of AON (Wopereis et al., 2000; Murray et al., 2007). It is, therefore, likely that these two mechanisms work in conjunction to establish the homeostasis of the infected root, with cytokinin playing a significant role in both of these events.

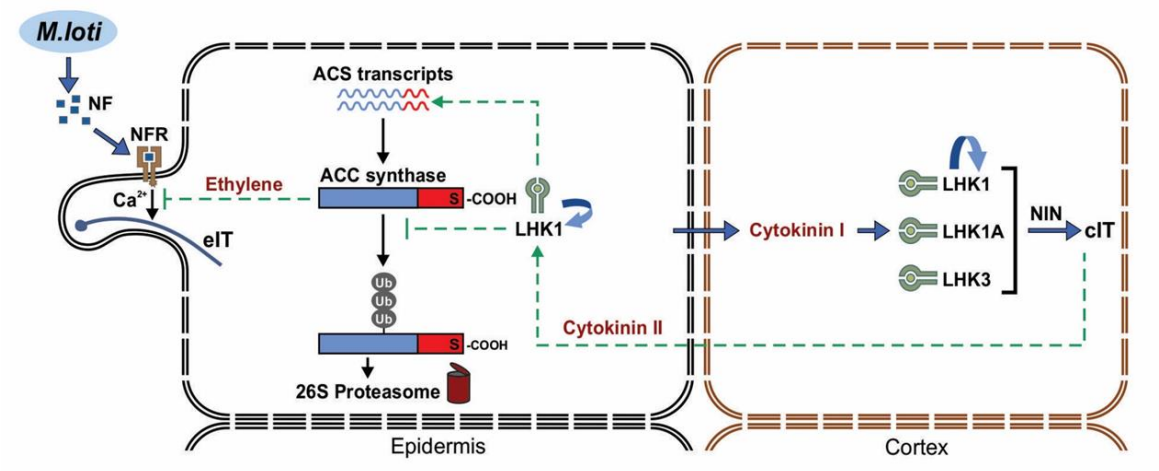

Figure 3.5 A conceptual model for cytokinin-dependent regulation of *M. loti* infection in *L. japonicus*.

The *M. loti* infection and perception of NF by the NF receptor complex (NFR) generate a presumed cell non-autonomous signaling event (the blue arrow that crosses an epidermis/cortex boundary), triggering the first cytokinin activity peak within the root cortex (Cytokinin I). As perceived by LHK cytokinin receptors and in a NIN-cortex (NIN) dependent manner, the permissive conditions for cIT formation are generated. The same signaling events contribute to a negative feedback-loop, which leads to the second cytokinin activity peak that includes root epidermis (Cytokinin II); this is presumed to locally block subsequent eIT. Cytokinin might increase the level of ethylene production in a LHK1-dependent manner by enhancing the steady-state level of mRNA encoding 1-aminocyclopropane-1-carboxylic acid synthase (ACS) transcripts and/or by increasing the stability of the type-2 ACS proteins, preventing their degradation via a ubiquitin-proteasome pathway. Ethylene blocks calcium signaling, which is required for eIT formation. The "u-turn" arrows denote auto-activation of the LHK1 gene expression, which is alleged to increase sensitivity of cells to cytokinin. Positive and negative regulatory actions are indicated by broken green lines with arrows and bars, respectively.

It is possible that both of the cytokinin activity peaks, as induced by *M. loti* infection, contribute to increased ethylene synthesis within roots. We favor a model wherein the second, more extensive burst of cytokinin activity delineates a mechanism that restricts subsequent infection events at the root epidermis (Figure 3.5). This negative feedback is presumed here to involve the cytokinin-dependent up-regulation of the ACS enzyme activity in infected roots. ACSs mediate the first committed step in the ethylene biosynthetic pathway and are regulated by many cues, including cytokinin (Hansen et al., 2009). Cytokinin exerts this function at both transcriptional and post-transcriptional levels (Argueso et al., 2007; Hansen et al., 2009), with the latter conferring increased stability of type-2 ACSs (Hansen et al., 2009) (see Chapter 4 for details).

Our working model incorporates a simple hypothesis, wherein the second cytokinin peak contributes to a significant, local increase in ACS activity and, consequently, ethylene production. The ethylene level, in turn, reaches a threshold that is necessary to block the NF-dependent calcium signaling, thus impairing initiation of new and progression of already initiated eITs (Figure 3.5). The late arrival of the cytokinin activity in the root epidermis following the primary *M. loti* infection (Held et al., 2014) might be of particular relevance to this regulatory process. Cytokinin rapidly increases the steady-state level of the *Lhk1* mRNA, which may also dictate the magnitude of ethylene production. These distinctive attributes of *Lhk1* might, therefore, account for its central role in local signaling for restriction of eIT formation (Held et al., 2014).

Recently, evidence was provided that in *M. truncatula* the majority of transcriptional changes that occur in roots within the first three hours after NF application are cytokinin and MtCRE1 receptor-dependent (van Zeijl et al., 2015). This work revealed also the presence of regulatory feedback loops, including a cytokinin-ethylene crosstalk, which was postulated to inhibit NF-dependent signaling and restrict further nodule primordia formation events. Although not investigated, the same work hints at the possibility of a similar cytokinin-ethylene crosstalk partaking in the LHK1-dependent regulation of *M. loti* infection in *L. japonicus.*

3.2.4 Concluding remarks

Further understanding of the fundamental mechanisms should clarify the *modus operandi* during colonization of roots by rhizobia, but cytokinin signaling clearly emerges as an important mediator of infection thread-dependent infection. Interestingly, a NF- and infection thread-independent mode of cortical cell colonization was described for *Aeschynomene indica* (Indian *vetch*) *Bradyrhizobium* sp. strain ORS285 symbiosis (Giraud et al., 2007; Bonaldi et al., 2011). This direct symbiotic infection, considered to be more ancient, has been shown to require an intact purine biosynthesis pathway (Giraud et al., 2007), from which cytokinin is derived. This suggests that cytokinin or its precursors might have been consequential during the evolution of predisposition for endosymbiotic entry of bacteria into the root. However, similar to NF-dependent infection, the available data do not support the notion that bacterial (*Bradyrhizobium* ORS285)-derived cytokinins are essential for NF-independent mode of root colonization in *Aeschynomene* plants (Podleáková et al., 2013).

3.3 Experimental Procedures

3.3.1 Plant growth conditions

Seeds of *L. japonicus* wild-type Gifu, the *lhk1-1* mutant (Murray et al., 2007) and the *lhk1-1 lhk1a-1 lhk3-1* mutant (Held et al., 2014) were sterilized and grown as described in Section 2.5.1.

Seeds of *M. truncatula* wild-type A17 and *Mtcre1-1* (kind gift from Dr. Florian Frugier, Institute of Plant Sciences Paris-Saclay) were scarified lightly with sand paper, surface-sterilized using sulfuric acid for five minutes, followed by five rinses with sterile Milli-Q water, and incubation in 30% bleach solution for 10 minutes. Sterilized seeds were rinsed at least 10 times with sterile Milli-Q water and allowed to imbibe overnight. Imbibed seeds were left to germinate on Petri plates containing sterilized Whatmann filter paper moistened with sterilized Milli-Q water. Plates were sealed with parafilm and placed under continuous light at 23 ºC for a period of two days.

3.3.2 Assessment of symbiotic phenotypes

Under sterile conditions, seven day old seedlings were transplanted into pots containing a 6:1 mixture of vermiculite and sand soaked with 1X B and D nutrient solution (Broughton and Dilworth, 1971), supplemented with 0.5 mM KNO3, under the standard growth condition of 18 hours light at 23 ºC and 6 hours dark at 18 ºC with 80% humidity. Seven days after sowing, the *L. japonicus* and *M. truncatula* seedlings were inoculated with a strain of either *M. loti* or *S. meliloti*, respectively, carrying the *hemA::LacZ* reporter cassette for visualization of bacterial infection. Pots containing 15 plants were inoculated with 10 ml of an aqueous suspension (OD_{600}: 0.8) of the rhizobial bacteria (Wopereis et al., 2000). For histochemical analysis of β-galactosidase reporter gene activity, roots were fixed, stained, and cleared (Wopereis et al., 2000) at different time points as stated for each experiment.

3.3.3 *NIN::GUS* epidermal staining

Sterilized, imbibed seeds were kept upside down on petri plates with filter paper for two days in dark. The seedlings were transferred to vertical plates containing ¼ B and D

nutrient solution (Broughton and Dilworth, 1971) with 0.8% agar. Seedlings were sown onto a pre-soaked filter paper that had been placed over the media, to avoid penetration of the roots into the agar. The filter papers were soaked in sterile Milli-Q water. Five germinated seedlings were placed on each plate and roots were covered with another wet filter paper. Vertical plates were kept in boxes such that the shoots were kept under continuous light while the roots were protected from light. After two days on the plates, each root was inoculated with 20 µl of *M. loti*. Plates were kept for another 24 hours under continuous light before roots were stained for GUS activity.

Detection of the GUS reporter activity was conducted using a staining solution which contained 0.1M potassium phosphate buffer, 5 mM EDTA, 0.5 mM potassium ferric- and ferrous-cyanides, and 0.5 mg/ml 5-bromo-4-chloro-3-indolyl glucuronide cyclohexylammonium salt (X-GLUC; Fermentas). Roots were gently placed on Fahraeus slides and stained with 1 ml of GUS staining solution per slide. Slides were placed into large plates containing a few drops of water and incubated at 37 ºC. Stained roots were cleared, as described previously (Wopereis et al., 2000).

3.4 References

Argueso, C.T., Hansen, M., and Kieber, J.J. (2007). Regulation of ethylene biosynthesis. J. Plant Growth Regul. **26:** 92-105.

Bonaldi, K., Gargani, D., Prin, Y., Fardoux, J., Gully, D., Nouwen, N., Goormachtig, S., and Giraud, E. (2011). Nodulation of *Aeschynomene afraspera* and *A. indica* by photosynthetic *Bradyrhizobium* sp. strain ORS285: The Nod-dependent versus the Nod-independent symbiotic interaction. Mol. Plant-Microbe Interact. **24:** 1359-1371.

Breakspear, A., Liu, C., Roy, S., Stacey, N., Rogers, C., Trick, M., Morieri, G., Mysore, K.S., Wen, J., and Oldroyd, G.E. (2014). The root hair "infectome" of *Medicago truncatula* uncovers changes in cell cycle genes and reveals a requirement for auxin signaling in rhizobial infection. Plant Cell **26:** 4680-4701.

Broghammer, A., Krusell, L., Blaise, M., Sauer, J., Sullivan, J.T., Maolanon, N., Vinther, M., Lorentzen, A., Madsen, E.B., Jensen, K.J., Roepstorff, P., Thirup, S., Ronson, C.W., Thygesen, M.B., and Stougaard, J. (2012). Legume receptors perceive the rhizobial lipochitin oligosaccharide signal molecules by direct binding. Proc. Natl. Acad. Sci. U. S. A. **109:** 13859-13864.

Broughton, W.J., and Dilworth, M.J. (1971). Control of leghaemoglobin synthesis in snake beans. Biochem. J. **125:** 1075-1080.

Chandler, J.W., and Werr, W. (2015). Cytokinin-auxin crosstalk in cell type specification. Trends Plant Sci. **20:** 291-300.

Cooper, J.B., and Long, S.R. (1994). Morphogenetic rescue of *Rhizobium meliloti* nodulation mutants by *trans*-zeatin secretion. Plant Cell **6:** 215-225.

Dugardeyn, J., and Van Der Straeten, D. (2008). Ethylene: Fine-tuning plant growth and development by stimulation and inhibition of elongation. Plant Sci. **175:** 59-70.

Fournier, J., Teillet, A., Chabaud, M., Ivanov, S., Genre, A., Limpens, E., Carvalho-Niebel, F.D., and Barker, D.G. (2015). Remodeling of the infection chamber before infection thread formation reveals a two-step mechanism for rhizobial entry into the host legume root hair. Plant Physiol. **167:** 1233-1242.

Frugier, F., Kosuta, S., Murray, J.D., Crespi, M., and Szczyglowski, K. (2008). Cytokinin: secret agent of symbiosis. Trends Plant Sci. **13:** 115-120.

Giraud, E., Moulin, L., Vallenet, D., Barbe, V., Cytryn, E., Avarre, J.C., Jaubert, M., Simon, D., Cartieaux, F., Prin, Y., Bena, G., Hannibal, L., Fardoux, J., Kojadinovic, M., Vuillet, L., Lajus, A., Cruveiller, S., Rouy, Z., Mangenot, S.,

Segurens, B., Dossat, C., Franck, W.L., Chang, W.S., Saunders, E., Bruce, D., Richardson, P., Normand, P., Dreyfus, B., Pignol, D., Stacey, G., Emerich, D., Verméglio, A., Médigue, C., and Sadowsky, M. (2007). Legumes symbioses: Absence of *Nod* genes in photosynthetic bradyrhizobia. Science **316:** 1307-1312.

Gleason, C., Chaudhuri, S., Yang, T., Muñoz, A., Poovaiah, B.W., and Oldroyd, G.E.D. (2006). Nodulation independent of rhizobia induced by a calcium-activated kinase lacking autoinhibition. Nature **441:** 1149-1152.

Gonzalez-Rizzo, S., Crespi, M., and Frugier, F. (2006). The *Medicago truncatula* CRE1 cytokinin receptor regulates lateral root development and early symbiotic interaction with *Sinorhizobium meliloti*. Plant Cell **18:** 2680-2693.

Groth, M., Takeda, N., Perry, J., Uchid, H., Dräxl, S., Brachmann, A., Sato, S., Tabata, S., Kawaguchi, M., Wang, T.L., and Parniskea, M. (2010). *NENA*, a *Lotus japonicus* homolog of *Sec13*, is required for rhizodermal infection by arbuscular mycorrhiza fungi and rhizobia but dispensable for cortical endosymbiotic development. Plant Cell **22:** 2509-2526.

Hansen, M., Chae, H.S., and Kieber, J.J. (2009). Regulation of ACS protein stability by cytokinin and brassinosteroid. Plant J. **57:** 606-614.

Hayashi, T., Shimoda, Y., Sato, S., Tabata, S., Imaizumi-Anraku, H., and Hayashi, M. (2014). Rhizobial infection does not require cortical expression of upstream common symbiosis genes responsible for the induction of Ca^{2+} spiking. Plant J. **77:** 146-159.

Heckmann, A.B., Sandal, N., Bek, A.S., Madsen, L.H., Jurkiewicz, A., Nielsen, M.W., Tirichine, L., and Stougaard, J. (2011). Cytokinin induction of root nodule primordia in *Lotus japonicus* is regulated by a mechanism operating in the root cortex. Mol. Plant-Microbe Interact. **24:** 1385-1395.

Heidstra, R., Yang, W.C., Yalcin, Y., Peck, S., Emons, A., Van Kammen, A., and Bisseling, T. (1997). Ethylene provides positional information on cortical cell division but is not involved in Nod factor-induced root hair tip growth in *Rhizobium*-legume interaction. Development **124:** 1781-1787.

Held, M., Hossain, M.S., Yokota, K., Bonfante, P., Stougaard, J., and Szczyglowski, K. (2010). Common and not so common symbiotic entry. Trends Plant Sci. **15:** 540-545.

Held, M., Hou, H., Miri, M., Huynh, C., Ross, L., Hossain, M.S., Sato, S., Tabata, S., Perry, J., Wang, T.L., and Szczyglowski, K. (2014). *Lotus japonicus* cytokinin receptors work partially redundantly to mediate nodule formation. Plant Cell **26:** 678-694.

Jain, M., Tyagi, A.K., and Khurana, J.P. (2006). Overexpression of putative topoisomerase 6 genes from rice confers stress tolerance in transgenic *Arabidopsis* plants. FEBS J. **273:** 5245-5260.

Karas, B., Murray, J., Gorzelak, M., Smith, A., Sato, S., Tabata, S., and Szczyglowski, K. (2005). Invasion of *Lotus japonicus root hairless 1* by *Mesorhizobium loti* involves the nodulation factor-dependent induction of root hairs. Plant Physiol. **137:** 1331-1344.

Kereszt, A., Mergaert, P., and Kondorosi, E. (2011). Bacteroid development in legume nodules: Evolution of mutual benefit or of sacrificial victims? Mol. Plant-Microbe Interact. **24:** 1300-1309.

Kondorosi, E., and Kondorosi, A. (2004). Endoreduplication and activation of the anaphase-promoting complex during symbiotic cell development. FEBS Lett. **567:** 152-157.

Kosuta, S., Held, M., Hossain, M.S., Morieri, G., MacGillivary, A., Johansen, C., Antolín-Llovera, M., Parniske, M., Oldroyd, G.E.D., Downie, A.J., Karas, B., and Szczyglowski, K. (2011). *Lotus japonicus* symRK-14 uncouples the cortical and epidermal symbiotic program. Plant J. **67:** 929-940.

Lévy, J., Bres, C., Geurts, R., Chalhoub, B., Kulikova, O., Duc, G., Journet, E.P., Ané, J.M., Lauber, E., Bisseling, T., Dénarié, J., Rosenberg, C., and Debellé, F. (2004). A putative Ca^{2+} and calmodulin-dependent protein kinase required for bacterial and fungal symbioses. Science **303:** 1361-1364.

Liao, J., Singh, S., Hossain, M.S., Andersen, S.U., Ross, L., Bonetta, D., Zhou, Y., Sato, S., Tabata, S., Stougaard, J., Szczyglowski, K., and Parniske, M. (2012). Negative regulation of CCaMK is essential for symbiotic infection. Plant J. **72:** 572-584.

Liu, C.W., Breakspear, A., Roy, S., and Murray, J.D. (2015). Cytokinin responses counterpoint auxin signaling during rhizobial infection. Plant Signaling Behav. **10**.

Madsen, L.H., Tirichine, L., Jurkiewicz, A., Sullivan, J.T., Heckmann, A.B., Bek, A.S., Ronson, C.W., James, E.K., and Stougaard, J. (2010). The molecular network governing nodule organogenesis and infection in the model legume *Lotus japonicus*. Nat. Commun. **1:** 10.

Miller, J.B., Pratap, A., Miyahara, A., Zhou, L., Bornemann, S., Morris, R.J., and Oldroyd, G.E.D. (2013). Calcium/calmodulin-dependent protein kinase is negatively and positively regulated by calcium, providing a mechanism for decoding calcium responses during symbiosis signaling. Plant Cell **25:** 5053-5066.

Morieri, G., Martinez, E.A., Jarynowski, A., Driguez, H., Morris, R., Oldroyd, G.E.D., and Downie, J.A. (2013). Host-specific Nod-factors associated with *Medicago truncatula* nodule infection differentially induce calcium influx and calcium spiking in root hairs. New Phytol. **200:** 656-662.

Müller, B., and Sheen, J. (2008). Cytokinin and auxin interaction in root stem-cell specification during early embryogenesis. Nature **453:** 1094-1097.

Murray, J.D., Karas, B.J., Sato, S., Tabata, S., Amyot, L., and Szczyglowski, K. (2007). A cytokinin perception mutant colonized by *Rhizobium* in the absence of nodule organogenesis. Science **315:** 101-104.

Oldroyd, G.E., and Downie, J.A. (2006). Nuclear calcium changes at the core of symbiosis signalling. Curr. Opin. Plant Biol. **9:** 351-357.

Oldroyd, G.E.D., Harrison, M.J., and Paszkowski, U. (2009). Reprogramming plant cells for endosymbiosis. Science **324:** 753-754.

Oldroyd, G.E.D., Murray, J.D., Poole, P.S., and Downie, J.A. (2011). The rules of engagement in the legume-rhizobial symbiosis. In Annual Review of Genetics, pp. 119-144.

Op den Camp, R.H.M., de Mita, S., Lillo, A., Cao, Q., Limpens, E., Bisseling, T., and Geurts, R. (2011). A phylogenetic strategy based on a legume-specific whole genome duplication yields symbiotic cytokinin type-A response regulators. Plant Physiol. **157:** 2013-2022.

Penmetsa, R.V., and Cook, D.R. (1997). A legume ethylene-insensitive mutant hyperinfected by its rhizobial symbiont. Science **275:** 527-530.

Plet, J., Wasson, A., Ariel, F., Le Signor, C., Baker, D., Mathesius, U., Crespi, M., and Frugier, F. (2011). MtCRE1-dependent cytokinin signaling integrates bacterial and plant cues to coordinate symbiotic nodule organogenesis in *Medicago truncatula*. Plant J. **65:** 622-633.

Podleáková, K., Fardoux, J., Patrel, D., Bonaldi, K., Novák, O., Strnad, M., Giraud, E., Spíchal, L., and Nouwen, N. (2013). Rhizobial synthesized cytokinins contribute to but are not essential for the symbiotic interaction between photosynthetic bradyrhizobia and aeschynomene legumes. Mol. Plant-Microbe Interact. **26:** 1232-1238.

Ried, M.K., Antolín-Llovera, M., and Parniske, M. (2014). Spontaneous symbiotic reprogramming of plant roots triggered by receptor-like kinases. eLife **3:** 1-17.

Saha, S., Dutta, A., Bhattacharya, A., and DasGupta, M. (2014). Intracellular catalytic domain of symbiosis receptor kinase hyperactivates spontaneous nodulation in absence of rhizobia. Plant Physiol. **166:** 1699-1708.

Sasaki, T., Suzaki, T., Soyano, T., Kojima, M., Sakakibara, H., and Kawaguchi, M. (2014). Shoot-derived cytokinins systemically regulate root nodulation. Nat. Commun. **5**.

Schauser, L., Roussis, A., Stiller, J., and Stougaard, J. (1999). A plant regulator controlling development of symbiotic root nodules. Nature **402:** 191-195.

Singh, S., Katzer, K., Lambert, J., Cerri, M., and Parniske, M. (2014). CYCLOPS, A DNA-binding transcriptional activator, orchestrates symbiotic root nodule development. Cell Host Microbe **15:** 139-152.

Soyano, T., Hirakawa, H., Sato, S., Hayashi, M., and Kawaguchi, M. (2014). NODULE INCEPTION creates a long-distance negative feedback loop involved in homeostatic regulation of nodule organ production. Proc. Natl. Acad. Sci. U. S. A. **111:** 14607-14612.

Suzaki, T., and Kawaguchi, M. (2014). Root nodulation: A developmental program involving cell fate conversion triggered by symbiotic bacterial infection. Curr. Opin. Plant Biol. **21:** 16-22.

Suzaki, T., Yoro, E., and Kawaguchi, M. (2015). Leguminous plants: Inventors of root nodules to accommodate symbiotic bacteria. In International review of cell and molecular biology (Elsevier Inc.), pp. 111-158.

Takahashi, N., Kajihara, T., Okamura, C., Kim, Y., Katagiri, Y., Okushima, Y., Matsunaga, S., Hwang, I., and Umeda, M. (2013). Cytokinins control endocycle onset by promoting the expression of an APC/C activator in arabidopsis roots. Curr. Biol. **23:** 1812-1817.

Tirichine, L., Sandal, N., Madsen, L.H., Radutoiu, S., Albrektsen, A.S., Sato, S., Asamizu, E., Tabata, S., and Stougaard, J. (2007). A gain-of-function mutation in a cytokinin receptor triggers spontaneous root nodule organogenesis. Science **315:** 104-107.

van Zeijl, A., Op Den Camp, R.H.M., Deinum, E.E., Charnikhova, T., Franssen, H., Op Den Camp, H.J.M., Bouwmeester, H., Kohlen, W., Bisseling, T., and Geurts, R. (2015). Rhizobium Lipo-chitooligosaccharide signaling triggers accumulation of cytokinins in *Medicago truncatula* Roots. Molecular Plant **8:** 1213-1226.

Wang, Y., Wang, L., Zou, Y., Chen, L., Cai, Z., Zhang, S., Zhao, F., Tian, Y., Jiang, Q., and Ferguson, B.J. (2014). Soybean miR172c targets the repressive AP2 transcription factor NNC1 to activate *ENOD40* expression and regulate nodule initiation. Plant Cell **26:** 4782-4801.

Wopereis, J., Pajuelo, E., Dazzo, F.B., Jiang, Q., Gresshoff, P.M., De Bruijn, F.J., Stougaard, J., and Szczyglowski, K. (2000). Short root mutant of *Lotus japonicus* with a dramatically altered symbiotic phenotype. Plant J. **23:** 97-114.

Yang, W.C., De Blank, C., Meskiene, I., Hirt, H., Bakker, J., Van Kammen, A., Franssen, H., and Bisseling, T. (1994). *Rhizobium* nod factors reactivate the cell cycle during infection and nodule primordium formation, but the cycle is only completed in primordium formation. Plant Cell **6:** 1415-1426.

Yoon, H.J., Hossain, M.S., Held, M., Hou, H., Kehl, M., Tromas, A., Sato, S., Tabata, S., Andersen, S.U., Stougaard, J., Ross, L., and Szczyglowski, K. (2014). *Lotus japonicus SUNERGOS1* encodes a predicted subunit A of a DNA topoisomerase VI that is required for nodule differentiation and accommodation of rhizobial infection. Plant J. **78:** 811-821.

Yoro, E., Suzaki, T., Toyokura, K., Miyazawa, H., Fukaki, H., and Kawaguchi, M. (2014). A Positive regulator of nodule organogenesis, NODULE INCEPTION, acts as a negative regulator of rhizobial infection in *Lotus japonicus*. Plant Physiol. **165:** 747-758.

Chapter 4

4 Cytokinin-ethylene crosstalk regulates rhizobial infection in *Lotus japonicus*

Mandana Miri[1,2], Dugald Reid[3], Jens Stougaard[3], Preetam Janakirama[1], Stig Andersen[3] and Krzysztof Szczyglowski[1,2]

[1]Agriculture and Agri-Food Canada, Southern Crop Protection and Food Research Centre, London, Ontario, N5V 4T3 Canada

[2]Department of Biology, University of Western Ontario, London, Ontario, N6A 5BF Canada

[3]Plant Molecular Biology, Department of Molecular Biology and Genetics, 8000 Aarhus C, Denmark

A version of this chapter will be submitted to the *Plant Molecular Biology* journal.

In this chapter, it is shown that in Lotus japonicus, the ACS1 *and* ACS2 *ethylene biosynthesis genes are likely to function redundantly to regulate the extent of rhizobial infection in an LHK1-dependent manner. I also demonstrate that ETO1/EOLs proteins work redundantly in fine-tuning the rhizobially-induced ethylene production, thus contributing to the homeostasis of the symbiotic infection.*

4.1 Introduction

Ethylene (C_2H_4) has been recognized as a plant growth regulator since the turn of the last century (Crocker and Knight, 1908; Knight et al., 1910). As a signaling molecule, it is an important gaseous phytohormone that has long been known to play important roles in a diverse array of developmental processes, including seed germination, seedling growth, leaf and flower senescence and abscission, fruit ripening, and the response to a wide variety of biotic and abiotic stresses (Light et al., 2016).

The biosynthetic capacity for ethylene is nearly ubiquitous throughout the plant body, but ethylene production is stringently regulated (Argueso et al., 2007). This permits the maintenance of low ethylene levels through a regulatory network which is highly dynamic and allows for rapid and dramatic increases in ethylene levels in response to both endogenous cues and varying external conditions including light, temperature, and presence of pathogens or microsymbionts (Chae and Kieber, 2005; De Paepe and Van Der Straeten, 2005).

The biosynthesis of ethylene occurs through a relatively simple metabolic pathway (Figure 4.1) that has been extensively studied and well-documented in several plant species (Yang and Hoffman, 1984; Argueso et al., 2007; Lin et al., 2009). In short, ethylene is derived from the amino acid methionine and is produced in the following three enzymatic steps: (1) conversion of methionine to S-adenosyl methionine (SAM) by SAM synthetase (SAMS); (2) conversion of SAM to 1-aminocyclopropane-1-carboxylic acid (ACC) by ACC synthase (ACS); and lastly, (3) conversion of ACC to ethylene by ACC oxidase (ACO). The conversion of SAM to ACC by ACS is the first committed, and generally the rate-limiting step in the ethylene biosynthesis during vegetative growth (Adams and Yang, 1979). The level of ACS activity closely parallels the level of ethylene

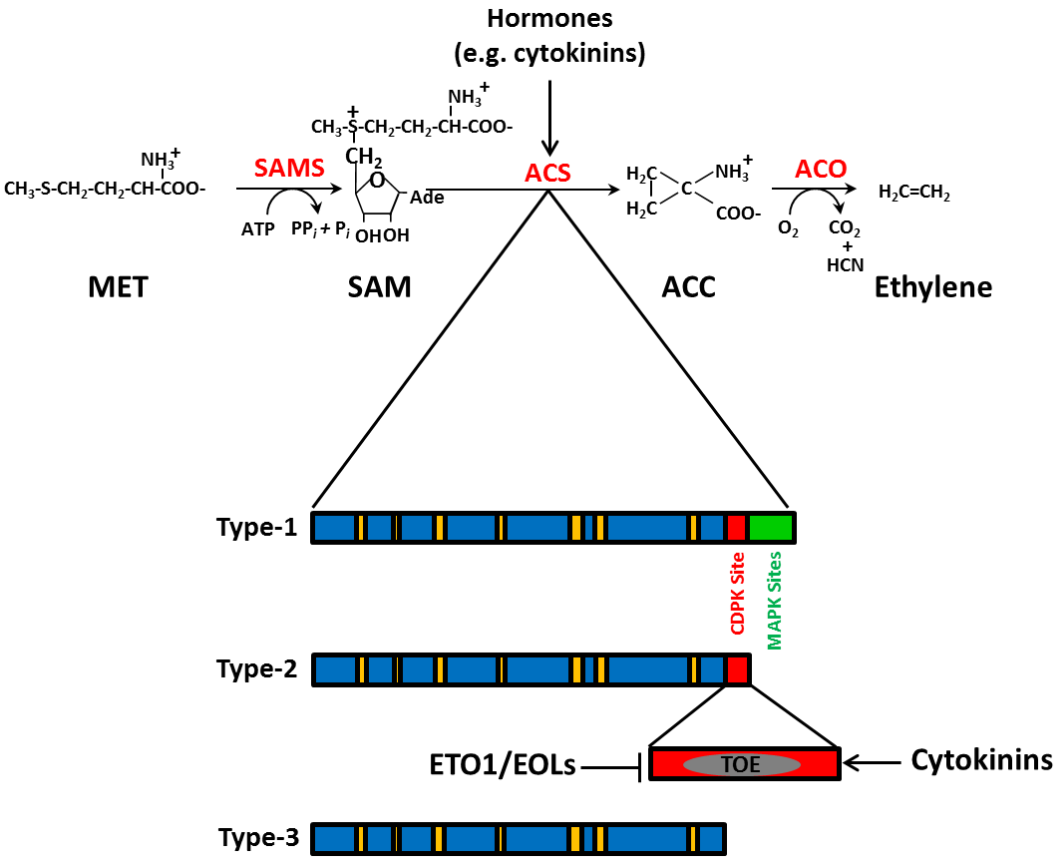

Figure 4.1 Ethylene biosynthesis pathway.

Ethylene is produced in three steps from methionine (see the text for details). The enzymes catalyzing each step are shown in red above the arrows. Several inputs, including plant hormone cytokinins can regulate the enzymes (mostly ACS) involved in ethylene biosynthesis via either transcriptional or post-transcriptional mechanisms**.** Based on their C-terminal amino acid sequence motifs, ACS proteins are classified in three subfamilies; type-1, type-2, and type-3. Consensus sites for CDPK and MAPK sites are shown as red and green, respectively. Type-2 ACS proteins contain the TOE sequence which is required for interaction with ETO1/EOLs. Type-2 ACSs are stabilized by cytokinin and are ubiquitinated and targeted for degradation by ETO1/EOLs. Modified from (Lyzenga and Stone, 2012).

MET, methionine; SAM, S-adenosyl-methionine; ACC, 1-aminocyclopropane-1-carboxylic acid; SAMS, SAM synthetase; ACO, ACC oxidase; TOE, Target of ETO1.

production in most plant tissues (Yang and Hoffman, 1984). In *Arabidopsis thaliana* seedlings, increasing ACS protein levels drives ethylene synthesis to a high degree (Chae et al., 2003; Joo et al., 2008; Christians et al., 2009). In fact, it has been well-established that the regulation of ethylene biosynthesis by internal signals (e.g. hormones) or in response to environmental factors, is mostly mediated through modulating ACS activity (Chae et al., 2003; Argueso et al., 2007; Joo et al., 2008; Christians et al., 2009; Zdarska et al., 2015).

ACS is encoded by a multi-gene family in all plant species examined thus far (Bleecker and Kende, 2000). In *A. thaliana*, this family consists of nine members (ACS1, ACS2, ACS4-9 and ACS11), of which eight (ACS2, ACS4-9 and ACS11) have ACS activities as homodimers, while ACS1 forms a non-functional homodimer (Yamagami et al., 2003; Tsuchisaka and Theologis, 2004). The sequence of the catalytic core is highly conserved, but C-terminal regions of ACS proteins are divergent. Based on the composition of the C-terminal regions, the ACS proteins are divided into three subfamilies (Yamagami et al., 2003) (Figure 4.1). Type-1 ACS proteins have the longest C-terminus with a single, putative calcium-dependent protein kinase (CDPK) phosphorylation site and three mitogen-activated protein kinase (MAPK) phosphorylation sites. Type-2 ACS proteins have an intermediate length C-terminus containing a single putative CDPK phosphorylation site, while type-3 ACS proteins have a very short C-terminus and no predicted kinase phosphorylation sites (Tatsuki and Mori, 2001; Liu and Zhang, 2004; Sebastià et al., 2004; Chae and Kieber, 2005; Yoshida et al., 2005).

Studies have shown that ACSs are regulated by many biotic and abiotic cues, transcriptionally and post-translationally, including proteasome-mediated degradation (Chae et al., 2003; Liu and Zhang, 2004; Wang et al., 2004; Skottke et al., 2011). The highly variable C-terminal regions of the proteins serve as targets for post-translational regulation (Chae et al., 2003; Yoshida et al., 2005; Hansen et al., 2009). The underlying mechanisms for regulation of different ACSs, however, are complex and diverse. For instance, in *A. thaliana* phosphorylation of the type-1 AtACS2 and AtACS6 proteins by stress-responsive MAPKs (MPK3 and MPK6) results in increased ethylene synthesis through protein stabilization (Liu and Zhang, 2004; Joo et al., 2008; Han et al., 2010).

Similarly, in wounded tomato (*Lycopersicon esculentum*) tissues, the CDPK-mediated phosphorylation of LeACS2, a type-1 ACS, stabilizes the enzyme leading to increased ACS activity and ACC content (Tatsuki and Mori, 2001; Kamiyoshihara et al., 2010). Conversely, un-phosphorylated type-1 isozymes are rapidly turned over via a 26S proteasome-dependent pathway (Joo et al., 2008).

The CDPK motif of type-2 ACS proteins can also be phosphorylated (Sebastià et al., 2004), but this seems to have a negative effect (Tan and Xue, 2014). Protein phosphatase 2A, which regulates the reversible de-phosphorylation of ACS proteins, positively regulates type-2 ACSs (AtACS5 and AtACS9) while negatively regulating type-1 ACSs (AtACS2 and AtACS6) (Skottke et al., 2011). Also, the phosphatase inhibitor cantharidin, by increasing the phosphorylation status of AtACS5, results in increased degradation (Skottke et al., 2011).

Members of the type-2 ACS protein family are specifically targeted by Ethylene Over-Producer1 (ETO1) protein for ubiquitination and rapid degradation via the 26S proteasome pathway (Lin et al., 2009) (Figure 4.1). It has been shown that in *A. thaliana*, ETO1 and its two paralogs, ETO1-like (EOL1) and EOL2, work redundantly to target type-2 ACSs (AtACS5 and AtACS9) for degradation (Christians et al., 2009). ETO1, EOL1, and EOL2 are Broad complex/Tramtrack/Bric-a-brac (BTB)-domain containing proteins. The BTB domain functions as a substrate-recruiting component of a cullin (CUL) 3a/b based E3 ligase complex (Gingerich et al., 2005; Lyzenga and Stone, 2012). ETO1 and EOLs target a C-terminal sequence specific to type-2 ACS proteins called Target of ETO1 (TOE) (Yoshida et al., 2006; Christians et al., 2009). Dominant mutations within the TOE sequence (*eto2*, and *eto3* in AtACS5 and AtACS9, respectively) eliminate the recognition by ETO1/EOLs, thus increasing the stability of ACS proteins, and resulting in ethylene over production (Chae et al., 2003; Hansen et al., 2009). It has also been shown that a phosphor-binding protein called 14-3-3 positively regulates ethylene production by direct interactions with the ACS and ETO1/EOL proteins. These interactions stabilize the type-2 ACS proteins (for instance, AtACS5), while destabilizing the ETO/EOLs, contributing to increased ethylene production (Yoon and Kieber, 2013). Recently, Casein Kinase1 (CK1) was shown to promote the

phosphorylation of AtACS5, thereby increasing its interaction with ETO1, and leading to its degradation (Tan and Xue, 2014).

It has been known for decades that cytokinins play an important role in modulating ethylene levels (Vogel et al., 1998). Exogenous cytokinin, for example, induces ethylene production and thus triggers the characteristic, ethylene-related "triple response" (thickening and shortening of the hypocotyl with a pronounced apical hook) in dark-grown *Arabidopsis* seedlings (Cary et al., 1995; Vogel et al., 1998). One of the mechanisms involved is a cytokinin-dependent increase in stability of AtACS5 and AtACS9 proteins (Chae et al., 2003; Hansen et al., 2009). This effect requires cytokinin signaling components, including cytokinin receptors, histidine phosphotransfer proteins, and response regulators (Hansen et al., 2009). In addition to ACS proteins, proteomic analysis showed that cytokinin treatment specifically induces the levels of other two ethylene biosynthetic enzymes, SAMS and ACO, in *Arabidopsis* root but not shoot tissues (Zdarska et al., 2013).

In the context of symbiosis, ethylene has been shown to have an important role as a negative regulator of both rhizobial infection and nodule formation. A pioneering study in *Medicago truncatula* showed that the *Mtein2* mutant, named *sickle*, is ethylene insensitive and is hyperinfected by *Sinorhizobium meliloti*, its nitrogen-fixing microsymbiont (Penmetsa and Cook, 1997; Penmetsa et al., 2008). Interestingly, deleterious mutations in the *L. japonicu*s cytokinin receptor *LHK1* gene, such as *lhk1-1*, were also shown to result in an excessive number of infection thread formation events (Murray et al., 2007). Consequently, we sought to determine whether a crosstalk between cytokinin and ethylene regulates the number of infection threads in *L. japonicus*.

In this study, we followed a simple hypothesis that the hyperinfection phenotype of the *lhk1-1* mutant is due at least in part to an altered ethylene level in this cytokinin perception mutant. The focus of this research, therefore, was mainly on *ACS(s)* and *ETO1/EOLs* and their possible involvement in the cytokinin-dependent regulation of infection thread formation during *L. japonicus-Mesorhizobium loti* symbiosis.

4.2 Results

4.2.1 LHK1 cytokinin receptor regulates the number of infection threads

The results presented in Chapters 2 and 3 highlight the importance of the LHK1 cytokinin receptor in regulating at least two key aspects of the symbiotic interaction between *L. japonicus* and *M. loti*, namely the initiation of nodule primordia and the restriction of root colonization by the microsymbiont.

Given the availability of both loss- (*lhk1-1*) and gain-of-function (*snf2*) alleles of *LHK1*, the role of this cytokinin receptor during the infection process was further evaluated by comparing the number of epidermal infection threads that formed in wild type and the mutants, 7 days after inoculation (DAI) with *M. loti* (Figure 4.2). If, as predicted by our model (Figure 3.5), cytokinin indeed restricts epidermal infection events in an LHK1-dependent manner, this should be reflected by contrasting phenotypes of the two mutants.

Confirming pervious observations (Murray et al., 2007), the *lhk1-1* mutant was hyperinfected by *M. loti*, forming almost five times more infection threads compared to the wild-type control. By contrast, in the *snf2* mutant, where LHK1 is constitutively activated by a gain-of-function mutation in the cytokinin-binding (CHASE) domain (Tirichine et al., 2007), the number of infection threads was decreased approximately 25-fold compared to wild type (Figure 4.2). Together, these results convincingly demonstrate the essential role of the LHK1 cytokinin receptor in restricting the extent of *M. loti* epidermal infections in *L. japonicus*.

4.2.2 Cytokinin and ethylene regulate the number of infection threads in *L. japonicus*

We have shown that LHK1 is the main sensor of exogenous cytokinin in *L. japonicus* (Chapter 2, Section 2.3.8). When applied to roots, cytokinin induces ethylene production which in turn limits root elongation in several plants (Dugardeyn and Van Der Straeten, 2008), including *L. japonicus* (Wopereis et al., 2000). In order to directly demonstrate the roles of cytokinin and ethylene in the regulation of epidermal infection thread formation,

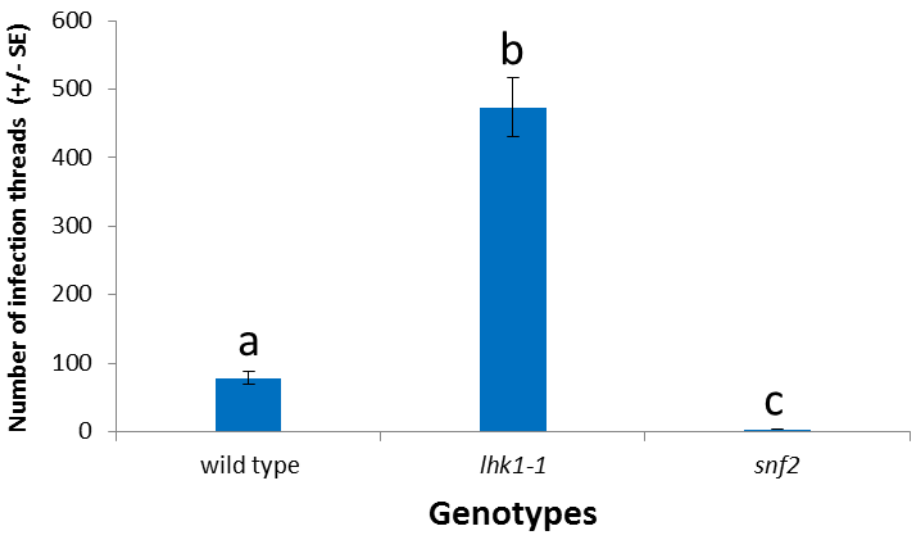

Figure 4.2 LHK1 regulates the number of infection threads.

The number of epidermal infection threads was scored in the *lhk1-1* and *snf2* mutants at 7 DAI with an *M. loti* strain tagged with the *hemA::LacZ* reporter and this was compared to the *L. japonicus* wild-type control. In all cases, values represent mean ± standard error (SE) (n = 10). Statistical grouping is indicated by the same lower case letter (one-way ANOVA, $p < 0.05$).

wild type and *lhk1-1* were exposed to the synthetic cytokinin, 6-benzylaminopurine (BA) and the ethylene precursor, ACC.

As shown in Figure 4.3, both wild-type and *lhk1-1* roots had decreased root lengths in the presence of either BA or ACC. At 5×10^{-8} M BA, the length of wild-type roots was reduced by approximately 80%, compared to the untreated control samples, while *lhk1-1* root length decreased by approximately 30%, demonstrating that *lhk1-1* is much less perceptive/sensitive to exogenous cytokinin than wild type. Similarly, the *lhk1-1* roots showed less sensitivity to 5×10^{-8} M ACC compared to wild type, perhaps reflecting a lower endogenous level of ethylene in the mutant (see below in Figure 4.14). Consistent with the latter, treatment with aminoethoxyvinylglycine (AVG), a known inhibitor of ethylene biosynthesis (Yu et al., 1979), significantly increased the relative wild-type root length (Figure 4.3), while having no (12 days) or a significantly less pronounced effect (16 days) on the *lhk1-1* root growth (Figure 4.3).

In the same roots, the number of epidermal infection threads was determined in the presence of BA or ACC and compared with untreated roots at 10 DAI (Figure 4.4). The number of epidermal infection threads formed in the presence of the given concentrations of BA and ACC was significantly reduced in comparison to untreated samples. However, the effect of the BA treatment in reducing the number of infection threads in *lhk1-1* is less dramatic compared to wild type. The impact of AVG was evaluated only in wild type and resulted in a significant increase in the number infection threads (Figure 4.5). Taken together, these observations are consistent with important roles for cytokinin and ethylene in the regulation of infection thread formation. The underlying mechanism was therefore investigated.

4.2.3 *L. japonicus* genome contains a family of at least seven *ACSs*

As the rate-limiting step in ethylene biosynthesis in plants is generally mediated by ACSs (Argueso et al., 2007), and it was predicted that ACSs are subjected to LHK1-dependent regulation during symbiosis (Figure 3.5), ACSs were targeted for detailed analyses. Using the Basic Local Alignment Search Tool (BLAST) server and available protein sequences of the nine *A. thaliana* ACSs as queries, at least seven genes predicted to encode

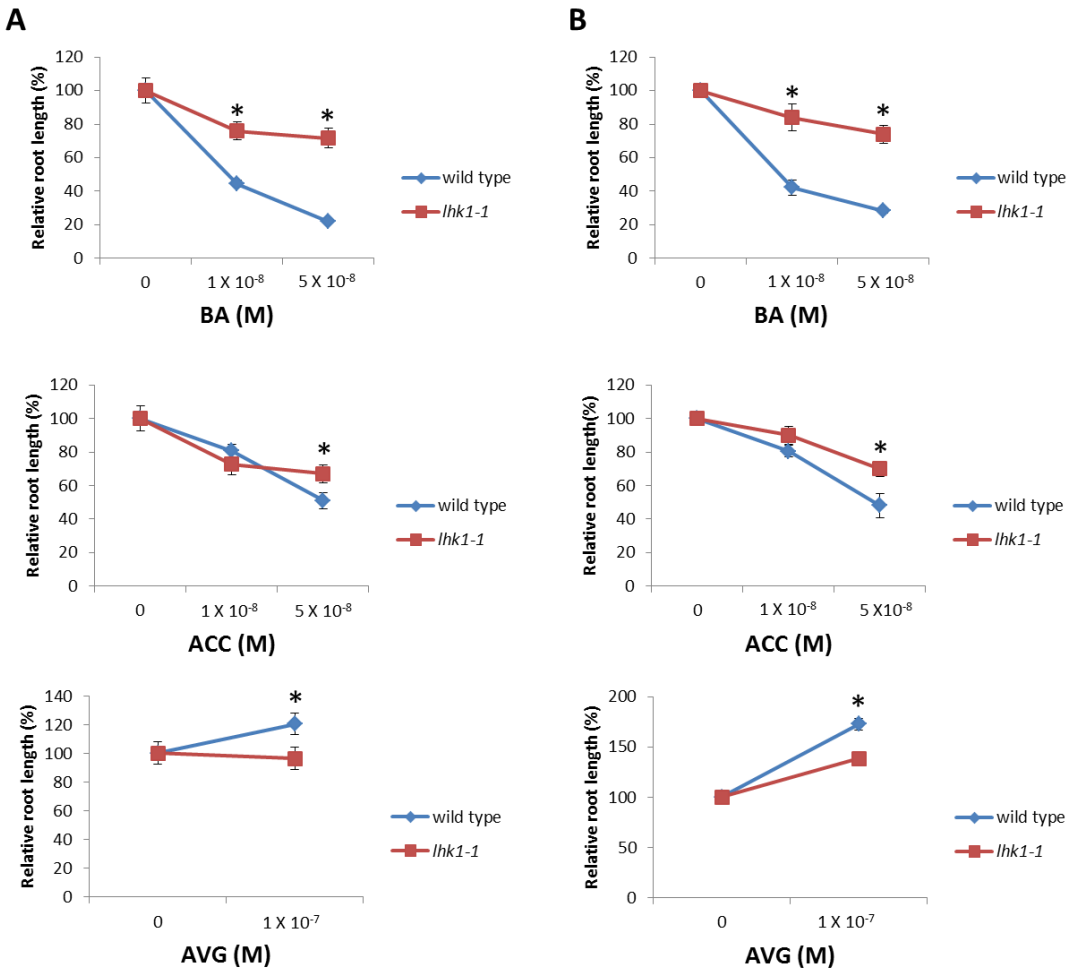

Figure 4.3 Effect of exogenous cytokinin (BA), ethylene precursor (ACC), and ethylene biosynthesis inhibitor (AVG) on root elongation in *L. japonicus* wild type and the *lhk1-1* mutant.

Plant seedlings were grown on the surface of agar plates under continuous light, in the presence of the given concentrations of BA, ACC, or AVG. Plants were inoculated with *M. loti* two days after sowing. The root length was measured 12 days **(A)** and 16 days **(B)** after sowing. The relative root length is given, where the length of the control, untreated roots (0) was set as 100%. Asterisks indicate significant differences between the wild type and *lhk1-1* samples (Student's t-Test, $P<0.05$). BA: 6-benzylaminopurine, ACC: 1-aminocyclopropane-1-carboxylic acid, AVG: aminoethoxyvinylglycine.

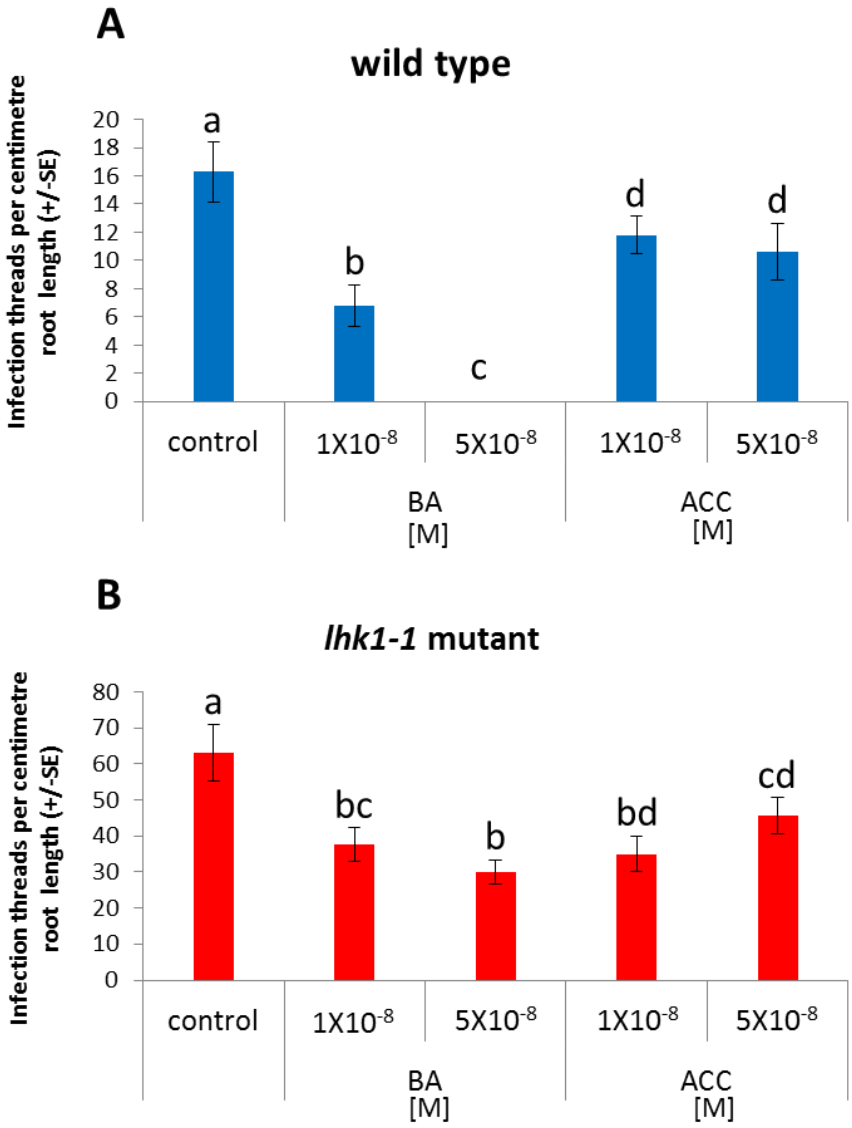

Figure 4.4 Effect of exogenous application of BA and ACC on the number of infection threads in wild type and the *lhk1-1* mutant.

The number of epidermal infection threads was scored and calculated in relation to the root length (i.e. per centimetre of the root length) in wild type **(A)** and *lhk1-1* **(B)** at 10 DAI with *M. loti* and compared to the untreated, control samples. Plant growth conditions were as described in the legend to Figure 4.3. In all cases, values reported are the mean +/- SE (n = 10). Statistical grouping is indicated by the same lower case letter (one-way ANOVA, $p < 0.05$). BA: 6-benzylaminopurine, ACC: 1-aminocyclopropane-1-carboxylic acid.

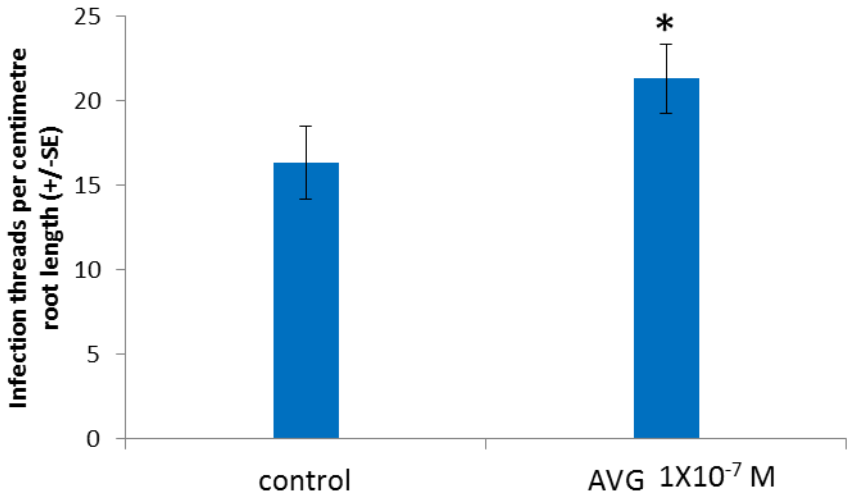

Figure 4.5 Effect of AVG on infection thread formation in wild-type roots.

The number of epidermal infection threads was scored 10 DAI with *M. loti* and calculated per centimetre of the wild-type root length, in the absence (control) or presence of 1×10^{-7} M of AVG. Values reported are the mean +/- SE (n = 10). Plant growth conditions are as described in the legend to Figure 4.3. Asterisk indicates a significant difference between the untreated control and AVG-treated samples (Student's t-Test, $P<0.05$). AVG: aminoethoxyvinylglycine.

ACS proteins were identified in the *L. japonicus* genome (Figure 4.6A). These genes were positioned onto the *L. japonicus* genetic map using the available genomic sequence information (Sato et al., 2008) and their corresponding full-length transcripts were obtained from the *L. japonicus* genome assembly website (http://www.kazusa.or.jp/lotus/). Using the online tool Spidey (Wheelan et al., 2001), the intron-exon structures for each of the seven genes were predicted (Figure 4.6B). Not surprisingly, the length and number of exons were more conserved within each of the three *L. japonicus* ACS subfamilies (Figure 4.6B).

4.2.4 *L. japonicus* ACS proteins contain known conserved domains of 1-aminocyclopropane-1-carboxylate synthase

A list of the predicted *L. japonicus* ACS proteins (LjACSs) and their counter parts in *A. thaliana* (AtACSs), including the length of amino acid sequences and the predicted molecular masses (http://web.expasy.org/compute_pi/) is provided in Table 4.1. The ACS proteins of these two species are quite similar in size, ranging between about 49.7 to around 55.5 kDa (Table 4.1). Pairwise amino acid sequence comparisons between *L. japonicus* and *A. thaliana* ACSs show identity values ranging from 49.46 to 91.70% (Table 4.2).

The LjACS proteins contain seven strongly conserved regions (BOXES1-7) (Yamagami et al., 2003). The 12 conserved amino acid residues, known to be important for catalysis and structure of ACSs, are also predicted to be invariably present in LjACS proteins (Figure 4.7) (Mehta and Christen, 1994; McCarthy et al., 2001; Jakubowicz, 2002). Alignment of LjACSs with AtACSs (Figure 4.8) partitioned these proteins into three subfamilies. Although ACS proteins all share a highly conserved catalytic core, the C-terminal region is divergent (Lin et al., 2009) (Figure 4.9).

4.2.5 Do any of the *ACS* genes respond to *M. loti* infection?

Different subsets of *ACS* genes are expressed in response to various developmental, environmental and hormonal factors (Lin et al., 2009). To understand the possible involvement of cytokinin-ethylene crosstalk in restricting the extent of infection thread

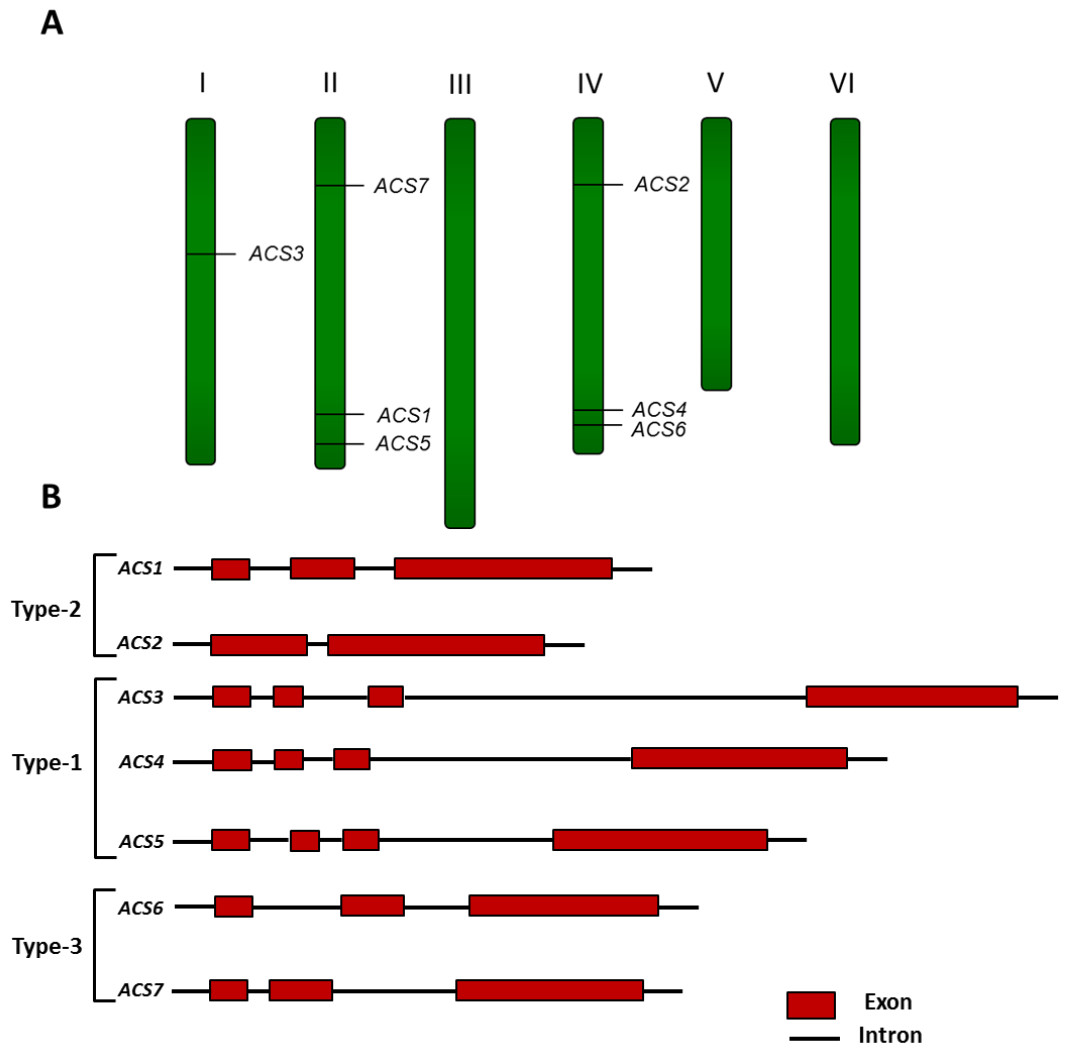

Figure 4.6 Chromosomal location and predicated intron-exon structure of *L. japonicus ACS* genes.

(A) The locations of seven predicted *ACS* loci on the six (I – VI) *L. japonicus* chromosomes are shown, according to version 3.0 of the *L. japonicus* genome annotation (http://www.kazusa.or.jp/lotus/).

(B) The predicted intron-exon structure of *LjACS* genes is shown. Boxes represent predicted exons while lines denote 5' and 3' UTRs and introns. Members of the ACS family fall within three sub-families named type-1, type-2, and type-3. For more information see Figure 4.9.

Table 4.1 Amino acid lengths and the predicted molecular mass of *L. japonicus* and *A. thaliana* ACS proteins.

	Amino Acid Length (aa)	Predicted Molecular Mass (Da)
LjACS1	480	53803.51
LjACS2	479	53853.30
LjACS3	480	54503.78
LjACS4	485	54612.47
LjACS5	483	54341.13
LjACS6	442	49942.97
LjACS7	440	49795.63
AtACS1	488	55003.00
AtACS2	496	55531.52
AtACS4	474	53795.41
AtACS5	470	53312.93
AtACS6	495	55524.37
AtACS7	447	50665.53
AtACS8	469	53370.88
AtACS9	470	53169.75
AtACS11	460	51798.94

aa: amino acid, Da: Dalton

Table 4.2 Pairwise comparisons of the predicted ACS gene and protein sequences from *L. japonicus* and *A. thaliana.*

Protein \ Nucleotide	AtACS1	AtACS2	AtACS4	AtACS5	AtACS6	AtACS7	AtACS8	AtACS9	AtACS11	LjACS1	LjACS2	LjACS3	LjACS4	LjACS5	LjACS6	LjACS7
AtACS1	**100**	67.28	55.26	56.34	61.47	60.28	55.99	56.77	56.78	56.42	55.60	66.55	63.15	62.99	58.39	59.31
AtACS2	67.08	**100**	56.74	58.42	61.69	60.47	56.68	58.56	56.07	56.19	55.75	65.76	64.18	62.99	58.64	59.44
AtACS4	51.67	50.65	**100**	71.90	55.51	60.02	79.29	71.27	65.58	67.87	67.74	56.34	56.07	55.80	60.03	60.93
AtACS5	52.64	52.52	73.83	**100**	57.37	59.78	72.77	84.29	66.02	68.59	70.03	56.70	55.64	55.23	58.95	59.77
AtACS6	61.41	60.57	49.46	51.74	**100**	59.11	57.85	58.44	59.90	55.19	56.34	63.09	65.08	65.70	57.79	59.19
AtACS7	55.32	52.51	58.31	57.14	55.81	**100**	61.61	60.17	59.98	58.86	59.27	60.24	59.33	58.86	69.63	70.54
AtACS8	54.30	54.17	80.17	76.97	52.94	59.02	**100**	73.55	67.03	68.45	69.10	58.05	57.27	55.85	60.17	61.75
AtACS9	52.42	54.05	74.68	91.70	51.74	58.08	77.19	**100**	66.45	69.02	70.31	58.79	55.93	54.94	59.88	60.16
AtACS11	50.56	52.99	63.91	65.65	54.08	58.82	67.32	65.87	**100**	65.48	65.16	57.77	55.67	55.69	58.35	59.80
LjACS1	50.77	49.89	71.76	73.02	51.19	59.48	74.03	74.09	65.50	**100**	82.08	57.83	57.37	55.10	59.03	59.22
LjACS2	50.77	51.30	71.31	76.24	51.41	58.18	73.59	75.38	66.15	85.32	**100**	59.18	57.58	56.63	60.29	59.80
LjACS3	67.23	63.50	53.46	51.63	66.60	56.65	54.80	51.85	53.86	51.95	52.06	**100**	70.14	70.42	61.71	61.84
LjACS4	62.87	61.38	50.87	50.54	67.08	54.34	53.28	50.76	50.99	52.05	51.40	70.56	**100**	81.57	61.33	61.68
LjACS5	64.83	61.76	51.08	50.33	67.29	53.44	52.84	50.54	52.32	50.97	51.08	67.86	79.25	**100**	60.29	61.78
LjACS6	54.67	52.76	57.48	57.48	55.40	74.89	60.51	58.18	59.15	58.41	58.51	57.18	55.30	55.20	**100**	84.05
LjACS7	55.63	54.40	58.08	58.08	56.58	77.40	59.72	57.85	59.53	58.78	58.41	57.21	53.94	55.22	58.68	**100**

Nucleotide (top triangle, highlighted in red) and amino acid (bottom triangle, highlighted in blue) sequence conservation (%) among candidate ACSs. Nucleotide sequences of the coding regions for each gene and the corresponding protein sequences were acquired from either the *L. japonicus* (http://www.kazusa.or.jp/lotus/) or *A. thaliana* (https://www.arabidopsis.org/index.jsp) genome resources. Alignment of sequence and percentage identities calculations were performed by Clustal Omega (http://www.ebi.ac.uk/Tools/msa/clustalo/).

Figure 4.7 Amino acid sequence alignment of seven predicted LjACS proteins.

The open circles and red color indicate the 12 invariant amino acids conserved among ACSs (Yamagami et al., 2003). The seven highly conserved domains of ACSs (Boxes 1-7) are marked by yellow. The alignments were generated by Clustal Omega using default settings (http://www.ebi.ac.uk/Tools/msa/clustalo/).

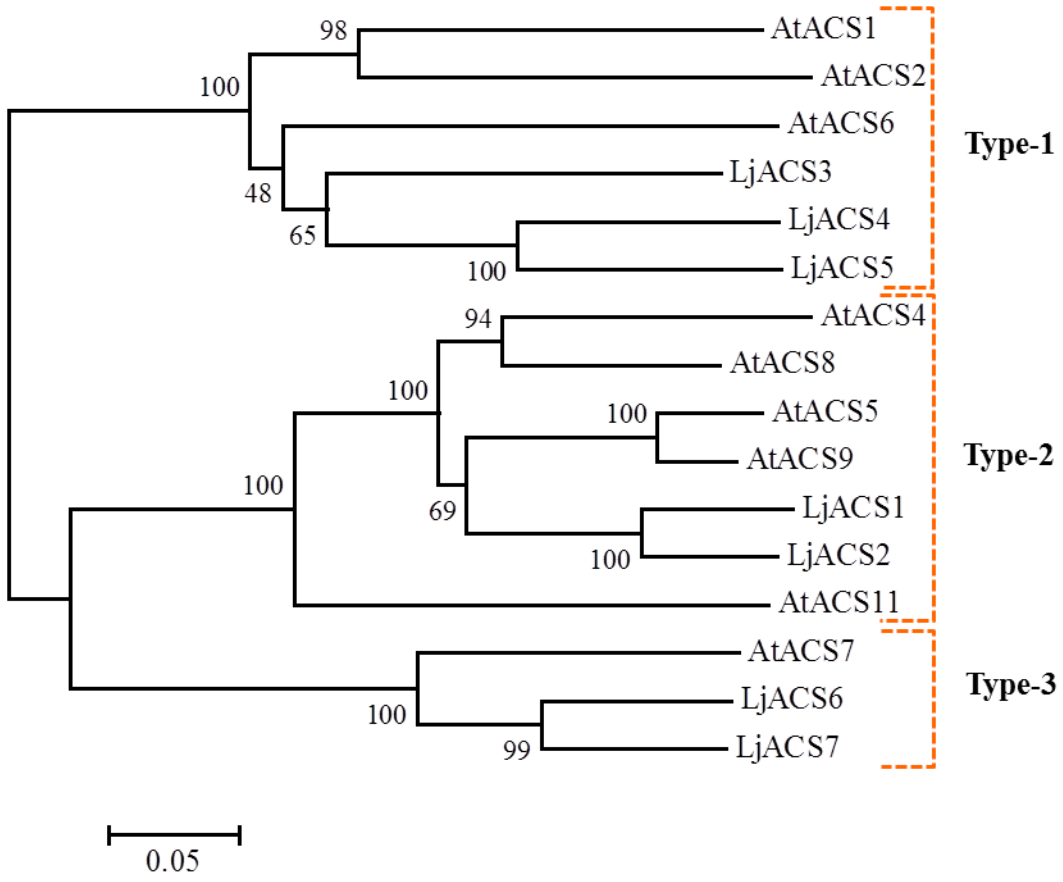

Figure 4.8 Phylogeny of ACS proteins.

An unrooted relationship tree was constructed based on amino acid alignment of predicted, full-length ACS sequences from *A. thaliana* and *L. japonicus*. The following are the gene IDs for sequences used: *A. thaliana*: AtACS1 (AT3G61510); AtACS2 (AT1G01480); AtACS4 (AT2G22810); AtACS5 (AT5G65800); AtACS6 (AT4G11280); AtACS7 (AT4G26200); AtACS8 (AT4G37770); AtACS9 (AT3G49700); AtACS11 (AT4G08040) and *L. japonicus*: LjACS1 (Lj2g3v1982940.1); LjACS2 (Lj4g3v0706600.1); LjACS3(Lj1g3v2766570.1); LjACS4 (Lj4g3v2990130.1); LjACS5 (Lj2g3v2051190.1); LjACS6 (Lj4g3v3017360.1); LjACS7(Lj2g3v0909590.1). Protein sequences were aligned using the default settings of the software MEGA version 6 and the Neighbor-Joining method with 1000 bootstrap repetition was utilized to portray the relationships between proteins.

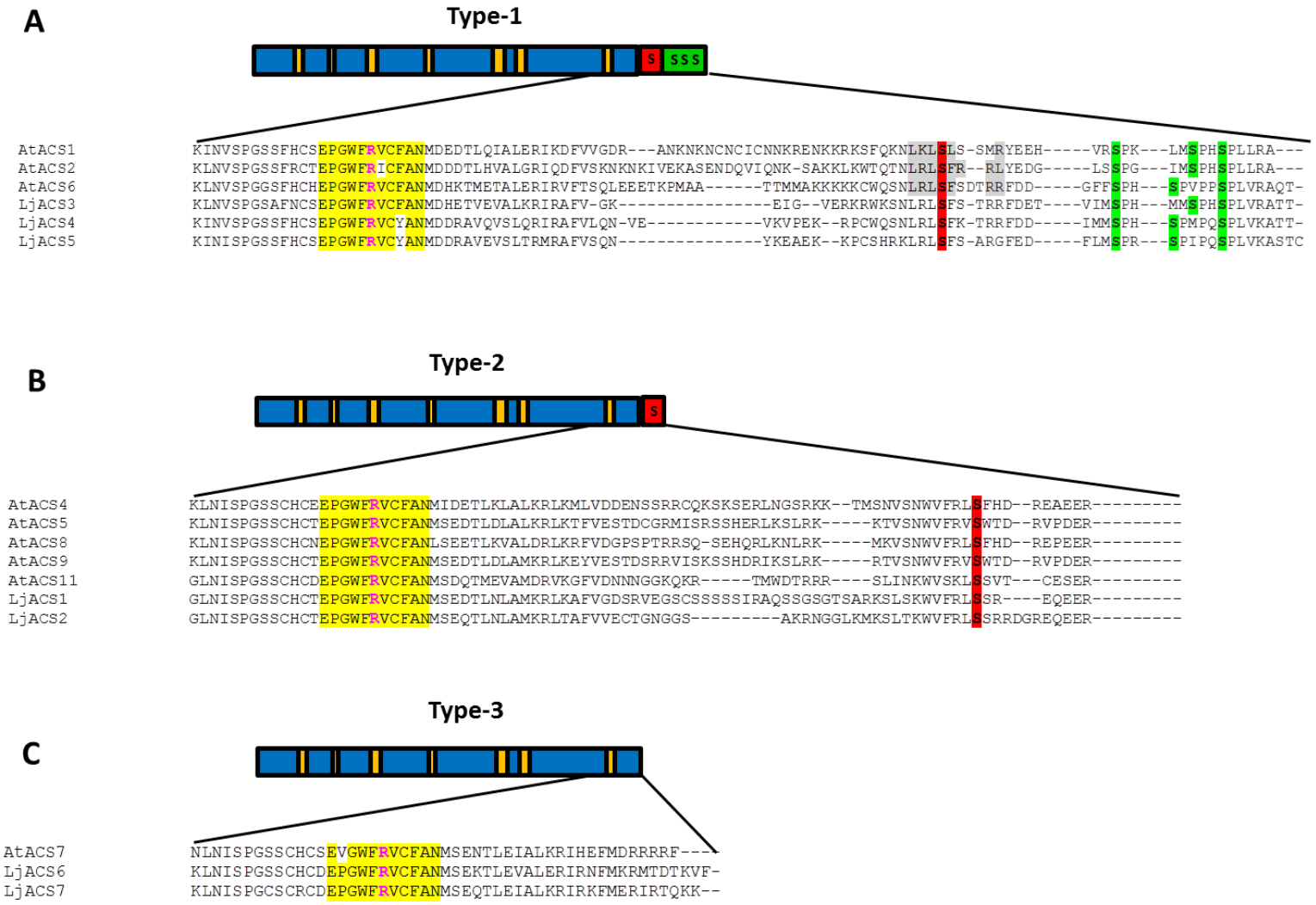
A
Type-1
S
SSS
AtACS1 KINVSPGSSFHCSEPGWFRVCFANMDEDTLQIALERIKDFVVGDR---ANKNKNCNCICNNKRENKKRKSFQKNLKLSLS-SMRYEEH-----VRSPK---LMSPHSPLLRA---
AtACS2 KLNVSPGSSFRCTEPGWFRICFANMDDDTLHVALGRIQDFVSKNKNKIVEKASENDQVIQNK-SAKKLKWTQTNLRLSFR--RLYEDG-----LSSPG---IMSPHSPLLRA---
AtACS6 KLNVSPGGSFHCHEPGWFRVCFANMDHKTMETALERIRVFTSQLEEETKPMAA------TTMMAKKKKKCWQSNLRLSFSDTRRFDD-----GFFSPH---SPVPPSPLVRAQT-
LjACS3 KLNVSPGSAFNCSEPGWFRVCFANMDHETVEVALKRIRAFV-GK----------------EIG--VERKRWKSNLRLSFS-TRRFDET----VIMSPH---MMSPHSPLVRATT-
LjACS4 KINVSPGSSFHCSEPGWFRVCYANMDDRAVQVSLQRIRAFVLQN-VE------------VKVPEK--RPCWQSNLRLSFK-TRRFDD-----IMMSPH---SPMPQSPLVKATT-
LjACS5 KINISPGSSFHCSEPGWFRVCYANMDDRAVEVSLTRMRAFVSQN--------------YKEAEK--KPCSHRKLRLSFS-ARGFED-----FLMSPR---SPIPQSPLVKASTC
B
Type-2
S
AtACS4 KLNISPGSSCHCEEPGWFRVCFANMIDETLKLALKRLKMLVDDENSSRRCQKSKSERLNGSRKK--TMSNVSNWVFRLSFHD--REAEER---------
AtACS5 KLNISPGSSCHCTEPGWFRVCFANMSEDTLDLALKRLKTFVESTDCGRMISRSSHERLKSLRK-----KTVSNWVFRVSWTD--RVPDER---------
AtACS8 KLNISPGSSCHCNEPGWFRVCFANLSEETLKVALDRLKRFVDGPSPTRRSQ-SEHQRLKNLRK-----MKVSNWVFRLSFHD--REPEER---------
AtACS9 KLNISPGSSCHCTEPGWFRVCFANMSEDTLDLAMKRLKEYVESTDSRRVISKSSHDRIKSLRK-----RTVSNWVFRVSWTD--RVPDER---------
AtACS11 GLNISPGSSCHCDEPGWFRVCFANMSDQTMEVAMDRVKGFVDNNNGGKQKR-----TMWDTRRR----SLINKWVSKLSSVT---CESER---------
LjACS1 GLNISPGSSCHCTEPGWFRVCFANMSEDTLNLAMKRLKAFVGDSRVEGSCSSSSSIRAQSSGSGTSARKSLSKWVFRLSSR----EQEER---------
LjACS2 GLNISPGSSCHCTEPGWFRVCFANMSEQTLNLAMKRLTAFVVECTGNGGS---------AKRNGGLKMKSLTKWVFRLSSRRDGREQEER---------
C
Type-3
AtACS7 NLNISPGSSCHCSEVGWFRVCFANMSENTLEIALKRIHEFMDRRRRF----
LjACS6 KLNISPGSSCHCDEPGWFRVCFANMSEKTLEVALERIRNFMKRMTDTKVF-
LjACS7 KLNISPGCSCRCDEPGWFRVCFANMSEQTLEIALKRIRKFMERIRTQKK--

Figure 4.9 Predicted sub-families of *L. japonicus* ACSs along with their corresponding *A. thaliana* counterparts.

ACS proteins fall into three subfamilies: type-1, type-2, and type-3. The protein sequence of the catalytic core (blue box on the schematics) is conserved. The highly conserved region of BOX7 is shown in yellow on the schematics. An alignment of C-terminus residues of the members belonging to each type is presented below the schematics.

(A) Type-1 ACS proteins have the longest C-terminus with a single putative CDPK phosphorylation site (red box) and three MAPK phosphorylation sites (green box). The conserved serine residue which is a phosphorylation target for CDPK is highlighted in red (Sebastià et al., 2004). The three conserved serine residues that are presumably targets for MAPK are marked in green (Liu and Zhang, 2004). The known CDPK phosphorylation motifs in *A. thaliana* are highlighted in gray (Sebastià et al., 2004).

(B) Type-2 ACS proteins have intermediate length C-termini, containing a single putative CDPK phosphorylation site. The conserved serine residue which is a phosphorylation target for CDPK is highlighted in red.

(C) Type-3 ACS proteins have very short C-termini and no predicted kinase phosphorylation sites.

formation, a possible role for ACSs in the negative regulation of rhizobia infection was investigated. Three selection criteria were initially applied to determine which *L. japonicus* ACSs might play a major role. Following the model presented in Figure 3.5, a candidate ACS involved in the regulation of *M. loti* infection, would be expected to be (1) responsive to *M. loti* infection, (2) responsive to cytokinin, and (3) regulated in an LHK1 receptor-dependent manner.

In order to determine whether any of the *ACSs* respond to rhizobial infection transcriptionally, the steady state levels of all seven *ACS* transcripts were quantified in uninoculated control roots and the corresponding roots collected 2, 3, 4, 5, 6, and 7 DAI with *M. loti* (Figure 4.10), using quantitative real-time PCR (qRT-PCR). Among seven ACSs, only *ACS2* transcript levels consistently responded to *M. loti* inoculation. Except for 2 DAI, the *ACS2* transcript level was significantly increased above the corresponding control samples at all time points analyzed. The steady state level of the *ACS2* mRNA was elevated almost five- and nine-fold in response to *M. loti* inoculation as early as 3 and 4 DAI, respectively (Figure 4.10).

4.2.6 Does cytokinin regulate ACSs in an LHK1-dependent manner *L. japonicus*?

In order to ascertain which of the *ACSs* might be regulated by cytokinin, wild-type *L. japonicus* roots were ectopically exposed to 50 nM BA for 3, 6, and 12 hours and the steady state levels of *ACS* mRNAs were determined (Figure 4.11). The transcript level of *Lhk1* was also quantified as a positive control. Consistently across all time points analyzed, three of the seven *ACS* genes, namely *ACS1*, *ACS2*, and *ACS6* responded to the ectopic cytokinin. The steady levels of their mRNAs were significantly increased above the control, untreated roots as early as 3 hours after cytokinin treatment (Figure 4.11A). To determine whether this response is LHK1-dependent, a comparable experiment was performed using *lhk1-1* mutant roots (Figure 4.12). The level of *ACS* transcripts did not significantly change upon cytokinin application in the *lhk1-1* roots indicating that the observed upregulation of *ACS1*, *ACS2*, and *ACS6* transcripts is indeed LHK1-dependent (Figure 4.12).

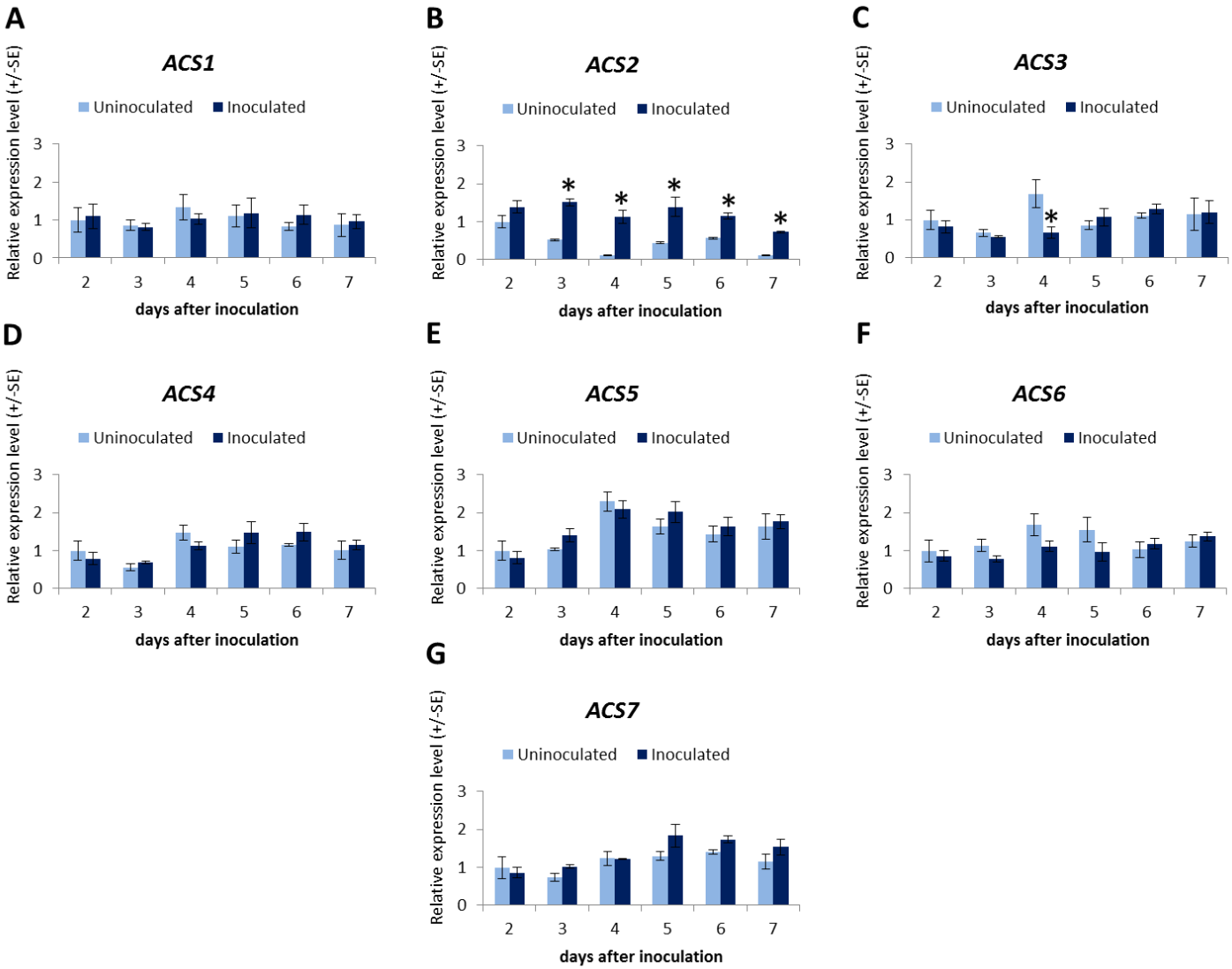
A
ACS1
Uninoculated
Inoculated
Relative expression level (+/-SE)
days after inoculation
B
ACS2
C
ACS3
D
ACS4
E
ACS5
F
ACS6
G
ACS7

Figure 4.10 Quantification of *L. japonicus ACS* transcripts in wild-type roots.

The relative steady state levels of *ACS* mRNAs **(A-G)** were quantified at 2, 3, 4, 5, 6, and 7 DAI with *M. loti* and in the corresponding uninoculated control roots of the same age. Plants were inoculated with *M. loti* 7 days after sowing. Average values for three biological replicates ± SE are given. Asterisks denote significant differences between the corresponding inoculated and uninoculated samples (Student's t test, $P < 0.05$). For each transcript, the expression values were normalized to the level of 9-day-old uninoculated samples (corresponding to the 2 DAI samples).

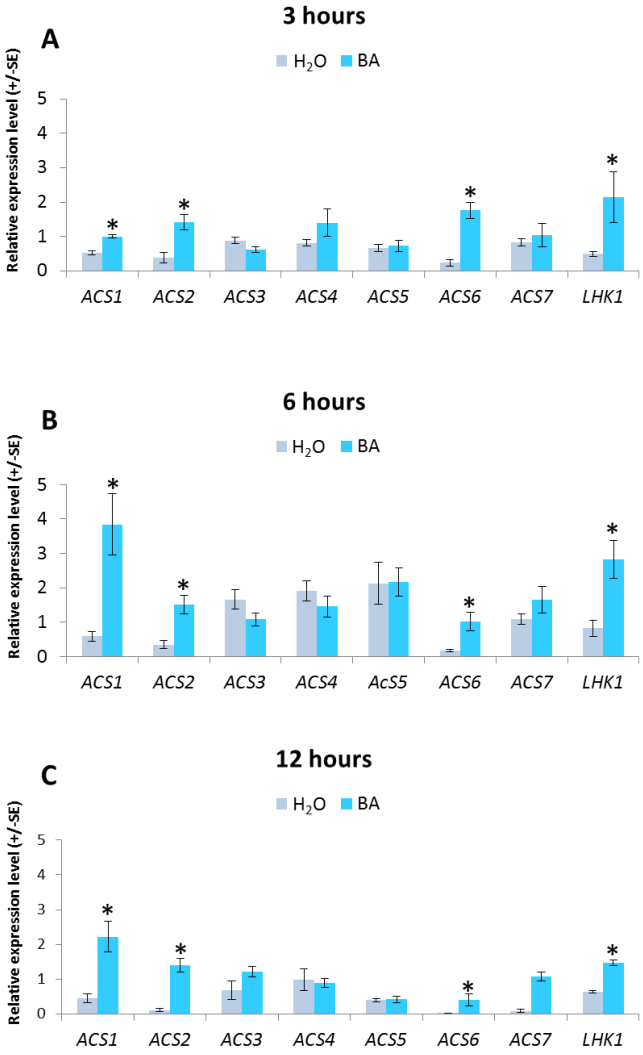

Figure 4.11 Effect of ectopic cytokinin on the steady state level of the mRNA of *ACSs* in wild-type *L. japonicus* roots.

The relative steady state levels of *ACS1*, *ACS2*, *ACS3*, *ACS4*, *ACS5*, *ACS6*, *ACS7*, and *LHK1* transcripts in untreated (H_2O) and cytokinin-treated (50 nM BA) *L. japonicus* wild type roots are given. Values represent mean ± SE for three biological replicates for roots that were incubated in the absence or presence of 50 nM BA for 3 hours **(A)**, 6 hours **(B)**, and 12 hours **(C).** The steady state level of *LHK1* transcript serves as a positive control as it is known to be increased upon cytokinin treatment. Asterisks denote significant differences between the corresponding untreated and BA-treated samples (Student's t-Test, $P<0.05$). BA: 6-benzylaminopurine.

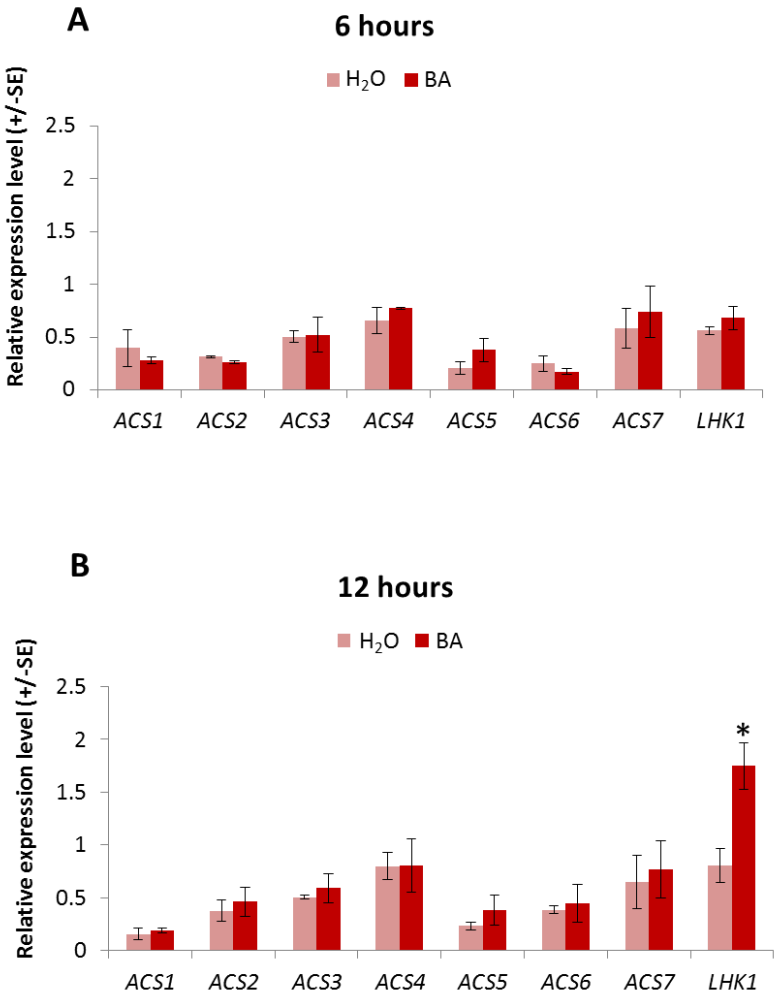

Figure 4.12 Effect of ectopic cytokinin on the steady state level of the mRNA of *ACSs* in the *lhk-1* mutant roots.

The relative steady state levels of *ACS1*, *ACS2*, *ACS3*, *ACS4*, *ACS5*, *ACS6*, *ACS7*, and *LHK1* transcripts in untreated (H_2O) and cytokinin-treated (50 nM BA) *L. japonicus lhk-1* roots are given. Values represent means ± SE for three biological replicates for 6 hours **(A)** and 12 hours **(B)** of incubation time. The steady state level of the *LHK1* transcript was measured as a control as it is expected to be increased only 12 hours after cytokinin treatment. Asterisks denote significant differences between the corresponding untreated control and BA-treated samples (Student's t-Test, $P<0.05$). BA: 6-benzylaminopurine.

Subsequent quantification in *M. loti* infected wild-type and *lhk1-1* mutant roots, 3 and 7 DAI, showed that the relative steady-state levels of *ACS1* and *ACS2* but not *ACS6* transcripts were significantly lower in *lhk1-1* compared to the corresponding wild-type samples. This observation indicated that in infected roots of *lhk1-1*, the activity of these two ACSs, both belonging to the type-2 ACS subfamily, is likely to be diminished (Figure 4.13).

4.2.7 Cytokinin and *M. loti* induce ethylene production in an LHK1-dependent manner

Based on the obtained results, it was reasoned that ACS2 and possibly also ACS1 might participate in the negative regulation of *M. loti* infection. In order to confirm whether the observed changes in levels of the *ACS* transcripts are correlated with ethylene production, its emissions were measured in wild-type *L. japonicus* in response to ectopic cytokinin or *M. loti* infection and compared to *lhk1-1* (Figure 4.14).

The ectopic cytokinin significantly enhanced ethylene levels in both wild-type and the *lhk1-1* mutant, albeit to a much lesser extent in the mutant. Similarly, inoculation of roots with *M. loti* also led to a significant increase in the ethylene levels in both wild-type and *lhk1-1* seedlings. However, the direct comparison of the relative ethylene emission levels in wild-type and *lhk1-1* seedlings revealed that a significantly lower level of ethylene was produced by the mutant (Figure 4.14).

4.2.8 In search of null alleles of *ACS1* and *ACS2* genes

Different reverse genetic approaches were employed to further understand the relevance of the *ACS* genes, particularly *ACS1* and *ACS2* in regulating *M. loti* infection. Firstly, by screening a population of *L. japonicus* LORE1 retrotransposon insertion lines (http://users-mb.au.dk/pmgrp/) (Fukai et al., 2012; Urbański et al., 2012), exonic insertions, predicted to generate null alleles, were identified in *ACS1*, *ACS4*, *ACS5*, *ACS6*, and *ACS7* loci but not in *ACS2* and *ACS3* (Figure 4.15). LORE1 is a stable, long terminal repeat (LTR) retrotransposon that amplifies in the *L. japonicus* genome by a copy-and-paste mechanism (Malolepszy et al., 2016). The insertion of the 5.041 kb long LORE1 sequence in the coding region introduces multiple premature, translational stop codons

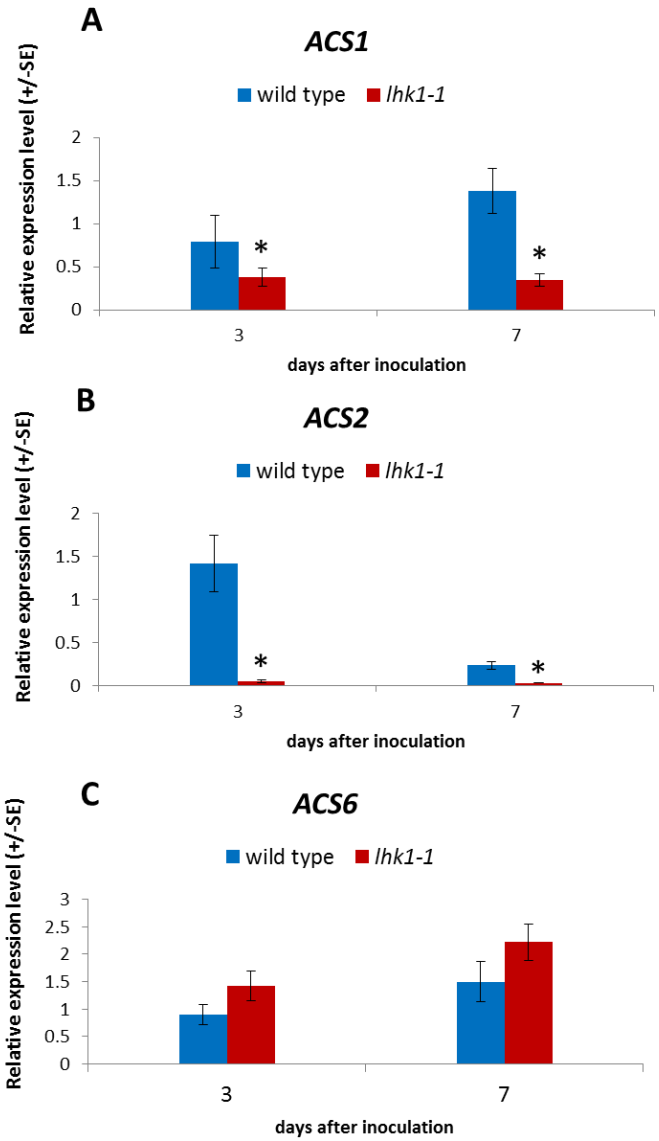

Figure 4.13 Relative expression levels of *ACS1*, *ACS2*, and *ACS6* in infected wild-type and *lhk1-1* roots.

The relative steady-state levels of *ACS1* **(A)**, *ACS2* **(B)**, and *ACS6* **(C)** mRNAs were determined in wild-type and *lhk1-1* root samples, 3 and 7 DAI with *M. loti*. Values represent mean ± SE for three biological replicates. Asterisks denote significant differences between the corresponding wild-type and *lhk1-1* samples (Student's t test, $P < 0.05$).

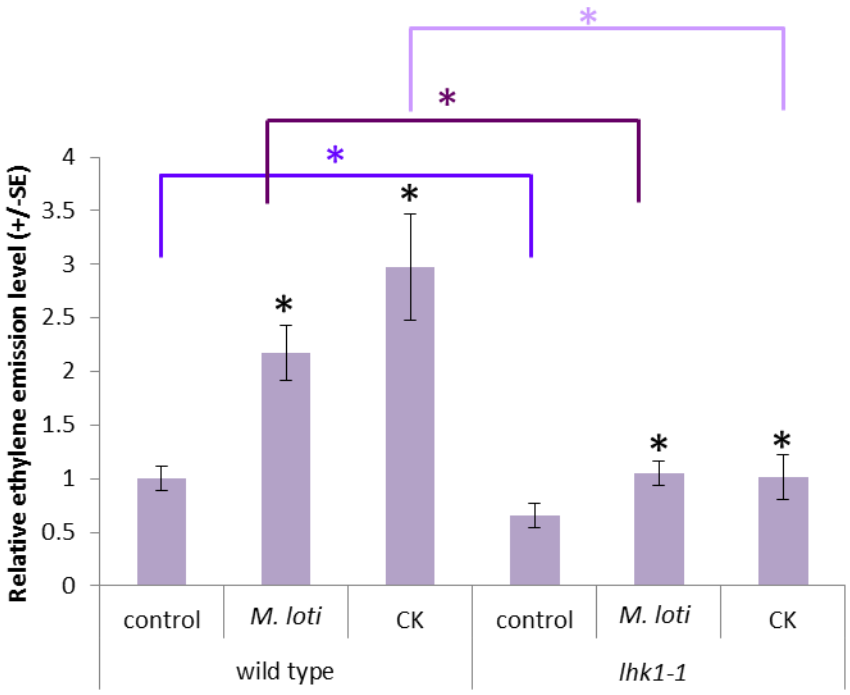

Figure 4.14 Measurement of ethylene emission.

Ethylene production was measured in wild-type and *lhk1-1* seedlings 24 hours post treatment with 10 µM BA (CK) or *M. loti* inoculation and compared to control samples. Values represent mean ± SE for ten biological replicates. The ethylene levels were normalized in relation to control wild-type samples. Black asterisks denote significant differences between the treatment and its corresponding control and colored asterisks denote significant differences between wildtype and *lhk1-1* treatments (Student's t test, $P < 0.05$).

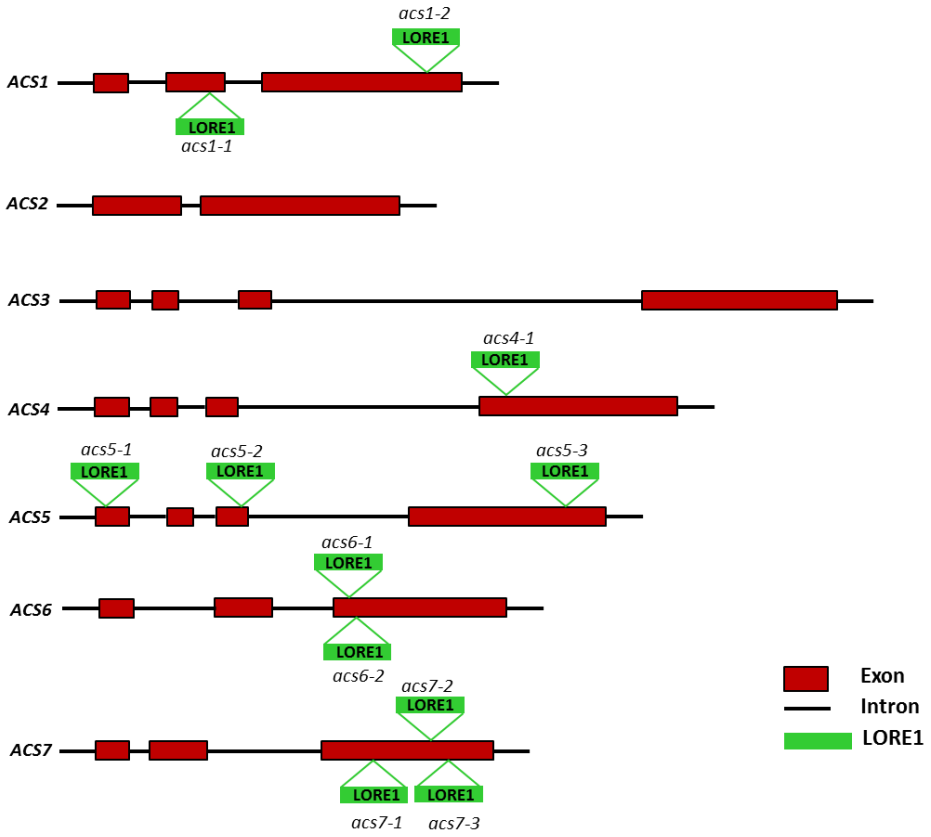

Figure 4.15 LORE1 insertions in the *L. japonicus ACS* genes.

The predicted intron-exon structures of the *L. japonicus ACS* genes are shown with positions of LORE1 insertions indicated. Red boxes represent predicted exons while lines denote 5' and 3' UTRs and introns. The green boxes represent the 5.041 kb long *L. japonicus* retrotransposon1 (LORE1) sequence (not to scale). Lower cases letters with number denote corresponding mutant allele names.

(Urbański et al., 2012). It has been previously shown that the activity of LORE1 can lead to gene inactivation and generation of null mutant alleles (Madsen et al., 2005). As the entire LORE1 sequence remains within the transcripts, we considered these insertional *ACS* alleles (Figure 4.15) as strong loss-of-function alleles.

As the search for LORE1 insertional mutations in the *ACS2* locus failed, the Targeted Induced Localized Lesions IN Genomes (TILLING) approach (Perry et al., 2009) was employed to look for an informative *ACS2* mutant. The entire *ACS2* locus (1440 bp) was targeted in two separate TILLING attempts. 12 *L. japonicus* lines carrying single nucleotide substitutions within the *ACS2* locus were identified (Table 4.3). The exact positions of the predicted amino acids changes resulting from these mutations are shown in Figure 4.16A.

Several nonsynonymous mutations were identified, however, none of them were predicted to result in a premature stop codon or affect either of the two splice sites. Furthermore, no mutations were found in any of the 12 evolutionarily conserved ACS amino acid residues (Figure 4.16A). Therefore, it was deemed unlikely that any of these mutations would have a deleterious effect on the ACS2 activity. Consistent with this prediction, *L. japonicus* mutant lines, each carrying one of the three selected *acs* TILLING mutant alleles (*acs2-7*, *acs2-8*, and *acs2-10*) showed the wild-type symbiotic phenotype, including the number of epidermal infection threads (Figure 4.16B).

Given the possibility of redundant or partially redundant function of ACS2, which could mask any phenotypic effects, the work with the *ACS2* TILLING lines was not continued. Instead, a more targeted approach, using **c**lustered **r**egularly **i**nterspaced **s**hort **p**alindromic **r**epeats (CRISPR)/CRISPR-associated protein 9 (Cas9) technology was initiated. Briefly, using the CRISPR-P web tool (http://cbi.hzau.edu.cn/cgi-bin/CRISPR), three *LjACS2*-highly specific single-guide RNAs (sgRNAs), with the lowest prediction for the off-target effects, were designed to target the 5'end of LjACS2 (Figure 4.17A). The binary Cas9 vectors containing one of the sgRNAs under the *M. truncatula* U6 promoter (Figure 4.17B), were introduced to hypocotyl segments of wild-type *L. japonicus* via an *A. tumefaciens*-mediated transformation. 96 individual T0 stable *L.*

Table 4.3 A list of *acs2* mutant alleles identified by a TILLING approach.

Plant line number	*acs2* mutant allele	Nucleotide Change *	Amino acid substitution +	Type of amino acid change
SL6609-1	*acs2-1*	G_{64} - *A*	G_{22} - *R*	Polar-Basic
SL4778-1	*acs2-2*	G_{166} -*A*	E_{56} -*K*	Acidic-Basic
SL1688-1	*acs2-3*	C_{725} - *T*	T_{206} -*I*	Polar-Nonpolar
SL5650-1	*acs2-4*	G_{778} - *A*	G_{224} - *E*	Polar-Acidic
SL4345-1	*acs2-5*	G_{802} - *A*	E_{232} - *K*	Acidic-Basic
SL1568-1	*acs2-6*	G_{898} - *A*	D_{264} -*N*	Acidic-Polar
JI8910-1	*acs2-6*	G_{898} - *A*	D_{264} - *N*	Acidic-Polar
SL4616-1	*acs2-7*	C_{949} - *T*	L_{281} - *F*	Nonpolar-Nonpolar
SL0518-1	*acs2-8*	C_{998} - *T*	S_{297} - *F*	Polar-Nonpolar
SL5911-1	*acs2-9*	C_{1019} - *A*	S_{304} - *Y*	Polar-Polar
SL4685-1	*acs2-10*	C_{1028} - *T*	T_{307} - *I*	Polar-Nonpolar
JI7203-1	*acs2-11*	C_{1075} - *T*	L_{323} - *F*	Nonpolar-Nonpolar
JI9049-1	*acs2-12*	G_{14602} - *A*	R_{451} - *K*	Basic-Basic

* DNA: nucleotide changes are listed; + Amino acid: predicted amino acid changes are listed.

Adenine in the predicted ATG initiation codon and the initiating methionine were set as 1 for defining the positions of the mutations on the DNA and amino acid levels, respectively.

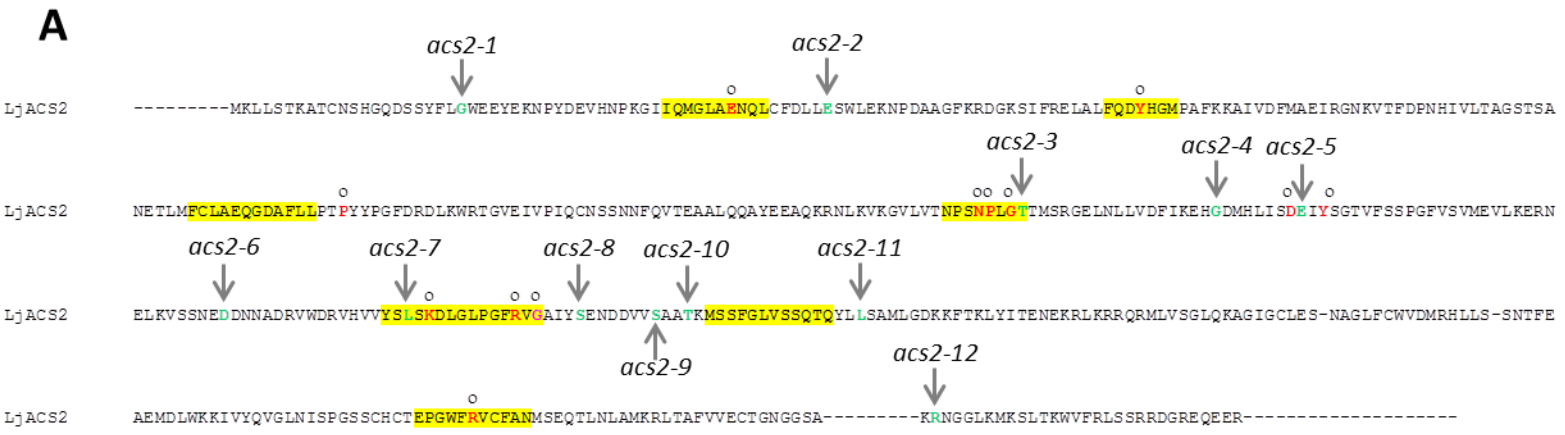
A
acs2-1
acs2-2
acs2-3
acs2-4
acs2-5
acs2-6
acs2-7
acs2-8
acs2-10
acs2-11
acs2-9
acs2-12
LjACS2 ---------MKLLSTKATCNSHGQDSSYFLGWEEYEKNPYDEVHNPKGIIQMGLAENQLCFDLLESWLEKNPDAAGFKRDGKSIFRELALFQDYHGMPAFKKAIVDFMAEIRGNKVTFDPNHIVLTAGSTSA
LjACS2 NETLMFCLAEQGDAFLLPTPYYPGFDRDLKWRTGVEIVPIQCNSSNNFQVTEAALQQAYEEAQKRNLKVKGVLVTNPSNPLGTTMSRGELNLLVDFIKEHGDMHLISDEIYSGTVFSSPGFVSVMEVLKERN
LjACS2 ELKVSSNEDDNNADRVWDRVHVVYSLSKDLGLPGFRVGAIYSENDDVVSAATKMSSFGLVSSQTQYLLSAMLGDKKFTKLYITENEKRLKRRQRMLVSGLQKAGIGCLES-NAGLFCWVDMRHLLS-SNTFE
LjACS2 AEMDLWKKIVYQVGLNISPGSSCHCTEPGWFRVCFANMSEQTLNLAMKRLTAFVVECTGNGGSA---------KRNGGLKMKSLTKWVFRLSSRRDGREQEER----------

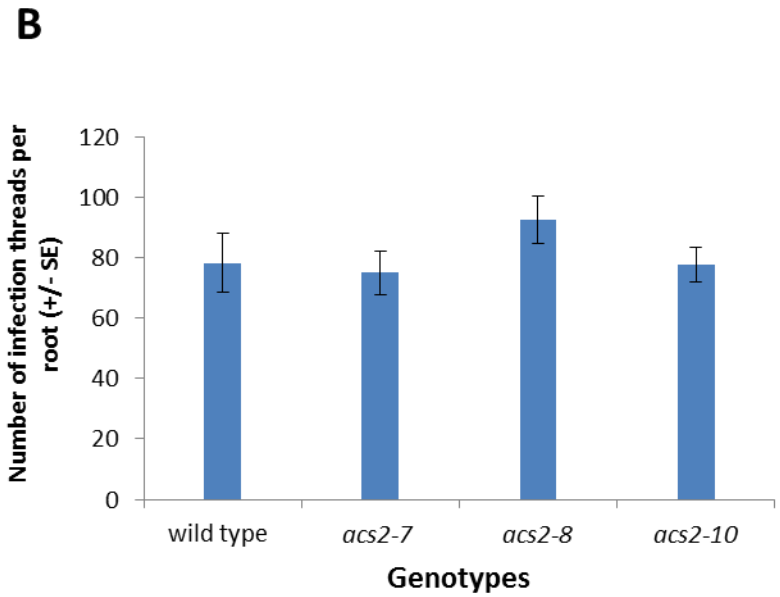
B
Number of infection threads per root (+/- SE)
120
100
80
60
40
20
0
wild type
acs2-7
acs2-8
acs2-10
Genotypes

Figure 4.16 *ACS2* mutant alleles as identified by TILLING approach.

(A) The positions of predicted amino acid changes identified through the TILLING approach are marked (arrows) and shown in green. Note that the open circles and red color indicate the 12 invariant amino acids conserved among ACS proteins. The seven conserved domains of ACS proteins are marked by yellow boxes. Lower case letter names with number denote corresponding mutant allele names.

(B) The infection threads were scored in the selected *acs2* TILLING mutant lines at 7 DAI with an *M. loti* strain tagged with the *hemA::LacZ* reporter and this was compared to the *L. japonicus* wild-type control. In all cases, values reported are the mean ± SE (n = 10). No significant differences between the mutant and wild-type control were identified (Student's t-Test, $P<0.05$).

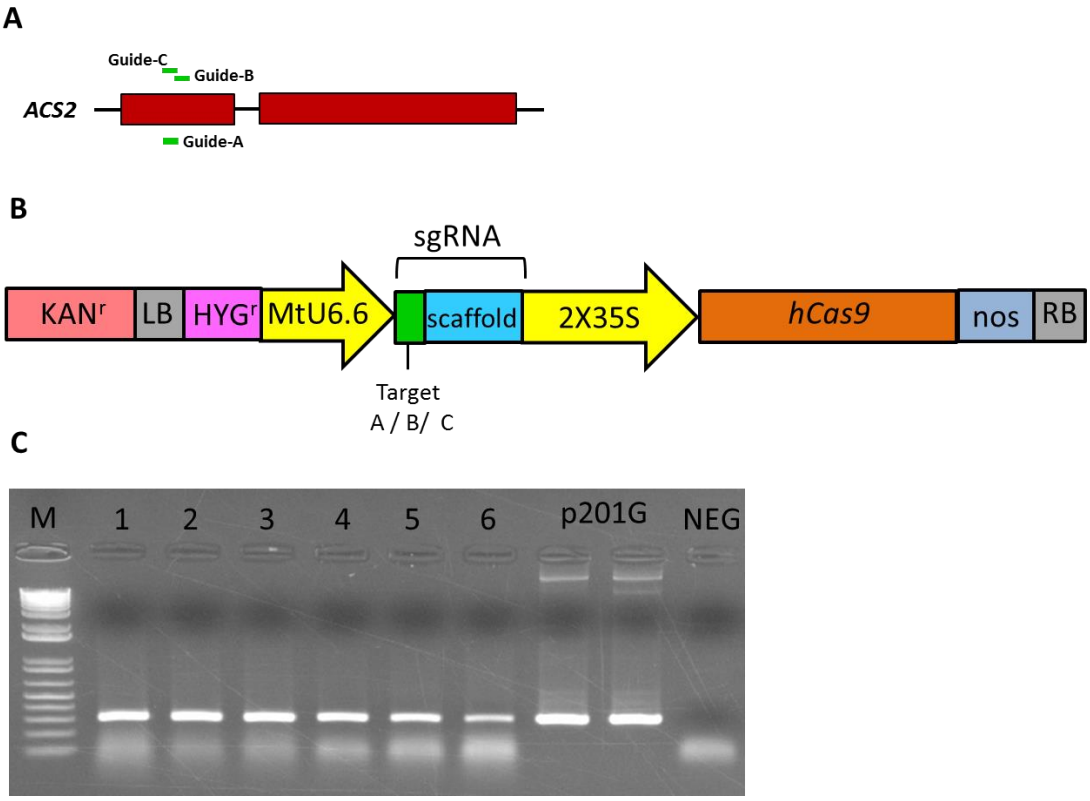

Figure 4.17 *cas9* targeting the *ACS2* in *L. japonicus* transgenic plants.

(A) Schematic showing the three $GN_{20}GG$ target motifs (green lines) on the *LjACS2* predicted intron-exon structure.

(B) A schematic of construct(s) used to target *LjACS2* using CRISPR/Cas9 system.

(C) The leaves of the transgenic plants were genotyped for the presence of the *Cas9* transgene using a PCR-based method and *Cas9* specific primers. 96 different transgenic plants were tested. The PCR results for transgenic plants 1 to 6 are shown, alongside the p201G vector (https://www.addgene.org/59176/) as the positive control.

KAN^r, kanamycin resistance; LB, T-DNA left border; HYG^r, hygromycin resistance; MtU6.6, *M. truncatula* U6.6 polymerase III promotor; sgRNA, single guide RNA, 2X35S, constitutive promotor; hCas9, human codon optimized *Cas9*, nos: terminator; RB, T- DNA right border; M; 1KB plus DNA ladder Marker; p201G: Positive control (p201G vector); NEG, Negative control

japonicus transgenic lines (Figure 4.17C) were regenerated and selected for custom-amplicon sequencing to determine the genetic modification at the *ACS2* locus. It has yet to be determined if this genome editing approach has successfully resulted in any deleterious mutations at the *ACS2* locus.

4.2.9 ACS1 participates in the negative regulation of infection thread formation in *L. japonicus*

The availability of *L. japonicus* lines carrying *acs1-1* and *acs1-2* mutant alleles (Figure 4.15), prompted follow-up experiments. Homozygous *acs1-1* and *acs1-2* lines, in addition to the wild-type control, were tested for their symbiotic phenotypes. While nodule number was unchanged (Figure 4.18A), the number of infection threads was significantly increased in both *acs1* allelic mutant lines, reaching almost twice the number in wild-type roots (Figure 4.18B). Nonetheless, this number was still significantly lower than that of hyper-infected *lhk1-1*, where at least five times more infection threads were formed in comparison to wild type (Figure 4.2). This observation indicated that it is unlikely for ACS1 to be the only player in the regulatory mechanism that limits *M. loti* infection, thus emphasizing the need for further research into the role of the *ACS2* locus.

4.2.10 Characterization of *ACS1* and *ACS2* promoter expression profiles in transgenic *L. japonicus* roots

If *ACS1* and *ACS2* indeed partake during regulation of *M. loti* infection, this should be reflected by the activity of their promoters. It is expected that they should be active in association with nodule development. Therefore, binary vectors carrying the *ACS1* and *ACS2* promoters fused to the *GUS/GFP* reporter genes were developed (Figure 4.19A) and transgenic hairy roots formed via the *Agrobacterium rhizogenes*-mediated transformation of wild-type *L. japonicus* shoots were stained for *β-glucuronidase* reporter gene activity.

When examined 10 DAI with *M. loti*, expression profiles of *ACS1* and *ACS2* were found to be nearly identical (Figure 4.19B). At an early stage, both promoters were active in dividing cortical cells of nodule primordia. With further advancement in nodule development, the activity of the promoters expanded to all dividing cells. In young nodules,

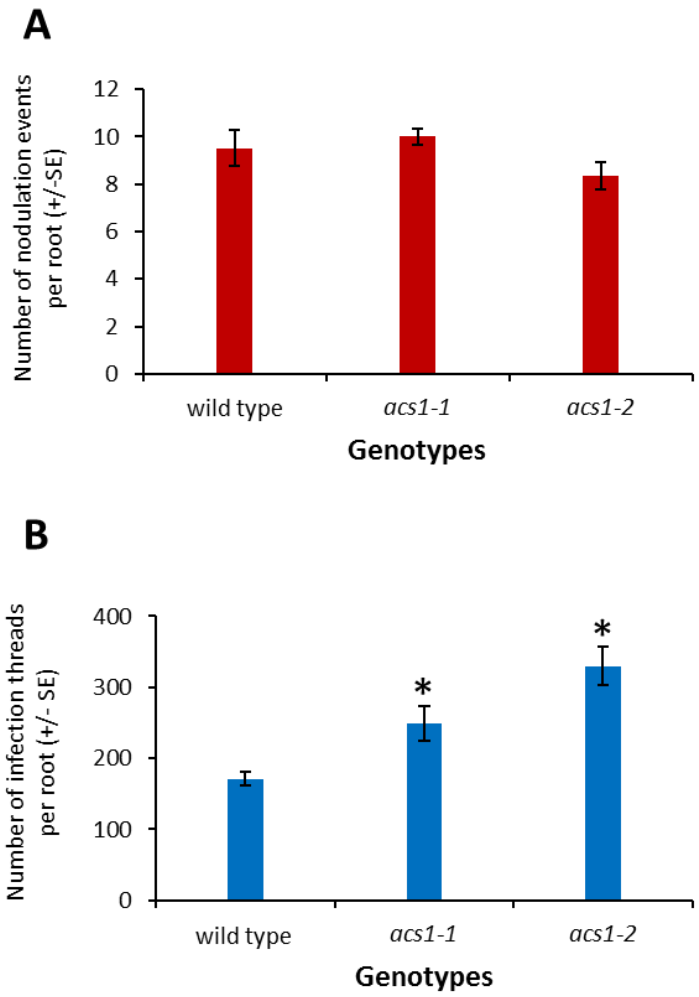

Figure 4.18 *acs1-1* and *acs1-2* have no impact on nodule number but show an increased level of epidermal infection.

The number of nodulation events (combination of nodules and nodule primordia) **(A)** and epidermal infection threads **(B)** were scored in *acs1* mutants at 7 DAI with the *M. loti* strain tagged with the *hemA::LacZ* reporter and this was compared to the *L. japonicus* wild-type control. In all cases, values reported are mean ± SE (n = 10). An asterisk denotes significant differences between the mutants and the wild-type control (Student's t-Test, $P<0.05$).

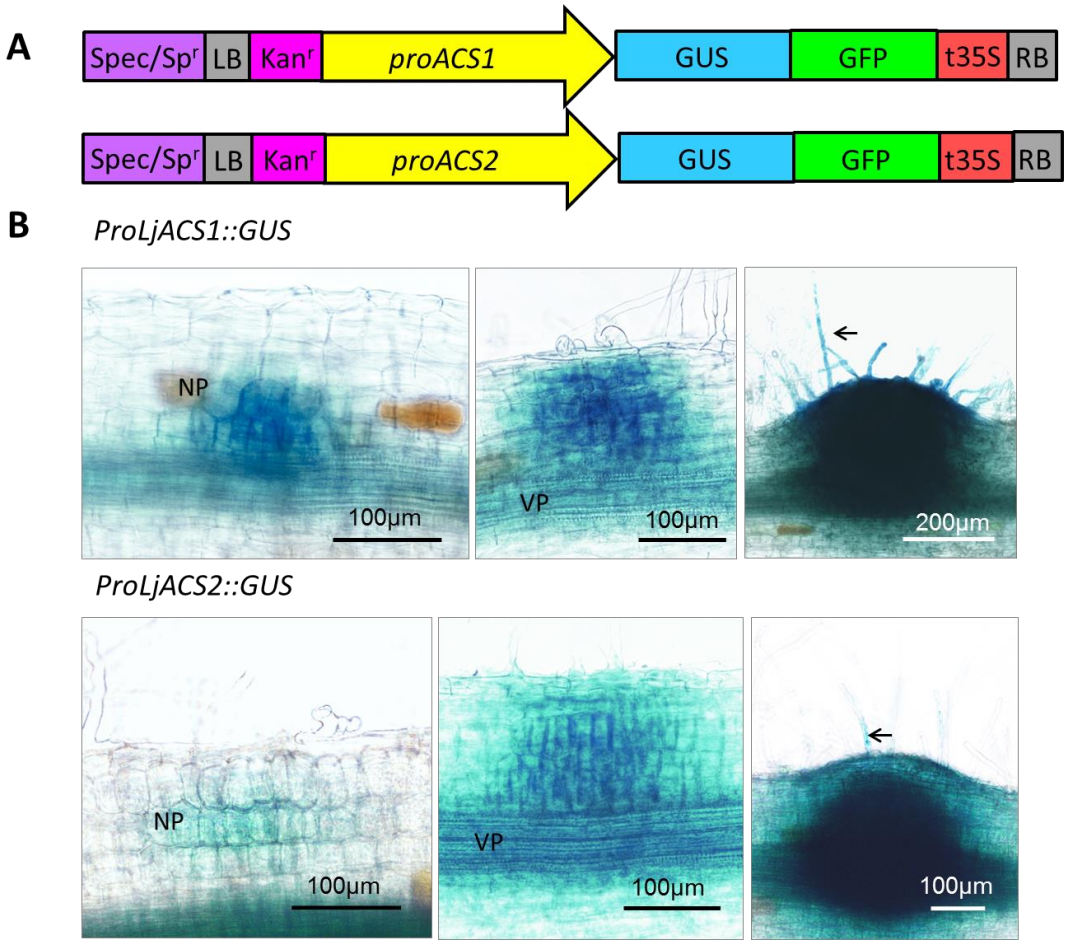

Figure 4.19 Localization of *proACS1::GUS* and *proACS2::GUS* reporter gene activities in *L. japonicus* transgenic hairy roots after *M. loti* inoculation.

(A) Schematics of constructs used to localize the *ACS1* and *ACS2* promoter activities.

(B) Histochemical detection of *LjACS1* and *LjACS2* promoter activities at different stages of nodule development. Transgenic hairy roots were stained for *β-glucuronidase* reporter gene activity at 10 DAI with *M. loti*. Arrows point to root hair showing GUS activity.

Spec/Sp^r, Spectinomycin and Spectinomycin resistance; LB, T-DNA left border; Kan^r, kanamycin resistance; GUS, β-glucoronidase; GFP, green fluorescence protein; t35S: terminator of CaMV; RB, T-DNA right border; NP, nodule primordium; VB, vascular bundle.

the GUS activity was apparent in most cells including the root epidermis and root hairs.

4.2.11 ACS1 and ACS2 might be regulated post-transcriptionally by ETO1 family proteins

Both LjACS1 and LjACS2 belong to the type-2 ACS subfamily (See Figure 4.9). Although not studied in *L. japonicus*, in several plant organisms tested type-2 ACS proteins are ubiquitinated by ETO1/EOL proteins, which promotes their degradation by a proteasome-dependent pathway (Lyzenga and Stone, 2012).

Both LjACS1 and LjACS2 contain the signature TOE sequence (WVF, RLS, and the R/D/E-rich region), at the C-terminal end which makes them potential targets of ETO1/EOLs (Figure 4.20A). Consequently, the potential role of *L. japonicus* ETO1/EOL proteins during rhizobial infection was studied.

4.2.11.1 *L. japonicus* genome contains a family of at least three ETO1/EOLs

At least three *ETO1/EOL* genes were predicted to be present in the *L. japonicus* genome by performing a homology search using the *A. thaliana* AtETO1, AtEOL1, and AtEOL2 sequences (Figure 4.20B). Based on the overall amino acid sequence homology (Figure 4.21), and the clustering pattern with the corresponding *A. thaliana* proteins (Figure 4.20B), the three *L. japonicus* ETO1/EOLs were named LjETO1, LjEOL1, and LjEOL2. Using available *L. japonicus* genome sequence information (Sato et al., 2008), *LjETO1* and *LjEOL1* loci were positioned at the upper arms of chromosome 1 and 5, respectively. *LjEOL2* was located at the lower arm of chromosome 2.

Full-length transcripts for the three *ETO1/EOLS* were obtained from the *L. japonicus* genome assembly website (http://www.kazusa.or.jp/lotus/). Using Spidey (Wheelan et al., 2001), the intron-exon structures for each of the loci were predicted (Figure 4.20C). *LjETO1* and *LjEOL2* both contain four exons, while LjEOL1 has five exons. The lengths of the predicted open reading frames were found to be 2874, 2661, and 2739 bp for *LjETO1*, *LjEOL1*, and *LjEOL2*, respectively. These reflect corresponding proteins of 957, 886, and 912 amino acids in length.

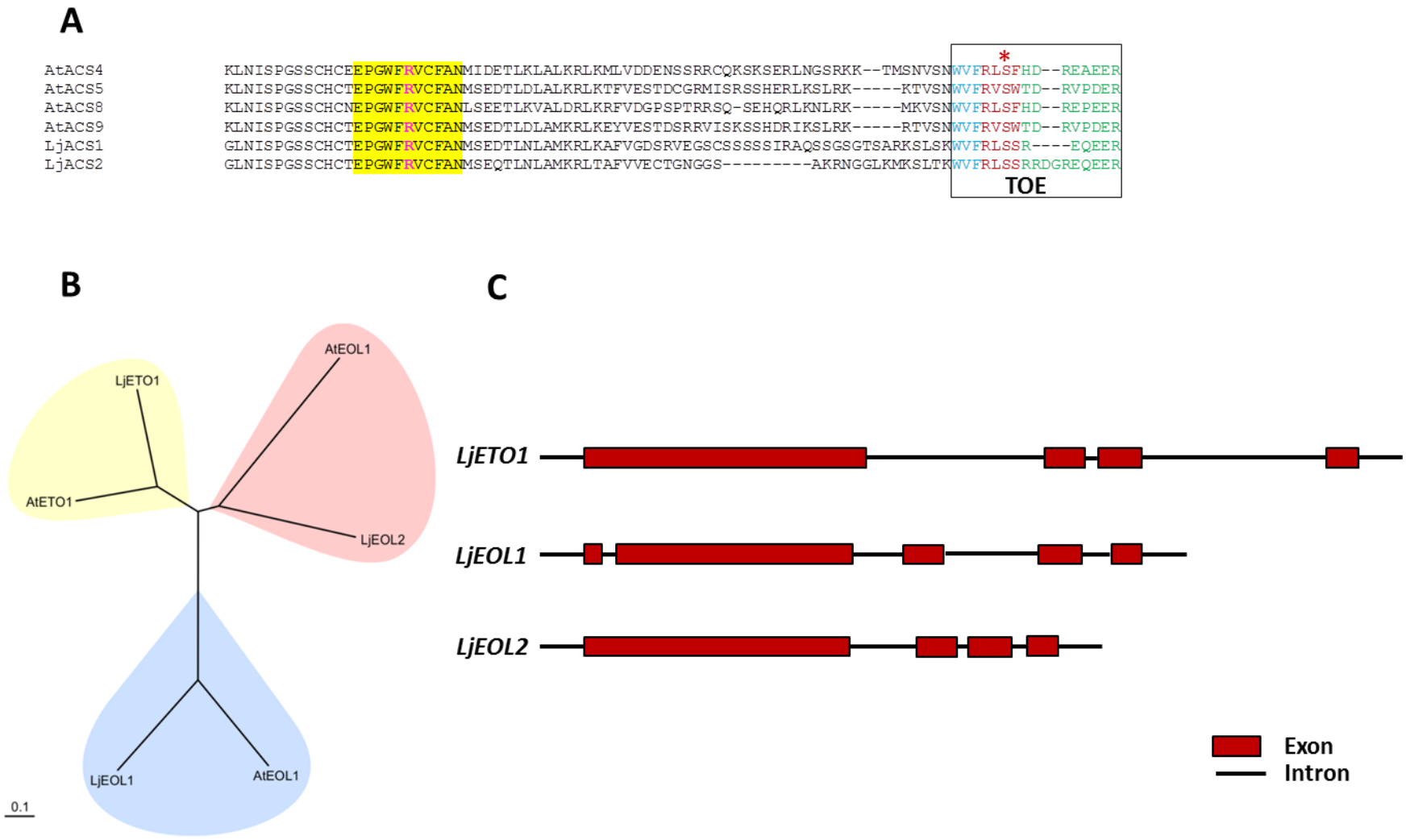
A
AtACS4 KLNISPGSSCHCEEPGWFRVCFANMIDETLKLALKRLKMLVDDENSSRRCQKSKSERLNGSRKK--TMSNVSNWVFRLSFHD--REAEER
AtACS5 KLNISPGSSCHCTEPGWFRVCFANMSEDTLDLALKRLKTFVESTDCGRMISRSSHERLKSLRK-----KTVSNWVFRVSWTD--RVPDER
AtACS8 KLNISPGSSCHCNEPGWFRVCFANLSEETLKVALDRLKRFVDGPSPTRRSQ-SEHQRLKNLRK-----MKVSNWVFRLSFHD--REPEER
AtACS9 KLNISPGSSCHCTEPGWFRVCFANMSEDTLDLAMKRLKEYVESTDSRRVISKSSHDRIKSLRK-----RTVSNWVFRVSWTD--RVPDER
LjACS1 GLNISPGSSCHCTEPGWFRVCFANMSEDTLNLAMKRLKAFVGDSRVEGSCSSSSSIRAQSSGSGTSARKSLSKWVFRLSSR----EQEER
LjACS2 GLNISPGSSCHCTEPGWFRVCFANMSEQTLNLAMKRLTAFVVECTGNGGS---------AKRNGGLKMKSLTKWVFRLSSRRDGREQEER
*
TOE
B
AtEOL1
LjETO1
AtETO1
LjEOL2
LjEOL1
AtEOL1
0.1
C
LjETO1
LjEOL1
LjEOL2
Exon
Intron

Figure 4.20 *L. japonicus* type-2 ACSs contain the TOE sequence and *L. japonicus* genome contains a family of at least three ETO1/EOLs.

(A) An alignment of C-terminal amino acid sequences of type-2 ACS from *A. thaliana* and *L. japonicus*. WVF (blue), RLS (red), and the R/D/E-rich region (green) are collectively known as TOE (Target of ETO) sequence. The RLS motif, which is common to both type-1 and type-2 ACSs, is shown in red. The conserved serine residue, which is a phosphorylation target for CDPK, is marked by a star. The conserved BOX7 is shown in yellow.

(B) An unrooted relationship tree based on an amino acid alignment of predicted, full-length ETO1/EOL sequences from *A. thaliana* and *L. japonicus*. The following are the gene IDs for sequences used: *A. thaliana:* AtETO1 (AT3G51770); AtEOL1 (AT4G02680); AtEOL2 (AT5G58550) and *L. japonicus*: LjETO1 (Lj1g3v2372430.1); LjEOL1 (Lj5g3v1003910.1); LjEOL2 (Lj2g3v2314890.2). Protein sequences were aligned using the default settings of the software MEGA version 6 and the Neighbor-Joining method with 1000 bootstrap repetition was utilized to portray the relationships between proteins.

(C) Predicted intron-exon structure of the *L. japonicus ETO1/EOL* genes is shown. Boxes represent predicted exons while lines denote 5' and 3' UTRs and introns.

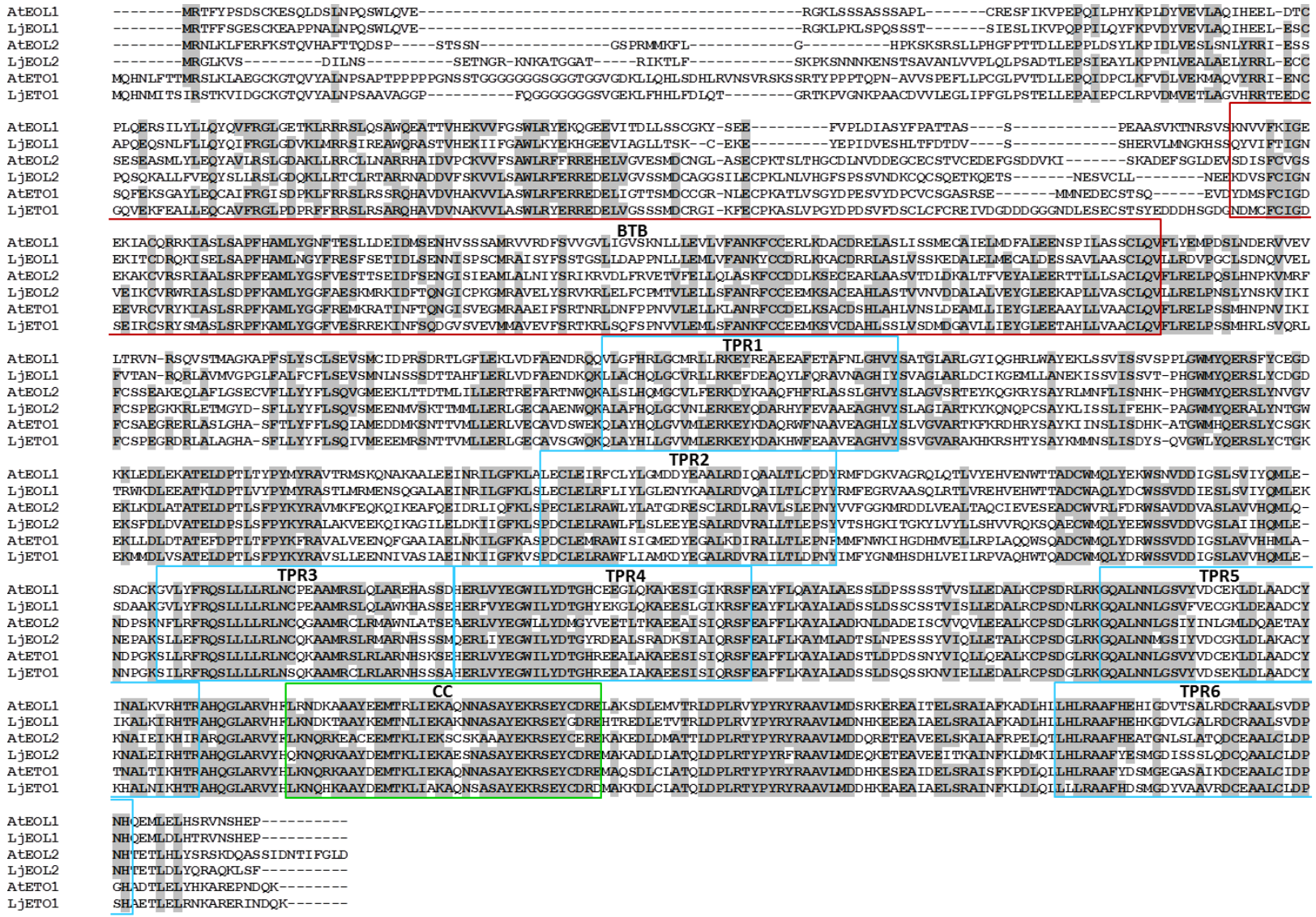
BTB
TPR1
TPR2
TPR3
TPR4
TPR5
CC
TPR6

Figure 4.21 Alignment of LjEOL1, LjEOL2, and LjETO1with their *A. thaliana* counterparts.

Predicted structural motifs of ETO1/EOL family members including the BTB domain (red box), the six TPR motifs (blue boxes), and the CC motif (green box), are indicated based on the predication made for *A. thaliana* ETO1/EOLs (Wang et al., 2004; Yoshida et al., 2006). The alignments were generated using Clustal Omega (http://www.ebi.ac.uk/Tools/msa/clustalo/).

4.2.11.2 *L. japonicus* ETO1/EOL proteins contain domains characteristic of E3 ubiquitin ligase complex members

ETO1 and the other EOL proteins are constituents of the E3 ubiquitin ligase complex (Lyzenga and Stone, 2012). *A. thaliana* ETO1/EOLs contain a BTB domain in the N-terminus, and six Tetratricopeptide Repeat (TPR) motifs and a Coiled-Coil (CC) structural motif in the C-terminus (Wang et al., 2004). The BTB, TPR and CC motifs are involved in protein-protein interactions (Lupas, 1996; Collins et al., 2001; D'Andrea and Regan, 2003). It has been suggested that the BTB domain in ETO1/EOLs is essential for interaction with CUL3 proteins, which are also constituents of the E3 ubiquitin ligase complex. In *L. japonicus* ETO1/EOLs, as in every plant species examined thus far, the arrangement of TPR and CC motifs is highly conserved (Figure 4.21). It has been suggested that TPRs are required for the specific interaction with type-2 ACS target proteins (Yoshida et al., 2006). The strong similarity of LjETO1, LjEOL1, and LjEOL2 proteins to their *A. thaliana* counterparts strongly suggests that they are involved in the regulation of ethylene biosynthesis in *L. japonicus.*

4.2.11.3 *M. loti* infection downregulates the *EOL2* transcript

In *A. thaliana* it has been shown that cytokinin increases the stability of AtACS5 and AtACS9 (type-2) by preventing their degradation by an ETO1/EOLs-dependent mechanism (Chae et al., 2003; Hansen et al., 2009). However, whether cytokinin regulates the ETO1/EOL activities is currently unknown.

The steady state levels of *ETO1*, *EOL1*, and *EOL2* transcripts were unchanged in *L. japonicus* wild-type roots upon 6 hour cytokinin treatment (Figure 4.22A). Interestingly, however, the relative normalized level of the *EOL2* mRNA was downregulated upon *M. loti* inoculation at all of the time points tested (Figure 4.22B). Importantly, our recent RNAseq data confirmed the qPCR results by showing that the level of *ACS2* and *EOL2* transcripts are significantly up- and down-regulated, respectively, in wild-type roots at 4 DAI with *M. loti* (Figure 4.23). It is plausible that the upregulation of the *ACS2* transcript and simultaneous downregulation of *EOL2* might contribute together to the increased

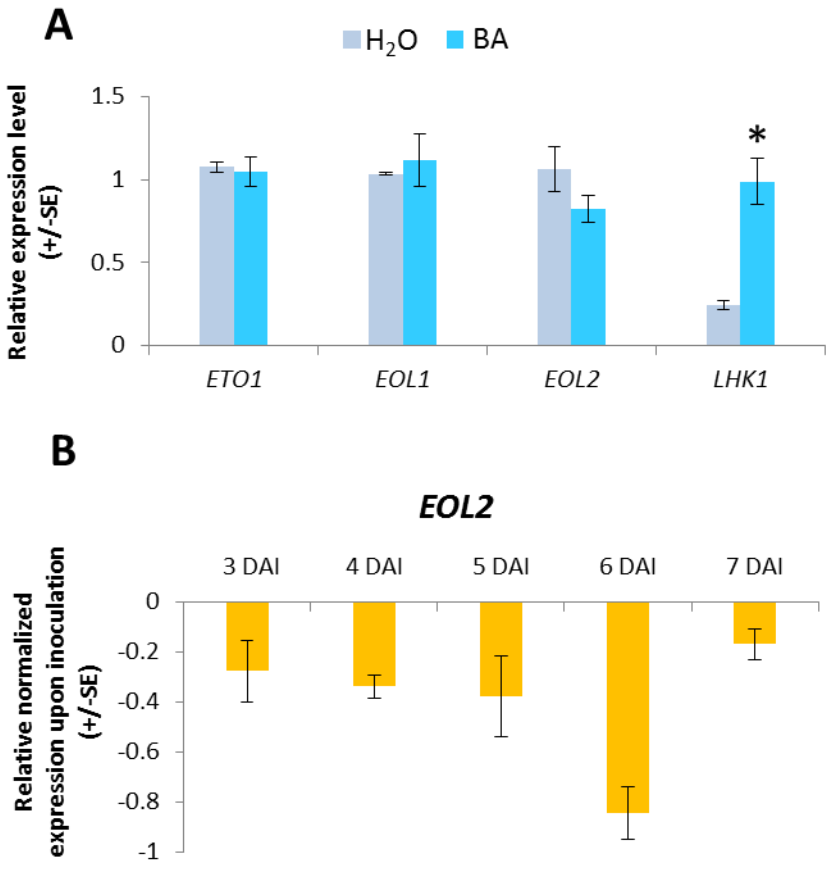

Figure 4.22 The transcript levels of *LjETO1*, *LjEOL1*, and *LjEOL2* in response to cytokinin and *M. loti* inoculation.

(A) The relative steady state levels of *LjETO1*, *LjEOL1*, *LjEOL2*, and *LHK1* mRNAs in untreated (H_2O) and cytokinin-treated (BA) *L. japonicus* wild-type roots are given. Values represent mean ± SE of three biological replicates for roots that were incubated in the absence or presence of 50 nM BA for 6 hours. The steady state level of *LHK1* was measured and used as a positive control. Asterisks denote significant differences between the corresponding untreated control and BA-treated samples (Student's t-Test, $P<0.05$). BA: 6-benzylaminopurine.

(B) The relative normalized expression levels of *EOL2* mRNA in *L. japonicus* wild type roots at 3, 4, 5, 6, 7 DAI are given. Values represent means of the expression levels for three biological replicates from inoculated samples minus corresponding values of control, uninoculated samples. Bars represent standard errors.

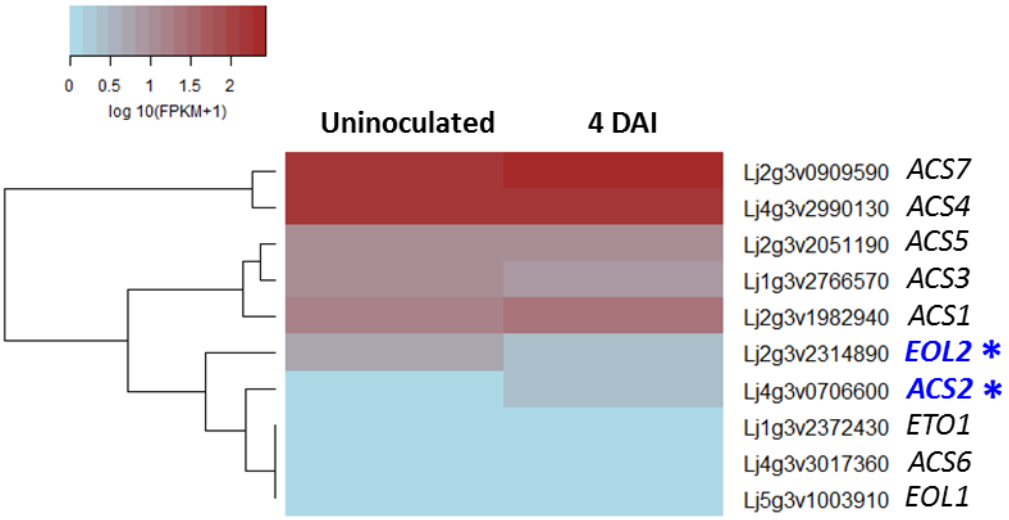

Figure 4.23 A heat map representing the expression patterns of *L. japonicus ACSs* and *ETO1/EOLs* genes in an RNA-seq experiment.

The average of log10 (FPKM+1) values are shown for normalized transcript levels of *LjACSs* and *LjETO/EOLs* in wild-type control, uninoculated samples and roots harvested 4 DAI with *M. loti*. Values are the mean of three independent biological replicates, which were grown and sequenced separately. Genes marked with blue asterisk showed statistically significantly changes in transcript levels upon inoculation with *M. loti* (FDR ≤0.001), The vertical axis dendrogram organizes genes according to co-expression. FPKM; fragments per kilobase of transcript per million mapped reads, FDR; False discovery rate

level of ethylene production upon *M. loti* infection (See Figure 4.14) which limits subsequent infection events.

4.2.11.4 Plants carrying loss-of-function alleles in *ETO1*, *EOL1*, and *EOL2* form fewer infection threads than wild type

The quantitative real time PCR and RNAseq results pointed to a possible involvement of *EOL2* in the regulation of ethylene level in response to *M. loti* inoculation. Exonic LORE1 insertions lines for *ETO1*, *EOL1*, and *EOL2* were identified (Figure 4.24A). Interestingly, they displayed a shortened hypocotyl length phenotype, possibly reflecting an increased endogenous ethylene level (Figure 4.24B). When tested for their symbiotic phenotype 7 DAI with *M. loti*, *eto1-1*, *eol1-1*, and *eol2-3* formed slightly yet significantly fewer infection threads compared to the *L. japonicus* wild-type control (Figure 4.24C).

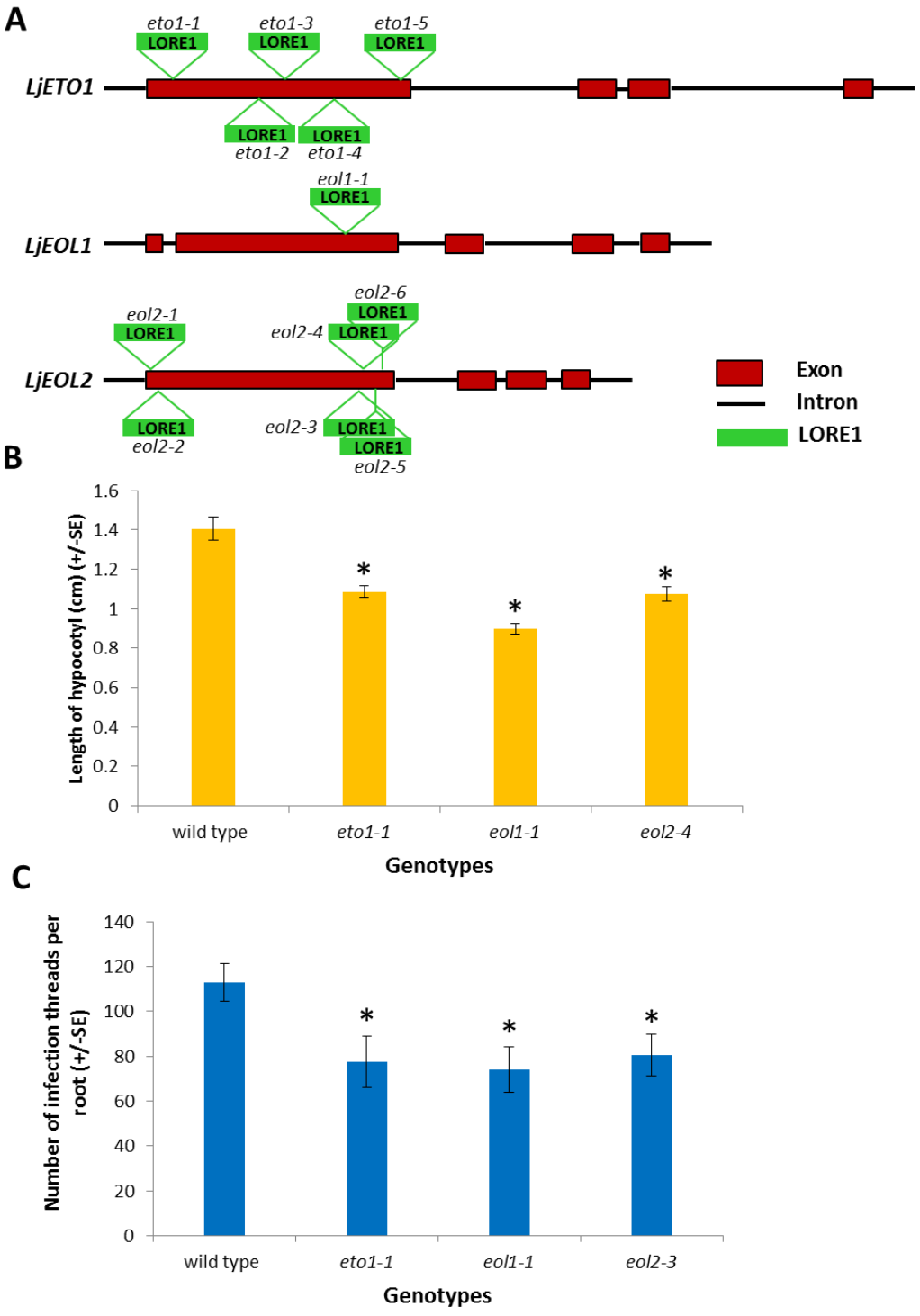
A
eto1-1
LORE1
eto1-3
LORE1
eto1-5
LORE1
LjETO1
LORE1
eto1-2
LORE1
eto1-4
eol1-1
LORE1
LjEOL1
eol2-6
LORE1
eol2-1
LORE1
eol2-4
LORE1
LjEOL2
LORE1
eol2-2
eol2-3
LORE1
LORE1
eol2-5
Exon
Intron
LORE1
B
Length of hypocotyl (cm) (+/-SE)
1.6
1.4
1.2
1
0.8
0.6
0.4
0.2
0
*
*
*
wild type
eto1-1
eol1-1
eol2-4
Genotypes
C
Number of infection threads per root (+/-SE)
140
120
100
80
60
40
20
0
*
*
*
wild type
eto1-1
eol1-1
eol2-3
Genotypes

Figure 4.24 LORE1 insertional mutations in *LjETO1*, *LjEOL1*, and *LjEOL2*.

(A) The predicted intron-exon structures of the *LjETO1/EOL* genes with the position of LORE1 insertion indicated. Red boxes represent predicted exons while lines denote 5' and 3' UTRs and introns. The green boxes represent the 5.041 kb long *L. japonicus* retrotransposon1 (LORE1) sequence. Lower case letter names with number denote corresponding mutant alleles.

(B) Hypocotyl length of 6-day-old etiolated seedlings of *eto1-1*, *eol1-1*, and *eol2-4* mutants were measured and compared to wild type. In all cases, values reported are mean ± SE ($n \geq 40$). An asterisk denotes significant differences between the mutant and wild-type control (Student's t-Test, $P<0.05$).

(C) The number of infection threads was scored in *eto1/eol* mutants at 7 DAI with the *M. loti* strain tagged with the *hemA::LacZ* reporter and this was compared to the *L. japonicus* wild-type control. In all cases, values reported are mean ± SE ($n = 10$). An asterisk denotes significant differences between the mutant and wild-type control (Student's t-Test, $P<0.05$).

4.3 Discussion

That *lhk1-1* is hyperinfected by *M. loti* has been known for almost a decade (Murray et al., 2007). The underlying mechanism, however, has not been investigated. As cytokinin and ethylene both negatively regulate the extent of rhizobial infection in legume roots (Penmetsa and Cook, 1997; Murray et al., 2007) (See also Chapter 3), we have tested a hypothesis that a molecular crosstalk between these two plant hormones partakes in establishing this homeostatic mechanism. In this chapter, we described the identification and characterization of the *L. japonicus ACS* gene family, encoding a group of isoenzymes that mediate the rate-limiting step in ethylene biosynthesis. The obtained data suggest that while operating in an LHK1-dependent manner, the *L. japonicus* type-2 ACS proteins, ACS1 and ACS2 contribute to the regulation of *M. loti* infection. Furthermore, the three members of the *L. japonicus* ETO1/EOLs family, which are the negative regulators of type-2 ACS proteins, also emerged as likely participants in this regulation. We have proposed a model in which combined effects of ACS1/ACS2 and ETO1/EOLs contribute during the regulation of ethylene and hence, *M. loti*-induced infection thread formation.

4.3.1 Cytokinin negatively regulates rhizobial infection

Compared to wild type, the loss- and gain-of-function alleles of *LHK1*, namely *lhk1-1* (Murray et al., 2007) and *snf2* (Tirichine et al., 2007), show hyperinfection and low infection phenotypes, respectively (Figure 4.2). This provides genetic evidence that the innate rates of cytokinin perception and the resulting cytokinin signaling are important regulators of infection thread (IT) formation. Importantly, while having a strongly negative effect on the ability of *L. japonicus* to initiate ITs, *snf2* has a relatively minor impact on the overall plant growth, hence it has been considered as a weak, gain-of-function allele (Tirichine et al., 2007). Together, this indicates that IT formation is highly sensitive to cytokinin levels. Indeed, at 50 nM concentration, ectopic cytokinin dramatically reduced the IT formation. This effect was apparent in both *L. japonicus* wild type and *lhk1-1* (Figure 4.3 and 4.4). We showed (see Chapter 2, Section 2.3.8) that LHK1 is the main sensor of exogenous cytokinin in *L. japonicus* (Held et al., 2014). However, when exposed to ectopic cytokinin for a longer time (e.g. for 12 and 16 days),

lhk1-1 was able to respond by reducing the root length and the number of ITs. This is likely due to the presence of other, partially redundantly functioning cytokinin receptors within the root cortex (see Figure 2.20) (Held et al., 2014). Nonetheless, this response was very limited in comparison to wild type (Figure 4.3 and 4.4). Taken together, the genetic and physiological observations are in agreement with our model (Figure 3.5), showing that cytokinin is indeed involved in the mechanism that locally restricts the number of ITs and in *L. japonicus* this process is primarily LHK1-dependent (Miri et al., 2016).

4.3.2 *lhk1-1* is ACC-sensitive

Ethylene is known to be a potent inhibitor of early responses to Nodulation factor (NF) and was shown to dynamically regulate infection and nodule formation events by inhibiting or modulating the epidermal calcium spiking in a concentration-dependent manner (Oldroyd et al., 2001; Oldroyd and Downie, 2006; Morieri et al., 2013). Furthermore, it has been shown that IT formation is inhibited by ACC but stimulated by AVG (Oldroyd et al., 2001). Also, ethylene insensitive *M. truncatula* and *L. japonicus* mutants (Penmetsa and Cook, 1997; Nukui et al., 2000; Lohar et al., 2009) show a significantly higher number of ITs, indicating that endogenous ethylene acts to limit this process. In agreement with these results, ACC significantly reduced the number of ITs in both the *L. japonicus* wild-type and *lhk1-1* (Figure 4.4). This was expected, as *lhk1-1* has no known defects in the ethylene perception mechanism. However, the amount of ethylene emitted by *lhk1-1* roots was found to be significantly lower than in wild type and this was further accentuated in the cytokinin-treated or *M. loti*-inoculated roots (Figure 4.14). This observation indicates that in addition to its role in mediating the ethylene production in response to *M. loti* inoculation or presence of exogenous cytokinin, LHK1 is also required to maintain the endogenous ethylene level. Consistent with the diminished endogenous level of ethylene, compared to wild type the growth of *lhk1-1* roots was less sensitive to the inhibitory and stimulatory effect of ACC and AVG, respectively (Figure 4.3).

The ability of *lhk1-1* to respond to *M. loti* inoculation by increasing ethylene level indicates that ethylene production can proceed during the symbiotic interaction

independent from LHK1, although to a much lesser extent (Figure 4.14). This ethylene level is likely insufficient to block the subsequent infection events, thus resulting in hyperinfection. Interestingly, the ethylene insensitive *Mtskl* mutant was shown to exhibit reduced sensitivity to cytokinin in the root elongation assay (Penmetsa et al., 2008), highlighting the existence of feedback mechanisms. Furthermore, Reid *et al* showed that the reduced number of ITs formed in the cytokinin oxidase/dehydrogenase3 (*ckx3*) mutants due to elevated cytokinin levels could be rescued by AVG treatment (Reid et al., 2016). Taken together, these observations further support our model (Figure 4.5) for the cytokinin-stimulated, ethylene-dependent inhibition of *M. loti* infection.

4.3.3 ACS2 might participate in negative regulation of rhizobial infection

The lower level of ethylene in the *lhk1-1* mutant roots could be, at least in part, due to defect in cytokinin-dependent ethylene biosynthesis. Here, we show that *LjACS2* is the only member of the *L. japonicus ACS* gene family that responds to both ectopic cytokinin and *M. loti* inoculation by increasing the steady state level of its mRNA. Importantly, this response is LHK1-dependent (Figure 4.10, Figure 4.11, Figure 4.12 and Figure 4.13). Meeting the three operational criteria makes *ACS2* a viable candidate in the postulated cytokinin-ethylene crosstalk which negatively regulates *M. loti* infection at the root epidermis. Such an interpretation is supported by additional observations, including the *L. japonicus* Gene Atlas data (http://ljgea.noble.org/v2/) (Verdier et al., 2013) and our recent RNAseq experiment (Figure 4.23) which both show that the *ACS2* but not the other *ACS* transcript levels are upregulated 3 and 4 DAI with *M. loti*, respectively. Furthermore, the transcript level of the *LjACS2* counterparts in *M. truncatula* have also been shown to be increased upon *S. meliloti* inoculation or NF application in an MtCRE1- and MtEIN2- dependent manner (Larrainzar et al., 2015; van Zeijl et al., 2015). Other studies have shown that expression of *LjACO2* and *MtACOs*, which mediate the final step in ethylene biosynthesis, are also upregulated early on upon rhizobial inoculation (Miyata et al., 2013; Larrainzar et al., 2015). Collectively, these data confirm that *de novo* ethylene production occurs early on during symbiotic interaction and imply

an important role for ACS2 in mediating the cytokinin-dependent inhibition of subsequent IT formation events in *L. japonicus*.

Attempts to identify a deleterious mutation at the *ASC2* locus through either insertional or chemical mutagenesis schemes have not been successful (Figure 4.15 and Figure 4.16). This has effectively precluded direct testing of the ACS2 role during *M. loti* infection of *L. japonicus* roots. Since obtaining an *asc2* mutant is crucial, a CRISPR/Cas9 system (Jacobs et al., 2015) was deployed to introduce site-specific double-stranded DNA breaks at the *ACS2* locus (Figure 4.17). An imprecise cellular repair mechanism is known to generate random insertion and/or deletion of sequences at the breakage sites, typically leading to frameshift mutations that result in knock-out alleles (Belhaj et al., 2013). The offspring of the fully transgenic plants carrying the *ACS2*-targeted CRISPR/Cas9 constructs will have to be analyzed to determine whether any deleterious mutations at the *ACS2* locus were obtained through this process. If ACS2 indeed plays a major role in the cytokinin-dependent regulation of epidermal infections, the corresponding mutant plants would be expected to develop significantly more ITs than wild type.

4.3.4 *acs1* mutants form more infection threads

Even though no significant differences could be observed in the steady state levels of the *ACS1* mRNA upon *M. loti* infection, it was still possible to consider that ACS1 might work at least partially redundantly with ACS2 to inhibit the excessive infection. ACS1 and ACS2 both belong to the type-2 subfamily and they also share more than 85% similarity at the amino acid sequence level (Table 4.2). Furthermore, like *ACS2*, *ACS1* responded to ectopic cytokinin and its transcript level was lower in the *lhk1-1* mutant (Figure 4.11 and Figure 4.13). Consistent with the prediction, *L. japonicus* plants carrying one of the two independent LORE1 insertion *acs1* alleles exhibited significantly increased levels of *M. loti* infection (Figure 4.18). Thus, ACS1 must be involved in the regulation of rhizobial infection, but the mechanism by which the gene expression is regulated during symbiosis remains unclear. *Arabidopsis* type-2 ACSs are known to be regulated by cytokinin primarily on a post-translational level (Hansen et al., 2009). It is, therefore, intriguing to think that rhizobially-induced cytokinin can also increase the stability of the ACS1 and ACS2 proteins, thus contributing to a local ethylene production that regulates

the extent of IT formation events. Whether indeed the stability of ACS1 and ASC2 is altered in *lhk1-1* remains to be determined.

Notably, the number of ITs formed by *acs1* mutants, although almost doubled compared to wild type, was not even close to the level of hyperinfection seen in *lhk1-1* (Figure 4.18B). This observation is consistent with the prediction that ACS1 might not be the only player in this context. Therefore, determining whether an *acs1 acs2* double mutant would be as hyperinfected as *lhk-1* is important. However, given the fact that cytokinins also partake in suppressing subsequent nodulation events as part of the systemic autoregulation of nodulation (AON) mechanism (Sasaki et al., 2014; Soyano et al., 2014), it is tempting to speculate that they might also contribute to systemically-mediated restriction of IT formation. This effect would be in addition to their local role, as mediated through ACSs. If this is indeed the case, then *acs1 acs2* would be expected to form more ITs than the corresponding single mutants but it would still not be as hyperinfected by *M. loti* as *lhk1-1*.

4.3.5 *eto1/eol* mutants form less infection threads

This study suggests that three members of the ETO1/EOL protein family are likely to play a role in fine-tuning *M. loti* infection. The *L. japonicus* mutant plants, each carrying a LORE1 insertion allele in one of these three loci showed a slightly but significantly lower number of ITs compared to wild type (Figure 4.24). This phenotype suggests that by overproducing ethylene the *eto1/eols* insertion mutants might contribute to the enhanced negative regulation of *M. loti* infection, potentially by affecting the degradation rate of type-2 ACS proteins. Importantly in this context, the steady-state level of the *EOL2* mRNA was significantly downregulated upon *M. loti* infection (Figure 4.22 and Figure 4.23), showing that the expression of this gene is symbiotically regulated.

Our results suggested that *L. japonicus* ETO1, EOL1, and EOL2 might function redundantly and their activity might be curtailed by *M. loti* infection, contributing to increased stability of ACSs and thus ethylene production, which limits subsequent infections (Figure 4.14). Consequently, a triple *eto1 eol1 eol2* mutant would be expected to have a low infection phenotype. If symbiotically-induced cytokinin negatively regulates the activity of ETO1/EOLs in an LHK1-dependent manner, then combining

eto1/eols mutant alleles with *lhk1-1* should result in the reversion or partial reversion of the *lhk1-1* hyperinfected phenotype.

4.3.6 *ACS1/2* expression profiles follow the cytokinin output activity

Expression patterns of *ACS1* and *ACS2* after rhizobial infection (Figure 4.19) are reminiscent of the expression of both the *Lhk1* cytokinin receptor promotor (Figure 2.13) and the cytokinin two- component output sensor (*TCS*)::*GUS* reporter (Figure 2.11) (Held et al., 2014). In all cases, the GUS reporter activity was initially associated with the dividing cells of a developing nodule primordium. These profiles are consistent with the notion that ACS1 and ACS2 are regulated by cytokinin and LHK1 as their spatial and temporal expression patterns are similar. They suggest, however, that in contrast to the model presented (Figure 3.5), the increased ACS(s) activity is not restricted to the root epidermis. It is more likely that both of cytokinin activity peaks, in the root cortex and the root epidermis, can contribute to the total ACS activity.

Interestingly, comparing the output of cytokinin signaling upon rhizobial inoculation in *L. japonicus* and *M. truncatula* revealed a remarkable difference (Held et al., 2014; Jardinaud et al., 2016). While in *L. japonicus*, the first peak of cytokinin activity is detectable within dividing cortical cells (Figure 2.11) (Held et al., 2014), in *M. truncatula* this is located in the root epidermis (Jardinaud et al., 2016). Importantly, the histochemical staining also showed only a weak signal associated with MtCRE1in root hair only after prolonged staining (Jardinaud et al., 2016), which is also in striking contrast with the strong expression of LHK1 promotor in the epidermis (Figure 2.13) (Held et al., 2014). These differences could be reflective of determinate and indeterminate nodulation in *L. japonicus* and *M. truncatula*, respectively, possibly also explaining the lack of hyperinfection in the *Mtcre1* mutants (Plet et al., 2011).

Taken together, ACS1 and ACS2 have emerged as the likely mediators of the cytokinin-ethylene crosstalk that regulate *M. loti* infection in *L. japonicus* (Figure 4.25). As dependent on *M. loti* infection and LHK1, the increased level of *ACS2* mRNA and the possible enhanced stability of ACS1 and ACS2 are likely to contribute to increased ethylene

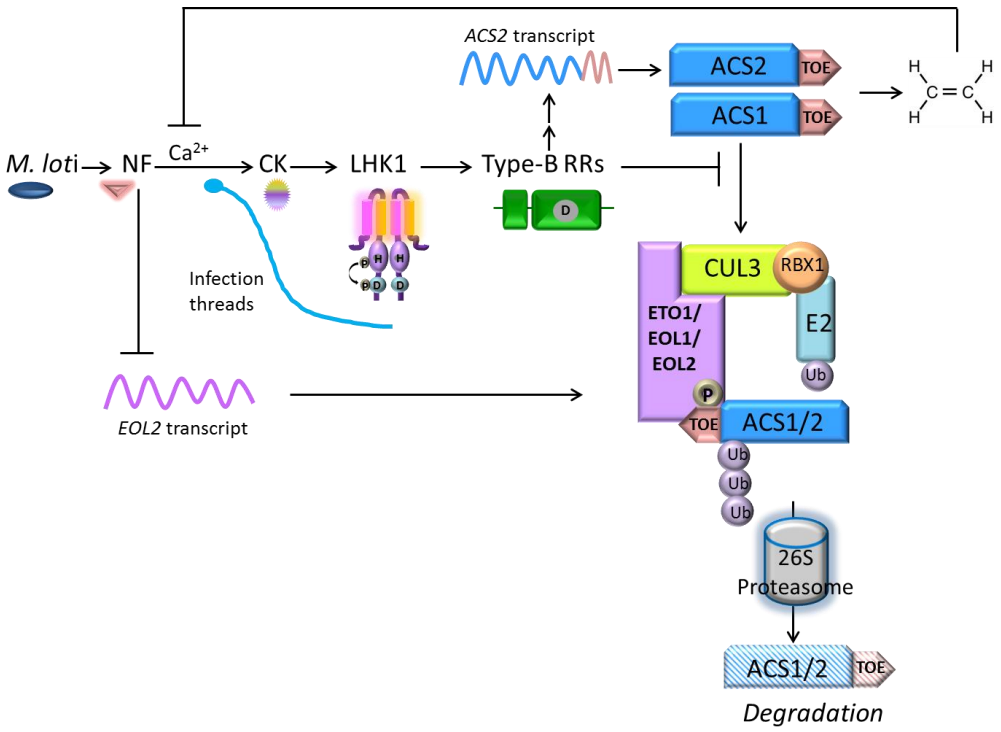

Figure 4.25 A working model for cytokinin-ethylene crosstalk in regulation of *M. loti* infection in *L. japonicus*.

Perception of *M. loti*-produced NF leads to accumulation of cytokinins (CK), which are perceived by cytokinin receptors, with the main function performed by LHK1. The auto-phosphorylation of LHK1 and the resulting activation of type-B response regulators (RRs) presumably lead to increased local ethylene production. Several cytokinin-dependent mechanisms appear to contribute to this effect, including the increased level of the *ACS2* mRNA and diminished ACS1 and ACS2 degradation via ubiquitination. ETO1/EOLs, CUL3, and RBX1 constitute a ubiquitin ligase (E3) protein complex. The ubiquitin moiety is transferred from the ubiquitin conjugating enzyme (E2) to phosphorylated ACS1 and ACS2. As a result, the enzymatic activities of ACS1 and ACS2 are inhibited and the proteins are targeted for proteasome-dependent degradation. *M. loti* infection also diminishes the level of the *EOL2* mRNA, apparently through a cytokinin-independent mechanism. A local increase in ethylene levels blocks calcium (Ca^{2+}) signaling, which is required for infection thread formation. NF; Nod factors, Ub; Ubiquitin, E2; ubiquitin conjugating enzyme.

production, which in turn locally restricts the subsequent infection events. Furthermore, downregulation of the *EOL2* mRNA level through a cytokinin-independent mechanism may also contribute to fine-tuning the ethylene production in response to *M. loti* infection. Unravelling the unique molecular mechanisms required for cytokinin-ethylene regulation of homeostasis of IT formation during the *L. japonicus-M. loti* interaction, can shed new light on how these ubiquitous hormonal signals have been co-opted during root nodule symbiosis.

4.4 Experimental Procedures

4.4.1 Plant growth conditions

Seeds of *L. japonicus* wild-type Gifu, the *lhk1-1* mutant (Murray et al., 2007), the *snf2* mutant (Tirichine et al., 2007), and other mutant plants described in this study were sterilized and grown as described in Section 2.5.1.

To assess the effect of various pharmacological treatments on the extent of root growth and infection thread formation, a modified version of the previously established protocol was followed (Wopereis et al., 2000; Heckmann et al., 2011). Briefly, sterilized seeds were sown onto plates containing 0.8% phytagel (Sigma) and the plates kept up-side down in the dark for one day. The seedlings were transferred to vertical plates containing ¼ B and D nutrient solution (Broughton and Dilworth, 1971) with 1.4% agar supplemented with BA, ACC, or AVG at the stated concentrations where appropriate. Seedlings were transferred onto a pre-soaked filter paper that had been placed over the media, to avoid penetration of the roots into the agar. The filter papers were soaked in sterile Milli-Q water that was supplemented with the required concentrations of chemicals where appropriate. Five plants were placed on each plate and roots were covered with another wet filter paper. Vertical plates were kept in boxes such that shoots were kept under continuous light while the roots were protected from light. After two days on the plates, each root was inoculated with 50 µl of 1:100 diluted *M. loti* (OD_{600}: 1). Root elongation and number of infection threads were measured at 10 and 14 DAI. An average was determined for 10 roots per genotype and treatment.

For studying the response of *L. japonicus* wild-type and *lhk1-1* plants to exogenous cytokinin, 10 day-old sand-vermiculate grown plants were transferred to beakers containing either sterile water or 50 nM BA and incubated at room temperature with constant aeration. Roots were collected 3, 6, and 12 hours post-treatment and used for total RNA extraction as described (Murray et al., 2007).

4.4.2 Assessment of symbiotic phenotypes

In order to visualize the infection threads and nodulation events in *L. japonicus* wild-type and mutant roots at various time points, the plants were inoculated with *M. loti* containing the *hemA::LacZ* reporter cassette following the procedure in Section 2.5.2. The infected roots were harvested at various time points post-inoculation, fixed and stained for *β*-galactosidase activity as previously described (Wopereis et al., 2000). The localization of *M. loti* was surveyed based on the resulting blue color, and compared between different genotypes. The number of infection threads and nodulation events were counted on at least ten plants.

4.4.3 Quantitative real-time RT-PCR Assay

To quantify the expression level of *ACS* and *ETO1/EOLs* transcripts in wild-type and the *lhk1-1* mutants, the RNA extraction, cDNA synthesis and real time quantitative PCR was performed as described in Section 2.5.8. Primer sequences used for the real time qPCR expression analyses can be found in Table 4.4.

4.4.4 The *ACS* and *ETO1/EOL* mutants

The LORE1 insertional mutation alleles called *acs1-1* (line no. 30095707), *acs1-2* (line no. 30060922), *acs4-1* (line no. 30080738), *acs5-1* (line no. 30061816), *acs5-2* (line no. 30059173), *acs5-3* (line no. 30068546), *acs6-1* (line no. 30050224), *acs6-2* (line no. 30102320), *acs7-1* (line no. 30016417), *acs7-2* (line no. 30052863), *acs7-3* (line no. 30053765), *eto1-1* (line no. 30014908), *eto1-2* (line no. 30033695), *eto1-3* (line no. 30005551), *eto1-4* (line no. 30009833), *eto1-5* (line no. 30050811), *eol1-1* (line no. 30056422), *eol2-1* (line no. 30005967), *eol2-2* (line no. 30020456), *eol2-3* (line no. 30008182), *eol2-4* (line no. 30049321), *eol2-5* (line no. 30008858), and *eol2-6* (line no. 30008689) were identified from the *L. japonicus* LORE1 retrotransposon mutant resource (https://lotus.au.dk/). The R3 generation seeds (3rd generation of tissue culture regenerated plants) carrying LORE1 insertions were received from Lotus Base. R3 is a segregating population. Therefore, seeds of the LORE1 insertion lines for each allele were sown and the seedlings were subjected to PCR-based genotyping using gene and LORE1 specific

primers, following an established procedure (Urbański et al., 2012). The primers used for genotyping were listed in Table 4.4.

Also, the TILLING approach (Perry et al., 2009) was utilized for the identification of mutant alleles at the *LjACS2* locus. In two attempts, two sets of primers were used to generate amplicons for TILLING which are listed in Table 4.4. To genotype plants carrying various point mutations in *ACS2* allele, combinations of sequence analysis, cleavage amplification polymorphisms (CAPS), and derived CAPS (dCAPS) markers were used. The primers used for genotyping are listed in Table 4.4.

4.4.5 Targeted *LjACS2* modification using CRISPR/Cas9 system

Three highly specific-*LjACS2* targeted nucleic acid sequences ($GN_{20}GG$), namely sgRNA-A, sgRNA-B, and sgRNA-C were designed using CRISPR-P web tool (http://cbi.hzau.edu.cn/cgi-bin/CRISPR). Using an Inverse PCR reaction with two 41-bp primers (see Table 4.4), followed by an In-Fusion® (Clontech) reaction, the three targeted sequences were cloned individually into the pUC gRNA shuttle vector (https://www.addgene.org/47024/). After validation of the inserts by Sanger sequencing, sgRNAS under *M. truncatula* U6.6 promoter were cut using the meganuclease *I-PpoI* (Promega) and ligated into the p201H Cas9 binary vector https://www.addgene.org/59176/. After confirmation of the insert by sequencing and restriction enzyme digest, the corresponding vectors were transferred to *Agrobacterium tumefaciens* LBA4404 using electroporation. Standard transformation protocols (Lombari et al., 2005) were used to regenerate fully transgenic plants from hypocotyl segments of wild-type (ecotype 'Gifu') and *acs1-2 L. japonicus* plants. 96 independent transgenic plants were tested for the presence of the transgene using PCR and *Cas9*-specifc primers (see Table 4.4) and then used to evaluate the possibility of any genetic modification in the *LjACS2* locus using custom-amplicon sequencing following an established method (Jacobs et al., 2015).

4.4.6 Gene expression analysis using GUS histochemical assay

To develop the gene expression localization constructs, the 3 kb *LjACS1, LjACS2, LjETO1, LjEOL1*, and *LjEOL2* promoter fragments were PCR amplified. The promotor

fragments were defined from position -1 to -3000 in the corresponding genomic sequences, where -1 denotes the first base upstream from the predicted ATG initiation codon. The sequences of the primers used can be found in Table 4.4. The promotor fragments were recombined into the pKGWFS7 destination vector containing a GFP/GUS reporter fusion (https://gateway.psb.ugent.be/search) using the Gateway™ technology (Invitrogen) and all constructs were confirmed by sequencing. After validation by sequencing, the corresponding vectors were transferred to both *A. rhizogenes* strains AR10 and AR1193. Standard transformation protocols were employed to generate non-transgenic *L. japonicus* shoots with hairy-roots expressing the binary constructs (Murray et al., 2007). At least ten independent hairy root systems were carefully inspected to define the expression patterns. The standard staining procedure for histochemical analysis of *β- glucuronidase* reporter gene activity was followed such that roots were fixed, stained, and cleared as described in Section 2.5.7 (Wopereis et al., 2000).

4.4.7 Ethylene measurement using gas chromatography

Wild-type Gifu and *lhk1-1* seeds were sterilized and plated on sterilized filter paper moistened with sterile water for three days. Seedlings were transferred to 5 mL glass vials (two seedlings / vial) which were sealed for three days. Seedling were exposed to BA (10 nM) in combination with AVG (1 M), or *M. loti* where appropriate. Ethylene accumulation over 24 hours was measured using an ETD-300 laser-based detection system (SensorSense) (Mohd-Radzman et al., 2016). Measurements were conducted in sampling mode with a flow rate of 2.5 L/min and a 6 min sample period. Ten samples were used for each treatment. The greater sensitivity of the laser-based system (Cristescu et al., 2013) enabled measurements to be made from individual seedlings, in contrast to other equipment types, which require pooled samples to generate detectable signals.

4.4.8 Ethylene “triple response” assay

Wild-type Gifu and mutant seeds were sterilized, germinated and transferred to plates containing ½ strength Gamborg’s B5 medium (Sigma) and 0.8% phytagel. The seedlings were incubated in the dark for six days at 24 ºC. Hypocotyl measurement was performed

under a Nikon SMZ25 stereomicroscope (Nikon) using NIS Elements imaging software (Nikon).

4.4.9 RNA sequencing

L. japonicus wild-type Gifu root samples were scarified, germinated, and grown as described in Section 4.4.1. Root samples were harvested 4 DAI with *M. loti* and from their uninoculated counterparts. Three independent biological replicates per treatment were collected. Total RNA was extracted using Total RNA Purification Kit (Norgen Biotek) and RNA library was constructed and sequenced on an Illumina Hi-Seq 2500 using paired-end reads at the Center for Applied Genomics (Sick Kids Hospital, Toronto, Canada). Briefly, the quality of total RNA samples was checked on an Agilent Bioanalyzer 2100 RNA Nano chip following manufacturer's instructions (Agilent Technologies). RNA library preparation was performed following the NEBNext Ultra Directional Library Preparation protocol (New England Biolabs); 400 ng of total RNA was used as the input material and enriched for poly-A mRNA, fragmented into the 200-300-bases range for 4 minutes at 94°C and converted to double stranded cDNA, end-repaired and adenylated at the 3' to create an overhang A to allow for ligation of Illumina adapters with an overhang T; library fragments were amplified under the following conditions: initial denaturation at 98 ºC for 10 seconds, followed by 15 cycles of 98 ºC for 10 seconds, 60 ºC for 30 seconds and 72 ºC for 30 seconds, and finally an extension step for 5 minutes at 72 ºC; at the amplification step, each sample was amplified with different barcoded adapters to allow for multiplex sequencing. Libraries were pooled in equimolar quantities and paired-end sequenced on 2 lanes of a High Throughput Run Mode flowcell with the V4 sequencing chemistry on an Illumina HiSeq 2500 platform following Illumina's recommended protocol to generate paired-end reads of 126-bases in length.

4.4.10 Microscopy and image analysis

All microscopic observations were performed on a Nikon SMZ25 (Nikon, Japan) dissecting or Zeiss Axioskop 2 compound (Zeiss, Germany) light microscope. Both microscopes were integrated with a Nikon digital camera using the Nikon NIS Elements

imaging software (Nikon). All images captured were taken in a TIFF format at a resolution of 3840 x 3072.

4.4.11 Statistical analysis

All statistical analyses were performed using Microsoft Excel spread sheet software. Pair-wise comparisons were made using a Student's t-Test assuming unequal variance or the significant differences between sample means were calculated using the one-way analysis of variance (ANOVA) where appropriate.

Table 4.4 Full primer sequences used in this study.

Name of primers	Primer sequence (5'-3')
qRT-PCR expression analysis	
LjACS1-qPCR-FWD	AGCCTGGTCATGATGGAAGC
LjACS1-qPCR-REV	ACCGATTTGGCTGTAACTCCA
LjACS2-qPCR-FWD	GCAGTGCTAAGAGGAACGGT
LjACS2-qPCR-REV	ACCAAAAATACCGGGGAGGC
LjACS3-qPCR-FWD	CAACCTTTGTGAGTGTCGCC
LjACS3-qPCR-REV	CCTGGAAGCCCCATGTCTTT
LjACS4-qPCR-FWD	CACCTATGCCACAGTCACCT
LjACS4-qPCR-REV	TCCAGCAGCAGCCATGTAAT
LjACS5-qPCR-FWD	GGTGGTTCAGGGTGTGCTAT
LjACS5-qPCR-REV	CTCACAAACGCACGCATTCT
LjACS6-qPCR-FWD	TGCTGGGTGGAAAGCCTATG
LjACS6-qPCR-REV	CTCAGCGTGCTCTTCCAAGT
LjACS7-qPCR-FWD	TCCAAATGGGGTTGGCAGAG
LjACS7-qPCR-REV	CCATGTGGATGCCTCAGAGT
LjETO1-qPCR-FWD	TGACCCTAGCCATGCTGAGA
LjETO1-qPCR-REV	TACTGGGTGGTTTGGCGTAA
LjEOL1-qPCR-FWD	GGAAGATCTGGAGACGGTGAC
LjEOL1-qPCR-REV	GCGCACCTAATACATCCCCC
LjEOL2-qPCR-FWD	CGAGCAGCGTTTTACGAGTC
LjEOL2-qPCR-REV	TCACGTTGCACTCGATTGGT
Lhk1-qPCR-FWD	GTGCTTAAATTGTGGGATGGA
Lhk1-qPCR-REV	ATTGATGCTGGGAGAAGTTGA
UBC-FWD	ATGTGCATTTTAAGACAGGG
UBC-REV	GAACGTAGAAGATTGCCTGAA
PP2A-FWD	GTAAATGCGTCTAAAGATAGGGTCC
PP2A-REV	ACTAGACTGTAGTGCTTGAGAGGC
TB2C-FWD	GCTCACCACCCCAAGCTTTGG
TB2C-REV	TGTCAATGGAGCAAACCCAACC
ATP-S-FWD	AACACCACTCTCGATCATTTCTCTG
ATP-S-REV	CAATGTCGCCAAGGCCCATGGTG
PUBQ-FWD	ATGCAGATCTTTTGTGAAGAC
PUBQ-REV	ACCACCACGGAAGACGGAG
Genotyping for LORE1 insertional alleles	
eto1-1-30014908-FWD	GCCGGAAGAATCTAGGATCCGGCA
eto1-1-30014908-REV	TCTCATCCTCCACCACCACCACCA
eto1-2-30033695-FWD	TGCCTCAACAGCAGCCTCAAACCA

eto1-2-30033695-REV	GATGGCCTCGCTTTCGAGACCCTTT
eto1-3-30005551-FWD	CGGCTTGCTTGCAGGTGTTTCTGA
eto1-3-30005551-REV	CCTCCAGCAAAGAAACAGCCCGGT
eto1-4-30009833-FWD	AGTGTGCGGTGAGTGGTTGGCAGA
eto1-4-30009833-REV	TGGGCGGAGGATTTCAACCAAGTG
eto1-5-30050811-FWD	CACTTGGTTGAAATCCTCCGCCCA
eto1-5-30050811-REV	TCCACACAGGATATGATAGCACCAACTGA
eol1-1-30056422-FWD	TGAGGATTGCTTGAACATCGCGGA
eol1-1-30056422-REV	TGTTCCCGGCTGCTTGAGTGACAA
eol2-1-30005967-FWD	TTTCTCTTCCTTGCAAAGTGCACACA
eol2-1-30005967-REV	GGGCAGCACTCAAGCCTGCGATAC
eol2-2-30020456-FWD	CAATGCGTGGCCTGAAGGTCAGTG
eol2-2-30020456-REV	CCCACAAGCTCGTCCTCCCTCCTC
eol2-3-30008182-FWD	GCAGGCTCTTTGCAGGCTCATTCTC
eol2-3-30008182-REV	GCTGGGTGGATGTACCAGGAGCGT
eol2-4-30049321-FWD	TCCGGATTGCCTAGAATTGCGAGC
eol2-4-30049321-REV	CCGCAATTGCAGTTGTTTTGACCG
eol2-5-30008858-FWD	GCCTTGAGAGATGTTCGCGCATTG
eol2-5-30008858-REV	GACCGCAGCCGCAATTTAAAACCC
eol2-6-30008689-FWD	TCCGGATTGCCTAGAATTGCGAGC
eol2-6-30008689-REV	CCGCAATTGCAGTTGTTTTGACCG
acs1-1-30095707-FWD	TGCAGGCTTGTTCTGCTGGGTTGA
acs1-1-30095707-REV	GCTCACACTTCACATCCAAATGGACCG
acs1-2-30060922-FWD	TGCCTAGTGGGTTCGATGGGTTCG
acs1-2-30060922-REV	TGTCATTTGCTTGCAGCTCTCTTTCG
acs4-1-30080738-FWD	ATGATTGCCATGAGTTGCGATGCG
acs4-1-30080738-REV	CCAGGGAACCCCATGTCCTTTGAA
acs5-1-30061816-FWD	TCCTTCAGGAGTGCAAATGGATGCC
acs5-1-30061816-REV	CGCGCGCTCAACTCTGAAAATCAA
acs5-2-30059173-FWD	GCGGCCAAAATGGAGAACCATTGC
acs5-2-30059173-REV	TCATGGATTGCCTGAGTTCAGAGAAGTGA
acs5-3-30068546-FWD	CAAAGGACATGGGGTTCCCTGGCT
acs5-3-30068546-REV	CAAGTGGTGGCTTTAACAAGTGCTGGC
acs6-1-30050224-FWD	TCAACATCGCAGTGCACAAAAACAA
acs6-1-30050224-REV	TGGTGCCAACTCTGAAACCTGGAA
acs6-2-30102320-FWD	TGAGGTGGAGAACTGGGGTGAACA
acs6-2-30102320-REV	TCCAATTCCCCTTCCCTTGTTGGC
acs7-1-30016417-FWD	TGGACAACATGGAAGCCAACAAGTGC
acs7-1-30016417-REV	TGGAACTTGAAAGCGCGTAGCAGA
acs7-2-30052863-FWD	CCCGCAAATACAAAGAGGCCGAGC

acs7-2-30052863-REV	CAAAATGGCCACAACCATTTGGAA
acs7-3-30053765-FWD	CCCGCAAATACAAAGAGGCCGAGC
acs7-3-30053765-REV	CAAAATGGCCACAACCATTTGGAA
LORE1-specific-P2	CCATGGCGGTTCCGTGAATCTTAGG
Generate amplicon for TILLING experiment	
ACS2-FWD1	TGAAGTGGAGAACTGGAGTGGAGATTG
ACS2-REV2	TTTTCATGGGCTACTCCACCAAAAATACC
LjACS2-FWD3	GATGTGATAAATGGTAAGAGGAGAGAG
LjACS2-REV3	TGCATTTTATAAATTGAACTTACCCTGG
Genotyping for the point mutations in ACS2	
ACS2-Seq-FWD-1	TTCTGCAATACCATGTGGCCT
ACS2-Seq-FWD-2	TAGTCTCTCCAAAGACTTGGGTTT
ACS2-Seq-REV-1	GCTTCAGTGACTTGGAAGTTGTT
ACS2-Seq-REV-2	ACATCCACATGGGCAGAGTG
acs2-5-EcoRV-FWD	CTAAAAACTGTCCCGGAGTAGATAT
acs2-5-BcoRV-REV	TCCAAGTCACTGAAGCAGCA
acs2-7-HinfI-FWD	GGGACAGAGTTCATGTTGTCTAGAGT
acs2-7-HinfI-REV	AGCATTCTCTGTCGTCGCTT
acs2-8-XhoI-FWD	TTTCCGCGTAGGCGCCATCTACC
acs2-8-XhoI-REV	GGCTTTTTGCAATCCTGAAA
acs2-10-MboI-FWD	ACGATGTTGTGTCTGCAGCGA
acs2-10-MboI-REV	GGCTTTTTGCAATCCTGAAA
LjACS2CRSISPR/Cas9	
*ACS2*_GuideA_FWD	GAACCCCGCTGCATCGGTTTTAGAGCTAG AAATAGCAAGTT
*ACS2*_GuideA_REV	GATGCAGCGGGGTTCAAGCAAGCCTACT GGTTCGCTTGAAG
*ACS2*_GuideB_FWD	CGGGGTTCAAGCGTGAGTTTTAGAGCTAG AAATAGCAAGTT
*ACS2*_GuideB_REV	CACGCTTGAACCCCGCTGCAAGCCTACTG GTTCGCTTGAAG
*ACS2*_GuideC_FWD	AGAACCCCGATGCAGCGTTTTAGAGCTAG AAATAGCAAGTT
*ACS2*_GuideC_REV	CTGCATCGGGGTTCTTCTCAAGCCTACTG GTTCGCTTGAAG
ACS2-Cas9-FWD	ACATCAATCGGCTCTCCGAC
ACS2-Cas9-REV	TTGGTGATCTGGCGTGTCTC
Localization analysis	
ACS1-Promoter-D-FWD	CACCAATTTTTCTCCGTACATGAAGCA
ACS1-Promoter-D-REV	TTTCGTTTTCTTTTTTGTGTGGTGGG
ACS2-Promoter-D-FWD	CACCGGTGGCTTTCAACTCACATGC
ACS2-Promoter-D-REV	ATTTTTTGTGGAATGCTAACTTGTACG

ACS6-Promoter-D-FWD	CACCCATGACTTTCAGTGCTTTCTAGC
ACS6-Promoter-D-REV	CAAAAGCTTACTCTTGCCAA
ETO1-Promoter-D-FWD	CACCTCCAACCGTTGCAGAAAATCA
ETO1-Promoter-D-REV	CGAGGTGATCATGTTGTGCTGC
EOL1-Promoter-D-FWD	CACCCGACGGCTGAAGAAAGGAGA
EOL1-Promoter-D-REV	GGGGCATAACAGACGAAACAAG
EOL2-Promoter-D-FWD	CACCGAAAAATTTGCGATCACGGCA
EOL2-Promoter-D-REV	AGCATCCCTATAAAGTAAGCCGA

4.5 References

Adams, D.O., and Yang, S.F. (1979). Ethylene biosynthesis: identification of 1-aminocyclopropane-1-carboxylic acid as an intermediate in the conversion of methionine to ethylene. Proc. Natl. Acad. Sci. U. S. A. **76:** 170-174.

Argueso, C.T., Hansen, M., and Kieber, J.J. (2007). Regulation of ethylene biosynthesis. J. Plant Growth Regul. **26:** 92-105.

Belhaj, K., Chaparro-Garcia, A., Kamoun, S., and Nekrasov, V. (2013). Plant genome editing made easy: Targeted mutagenesis in model and crop plants using the CRISPR/Cas system. Plant Methods **9**.

Bleecker, A.B., and Kende, H. (2000). Ethylene: a gaseous signal molecule in plants. Annual review of cell and developmental biology **16:** 1-18.

Broughton, W.J., and Dilworth, M.J. (1971). Control of leghaemoglobin synthesis in snake beans. Biochem. J. **125:** 1075-1080.

Cary, A.J., Liu, W., and Howell, S.H. (1995). Cytokinin action is coupled to ethylene in its effects on the inhibition of root and hypocotyl elongation in *Arabidopsis thaliana* seedlings. Plant Physiol. **107:** 1075-1082.

Chae, H.S., and Kieber, J.J. (2005). Eto Brute? Role of ACS turnover in regulating ethylene biosynthesis. Trends Plant Sci. **10:** 291-296.

Chae, H.S., Faure, F., and Kieber, J.J. (2003). The *eto1*, *eto2*, and *eto3* mutations and cytokinin treatment increase ethylene biosynthesis in Arabidopsis by increasing the stability of ACS protein. Plant Cell **15:** 545-559.

Christians, M.J., Gingerich, D.J., Hansen, M., Binder, B.M., Kieber, J.J., and Vierstra, R.D. (2009). The BTB ubiquitin ligases ETO1, EOL1 and EOL2 act collectively to regulate ethylene biosynthesis in Arabidopsis by controlling type-2 ACC synthase levels. Plant J. **57:** 332-345.

Collins, T., Stone, J.R., and Williams, A.J. (2001). All in the family: The BTB/POZ, KRAB, and SCAN domains. Mol. Cell. Biol. **21:** 3609-3615.

Cristescu, S.M., Mandon, J., Arslanov, D., De Pessemier, J., Hermans, C., and Harren, F.J.M. (2013). Current methods for detecting ethylene in plants. Ann. Bot. **111:** 347-360.

Crocker, W., and Knight, L.I. (1908). Effect of illuminating gas and ethylene upon flowering carnations. Botanical Gazette**:** 259-276.

D'Andrea, L.D., and Regan, L. (2003). TPR proteins: The versatile helix. Trends Biochem. Sci. **28:** 655-662.

De Paepe, A., and Van Der Straeten, D. (2005). Ethylene biosynthesis and signaling: an overview. Vitamins & Hormones **72:** 399-430.

Dugardeyn, J., and Van Der Straeten, D. (2008). Ethylene: Fine-tuning plant growth and development by stimulation and inhibition of elongation. Plant Sci. **175:** 59-70.

Fukai, E., Soyano, T., Umehara, Y., Nakayama, S., Hirakawa, H., Tabata, S., Sato, S., and Hayashi, M. (2012). Establishment of a *Lotus japonicus* gene tagging population using the exon-targeting endogenous retrotransposon *LORE1*. Plant J. **69:** 720-730.

Gingerich, D.J., Gagne, J.M., Salter, D.W., Hellmann, H., Estelle, M., Ma, L., and Vierstra, R.D. (2005). Cullins 3a and 3b assemble with members of the broad complex/tramtrack/ bric-a-brac (BTB) protein family to form essential ubiquitin-protein ligases (E3s) in *Arabidopsis*. J. Biol. Chem. **280:** 18810-18821.

Han, L., Li, G.J., Yang, K.Y., Mao, G., Wang, R., Liu, Y., and Zhang, S. (2010). Mitogen-activated protein kinase 3 and 6 regulate *Botrytis cinerea*-induced ethylene production in Arabidopsis. Plant J. **64:** 114-127.

Hansen, M., Chae, H.S., and Kieber, J.J. (2009). Regulation of ACS protein stability by cytokinin and brassinosteroid. Plant J. **57:** 606-614.

Heckmann, A.B., Sandal, N., Bek, A.S., Madsen, L.H., Jurkiewicz, A., Nielsen, M.W., Tirichine, L., and Stougaard, J. (2011). Cytokinin induction of root nodule primordia in *Lotus japonicus* is regulated by a mechanism operating in the root cortex. Mol. Plant-Microbe Interact. **24:** 1385-1395.

Held, M., Hou, H., Miri, M., Huynh, C., Ross, L., Hossain, M.S., Sato, S., Tabata, S., Perry, J., Wang, T.L., and Szczyglowski, K. (2014). *Lotus japonicus* cytokinin receptors work partially redundantly to mediate nodule formation. Plant Cell **26:** 678-694.

Jacobs, T.B., LaFayette, P.R., Schmitz, R.J., and Parrott, W.A. (2015). Targeted genome modifications in soybean with CRISPR/Cas9. BMC Biotechnol. **15**.

Jakubowicz, M. (2002). Structure, catalytic activity and evolutionary relationships of 1-aminocyclopropane-1-carboxylate synthase, the key enzyme of ethylene synthesis in higher plants. Acta Biochim. Pol. **49:** 757-774.

Jardinaud, M.F., Boivin, S., Rodde, N., Catrice, O., Kisiala, A., Lepage, A., Moreau, S., Roux, B., Cottret, L., Sallet, E., Brault, M., Emery, R.J.N., Gouzy, J., Frugier, F., and Gamas, P. (2016). A laser dissection-RNAseq analysis

highlights the activation of cytokinin pathways by nod factors in the Medicago truncatula root epidermis. Plant Physiol. **171:** 2256-2276.

Joo, S., Liu, Y., Lueth, A., and Zhang, S. (2008). MAPK phosphorylation-induced stabilization of ACS6 protein is mediated by the non-catalytic C-terminal domain, which also contains the *cis*-determinant for rapid degradation by the 26S proteasome pathway. Plant J. **54:** 129-140.

Kamiyoshihara, Y., Iwata, M., Fukaya, T., Tatsuki, M., and Mori, H. (2010). Turnover of LeACS2, a wound-inducible 1-aminocyclopropane-1-carboxylic acid synthase in tomato, is regulated by phosphorylation/dephosphorylation. Plant J. **64:** 140-150.

Knight, L.I., Rose, R.C., and Crocker, W. (1910). Effects of various gases and vapors upon etiolated seedlings of the sweet pea. Science **31:** 1.

Larrainzar, E., Riely, B.K., Kim, S.C., Carrasquilla-Garcia, N., Yu, H.J., Hwang, H.J., Oh, M., Kim, G.B., Surendrarao, A.K., Chasman, D., Siahpirani, A.F., Penmetsa, R.V., Lee, G.S., Kim, N., Roy, S., Mun, J.H., and Cook, D.R. (2015). Deep sequencing of the Medicago truncatula root transcriptome reveals a massive and early interaction between nodulation factor and ethylene signals. Plant Physiol. **169:** 233-265.

Light, K.M., Wisniewski, J.A., Vinyard, W.A., and Kieber-Emmons, M.T. (2016). Perception of the plant hormone ethylene: known-knowns and known-unknowns. J. Biol. Inorg. Chem. **21:** 715-728.

Lin, Z., Zhong, S., and Grierson, D. (2009). Recent advances in ethylene research. J. Exp. Bot. **60:** 3311-3336.

Liu, Y., and Zhang, S. (2004). Phosphorylation of 1-aminocyclopropane-1-carboxylic acid synthase by MPK6, a stress-responsive mitogen-activated protein kinase, induces ethylene biosynthesis in arabidopsis. Plant Cell **16:** 3386-3399.

Lohar, D., Stiller, J., Kam, J., Stacey, G., and Gresshoff, P.M. (2009). Ethylene insensitivity conferred by a mutated *Arabidopsis* ethylene receptor gene alters nodulation in transgenic *Lotus japonicus*. Ann. Bot. **104:** 277-285.

Lombari, P., Ercolano, E., El Alaouri, E., and Chiurazzi, M. (2005). *Agrobacterium*-mediated in vitro transformation. *Lotus japonicus* Handbook**:** 87-95.

Lupas, A. (1996). Coiled coils: New structures and new functions. Trends Biochem. Sci. **21:** 375-382.

Lyzenga, W.J., and Stone, S.L. (2012). Regulation of ethylene biosynthesis through protein degradation. Plant Signaling Behav. **7**.

Madsen, L.H., Fukai, E., Radutoiu, S., Yost, C.K., Sandal, N., Schauser, L., and Stougaard, J. (2005). LORE1, an active low-copy-number TY3-*gypsy* retrotransposon family in the model legume *Lotus japonicus*. Plant J. **44:** 372-381.

Malolepszy, A., Mun, T., Sandal, N., Gupta, V., Dubin, M., Urbański, D., Shah, N., Bachmann, A., Fukai, E., Hirakawa, H., Tabata, S., Nadzieja, M., Markmann, K., Su, J., Umehara, Y., Soyano, T., Miyahara, A., Sato, S., Hayashi, M., Stougaard, J., and Andersen, S.U. (2016). The *LORE1* insertion mutant resource. Plant J. **88:** 306-317.

McCarthy, D.L., Capitani, G., Feng, L., Gruetter, M.G., and Kirsch, J.F. (2001). Glutamate 47 in 1-aminocyclopropane-1-carboxylate synthase is a major specificity determinant. Biochemistry **40:** 12276-12284.

Mehta, P.K., and Christen, P. (1994). Homology of 1-aminocyclopropane-1-carboxylate synthase, 8-amino-7-oxononanoate synthase, 2-amino-6-caprolactam racemase, 2, 2-dialkylglycine decarboxylase, glutamate-1-semialdehyde 2, 1-aminomutase and isopenicillin-N-epimerase with aminotransferases. Biochem. Biophys. Res. Commun. **198:** 138-143.

Miri, M., Janakirama, P., Held, M., Ross, L., and Szczyglowski, K. (2016). Into the Root: How Cytokinin Controls Rhizobial Infection. Trends Plant Sci. **21:** 178-186.

Miyata, K., Kawaguchi, M., and Nakagawa, T. (2013). Two distinct EIN2 genes cooperatively regulate ethylene signaling in *Lotus japonicus*. Plant Cell Physiol. **54:** 1469-1477.

Mohd-Radzman, N.A., Laffont, C., Ivanovici, A., Patel, N., Reid, D., Stougaard, J., Frugier, F., Imin, N., and Djordjevic, M.A. (2016). Different pathways act downstream of the CEP peptide receptor CRA2 to regulate lateral root and nodule development. Plant Physiol. **171:** 2536-2548.

Morieri, G., Martinez, E.A., Jarynowski, A., Driguez, H., Morris, R., Oldroyd, G.E.D., and Downie, J.A. (2013). Host-specific Nod-factors associated with *Medicago truncatula* nodule infection differentially induce calcium influx and calcium spiking in root hairs. New Phytol. **200:** 656-662.

Murray, J.D., Karas, B.J., Sato, S., Tabata, S., Amyot, L., and Szczyglowski, K. (2007). A cytokinin perception mutant colonized by *Rhizobium* in the absence of nodule organogenesis. Science **315:** 101-104.

Nukui, N., Ezura, H., Yuhashi, K.I., Yasuta, T., and Minamisawa, K. (2000). Effects of ethylene precursor and inhibitors for ethylene biosynthesis and perception on nodulation in *Lotus japonicus* and *Macroptilium atropurpureum*. Plant Cell Physiol. **41:** 893-897.

Oldroyd, G.E., and Downie, J.A. (2006). Nuclear calcium changes at the core of symbiosis signalling. Curr. Opin. Plant Biol. **9:** 351-357.

Oldroyd, G.E.D., Engstrom, E.M., and Long, S.R. (2001). Ethylene inhibits the Nod factor signal transduction pathway of *Medicago truncatula*. Plant Cell **13:** 1835-1849.

Penmetsa, R.V., and Cook, D.R. (1997). A legume ethylene-insensitive mutant hyperinfected by its rhizobial symbiont. Science **275:** 527-530.

Penmetsa, R.V., Uribe, P., Anderson, J., Lichtenzveig, J., Gish, J.C., Nam, Y.W., Engstrom, E., Xu, K., Sckisel, G., Pereira, M., Baek, J.M., Lopez-Meyer, M., Long, S.R., Harrison, M.J., Singh, K.B., Kiss, G.B., and Cook, D.R. (2008). The *Medicago truncatula* ortholog of Arabidopsis EIN2, *sickle*, is a negative regulator of symbiotic and pathogenic microbial associations. Plant J. **55:** 580-595.

Perry, J., Brachmann, A., Welham, T., Binder, A., Charpentier, M., Groth, M., Haage, K., Markmann, K., Wang, T.L., and Parniske, M. (2009). TILLING in *Lotus japonicus* identified large allelic series for symbiosis genes and revealed a bias in functionally defective ethyl methanesulfonate alleles toward glycine replacements. Plant Physiol. **151:** 1281-1291.

Plet, J., Wasson, A., Ariel, F., Le Signor, C., Baker, D., Mathesius, U., Crespi, M., and Frugier, F. (2011). MtCRE1-dependent cytokinin signaling integrates bacterial and plant cues to coordinate symbiotic nodule organogenesis in *Medicago truncatula*. Plant J. **65:** 622-633.

Reid, D.E., Heckmann, A.B., Novák, O., Kelly, S., and Stougaard, J. (2016). CYTOKININ OXIDASE/DEHYDROGENASE3 maintains cytokinin homeostasis during root and nodule development in *Lotus japonicus*. Plant Physiol. **170:** 1060-1074.

Sasaki, T., Suzaki, T., Soyano, T., Kojima, M., Sakakibara, H., and Kawaguchi, M. (2014). Shoot-derived cytokinins systemically regulate root nodulation. Nat. Commun. **5**.

Sato, S., Nakamura, Y., Kaneko, T., Asamizu, E., Kato, T., Nakao, M., Sasamoto, S., Watanabe, A., Ono, A., Kawashima, K., Fujishiro, T., Katoh, M., Kohara, M., Kishida, Y., Minami, C., Nakayama, S., Nakazaki, N., Shimizu, Y., Shinpo, S., Takahashi, C., Wada, T., Yamada, M., Ohmido, N., Hayashi, M., Fukui, K., Baba, T., Nakamichi, T., Mori, H., and Tabata, S. (2008). Genome structure of the legume, *Lotus japonicus*. DNA Res. **15:** 227-239.

Sebastià, C.H., Hardin, S.C., Clouse, S.D., Kieber, J.J., and Huber, S.C. (2004). Identification of a new motif for CDPK phosphorylation in vitro that suggests ACC synthase may be a CDPK substrate. Arch. Biochem. Biophys. **428:** 81-91.

Skottke, K.R., Yoon, G.M., Kieber, J.J., and DeLong, A. (2011). Protein phosphatase 2A controls ethylene biosynthesis by differentially regulating the turnover of ACC synthase isoforms. PLoS Genet. **7**.

Soyano, T., Hirakawa, H., Sato, S., Hayashi, M., and Kawaguchi, M. (2014). NODULE INCEPTION creates a long-distance negative feedback loop involved in homeostatic regulation of nodule organ production. Proc. Natl. Acad. Sci. U. S. A. **111:** 14607-14612.

Tan, S.T., and Xue, H.W. (2014). Casein kinase 1 regulates ethylene synthesis by phosphorylating and promoting the turnover of ACS5. Cell Rep. **9:** 1692-1703.

Tatsuki, M., and Mori, H. (2001). Phosphorylation of tomato 1-aminocyclopropane-1-carboxylic acid synthase, LE-ACS2, at the C-terminal region. J. Biol. Chem. **276:** 28051-28057.

Tirichine, L., Sandal, N., Madsen, L.H., Radutoiu, S., Albrektsen, A.S., Sato, S., Asamizu, E., Tabata, S., and Stougaard, J. (2007). A gain-of-function mutation in a cytokinin receptor triggers spontaneous root nodule organogenesis. Science **315:** 104-107.

Tsuchisaka, A., and Theologis, A. (2004). Unique and overlapping expression patterns among the Arabidopsis 1-amino-cyclopropane-1-carboxylate synthase gene family members. Plant Physiol. **136:** 2982-3000.

Urbański, D.F., Małolepszy, A., Stougaard, J., and Andersen, S.U. (2012). Genome-wide *LORE1* retrotransposon mutagenesis and high-throughput insertion detection in *Lotus japonicus*. Plant J. **69:** 731-741.

van Zeijl, A., Op Den Camp, R.H.M., Deinum, E.E., Charnikhova, T., Franssen, H., Op Den Camp, H.J.M., Bouwmeester, H., Kohlen, W., Bisseling, T., and Geurts, R. (2015). Rhizobium Lipo-chitooligosaccharide signaling triggers accumulation of cytokinins in *Medicago truncatula* roots. Molecular Plant **8:** 1213-1226.

Verdier, J., Torres-Jerez, I., Wang, M., Andriankaja, A., Allen, S.N., He, J., Tang, Y., Murray, J.D., and Udvardi, M.K. (2013). Establishment of the *Lotus japonicus* Gene Expression Atlas (LjGEA) and its use to explore legume seed maturation. Plant J. **74:** 351-362.

Vogel, J.P., Schuerman, P., Woeste, K., Brandstatter, I., and Kieber, J.J. (1998). Isolation and characterization of Arabidopsis mutants defective in the induction of ethylene biosynthesis by cytokinin. Genetics **149:** 417-427.

Wang, K.L.C., Yoshida, H., Lurin, C., and Ecker, J.R. (2004). Regulation of ethylene gas biosynthesis by the *Arabidopsis* ETO1 protein. Nature **428:** 945-950.

Wheelan, S.J., Church, D.M., and Ostell, J.M. (2001). Spidey: A tool for mRNA-to-genomic alignments. Genome Res. **11:** 1952-1957.

Wopereis, J., Pajuelo, E., Dazzo, F.B., Jiang, Q., Gresshoff, P.M., De Bruijn, F.J., Stougaard, J., and Szczyglowski, K. (2000). Short root mutant of *Lotus japonicus* with a dramatically altered symbiotic phenotype. Plant J. **23:** 97-114.

Yamagami, T., Tsuchisaka, A., Yamada, K., Haddon, W.F., Harden, L.A., and Theologis, A. (2003). Biochemical diversity among the 1-amino-cyclopropane-1-carboxylate synthase isozymes encoded by the *Arabidopsis* gene family. J Biol Chem **278:** 49102-49112.

Yang, S.F., and Hoffman, N.E. (1984). Ethylene biosynthesis and its regulation in higher plants. Annu. Rev. Plant Physiol. **35:** 155-189.

Yoon, G.M., and Kieber, J.J. (2013). 14-3-3 regulates 1-aminocyclopropane-1-carboxylate synthase protein turnover in *Arabidopsis*. Plant Cell **25:** 1016-1028.

Yoshida, H., Nagata, M., Saito, K., Kevin, W.L.C., and Ecker, J.R. (2005). *Arabidopsis* ETO1 specifically interacts with and negatively regulates type 2 1-aminocyclopropane-1-carboxylate synthases. BMC Plant Biol. **5**.

Yoshida, H., Wang, K.L.C., Chang, C.M., Mori, K., Uchida, E., and Ecker, J.R. (2006). The ACC synthase TOE sequence is required for interaction with ETO1 family proteins and destabilization of target proteins. Plant Mol. Biol. **62:** 427-437.

Yu, Y.B., Adams, D.O., and Yang, S.F. (1979). 1-Aminocyclopropanecarboxylate synthase, a key enzyme in ethylene biosynthesis. Arch. Biochem. Biophys. **198:** 280-286.

Zdarska, M., Dobisova, T., Gelová, Z., Pernisová, M., Dabravolski, S., and Hejátko, J. (2015). Illuminating light, cytokinin, and ethylene signalling crosstalk in plant development. J. Exp. Bot. **66:** 4913-4931.

Zdarska, M., Zatloukalová, P., Benítez, M., Šedo, O., Potěšil, D., Novák, O., Svačinová, J., Pešek, B., Malbeck, J., Vašíčková, J., Zdráhal, Z., and Hejátko, J. (2013). Proteome analysis in Arabidopsis reveals shoot- and root-specific targets of cytokinin action and differential regulation of hormonal homeostasis. Plant Physiol. **161:** 918-930.

Chapter 5

5 General conclusions and perspectives

5.1 General conclusions and perspectives

To meet the demands for a global population that is predicted to reach nine billion people by 2050, sustainable and secure food production is a must (Tilman et al., 2011). Nitrogen availability is one of the major limiting factors to crop growth (Mueller et al., 2012). Synthetic nitrogen fertilizer, which has boosted crop yield, is a double-edged sword with substantial economic and environmental costs (Erisman et al., 2008). While profligate use of synthetic fertilizers across the developed world has severely impacted the integrity of the environment (Foley et al., 2011), too little or no access to fertilizers for smallholder farmers in developing nations in North Africa, the Middle East, and Sub-Saharan Africa has contributed to the cycle of poverty, and even political instability (Lagi et al., 2011; Tittonell and Giller, 2013).

There is a growing interest in increasing the contribution of biological nitrogen fixation to enhance crop productivity and food security while minimizing the associated environmental footprints (Charpentier and Oldroyd, 2010; Philippot et al., 2013; Rogers and Oldroyd, 2014; Mus et al., 2016). One of the most evolved nitrogen-fixing systems is the root nodule symbiosis (RNS) which is the result of the mutualistic associations between nitrogen-fixing bacteria, commonly referred to as rhizobia, and selected groups of plants within the Eurosid clade of angiosperms, most notably legumes (Sprent, 2007). This interaction enables the plants to tap into the otherwise unavailable pool of atmospheric nitrogen, thus limiting the need for synthetic nitrogen fertilizers in legumes (Graham and Vance, 2003). It has been estimated that approximately 40 to 60 million metric tons of atmospheric nitrogen is fixed annually by agriculturally-important legumes, which is equivalent to industrial fertilizer valued at 10 billion US dollars (Graham and Vance, 2003).

Engineering cereals with the ability to fix atmospheric nitrogen could circumvent the economic and environmental concerns associated with the overuse of synthetic fertilizers, while contributing to food sovereignty around the globe. Two major approaches are currently being explored towards the development of so-called self-fertilizing crops (Beatty and Good, 2011; Oldroyd and Dixon, 2014; Rogers and Oldroyd, 2014). One objective focuses on developing RNS in cereal crops. An alternative approach is to

directly engineer the expression of a nitrogenase enzyme, which reduces gaseous nitrogen to ammonia, into the organelles of plant cells. Although extremely attractive, the latter approach poses remarkable challenges, owing to the highly complex nature of the nitrogenase which requires the coordinated expression of at least 16 genes (Seefeldt et al., 2009). Additionally, nitrogenase activity, while being oxygen sensitive, is dependent on high levels of ATP. Therefore, finding a subcellular compartment that is suitable for nitrogenase activity in plant cells might be difficult. It is worth noting that the ability to fix atmospheric nitrogen is limited to only certain bacteria and archaea (Dos Santos et al., 2012) and no eukaryotes have evolved this capacity (Seefeldt et al., 2009). Consequently, direct transfer of nitrogenase to eukaryotic cells might face fundamental barriers (Rogers and Oldroyd, 2014).

Conferring a *Rhizobium*-legume type of symbiosis to non-legumes, however, while also highly challenging and unlikely to be implemented in the short term, seems feasible, considering legumes as the living prototypes for self-fertilizing crops. The *Rhizobium*-legume symbiosis results in novel specialized organs, called nodules, which accommodate the bacteria while providing a suitable, oxygen-limited environment for fixing nitrogen. It is thought that this evolutionary innovation, estimated to have evolved around 60 million years ago (MYA), recruited mechanisms pertinent to the already long-established and ancient (ca. 450 MYA) ability of plants to accommodate another group of intracellular endophytes, namely arbuscular mycorrhizal (AM) fungi (Kistner and Parniske, 2002; Markmann and Parniske, 2009). The signaling pathway that supports AM symbiosis is functionally conserved not only in legumes, but also in cereals, as at least some of its components from rice were shown to be able to rescue the nodulation and AM phenotypes of legume mutants (Banba et al., 2008; Gutjahr et al., 2008). Interestingly, unlike RNS, which occurs only in a restricted number of genera, AM symbiosis (AMS) is almost ubiquitous, and is found in the majority of extant plant species (Doyle, 2011). This implies that mimicking RNS in non-legume crops might be possible by tweaking the ubiquitous mechanism for AM symbiosis. The overall research objective of my thesis, therefore, has been to contribute to our understanding of the mechanisms governing the development of RNS in legumes.

The signaling pathway for root nodule development is divided into two diverse yet synchronized events: rhizobial infection (epidermal program) and nodule organogenesis (cortical program) (Figure 1.5). The available data strongly suggest that several plant hormonal pathways have been hijacked from the pre-existing mechanisms during the evolution of nitrogen-fixing root nodule symbiosis. In this research thesis, I have attempted to further dissect the involvement of two important phytohormones, cytokinin and ethylene, in the regulation of nodulation and rhizobial infection. Analysis of the *Lotus histidine kinase 1 (Lhk1)* cytokinin receptor gene showed that LHK1 is required and also sufficient for the initiation of nodule organogenesis (Murray et al., 2007; Tirichine et al., 2007). Nonetheless, mutant plants carrying the loss-of-function *lhk1-1* allele still form a limited number of nodules while being hyper-infected by their symbiotic partner (Murray et al., 2007). The unique and somewhat paradoxical phenotype of the *lhk1-1* mutant provided great insight into the regulatory mechanisms for nodule organogenesis within the root cortex and rhizobial infection at the root epidermis (see Chapters 2, 3, and 4).

Several studies indicated that cytokinins have a positive role in nodule organogenesis (Cooper and Long, 1994; Frugier et al., 2008; Heckmann et al., 2011). Chapter 2 of this thesis detailed the key function of cytokinin receptors in nodule structure formation by showing that *Lotus japonicus* contains a small family of four cytokinin receptor genes, namely *Lhk1*, *Lhk1A*, *Lhk2* and *Lhk3*, which all respond to *Mesorhizobium loti*. Phenotypic analysis of the single and double mutants revealed that unlike *lhk1-1*, deleterious mutations in *Lhk1A*, *Lhk2*, and *Lhk3* do not affect nodulation phenotype. Expression analyses and histochemical data, on the other hand, showed that *Lhk1*, *Lhk1A*, and *Lhk3* are expressed during early stages of nodule formation, suggesting specific and also partially redundant functions of these receptors in this process. I also showed that all four *Lhk* genes respond to rhizobial inoculation and also to an ectopic cytokinin application in wild-type roots but fail to do so in *lhk1-1*, indicating the unique role of LHK1 in these processes. When *lhk1-1* was combined with mutations that specifically block bacterial entry to the roots but leave the nodule formation intact, the resulting double mutant plants did not form nodules, showing that in the absence of LHK1, bacterial entry inside the root cortex is required for nodule formation. Importantly,

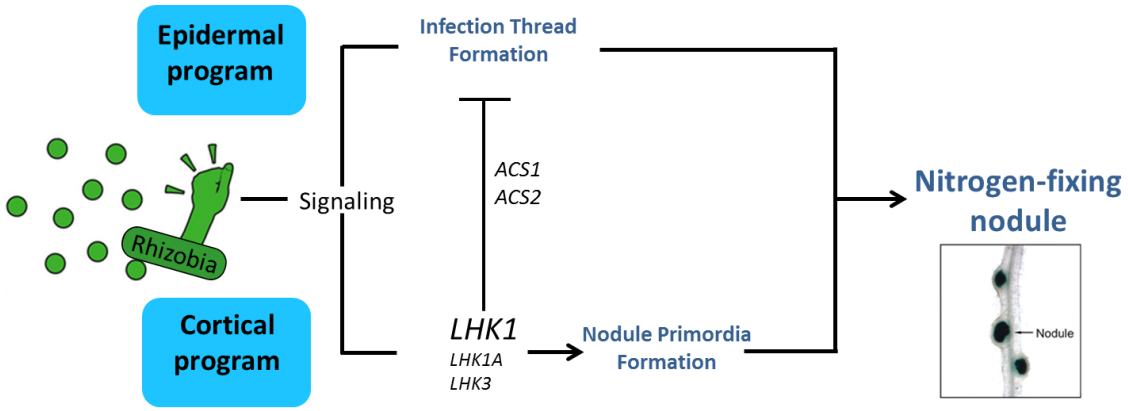

Figure 5.1 A proposed model for participation of cytokinin receptor and ethylene biosynthesis genes in regulation of nodule and infection thread formation.

unlike *lhk1-1*, triple mutant plants carrying deleterious mutations in *Lhk1*, *Lhk1A*, and *Lhk3* cytokinin receptor genes do not form nodules but remain hyperinfected by rhizobia, indicating a pivotal role of these cytokinin receptors in nodule structure formation. Based on these observations, I proposed a model for cytokinin receptor-dependent signaling for root nodule symbiosis. In this model, LHK1 exerts a unique function in the root epidermis but works partially redundantly with LHK1A and LHK3 in the cortex to mediate nodule formation (See Figure 2.20). The data presented in Chapter 2 of this thesis are in agreement with the current notion that plant production of cytokinins is a positive regulator of symbiosis in roots. Recently, it has been shown that a non-nodulating rhizobial strain is able to produce cytokinins in a manner similar to the nodulating rhizobia, indicating that rhizobially-derived cytokinins are not involved or may not be sufficient to trigger nodulation (Kisiala et al., 2013). Instead, rhizobially-produced nodulation factors (NFs) trigger a rapid accumulation of plant-derived cytokinins in roots of both *L. japonicus* and *Medicago truncatula* (van Zeijl et al., 2015; Reid et al., 2016). In fact, most transcriptional changes that occur in roots in response to NF application in *M. truncatula*, depend on MtCRE1, a homolog of LHK1 (van Zeijl et al., 2015).

Several recent studies have shown that the initial cellular response to NF signaling involves changes to the cytokinin homeostasis by *de novo* biosynthesis, activation, relocation and degradation of cytokinins (Chen et al., 2014; Mortier et al., 2014; van Zeijl et al., 2015; Reid et al., 2016). Thus the available pool of bioactive cytokinins directs nodule organogenesis in roots. These findings collectively indicate that cytokinin biosynthesis and the resulting signaling are essential and also sufficient for nodule organogenesis in legume roots.

Given that an external application of cytokinin and the constitutive activation of the LHK1 cytokinin receptor can both induce spontaneous nodule formation (Tirichine et al., 2007; Heckmann et al., 2011), and that timely nodule formation is prevented by *lhk1* mutations (Murray et al., 2007; Held et al., 2014), it was tempting to speculate that there might be a specific twist to the functioning of cytokinin receptors in legumes. However, using the *Arabidopsis AHK4* cytokinin receptor gene, I was able to demonstrate that this non-legume cytokinin receptor is able to functionally substitute for LHK1 during nodule

formation (see Figure 2.19). This observation indicates that the ability to control nodulation is unlikely to be determined by unique properties of *L. japonicus* cytokinin receptor. However, the same *Arabidopsis* receptor only partially rescued the defective nodulation phenotype of the *M. truncatula Mtcre1* mutant (Boivin et al., 2016). Whether this is related to different modes of nodule development in these two legume species is currently unknown but further insight will be important to fully comprehend various challenges as associated with the possibility of engineering nodule organogenesis in non-legumes.

The role of cytokinin as the endogenous plant inducer of nodule formation has now been firmly established. The involvement of cytokinin in mediating rhizobial entry into roots, however, has been overlooked. My data indicated that in *L. japonicus*, cytokinin receptors had no apparent function during the initial epidermal infection thread formation events. Nonetheless, in their absence, in the *lhk1-1 lhk1a-1 lhk3-1* triple receptor mutant, cortical infection threads did not develop (Miri et al., 2016) (see Chapter 3). Thus, cytokinin might be the primary, plant endogenous signal that conditions cortical cells for upcoming rhizobial infections. Arguably, cytokinin signaling must have been crucial during the evolution of plant cell predisposition for rhizobia colonization. Interestingly, I showed that the cytokinin-dependent signaling events which promote the development of infection threads in the cortex also appear to stimulate the negative feedback mechanism in the root epidermis which presumably functions through the ethylene biosynthesis pathway to restrict subsequent infection thread formation events (Chapter 3 and 4).

Although the hyperinfection phenotype of *lhk1-1* is reminiscent of those mutant/transgenic plants with ethylene insensitivity (Penmetsa and Cook, 1997; Nukui et al., 2004; Lohar et al., 2009), the mechanism by which ethylene is regulated during symbiosis remained obscure. Results presented in Chapter 4 showed that in *lhk1-1* the root growth and infection thread formation remained sensitive to ethylene precursor but the mutant produced less ethylene. This made it likely that the hyperinfection phenotype of *lhk1-1* is due, at least in part, to the altered ethylene level (Chapter 4). Consequently, I argued that upon *M. loti* infection, the increased cytokinin levels enhance the activity of ACS, the rate-limiting enzyme in ethylene biosynthesis pathway. This is presumed to

elevate the ethylene level, which in turn inhibits bacterial infection. My work suggests that two candidate type-2 ethylene biosynthesis genes, *ACS1* and *ACS2,* are likely to function redundantly to regulate the extent of rhizobial infection in an LHK1-dependent manner. In parallel, ETO1/EOLs proteins might also work redundantly in fine-tuning the rhizobially-induced ethylene production.

While a symbiotic relationship is generally beneficial to both partners, maintaining homeostasis is vital for the host plant as the nitrogen-fixation process is strongly energy-dependent. Therefore, understanding the mechanisms that govern the tight regulation of nodulation and infection thread formation is a requirement for the rational consideration of transferring RNS into cereals. In order to recapitulate nitrogen-fixing symbiosis in cereals four major steps need to be engineered; rhizobial recognition, nodule formation, rhizobial accommodation, and provision of an environment suitable for nitrogenase to reduce nitrogen (Rogers and Oldroyd, 2014). My thesis research has helped to further understanding of how two ubiquitous plant hormones, which are involved in many physiological processes, contribute to the regulation of RNS in legumes.

Nodule structures and the mechanisms by which plants are colonized by rhizobia are quite diverse. Nodules can vary from a simple swelling of roots or stems (due to limited cell divisions) to highly advanced structures like those formed in *L. japonicus* and *M. truncatula* (Sprent et al., 2013). Invasion of the root by rhizobia can occur by either a root hair-dependent mechanism that requires infection thread formation, as in *L. japonicus*, or a root hair-independent mechanism such as crack entry (Held et al., 2010). The root hair-independent mechanism is considered the more primitive form and is known to operate in about 25% of all legume genera (Sprent, 2007). Interestingly, even in legumes such as *L. japonicus* that support the more advanced route of rhizobial invasion, the crack entry process is still operable (Karas et al., 2005). Regardless of the type of nodules formed or the routes of rhizobial invasion, from the most basic to the most highly evolved, the host plant benefits from its close association with nitrogen-fixing bacteria. Clearly, the more intimate, endosymbiotic associations are more reliable in delivering fixed nitrogen to the plants.

Although the efficiency of the symbiotic nitrogen-fixation in a model legume such as *L. japonicus* can be the blueprint for transferring RNS to non-legumes, the first step in this challenging endeavor would be to demonstrate the ability to advance this process in cereals, regardless of the efficiency (Beatty and Good, 2011; Rogers and Oldroyd, 2014). Given the complexity of the processes involved, implementation of a more primitive association of cereals with nitrogen-fixing bacteria might be more feasible. Even a small increase in the amount of available nitrogen would be truly advantageous for subsistence farmers in developing countries (Tilman et al., 2011). This would also contribute to minimizing the existing yield gap, hence, contributing to global food security. Reaching a level of fixed nitrogen in cereals to a point that it could substitute for the intensive use of fertilizers in the developed countries will probably require stepwise improvement in the efficiency of nitrogen fixation. Achieving a scientific solution for the nitrogen dilemma will without doubt be extremely rewarding for mankind and the planet, but requires long-term commitment to research.

5.2 References

Banba, M., Gutjahr, C., Miyao, A., Hirochika, H., Paszkowski, U., Kouchi, H., and Imaizumi-Anraku, H. (2008). Divergence of evolutionary ways among common sym genes: CASTOR and CCaMK show functional conservation between two symbiosis systems and constitute the root of a common signaling pathway. Plant Cell Physiol. **49:** 1659-1671.

Beatty, P.H., and Good, A.G. (2011). Future prospects for cereals that fix nitrogen. Science **333:** 416-417.

Boivin, S., Kazmierczak, T., Brault, M., Wen, J., Gamas, P., Mysore, K.S., and Frugier, F. (2016). Different cytokinin histidine kinase receptors regulate nodule initiation as well as later nodule developmental stages in Medicago truncatula. Plant Cell Environ. **39:** 2198-2209.

Charpentier, M., and Oldroyd, G. (2010). How close are we to nitrogen-fixing cereals? Curr. Opin. Plant Biol. **13:** 556-564.

Chen, Y., Chen, W., Li, X., Jiang, H., Wu, P., Xia, K., Yang, Y., and Wu, G. (2014). Knockdown of *LjIPT3* influences nodule development in *Lotus japonicus*. Plant Cell Physiol. **55:** 183-193.

Cooper, J.B., and Long, S.R. (1994). Morphogenetic rescue of *Rhizobium meliloti* nodulation mutants by *trans*-zeatin secretion. Plant Cell **6:** 215-225.

Dos Santos, P.C., Fang, Z., Mason, S.W., Setubal, J.C., and Dixon, R. (2012). Distribution of nitrogen fixation and nitrogenase-like sequences amongst microbial genomes. BMC Genomics **13**.

Doyle, J.J. (2011). Phylogenetic perspectives on the origins of nodulation. Mol. Plant-Microbe Interact. **24:** 1289-1295.

Erisman, J.W., Sutton, M.A., Galloway, J., Klimont, Z., and Winiwarter, W. (2008). How a century of ammonia synthesis changed the world. Nat. Geosci. **1:** 636-639.

Foley, J.A., Ramankutty, N., Brauman, K.A., Cassidy, E.S., Gerber, J.S., Johnston, M., Mueller, N.D., O'Connell, C., Ray, D.K., West, P.C., Balzer, C., Bennett, E.M., Carpenter, S.R., Hill, J., Monfreda, C., Polasky, S., Rockström, J., Sheehan, J., Siebert, S., Tilman, D., and Zaks, D.P.M. (2011). Solutions for a cultivated planet. Nature **478:** 337-342.

Frugier, F., Kosuta, S., Murray, J.D., Crespi, M., and Szczyglowski, K. (2008). Cytokinin: secret agent of symbiosis. Trends Plant Sci. **13:** 115-120.

Graham, P.H., and Vance, C.P. (2003). Legumes: Importance and constraints to greater use. Plant Physiol. **131:** 872-877.

Gutjahr, C., Banba, M., Croset, V., An, K., Miyao, A., An, G., Hirochika, H., Imaizumi-Anraku, H., and Paszkowski, U. (2008). Arbuscular mycorrhiza-specific signaling in rice transcends the common symbiosis signaling pathway. Plant Cell **20:** 2989-3005.

Heckmann, A.B., Sandal, N., Bek, A.S., Madsen, L.H., Jurkiewicz, A., Nielsen, M.W., Tirichine, L., and Stougaard, J. (2011). Cytokinin induction of root nodule primordia in *Lotus japonicus* is regulated by a mechanism operating in the root cortex. Mol. Plant-Microbe Interact. **24:** 1385-1395.

Held, M., Hossain, M.S., Yokota, K., Bonfante, P., Stougaard, J., and Szczyglowski, K. (2010). Common and not so common symbiotic entry. Trends Plant Sci. **15:** 540-545.

Held, M., Hou, H., Miri, M., Huynh, C., Ross, L., Hossain, M.S., Sato, S., Tabata, S., Perry, J., Wang, T.L., and Szczyglowski, K. (2014). *Lotus japonicus* cytokinin receptors work partially redundantly to mediate nodule formation. Plant Cell **26:** 678-694.

Karas, B., Murray, J., Gorzelak, M., Smith, A., Sato, S., Tabata, S., and Szczyglowski, K. (2005). Invasion of *Lotus japonicus root hairless 1* by *Mesorhizobium loti* involves the nodulation factor-dependent induction of root hairs. Plant Physiol. **137:** 1331-1344.

Kisiala, A., Laffont, C., Emery, R.J.N., and Frugier, F. (2013). Bioactive cytokinins are selectively secreted by *Sinorhizobium meliloti* nodulating and nonnodulating strains. Mol. Plant-Microbe Interact. **26:** 1225-1231.

Kistner, C., and Parniske, M. (2002). Evolution of signal transduction in intracellular symbiosis. Trends Plant Sci. **7:** 511-518.

Lagi, M., Bertrand, K.Z., and Bar-Yam, Y. (2011). The food crises and political instability in North Africa and the Middle East. New England Complex Systems Institute, Cambridge, MA. Available at SSRN 1910031.

Lohar, D., Stiller, J., Kam, J., Stacey, G., and Gresshoff, P.M. (2009). Ethylene insensitivity conferred by a mutated *Arabidopsis* ethylene receptor gene alters nodulation in transgenic *Lotus japonicus*. Ann. Bot. **104:** 277-285.

Markmann, K., and Parniske, M. (2009). Evolution of root endosymbiosis with bacteria: how novel are nodules? Trends Plant Sci. **14:** 77-86.

Miri, M., Janakirama, P., Held, M., Ross, L., and Szczyglowski, K. (2016). Into the Root: How Cytokinin Controls Rhizobial Infection. Trends Plant Sci. **21:** 178-186.

Mortier, V., Wasson, A., Jaworek, P., De Keyser, A., Decroos, M., Holsters, M., Tarkowski, P., Mathesius, U., and Goormachtig, S. (2014). Role of LONELY GUY genes in indeterminate nodulation on *Medicago truncatula*. New Phytol. **202:** 582-593.

Mueller, N.D., Gerber, J.S., Johnston, M., Ray, D.K., Ramankutty, N., and Foley, J.A. (2012). Closing yield gaps through nutrient and water management. Nature **490:** 254-257.

Murray, J.D., Karas, B.J., Sato, S., Tabata, S., Amyot, L., and Szczyglowski, K. (2007). A cytokinin perception mutant colonized by *Rhizobium* in the absence of nodule organogenesis. Science **315:** 101-104.

Mus, F., Crook, M.B., Garcia, K., Costas, A.G., Geddes, B.A., Kouri, E.D., Paramasivan, P., Ryu, M.H., Oldroyd, G.E.D., Poole, P.S., Udvardi, M.K., Voigt, C.A., Ané, J.M., and Peters, J.W. (2016). Symbiotic nitrogen fixation and the challenges to its extension to nonlegumes. Appl. Environ. Microbiol. **82:** 3698-3710.

Nukui, N., Ezura, H., and Minamisawa, K. (2004). Transgenic *Lotus japonicus* with an ethylene receptor gene *Cm-ERS1/H70A* enhances formation of infection threads and nodule primordia. Plant Cell Physiol. **45:** 427-435.

Oldroyd, G.E.D., and Dixon, R. (2014). Biotechnological solutions to the nitrogen problem. Curr. Opin. Biotechnol. **26:** 19-24.

Penmetsa, R.V., and Cook, D.R. (1997). A legume ethylene-insensitive mutant hyperinfected by its rhizobial symbiont. Science **275:** 527-530.

Philippot, L., Raaijmakers, J.M., Lemanceau, P., and Van Der Putten, W.H. (2013). Going back to the roots: The microbial ecology of the rhizosphere. Nat. Rev. Microbiol. **11:** 789-799.

Reid, D.E., Heckmann, A.B., Novák, O., Kelly, S., and Stougaard, J. (2016). CYTOKININ OXIDASE/DEHYDROGENASE3 maintains cytokinin homeostasis during root and nodule development in *Lotus japonicus*. Plant Physiol. **170:** 1060-1074.

Rogers, C., and Oldroyd, G.E.D. (2014). Synthetic biology approaches to engineering the nitrogen symbiosis in cereals. J. Exp. Bot. **65:** 1939-1946.

Seefeldt, L.C., Hoffman, B.M., and Dean, D.R. (2009). Mechanism of mo-dependent nitrogenase. In Annual Review of Biochemistry, pp. 701-722.

Sprent, J.I. (2007). Evolving ideas of legume evolution and diversity: A taxonomic perspective on the occurrence of nodulation. New Phytol. **174:** 11-25.

Sprent, J.I., Ardley, J.K., and James, E.K. (2013). From North to South: A latitudinal look at legume nodulation processes. S. Afr. J. Bot. **89:** 31-41.

Tilman, D., Balzer, C., Hill, J., and Befort, B.L. (2011). Global food demand and the sustainable intensification of agriculture. Proc. Natl. Acad. Sci. U. S. A. **108:** 20260-20264.

Tirichine, L., Sandal, N., Madsen, L.H., Radutoiu, S., Albrektsen, A.S., Sato, S., Asamizu, E., Tabata, S., and Stougaard, J. (2007). A gain-of-function mutation in a cytokinin receptor triggers spontaneous root nodule organogenesis. Science **315:** 104-107.

Tittonell, P., and Giller, K.E. (2013). When yield gaps are poverty traps: The paradigm of ecological intensification in African smallholder agriculture. Field Crops Res. **143:** 76-90.

van Zeijl, A., Op Den Camp, R.H.M., Deinum, E.E., Charnikhova, T., Franssen, H., Op Den Camp, H.J.M., Bouwmeester, H., Kohlen, W., Bisseling, T., and Geurts, R. (2015). Rhizobium Lipo-chitooligosaccharide signaling triggers accumulation of cytokinins in *Medicago truncatula* roots. Molecular Plant **8:** 1213-1226.

Appendices

Appendix A: Copy right permission (Chapter 3)

Permission for inclusion of the article “Into the root: how cytokinin controls rhizobial infection” published in the Trends in Plant Science, Volume 21, pages 178-186, March 2016 as Chapter 3 of this thesis.

Curriculum Vitae

Mandana Miri

EDUCATION

2011- 2016 **PhD candidate in Cell & Molecular Biology**
Biology Department, University of Western Ontario,
London, Ontario, Canada **(92.25/100)**
Thesis: Gatekeepers of the nitrogen-fixing symbiosis: cytokinin-ethylene crosstalk regulates symbiotic interaction in *Lotus japonicus*

2014 PhD comprehensive exam- ***Passed with Distinction***

2006- 2009 **Masters of Science in Genetics**
Biology Department, Azad University,
Science & Research Branch, Tehran, Iran **(88.5/100)**
Thesis: Cloning and expression of an alkane hydroxylase system from *Alcanivorax borkumensis* in *Escherichia coli*, **20/20 (A^+)**

2002- 2006 **Bachelor of Science in Biology**
Biology Department, Tarbiat Moallem University,
Tehran, Iran
Thesis: Effects of UV on mutation rate of *Drosophila melanogaster*, **20/20 (A^+)**

ACADEMIC HONOURS AND AWARDS

2017 Great Ideas In Innovative Teaching Award (Runner-up)
2016 Cover of the *Molecular Plant-Microbe Interactions* journal
2016 Dr. John D. Detwiler Award
2016 SOGS Travel Subsidy
2016 PSAC 610 Outstanding Research Contributions Scholarship
2015 Dr. Jesus Caballero-Mellado Best Oral Presentation Award

2015	The Michael Locke Graduate Student Travel Grant
2015	Society of Graduate Students Teaching Award Nominee
2015	Dr. Roth Memorial Award
2014	Oral Presentation Award (Runner-up), Biology Graduate Research Forum
2014	Malcolm Ferguson Award in Life Sciences
2014	Biology Graduate Student Travel Award
2013	Best Oral Presentation Award, Biology Graduate Research Forum
2013	Society of Graduate Students Teaching Award Nominee
2013	René R. Roth Memorial Award
2012	Vanier Canadian Graduate Scholarship Institutional Nominee
2012	GTA Academic Achievement Scholarship
2012	Department of Biology Graduate Student Teaching Award
2012	Three Minute Thesis (3MT) Competition Finalist
2012	Society of Graduate Students Teaching Award Nominee
2009	Best Master's Thesis Award
2009	Best Oral Presentation Award, National Biotechnology Congress
2008	Best Poster Presentation Award, Iranian Genetics Congress

WORK EXPERIENCE

2011-2017	Teaching Assistant, Department of Biology, The University of Western Ontario, London, Ontario
2011-2017	Research Assistant, Agriculture and Agri-Food Canada London, Ontario
2010-2010	Research Associate, Molecular Parasitology Department, Pasteur Institute of Iran, Tehran, Iran
2006-2009	Director of Research and Development, BehshidZistFaravard Company, Biotechnology Incubator, Tehran, Iran
2005-2006	Research Assistant, Genetics Laboratory, Tarbiat Moallem University, Tehran, Iran

ARTICLES IN REFEREED JOURNALS

Miri, M., Ross, L., Huebert, T., Reid, D., Stougaard, J., Szczyglowski, K. (2017) Cytokinin-ethylene crosstalk limits bacterial infection in *Lotus japonicus*. *Molecular Plant Biology.* In preparation (PhD work).

Miri, M., Shrestha, A., Zhong, S., Janakirama, P., Ross, L., Szczyglowski, K. (2017) Nitrogen-fixing root nodule symbiosis: Life according to NIN? (2016) *The Plant Cell.* In preparation (PhD work).

Hossain, Md.S., Shrestha, A., Zhong, S., **Miri, M.**, Austin, R., Sato, S. Ross, L., Huebert, T., Tromas, A., Torres-Jerez, I., Torres-Jerez, I., Tang, Y., Murray, J., Udvardi, M., Szczyglowski, K. (2016). *Lotus japonicus* NF-YA1 plays an essential role during nodule differentiation and targets members of the *SHI/STY* gene family. *Molecular Plant-Microbe Interactions*. 29(12): 950-964 (PhD work)

[An image from this work was featured as the cover of the *Molecular Plant-Microbe Interactions* journal for the December 2016].

Miri, M., Janakirama, P., Held, M., Ross, L., Szczyglowski, K. (2016) Into the root: how cytokinin controls rhizobial infection. *Trends in Plant Science.* 2(3): 178-186 [**Special issue** on RHIZOSPHERE], (PhD work).

Held, M*., Hou, H*., **Miri, M*.**, Huynh, C., Ross, L., Hossain, Md.S., Sato, S., Tabata, S., Perry, J., Wang, T., Szczyglowski, K. (2014) *Lotus japonicus* cytokinin receptors work partially redundantly to mediate nodule formation. *The Plant Cell.* 26(2): 678-694 (PhD work).***These authors contributed equally to this work.**

Babaei, J., **Miri, M.**, Sadeghiani, G., Zare, M., Khalili, G., Golkar, M. (2011) Expression and single-step purification of GRA8 antigen of *Toxoplasma gondii* in *Escherichia coli*. *Avicenna Journal of Medical Biotechnology*. 3(2): 67-77 (Research Associate work).

Kamali, N., Bambai, B., Karkhaneh, A.A., Tavalayee, M., **Miri, M.** Site-directed mutagenesis enhanced NADH-FMN oxidoreductase (DszD) activity of *Rhodococcus erythropolis*. *Biotechnology Letters.* 32(7): 921-927 (MSc work).

Miri, M., Bambai, B., Tabandeh, F., Sadeghizadeh, M., Kamali, N. (2010) Production of a recombinant alkane hydroxylase (AlkB2) from *Alcanivorax borkumensis*. *Biotechnology Letters.* 32(4): 497-502 (MSc work).

Miri, M., Bambai, B., Tabandeh, F., Panahi, F., Sadeghizadeh M. (2010) Role of microorganisms in combating petroleum-marine pollution. *Farayandno.* 19(1): 60-74 (MSc work).

OTHER REFEREED PUBLICATIONS_ REGISTERED PATENTS

Tabandeh, F., Khodabandeh, M., Bambai, B., **Miri, M.**, Zamzamian, A.H., Shojayee, S., Davari, A., Mansoori, A.H. (2011) Production of a novel yogurt starter culture. Iranian Patents Office (Registration No.: 38911094).

Miri, M., Panahi, F., Bambai, B., Tabandeh, F. (2010) Construction of a multi-protein system for biotransformation of alkanes to alkanols. Iranian Patents Office (Registration No.: 12785984).

Panahi, F., **Miri, M.**, Bambai, B., Tabandeh, F. (2010) Design of a novel system process for converting alkanes to alkanols. Iranian Patents Office (Registration No.: 12785985).

ORAL PRESENTATIONS (PRESENTING AUTHOR IS UNDERLINED)

Miri, M., Szczyglowski, K. (2016) Gatekeepers of rhizobia entry: cytokinin-ethylene crosstalk might take us towards nitrogen-fixing crops. The 7th annual Biology Graduate Research Forum (BGRF), University of Western Ontario, London, Ontario, Canada (Institutional- PhD work).

Miri, M., Ross, L., Huebert, T., Szczyglowski, K. (2016) Gatekeepers of rhizobia entry: cytokinin-ethylene crosstalk regulates infection in *Lotus japonicus.* The joint meeting of

the Canadian Society of Plant Biologists (CSPB) and the Canadian Association of Plant Biotechnology (CAPB), Kingston, Ontario (National- PhD work).

Miri, M., Ross, L., Huebert, T., Szczyglowski, K. (2015) Cytokinin-ethylene crosstalk regulates infection in *Lotus japonicus*. 23rd North American Symbiotic Nitrogen Fixation Conference (NASNFC), Ixtapa, Mexico (International- PhD work).

Miri, M., Ross, L.M., and Szczyglowski, K. (2015). Into the root: how cytokinin controls symbiotic root nodule formation. 19th International Conference on Nitrogen Fixation, Pacific Grove, California, USA (International- PhD work).

Miri, M., Szczyglowski, K. (2014) Too many invasions? Cytokinin-ethylene cross-talk may limit bacterial infection in *Lotus japonicus.* The 5th annual Biology Graduate Research Forum (BGRF), University of Western Ontario, London, Ontario, Canada (Institutional- PhD work).

Miri, M., Hou, H., Ross, L., Perry, J., Wang, T., Held, M., Szczyglowski, K. (2014) Turning on the nitrogen tap: how legumes keep the nutrient flowing. International Food Legumes Research Conference & International Conference on Legume Genetics and Genomics (IFLRC & ICLGG), Saskatoon, Saskatchewan, Canada (International- PhD work).

Miri, M., Szczyglowski, K. (2013) Next green revolution; towards nitrogen-fixing crops. The 4th annual Biology Graduate Research Forum (BGRF), University of Western Ontario, London, Ontario, Canada, (Institutional- PhD work).

Szczyglowski, K., **Miri, M.**, Held, M., Hou, H., Huynh, C. Ross, L. (2013) Cytokinin receptors: footprints along the evolutionary path to symbiotic root nodule formation. The 22nd North American Symbiotic Nitrogen Fixation Conference (NASNFC), Minneapolis, Minnesota, USA (International- PhD work).

Miri, M., Hou, H., Held, M., Ross, L., Perry, J., Wang, T., Szczyglowski, K. (2012) Role of cytokinin receptors during symbiotic root nodule organogenesis in *Lotus japonicus*.

The Canadian Society of Plant Biologists, Eastern Regional Meeting (CSPB ERM), Waterloo, Ontario, Canada (Regional- PhD work).

Miri, M. (2012) Putting an end to the world hunger using plant-bacteria interaction. Three Minute Thesis (3MT) Competition, School of Graduate and Postdoctoral Studies, University of Western Ontario, London, Ontario, Canada (Institutional- PhD work).

Miri, M., Bambai, B., Farzaneh, P., Kashefi Mofrad, M.R. (2010) Production of a heat-resistant organophosphor anhydrase in *Escherichia coli*. The 11th Iranian Genetics Congress, Tehran, Iran, (National- R & D activities).

Miri, M., Tabandeh, F., Sadeghizadeh, M., Bambai B. (2009) Construction of a multi-protein system for alkane biotransformation. The 6th National Biotechnology Congress, Tehran, Iran (National- MSc work).

Miri, M., Tabandeh, F., Sadeghizadeh, M., Bambai, B. (2008) Cloning and co-expression of rubredoxin and rubredoxin reductase from *Alcanivorax borkumensis*. The 2nd International Student Conference of Biotechnology, Tehran, Iran (International- MSc work).

POSTER PRESENTATIONS (PRESENTING AUTHOR IS UNDERLINED)

Miri, M., Szczyglowski, K. (2016) Into the root: how cytokinin controls symbiotic root nodule formation. The 12th European Nitrogen Fixation Conference (ENFC), Budapest, Hungary (International- PhD work).

Miri, M., Ross, L., Szczyglowski, K. (2014) Cytokinin-ethylene crosstalk may limit bacterial infection in *Lotus japonicus*. The 11th European Nitrogen Fixation Conference (ENFC), Tenerife, Canary Islands, Spain (International- PhD work).

Miri, M., Held, M., Hou, H., Ross, L., Perry, J., Wang, T., Szczyglowski, K. (2013) Redundant role of cytokinin receptors during symbiotic root nodule organogenesis in *Lotus japonicus*. The 22nd annual North American Symbiotic Nitrogen Fixation Conference (NASNFC), Minneapolis, Minnesota, USA (International- PhD work).

Miri, M., Hou, H., Held, M., Huynh, C., Szczyglowski, K. (2012) Role of cytokinin receptors during symbiotic root nodule organogenesis in *Lotus japonicus*. The annual meeting of the American Society of Plant Biologists (ASPB), Austin, Texas, USA (International- PhD work).

Miri, M., Hou, H., Held, M., Huynh, C., Ross, L., Szczyglowski, K. (2011) Role of cytokinin receptors during root nodule organogenesis. The 2nd Biology Graduate Research Forum (BGRF), University of Western Ontario, London, Ontario, Canada (Institutional- PhD work).

Hou, H., Held, M., **Miri, M.**, Huynh, C., Ross, L., Perry, J., Wang, T., Szczyglowski, K. (2011) Superimposed signaling by cytokinin mediates root nodule organogenesis. The 8th Canadian Plant Genomics Workshop (CPGW), Niagara Falls, Ontario, Canada (National- PhD work).

Miri, M., Tabandeh, F., Sadeghizadeh, M., Bambai, B. (2009) Construction of a multi-protein system for alkanes biotransformation. The 6th National Biotechnology Congress, Tehran, Iran (National- MSc work).

Miri, M., Bambai, B., Farzaneh, P. Kashefi Mofrad, M.R. (2009) Recombinant expression of an organophosphor anhydrase in *Escherichia coli*. The 6th National Biotechnology Congress, Tehran, Iran (National- R & D activities).

Miri, M., Tabandeh, F., Sadeghizadeh, M., Bambai, B. (2008) Construction of a multi-protein system for biotransformation of alkanes. Biotechnology and Bioinformatics Symposium (BIOT-2008), Arlington, Texas, USA, (International- MSc work).

Miri, M., Bambai, B., Tabandeh, F., Sadeghizadeh, M. (2008) Cloning and expression of alkane hydroxylase from the oil-consuming marine bacterium *Alcanivorax borkumensis* in *Escherichia coli*. The 10th Iranian Genetics Congress, Tehran, Iran (National, MSc work)

Miri, M., Saberianfar, R., Tahmaseb, M. (2006) A study of the effects of UVA, UVB and UVC on mutation rate in *Drosophila melanogaster*. The 2nd International Conference of Biology, Teheran, Iran (International- Undergraduate work).

DEPARTMENTAL AND UNIVERSITY SERVICES

2015-2016	Graduate Education Committee Representative,
	Biology Department, University of Western Ontario, London, Ontario, Canada
2015-2016	Biology Steward for Graduate Teaching Assistant (GTA) Union
	University of Western Ontario, London, Ontario, Canada
2015-2016	Fundraising Sub-committee Member, Biology Graduate Research Forum,
	University of Western Ontario, London, Ontario, Canada
2016	Guest Speaker at the "Take Our Kids to Work Day" Event,
	Agriculture & Agri-Food Canada, London, Ontario, Canada
2016	Panel Discussion Moderator, Biology Graduate Research Forum,
	University of Western Ontario, London, Ontario, Canada
2016	Public Lecturer at "Doors Open to the Public" Event
	Agriculture & Agri-Food Canada, London, Ontario, Canada
2016	Panelist for the Graduate Students Orientation Day,
	Biology Department, University of Western Ontario, London, Ontario, Canada
2016	Co-instructor as a part of SHAD program
	Biology Department, University of Western Ontario, London, Ontario, Canada
2016	Graduate Student Teaching Assistant (GSTA) Award Committee

	Society of Graduate Students, University of Western Ontario, London, Ontario, Canada
2016	Oral Presentation Judge at Western Student Research Conference
	University of Western Ontario, London, Ontario, Canada
2015	National Scholarship Application Reviewer
	University of Western Ontario, London, Ontario, Canada
2015	Volunteer Recruiter at the Science Graduate Studies Fair
	Biology Department, University of Western Ontario, London, Ontario, Canada
2014	National Scholarship Application Reviewer
	University of Western Ontario, London, Ontario, Canada
2013	Poster Presentation Judge at Biology Graduate Research Forum
	University of Western Ontario, London, Ontario, Canada
2013	Volunteer at “Doors Open to the Public” Event
	Agriculture & Agri-Food Canada, London, Ontario, Canada
2013	National Scholarship Application Reviewer
	University of Western Ontario, London, Ontario, Canada
2011-2012	Biology Steward for Graduate Teaching Assistant (GTA) Union
	University of Western Ontario, London, Ontario, Canada